Development of advanced biofiltration process for hydrogen sulphide control

Duan, Huiqi

2007

Duan, H. Q. (2007). Development of advanced biofiltration process for hydrogen sulphide control. Doctoral thesis, Nanyang Technological University, Singapore.

https://hdl.handle.net/10356/12059

https://doi.org/10.32657/10356/12059

Development of Advanced Biofiltration Process for Hydrogen Sulphide Control

Duan Huiqi

School of Civil and Environmental Engineering

A thesis submitted to the Nanyang Technological University
in fulfillment of the requirement for the degree of
Doctor of Philosophy

2007

ACKNOWLEDGMENTS

I wish to express my sincere gratitude and appreciation to my supervisor, **Associate Professor Lawrence C.C. Koe** for his invaluable guidance and encouragement throughout the course of the research project.

I am indebted to my co-supervisor, **Dr. Yan Rong**, for her continuous and patient guidance and supervision in the past three years.

The author also extend her thanks to **all staff**, technicians, including Mr. Yong Fook Yew, Mrs. Phang-Tay Beng Choo, Mrs. Lim-Tay Chew Wang, Mr. Aw Wah Beng, Mrs. Ng-Chong, Melissa and Mr. Tan Han Khiang, Miss Wang Xiaoling, and students in the Environmental Laboratory and Institute of Environmental Science and Engineering of Nanyang Technological University for their kind assistance and cooperation that made this research project possible. Special thanks to **Dr. Chen Xiaoge** for her invaluable academic advices which have enabled this research to progress smoothly.

Thanks also due to her precious fellow research students in Environmental Laboratory and Institute of Environmental Science and Engineering, for their valuable advice and friendship like my family members during the course of this project. The assistance and cooperation of the staff at the Ulu Pandan Water Reclamation Plant are greatly appreciated.

Finally, I want to dedicate this thesis to my dearest Mom and Dad. Without their love, guide and support, I cannot reach where I am. Special thanks to my dear husband, Yan Jie, for his consistent love and support.

SUMMARY

Odor emission is a severe problem common to most wastewater treatment operations and particularly significant at urban treatment plants. Economical advantages coupled with environmental benefits make the process of odor biofiltration an attractive option, compared to the current chemical scrubber and activated carbon techniques. However, there still exist inefficiencies pertaining to the media used in biofiltration processes, such as the need for adequate residence time, limited life-time, and pore blockage of the media, which at present, render the technology economically unattractive. This study aims to develop a novel active medium, termed as biological activated carbon (BAC), through bacteria immobilization on activated carbon, a supporting medium with generally high specific surface area. It is expected that BAC could provide improved performance in removal of the major odorous pollutants such as hydrogen sulphide (H_2S) from the sewage air, by achieving an optimum balance and combination of the media adsorption capacity with the biodegradation of H_2S through the bacteria immobilized on the BAC.

The feasibility of developing BAC as a packing medium for H_2S removal was primarily evaluated in lab-scale biofilters. A mix culture of sulfide oxidizing bacteria dominated by *Acidithiobacillus Thiooxidans* acclimated from activated sludge was used as bacterial seeds and biofilm was mostly developed through culturing the bacteria in the presence of carbon pellets in mineral media. A rapid startup (a few days) was observed and the maximum elimination capacity of the BAC reached 181 $gH_2S \cdot m^{-3} \cdot h^{-1}$ at 94% removal efficiency (RE). If inlet concentration was within 30 ppm_v, over 99% of H_2S removal was achieved at a gas retention time (GRT) as low as 2s. The bacteria in the acidic biofilter demonstrated a capacity for H_2S removal in

a broad pH range (pH 1~7). Experimental evidences show that spent carbon (H_2S saturated carbon) could be re-used to develop BAC in a biofilter, thus provide some sense on the potential re-use or bio-regeneration of spent carbon.

To overcome the limitations found in the biofilter based on BAC, a horizontal, cross-flow biotrickling filter was designed to treat H_2S. It was found to be able to work efficiently from the first day of operation. The maximum elimination capacity (EC) of the system is 113 $gH_2S \cdot m^{-3} \cdot h^{-1}$ at RE of 96%. If inlet concentration was kept at around 20 ppm_v, H_2S removal of over 99% was achieved at a GRT of 3 s. The pH of the system should be maintained above 1 to avoid inhibition of microbial growth. Bacterial population in the recirculation sump should be controlled within the range of 10^6~10^9 $cfu \cdot mL^{-1}$ for optimal performance while avoiding clogging. High system buffer effect was evident because of the high carbon adsorption ability. Pressure drop test showed that the BAC bed had a much higher pressure drop than that of a conventional packing material in a chemical scrubber. Fortunately, the horizontal design alleviated this problem to some extent.

The mechanism of H_2S elimination on BAC was investigated following the horizontal biotrickling filter (HBTF) operation. A series of BAC samples were taken from inlet to outlet of the HBTF to examine the different effects of adsorption and biodegradation on H_2S removal. A correlation between the available surface area and pore volume with the extent of microbial immobilization and H_2S uptake is evidenced. Scanning electron microscopy (SEM) photographs show the direct carbon structure and biofilm coated on the surface of the carbon pellets. Fourier transform infrared (FTIR) spectra, differential thermogravimetric (DTG) curves and carbon-hydrogen-nitrogen-sulfur (CHNS) results indicate less diversity of H_2S oxidation products on BAC than those previously observed on exhausted carbon from H_2S adsorption only. The predominant oxidation product on BAC was sulfuric acid and the biofilm was believed to enhance the oxidation of H_2S on carbon surface. A mathematical modeling of the kinetics behavior of this HBTF was also developed in this work to achieve a better understanding to the key phenomena occurring in the process.

The combined effect of adsorption and biodegradation on activated carbon surface was studied with regards to the distribution of H_2S oxidation products. Four parallel lab-scale biofiltration columns were operated for 120 h to investigate in-depth the mechanisms involved in treating H_2S using BAC. Removal efficiency of the virgin (non-bacterial) activated carbon (VAC) bed dropped quickly to 30% within the first 8h, and eventually to 0% on saturation. Biofilter columns with the BAC, however, stay about 27% RE throughout their operation though the performance did fluctuate. The various S species in both aqueous and solid phases were determined using inductively coupled plasma optical emission spectrometry (ICP-OES), ion chromatography (IC), x-ray fluorescence (XRF) and carbon-hydrogen-nitrogen-sulfur (CHNS) element analyzer, respectively. It was found that sulfate sulfur percentage to total sulfur in the BAC system was twice that in the VAC system.

The findings of this research demonstrated that the combination of biodegradation and adsorption on BAC is capable of removing H_2S for a substantial period of time. A biotrickling filter using this new BAC is a viable biotechnology for the efficient removal of H_2S, the predominant odorous compound in sewage air. Studies on the mechanisms and modeling enable a better understanding to the biofiltration process applied in H_2S removal using BAC.

TABLE OF CONTENTS

LIST OF TABLES

LIST OF FIGURES

NOMENCLATURES

A	Cross section area of packing bed, m^2
ACF	Activated carbon fiber
A_p	Apparent surface area of particle, m^2
A_s	Effective diffusion surface area per volume of packing (specific area), m^{-1}
ASCE	American Society of Civil Engineering
ASTM	American Standard Test Method
BAC	Biological activated carbon
bar	A unit of pressure, 1 bar = 14.5 psi = 10^5 Pa
BET	Braunner-Emmett-Teller
BF	Biofilter
BTEX	Benzene, toluene, ethylbenzene, o-xylene
BTF	Biotrickling Filter
C	Concentration of substrate in air phase, $g \cdot m^{-3}$
C_f	Concentration of substrate in biofilm, $g \cdot m^{-3}$
cfu	Colony forming unit
CHNS	Carbon, hydrogen, nitrogen, sulphur
conc.	Concentration
Cs	Concentration of substrate in carbon, $g \cdot m^{-3}$
C-S	Combustible sulfur
d	Bulk density, $d=W_1/V$, $kg \cdot m^{-3}$
D	Dispersion coefficient in air phase, $m^2 \cdot s^{-1}$
D_f	Diffusivity of substrate in the biofilm, $m^2 \cdot s^{-1}$
DGGE	Denaturing gradient gel electrophoresis
DNA	Deoxyribonucleic acid

DO	Dissolved oxygen
D_s	Internal pore diffusivity of substrate within activated carbon pellet, $m^2 \cdot s^{-1}$
DTG	Differential thermogravimetric
DTS	Dissolved total sulfur
EC	Elimination capacity
EPS	Extracellular polymeric substance
FTIR	Fourier transform infrared spectroscopy
GRT	Gas retention time (=bed volume/air flow rate)
H	Henry's Constant, dimensionless
h	hour
H_2S	Hydrogen sulfide
HAPs	Hazardous air pollutants
HBF	Horizontal biofilter
HBTF	Horizontal biotrickling filter
HPE	High-pressure secondary effluent (~equivalent to industrial water)
HSDM	Homogeneous surface diffusion model
IC	Ion chromatography
ICP-OES	Inductively coupled plasma-optical emission spectrometry
k_0	Zero-order biodegradation rate constant, = $k_{max,}$ $g \cdot m^{-3} \cdot s^{-1}$
k_1	First-order biodegradation rate constant, = k_{max}/K_s, s^{-1}
k_{ad}	The first order reaction rate constant that describes absorption in activated carbon particles, s^{-1}.
k_b	Mass transfer coefficient between biofilm and solid, $m \cdot s^{-1}$
k_{max}	Maximum degradation rate, $g \cdot m^{-3} \cdot s^{-1}$
K_s	Half-saturate constant, $g \cdot m^{-3}$
l	Average carbon pellet length, m
L	Filter bed length, m
LDF	Linear driving force
m	Moisture content, $m=(W_1-W_2)/W_1$, %
MATLAB	Matrix Laboratory (Math software developed by Mathworks)
MEK	Methyl ethyl ketone
MIBK	Methyl isobutyl ketone
MLVSS	Mixed-liquor volatile suspended solids

MTBE	Methyl tert-butyl ether
NH_3	Ammonia
N_p	Number of the particles
OTF	odor treatment facility
PCR	Polymerase chain reaction
POTW	Publicly owned treatment works
ppb_v	Parts per billion by volume
ppm_v	Parts per million by volume
psi	Pounds per square inch
Q_g	Gas flow rate, $L \cdot min^{-1}$
Q_l	Liquid flow rate, $ml \cdot min^{-1}$
R	Equivalent radius of carbon pellet, m
r	Radius distance in carbon pellets, m
r_b	Substrate biodegradation rate, $g \cdot m^{-3} \cdot s^{-1}$
r_c	Average carbon pellet radius, m
RE	Removal efficiency
rpm	Revolutions per minute
SAC	Spent activated carbon
SDS	Sodium dodecyl sulfate
SEM	Scanning electron microscopy
S-S	Sulfate sulfur
STW	Sewage treatment works
t	Time, s
TAE	Tris-Acetate-EDTA
TCE	Trichloroethylene
TEA	Triethylamine
TGA	Thermogravimetric analysis
TS	Thiosulfate
T-S	Total sulfur
TSS	Total suspended solids
UPW	Ultra pure water
V	Packing volume, m^3

v	Axial interstitial air velocity, $m \cdot s^{-1}$
VAC	Virgin activated carbon
V_l	Recirculation liquid volume, L
VOCs	Volatile organic compounds
VSCs	Volatile sulfur compounds
W_1	Wet carbon weight, g
W_2	Dry carbon weight, g
W_g	Weight of glass beads, g
WWTP	Wastewater treatment plant
x	Distance in the biofilm, μm
XRF	X-ray
z	Distance of travel in filter, m
ΔW_1	Weight of evaporated water, g

Greek Letters

α	Percentage coverage of the particle by the biofilm
δ	Biofilm thickness, μm
ε	Bed porosity
ρ	Apparent density of activated carbon, $kg \cdot m^{-3}$
ρ_l	Aqueous density, $kg \cdot m^{-3}$
Φ	Thiele modulus

CHAPTER 1
INTRODUCTION

1.1 Background

"Odor" is defined as a sensation resulting from stimulation of the olfactory organs. Emission control of odorous gases is a growing concern in municipal wastewater treatment plants where the odor is primarily caused by hydrogen sulphide (H_2S) and other reduced sulfur compounds (e.g. methyl mercaptan, dimethyl sulfide, and dimethyl disulfide). These compounds have adverse effects on human health and cause corrosion of infrastructure and equipment located at treatment plants.

At present, odorous sewage air is mostly treated by a combination of chemical scrubbers and activated carbon towers. However, chemical scrubbing has been found to be very expensive in terms of the recurrent use of chemicals; also it is dangerous in view of the need to handle vast quantities of chemical solutions. Carbon adsorption systems are also expensive and require either costly regeneration or disposal of spent carbon. In addition, both techniques are producing secondary pollutants, which generally are environmentally unfavorable.

Odor biofiltration is a relatively new and attractive technology. It does not require a large amount of chemical addition or costly adsorbents/absorbents, and the operational cost is also much lower than conventional methods. In addition,

biological digestion of odorous compounds rather than chemical reaction makes biofiltration environmentally friendly. However, there exist inefficiencies pertaining to the media used in biofiltration processes, such as the need for adequate residence time (e.g. a conventional biofilter needs 15~30 s gas retention time when treating H_2S), limited life time, and pore blockage of the media, which at present render the technology economically unattractive.

Activated carbon has generally a high surface area to provide a strong adsorption capacity. Also, its external surface area can be substantially used for bacterial immobilization. The unique properties of activated carbon lead to an idea of developing a new medium to be used in a biosystem that can have capacities of not only biodegradation like a biofilter but also adsorption like activated carbon bed. This kind of combined effect could hopefully contribute to (1) shorten the gas retention time thus reduce the footprint of a conventional biofilter, and (2) prolong the activated carbon service life in odor control.

As a supporting medium for biofilters treating various gas phase contaminants, activated carbon has been used alone or in combination with other materials in a variety of applications over the past decades. However, the application of using activated carbon as in a biofilter to treat odorous compounds has rarely been reported. By developing a new biological activated carbon (BAC) medium with selective strains of bacteria immobilized onto the carbon bed, odorous compounds presented in the influent air streams, are now firstly adsorbed by the activated carbon and then progressively released for microbial degradation. Therefore, the gas retention time required would be much shorter than the conventional biofilters and the BAC bed could be designed as small as a typical activated carbon adsorption tower. As the adsorbed compounds are embedded in the carbon pellet, the bacteria may have a longer

time to degrade the "food" effectively. It is also expected that a well-developed BAC can treat odor more quickly than conventional biofilter with a higher efficiency. In addition, BAC could possibly be generated from spent carbons as the pre-adsorbed odorous compounds now serve as food to the bacteria immobilized on the carbon pellets, and the bacteria are able to condition themselves to degrade the adsorbed odorous compounds in their own time. Overall, the BAC biofiltration medium, if successfully developed, will allow a more efficient and economical means of treating odorous sewage air.

1.2 Objective and Scope

The primary aim of this research was to evaluate the feasibility of using BAC as an enhanced medium for the treatment of H_2S, a representative of predominant odorous compounds in sewage air. For this purpose the following objectives were set for the study:

1) Feasibility of immobilizing bacteria onto carbon pellets.
2) Determination of important characteristics of the BAC.
3) Ability of BAC to perform as a biofilter when treating H_2S.
4) Ability of BAC to perform as a biotrickling filter when treating H_2S.
5) The new understanding on the mechanisms by which BAC removes H_2S.

The scope of work covered in this study includes the following five phases of investigation:

Phase 1: Establishment of characteristics of the selected bacterial culture and the properties of the activated carbon pellets to evaluate the feasibility of immobilizing the bacteria on the carbon medium. This early phase of study is discussed in

Chapters 3 and 4. In this phase, a suitable bacterial mixed culture was acclimated from activated sludge and the optimum environment for their growth was investigated. Carbon pellets obtained from a commercial supplier was studied in detail to ascertain its physical and chemical properties. Analyses involving the use of H_2S breakthrough test, mercury porosimeters, Brunauer-Emmett-Teller (BET), and other laboratory techniques were used to determine the surface characteristics of carbon pellets. For BAC production, three methods were adopted to immobilize bacteria onto carbon surface (the production of BAC): the offline immersed immobilization, the online immobilization in a biofilter and the online immobilization in a biotrickling filter. All of the three methods produced BAC successfully and evidence of this through the use of scanning electron microscopy (SEM) is discussed. This study phase confirmed the feasibility of immobilizing bacteria onto activated carbon pellets and the use of BAC as a medium for treatment of odorous sewage air.

Phase 2: Preliminary assessment of the use of BAC as a biofilter for treatment of gaseous H_2S. In Chapter 5, laboratory-scale columns packed with BAC were set up to determine the operational performance of the BAC as a medium for removal of H_2S. Performance efficiency of the BAC biofilter was studied in detail under a variety of operating conditions. Parameters such as empty bed gas retention time (GRT), H_2S loading rate and treatment efficiency were investigated over a series of experimental runs. Scanning electron microscopy indicated clearly the presence of oxidation products on the carbon surface and confirmed the ability of BAC to degrade H_2S. This study phase provided insights into the development and behavior of the biofilm formed in the carbon bed when the BAC is operating as a biofilter. Nevertheless, some limitations of using the BAC as a biofilter were identified and the next study phase (Phase 3) attempted to overcome these limitations.

Phase 3: The assessment of the use of BAC as a biotrickling filter (BTF) was carried out in Chapter 6. In this phase, a cross-flow horizontal BTF was designed and set up in the laboratory to enable experiments to be conducted to investigate the feasibility of using the BAC in a biotrickling filtration mode. This was to largely overcome some of the limitations identified earlier in Phase 2 when the BAC was used in a biofilter mode. Operating conditions again were varied over a series of experimental runs. The ability of the BAC to remove H_2S under a variety of operating scenarios was studied in detail. This study phase confirmed the feasibility of using the BAC as a medium in a biotrickling filtration mode for the treatment of H_2S.

Phase 4: Study to understand the mechanisms by which H_2S is degraded in a BAC bed. Here in Chapter 7, investigation and analyses were carried out on the horizontal biotrickling filter process and through a series of experimental runs, to provide information that could explain the mechanisms through which BAC degrades H_2S into various products. Furthermore, the combined effect of adsorption and biodegradation of BAC on H_2S removal was investigated in-depth through a series of batch tests which focused on the sulfur balance. A mathematical model was also developed to explain the kinetic behaviour of the BAC during the transformation of H_2S in the biotrickling filter. This study phase provided important new thoughts on how the BAC degrades H_2S thus contributing to a better understanding of the use of this new medium in the treatment of gaseous H_2S.

Finally, an in-depth discussion was carried out through a comparison of the observations from biofilter and biotrickling filter studies, and that of the experimental studies and modeling. An overall conclusion is systematically provided with recommendation for further studies in Chapter 8.

1.3 Dissertation Organization Flow Chart

The organization of this dissertation is illustrated in the following flow chart:

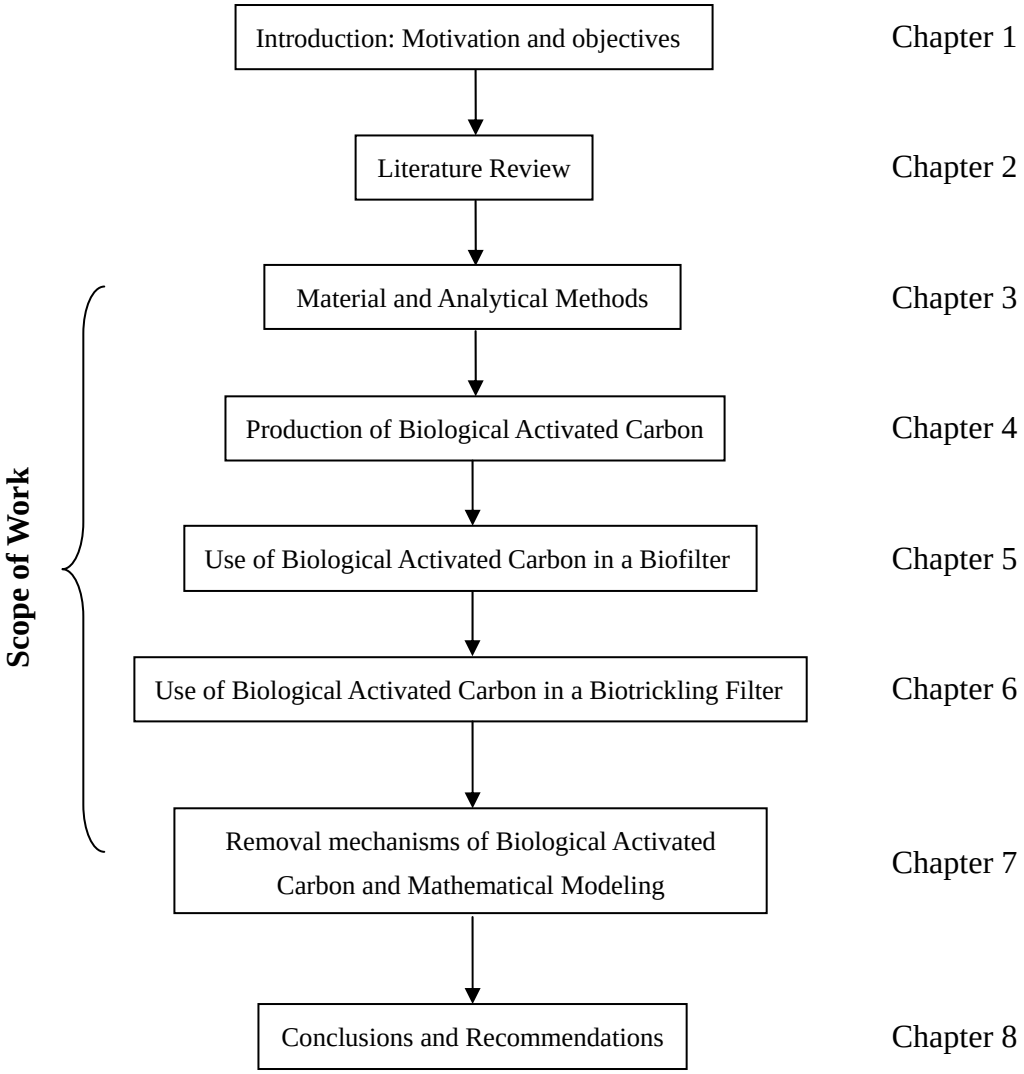

Figure 1.1 Dissertation organization flow chart

CHAPTER 2
LITERATURE REVIEW

In order to obtain a clear understanding of the state-of-the-art of odor biofiltration globally, a literature review is carried out and presented in this chapter, it includes: (1) Odorous air emissions; (2) Odor control technology; (3) Biofiltration on H_2S removal; (4) Biological activated carbon and (5) Mathematical modeling.

2.1 Odorous Air Emissions

Most odorants have the same characteristics that they are all vapor phase contaminants, which are found in off-gases from soil and groundwater remediation operations, from industrial processes and wastewater treatment systems. The odorous smell is principally caused by volatile organic compounds (VOCs) such as, acetaldehyde (CH_3CHO), chlorophenol (ClC_6H_5O); volatile sulfur compounds (VSCs) such as hydrogen sulfide (H_2S), methyl mercaptan (MeSH), dmethyl sulfide (Me_2S), demethyl disulfide (Me_2S_2), carbon disulfide (CS_2); and some inorganic gases such as ammonia (NH_3), chlorine (Cl_2), ozone (O_3). The most important characateristics of these compounds are their low odor thresholds, toxicity to human health, and potential corrosive effects to infrastructure and equipment. Table 2.1 provides the thresholds of odorous compounds indicating their low odor threshold down to ppb_v level. Both natural and anthropogenic sources contribute to the total

emission of odorous compounds. The anthropogenic sources are the main concerns. The anthropogenic sources of odor include anaerobic process, chemical processes, industrial applications, wastewater treatment processes, vehicle combustors, etc.

Table 2.1 Odorous substance (WPCF, 1979)

Compound name	***Formula***	***Molecular weight***	***Recognition Threshold, ppm_v***	***Odor Threshold, ppm_v***	***Characteristic Odor***
Acetaldehyde	CH_3CHO	44.05	0.21	0.004	Pungent, fruity
Allyl mercaptan	CH_2CHCH_2SH	74.15	—	0.00005	Strong garlic,coffee
Ammonia	NH_3	17.03	46.8	0.037	Sharp pungent
Amyl mercaptan	$CH_3(CH_2)_4SH$	104.22	—	0.0003	Unpleasant, putrid
Benzyl mercaptan	$C_6H_5CH_2SH$	124.21	—	0.00019	Unpleasant, strong
n-Butyl amine	$CH_3(CH_2)NH_2$	73.14	0.24	—	Sour, ammonia
Cadaverine	$H_2N(CH_2)_5NH_2$	102.18	—	—	Putrid,decaying flesh
Chlorine	Cl_2	70.91	0.314	0.01	Pungent, suffocating
Dibutylamine	$(C_4H_9)_2NH$	129.25	—	0.016	Fishy
Diisopropyl amine	$(C_3H_7)_2NH$	101.19	0.085	0.0035	Fishy
Dimethyl amine	$(CH_3)_2NH$	45.08	0.047	0.047	Putrid, fishy
Dimethyl sulphide	$(CH_3)_2S$	62.13	0.001	0.001	Decayed vegetable
Diphenyl sulphide	$(C_6H_5)_2S$	186.28	0.0021	0.000048	Unpleasant
Ethylamine	$C_2H_5NH_2$	45.08	0.83	0.83	Ammonia-like
Ethyl mercaptan	C_2H_5SH	62.1	0.001	0.00019	Decayed cabbage
Hydrogen sulphide	H_2S	34.1	0.0047	0.00047	Rotten eggs
Indole	$C_6H_4(CH)_2NH$	117.15	—	—	Faecal, nauseating
Methylamine	CH_3NH_2	31.05	0.021	0.021	Putrid, fishy
Methyl mercaptan	CH_3SH	48.1	0.0021	0.0011	Decayed cabbage
Ozone	O_3	48	—	0.001	Irritating above 2ppm
Propyl mercaptan	C_3H_7SH	76.16	—	0.000075	Unpleasant
Pyridine	C_5H_5N	79.1	—	0.0037	Irritating
Skatole	C_9H_9N	131.2	0.47	0.0012	Faecal, nauseating
Sulphur dioxide	SO_2	64.07	—	0.009	Pungent, irritating
Thiocresol	$CH_3C_6H_4SH$	124.21	—	0.0001	Skunky, rancid
Triethylamine	$(C_2H_5)_3N$	101.19	—	0.08	Ammoniacal, fishy

2.1.1 Anthropogenic Sources

In industrial applications, VSC emissions include their use for the synthesis of amino acid (e.g. methionine), their use as solvent, and some minor applications such as in flotation processes and cosmetics (Verschueren, 1983). CS_2 is widely used to produce rayon, carbon tetrachloride, rubber chemicals and cellulose film, and is a by-product of widely used dithiocarbamate pesticides (Tan et al., 2001). In the manufacturing of viscose rayon, NaOH and CS_2 are added to convert cellulose to sodium-cellulose-xanthogenate (viscose) prior to spinning. During the spinning process, CS_2 and H_2S are released and cause the typical odor in the vicinity of rayon plant (Chin and Davis, 1993). H_2S and SO_2 emissions are associated with chemical processes such as petroleum refining, the treatment of "sour" natural gas (Sublette and Sylvester, 1987), asphalt production (Cook et al., 1999), and electricity generation from coal (Sublette and Sylvester, 1987; Yang and Allen, 1994a).

Under anaerobic conditions, sulfur-reducing bacteria utilize sulfur-bearing compounds contained in wastewater as an electron acceptor and sulfide is the end -product of the reducing action. H_2S is generally considered to be the most important contributor to the sewer odors associated with municipal and industrial wastewater treatment (Schowengerdt et al., 1999). Animal feed operations and composting are known to cause odor problems because of microbial activity under anaerobic conditions. More than 160 compounds which contribute in various degree to the malodor of swine slurry have been detected (O'Neill and Phillips, 1992).

As a result of inefficient combustion of fuel, odors together with air pollutants are released from motor vehicle engines. Vehicle combustors are usually designed to achieve maximum power and performance, rather than minimizing air pollution. Major compounds released from vehicles are water vapor, NO_x, CO, CO_2, SO_x,

some hydrocarbon and lead.

2.1.2 Hydrogen Sulfide

De Zwart and Kuenen (1992) pointed out that the natural emission of sulfur to the atmosphere is mainly in the form of H_2S and Me_2S. In nature, hydrogen sulfide (H_2S) emits from dissimilatory sulfate reduction, heterotrophic organic sulfur compound catabolism, assimilatory sulfur metabolism, and the chemical reduction of seawater sulfate by ferrous ion in the basalts over which the water passes in hydrothermal systems of the submarine oceanic ridges (Kelly and Smith, 1990). Hydrogen sulfide in municipal sewer is the representative odor compound in this study, it is mostly caused by the decomposition of a large amount of organic materials and the biochemical reduction of inorganic sulfur compounds. High concentrations of H_2S may exist in some industrial wastes, mainly due to the bacteriological reduction of sulfate in the absence of oxygen and in the presence of organic matter.

Hydrogen sulfide has dominated the literature in studies on the control of sewer odors associated with municipal and industrial wastewater treatment and has clearly been the focus of past research. This is likely due to three characteristics of H_2S. First, it has an extremely low odor threshold relative to most other odorous compounds, with a reported threshold of only 8 ppb_v (Smet et al., 1998). Second, it is flammable and has a very high and acute toxicity so that it is often present at toxic levels (Table 2.2), e.g. during confined space entry to wastewater collection systems. The maximum permissible 8-hour H_2S concentration is about 20 ppm_v. A 5-minute exposure to 1000 ppm_v concentration in air can be fatal to humans (Patnaik, 1999). Finally, gaseous H_2S is highly soluble (2.80 $g \cdot L^{-1}$ at 30 ^oC to 5.65

$g \cdot L^{-1}$ at 5 ^{o}C). It can easily be absorbed into moisture, with subsequent biological conversion by sulfide oxidizing bacteria to sulfate. Based on above reasons, H_2S is chosen in this study as the target odorous pollutant to remove.

Table 2.2 Effect of H_2S gas on human health (ASCE, 1989)

Concentration (ppm_v)	Effect
<0.00021	Olfactory detection threshold
0.00047	Olfactory recognition threshold
0.5-30	Strong odor
10-50	Headache, nausea and eye, nose irritation
50-100	Eye and respiratory injury
300-500	Life threatening
Above 700	Immediate death

2.2 Odor Control Technology

A number of odor control technologies are available for comparison of their process residuals and by-products, energy costs, and process limitations as provided in Table 2.3. Basically, they could be divided into two types: (1) physico-chemical treatment and (2) biological treatment. Detailed discussion on each of them is presented in the following paragraphs.

Table 2.3 Comparison of odorous pollutant control technologies

Treatment technology	Residuals/ by-products	Cost	Comments
Masking	None	High	•Dangerous for high concentrations
Condensation	Compound not destroyed, however, potential for product recovery	High	•Low range of compounds at high concentrations
Incineration	NO_x, CO, HCl, potentially toxic organic compounds	Moderate to high	•Stable performance with sufficient time, temperature. •H_2S, SO_2, HCl, or particulate matter can destroy catalyst
Adsorption	Spent activated carbon (regenerable systems, usually combined with condensation or incineration)	Moderate	•Limited to low to moderate concentration emissions •High operating cost. •Creates secondary waste stream
Chemical Scrubbing	Chemical concentrated leachate	High	•Ability to handle high loading •Need complex chemical feed systems
Biofiltration	Compost media changed every 2-5 years	Low	•Low to moderate concentration biodegradable emissions • Moisture and pH difficult to control
Biotrickling filter	Synthetic media and further waste stream produced	Low to moderate	• Moderate to high concentration biodegradable emissions • Treats acid-producing contaminants

2.2.1 Physio-chemical Treatment

Numerous processes involving physico-chemical principles have been developed to effectively remove odorous compounds from air, waste gas and liquid including chemical scrubbing, masking, condensation, adsorption, incineration, and so on. The major disadvantage of the above conventional technologies is the high cost associated with the addition of chemicals, frequent medium replacement, or high

energy requirement, as Table 2.3 shows.

Masking: The process of masking involves overpowering the odorous molecules with a stronger and more pleasant molecule. Masking compounds frequently utilize one essential oil, usually vanilla, citrus, pine, or floral to permeate the area with its aroma. However, the application of these fragrant compounds becomes dangerous if they are used to mask odor compounds that have high or toxic pollutant concentrations (Planker, 1998).

Condensation: Waste gas contaminants that are concentrated and have a high boiling point may be partially removed by simultaneous cooling and compression of the gaseous vapors. Condensation is only economical for concentrated vapors where there is some recycle or recovery value. If the waste gas is a mixed pollutant stream, recycling will be virtually impossible. Further treatment of the condensed liquid may be required. Therefore, this technique is often followed by additional removal technologies for compliance with regulatory emission standards (Devinny et al., 1999).

Incineration: Thermal and catalytic incineration are widely used and effective but are expensive treatment processes for waste gases with low contaminant concentrations because large amount of fuel are required. Thermal incineration involves the combustion of pollutants at temperature of 700 to 1400 ^{o}C with gas residence times of 0.5 to 1s (Smet et al., 1998). Catalytic incineration allows process temperatures between 300 and 700 ^{o}C, and some known catalysts are platinum, palladium, and rubidium (Devinny et al., 1999). However, the catalyst can be poisoned by the presence of sulfur compounds such as H_2S and SO_2. Thermal oxidation of reduced sulfur compounds may lead to SO_2 emission, which requires

an additional post-treatment.

Adsorption: Adsorption generally occurs on a fixed or fluidized bed of material with large surface area such as activated carbon or zeolite. Adsorption is only applicable and efficient for treatment of low concentration vapors (Devinny et al., 1999). The effectiveness of a carbon adsorption system for a particular waste stream is a function of the air flow rate, the odorous compounds loading and the humidity of the stream (Bagreev et al., 2001). In addition to physical adsorption, activated carbon provides a catalytic surface for chemical oxidation, reduction, neutralization or catalytic reaction of contaminants after physical adsorption. For example, caustics impregnated (e.g. KOH) activated carbon was preferred to neutralize the absorbed H_2S in order to optimize H_2S abatement (Yan et al., 2004a). Impregnated carbon with noble metals or with transition metal oxides can catalyze the air oxidation of VOCs (Turk et al., 1993; Adib et al., 1999b). However, the use of impregnated agents decreases the surface area and pore volume available for physical adsorption and thus reduces the sorption of odorants.

Chemical scrubbing: Chemical scrubbing aims to transfer the pollutant from the gas to the aqueous phase by contacting the polluted air stream with a water phase in a packed bed. The mass transfer depends on the concentration and air/water partition (Henry) coefficient of the volatiles and the mass transfer resistance of the scrubber system. In a scrubber, the water solubility of the volatiles can be enhanced by making the water alkaline/acidic (for acidic/alkaline pollutants) or by their (catalytic) oxidation/reduction to a more water-soluble compound through certain chemical dosing. For waste gases containing particulates or fat aerosols, a venturi scrubber is normally installed to remove non-gas containments before the chemical scrubber to prevent clogging (Prokop and Bohn, 1985).

2.2.2 Biological Treatment

Within the past two decades, there has been increased interest in biological odor control systems, especially biofiltration technology. Biofiltration offers a relatively new and attractive technology for air pollution control because it doesn't require a large amount of chemical addition (nutrition can be the secondary effluent from a wastewater treatment plant) and can be operated at room temperature. In addition, biological digestion of odorous compounds rather than chemical reaction makes biofiltration environmentally friendly. Also, the operational cost is much lower than conventional methods.

Processes designed for biological treatment of vapor phase contaminants have been almost entirely packed beds. The first packed bed systems were used for control of odors from wastewater treatment plants (Carlson and Leisner, 1966; Pomeroy, 1982). Packing material used in the first systems was soil and volumetric gas fluxes were relatively low. The systems were named *soil filters,* and the term *biofilter* came into use when alternative packings began to be used. Biotechniques for air pollution control include bioscrubbers, biofilters and biotrickling filters. They can be distinguished by whether the liquid phase is stationary or moving and whether the microorganisms are immobilized or dispersed.

A bioscrubber consists of two units: a scrubber and a regeneration basin. In the scrubber the soluble gases and oxygen are continuously absorbed into water. Biological oxidation occurs in the regeneration unit which is typically an activated sludge basin in a wastewater treatment plan.

A biofilter consists of a filter bed, packed with inert, artificial or natural material (e.g. pall rings, compost, etc.) as indicated in Figure 2.1. Microbial communities

grow as biofilm on the packing surface. Biofilm are composed of microbial cells, extracellular polysaccharides, and bound water. A liquid film must exist around the microorganisms because they extract all of their nutrients from liquid phase. Whether a layer of water in addition to that in the biofilm is required to maintain a satisfactory environment is unclear. However, liquid films would be very thin in conventional biofilters operated at 40 to 60% moisture by weight (wet basis) (Van Lith et al., 1997). This technique is very attractive in cleaning complex odorous waste gases. As a drawback, large reactor volumes are required to obtain the high gas residence times that are usually used in the design of the biofilters (Smet et al., 1998).

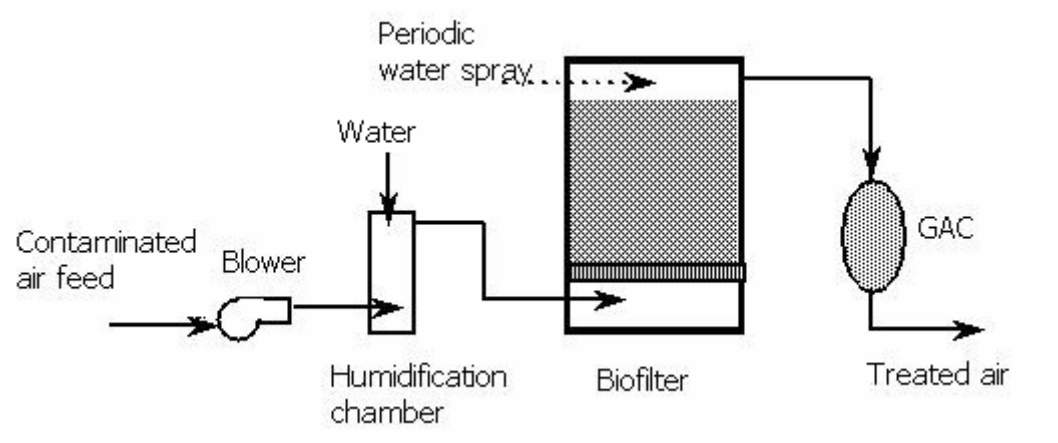

Figure 2.1 Typical biofilter system

Suggestion to treat odorous off-gases containing H_2S emission from sewage treatment plants using biofilters can be found in the literature as early as 1923 (Leson and Winer, 1991). Pomeroy (1982) described the deodorization of odorous waste gases emitted from sewage lines by a soil bed system which was used in Los Angeles, USA in 1957. In his work, he emphasized the microbial degradation of sulfur containing gases in the filter bed. During the 1970's, great improvements in biofiltration technology were made in Europe, where biological treatment was

applied to a wide range of environment problems. In several European countries, biological air treatment is now considered to be the state-of-the-art technology for odor removal at wastewater treatment plants (WWTPs) and chemical process industries (Hattermer-Fery et al., 1990).

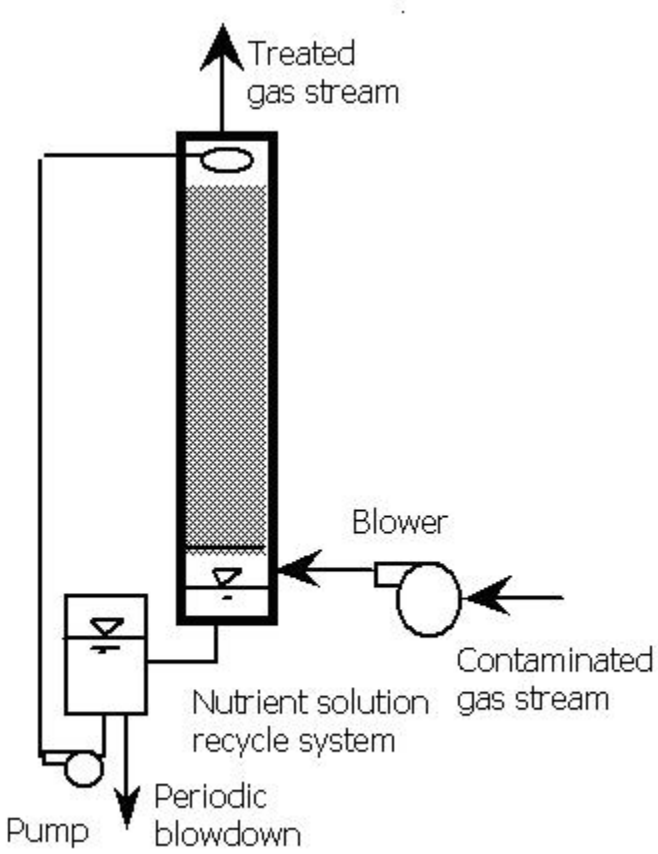

Figure 2.2 Sketch of biotrickling filter system.
(Air flow direction is optional).

Biotrickling filtration (Figure 2.2) is a relatively recent technology where the scrubbing and biological oxidation processes occur simultaneously in one unit as compared to two units in the case of bioscrubbers. Nutrients are supplied by a continuously recycled liquid stream added as a spray at the top of the column to maintain humidity in the media (Diks and Ottengraf, 1991a; Sorial et al., 1995). In a biotrickling filter, the reaction products are washed out of the media and packing

media acidification can be avoided when acidic foul gases such as H_2S are treated. The major drawback of this system is the problem of transferring the odorous pollutants from the gas phase to the liquid/biofilm phase because of the additional aqueous phase formed over the biofilm due to the continuous water trickling. Nevertheless, Kennes and Thalasso (1998) found that biotrickling filters can still be effective in the treatment of gaseous compounds with an air/water partition coefficient of less than 0.1.

Recent applications of biotechnique for H_2S removal are indicated in Table 2.4. As Table 2.4 shows, the elimination capacities of H_2S averaged about 70 $gH_2S \cdot m^{-3} \cdot h^{-1}$ with a reported maximum of 500 $gH_2S \cdot m^{-3} \cdot h^{-1}$. Biotechnological systems based on organic packing bed could achieve high elimination capacities with or without specific bacteria inoculation.

Biofiltration is now used in full-scale applications and is generally considered to be the cheapest odor-abatement method (Leson and Winer, 1991). It was estimated that the operation and maintenance costs of a lava rock biotrickling filter for odor control would be US$120 per million m^3 of air treated, which was only 20% of the cost of a sodium hydroxide chemical scrubber ($600 per million m^3 of air treated) (Morton and Caballero, 1996). In a study where odorous compounds from a combined sewer were treated (Laustsen et al., 1999), biofiltration was found to be more cost-effective compared to carbon adsorption and incineration. The estimated capital costs for a carbon adsorption bed, an incineration system and a biofilter were US$625,000, US$612,000, US$430,000, respectively, and the annual operation and maintenance costs were US$1,950,000, US$380,000 and US$94,000, respectively. The capital costs can be even less when full-scale biofiltration systems are retrofitted from the existing chemical scrubber.

Table 2.4 Removal capacities for H_2S in biotechnological system with/without microbial inoculation

Reactor Type	Inoculation	Removal Capacity ($gH_2S \cdot m^{-3} \cdot h^{-1}$)	Reference
BTF (granular activated carbon)	*Pseudous putida CH11*	6.25	Chung et al., 2005
BTF (plastic pall ring)	*Thiobacillus sp.*	31.25 (EC_{max})	Jin et al., 2005
BF	Granulated sludge	28.3 (EC_{max})	Malhautier et al. 2003
BTF (polyurethane foam)	*Thiobacillus sp.*	95~105 (>95%)	Gabriel and Deshusses, 2003a
BF (peat)	*T. Thioparus (ATCC 23645)*	55 (EC_{max})	Oyarzun et al., 2003
BF (pig mature & saw dust)	No	45 ($EC_{max)}$)	Elias et al. 2002
BTF (Polypropylene pall rings)	*Thiobacillus sp.*	20 (EC_{max})	Cox and Deshusses, 2002
BS (Polypropylene pall rings)	*Thiobacillus sp.*	120 (EC_{max})	Koe and Yang, 2000a
TF (Polypropylene pall rings)	*Thiobacillus sp.*	88.3	Wu, 2000
TF (Plastic fibers)	Activated sludge	63.4 (EC_{max})	Li et al., 1998
BS	Activated sludge	8.3 (100%)	Brandy et al., 1995
TF (act. carbon)	*Thiobacilli sp.*	142.5 (90%)	Guey et al., 1995
BF (peat)	No	10 (99%)	Bonnin et al., 1994a
BF (marl)	*Thiobacilli sp.*	60~70 (99%)	Bonnin et al., 1994a
BF (compost)	No	130 (EC_{max})	Yang and Allen, 1994a
TF (plastic etc.)	No	20.8~270.8 (85~98%)	Lanting and Shah, 1992
BF	Dry activated sludge	8.3~500 (100%)	Kowal et al., 1992
BF (peat)	*Thiobacillus HA43*	50.0 (EC_{max})	Cho et al., 1991

Remark: The performance of the reactors is expressed as the maximum elimination capacity (EC_{max}) and the removal efficiency (%) at the reported loading rate. BF=biofilter; TF=tickling filter; BTF=biotrickling filter; BS=bioscrubber.

2.3 H_2S Removal by Biofiltration

Since H_2S is the major contributor of sewage odor, this study will focus on the application of the biofiltration technology for H_2S removal. The following sections will provide a general view of the usage of the biofiltration technology for H_2S removal including types of bacteria and packing media, configurations of biofiltration, parameters that affect biofiltration operations and degradation mechanisms of H_2S abatement in a biofilter/biotrickling filter.

2.3.1 Microorganisms for H_2S Removal

Contaminant removal in a biofiltration system is a multi-step process involving partitioning to the liquid phase, transport to the bacterial cells in the biofilm, followed by transport across the cell membrane where metabolism occurs. There are many species of bacteria involved in the oxidation of sulfur-bearing substances in nature, including heterotrophic species such as *Xanthomonas, Pseudomons,* and autotrophic species such as *Thiomicrospira, Thiobacillus and Thiosphrera* (www.dsmz.de).

Hydrogen sulfide may be utilized by microorganisms in three different ways: assimilation, mineralization, and sulfur oxidation (Atlas and Bartha, 1981; Grant and Long, 1981). The rates of uptake of H_2S based on the assimilation processes are far too low to achieve reasonably high removal efficiencies from a highly loaded waste gas stream. The most important and efficient way for microorganisms to utilized H_2S is by the oxidation of H_2S to gain energy. The sulfur-oxidizing bacteria, such as *Beggiatoa, Thiothrix,* and *Thiobacillus sp.,* are gram-negative rods or spirals, which sometimes grow in filaments. They obtain energy by oxidizing reduced sulfur compounds (e.g. H_2S, S^o, $S_2O_3^{2-}$). Molecular oxygen serves as a terminal

electron acceptor, generating sulfuric acid. Certain bacteria in anaerobic environments can oxidize element sulfur. Examples of these are *Thioploca sp.* and the well known bacterium *Thiomargarita namibiensis*. They used nitrate as a terminal electron acceptor (Maier et al., 2000). The mechanisms of biological oxidation, with which energy source and terminal electron acceptor are found in two different environments, were shown in Table 2.5.

Table 2.5 Sulfur-oxidizing bacteria (Maier et al., 2000)

Group	***Sulfur conversion***	***Habitat interface***	***Habitat***	***Genera***
Obligate or facultative chemoautotrophs	$H_2S \rightarrow S^0 \rightarrow S_2O_3^{2-}$ $\rightarrow S_4O_6^{2-} \rightarrow S_3O_6^{2-}$ $\rightarrow SO_3^{2-} \rightarrow SO_4^{2-}$	H_2S-O_2 interface	Mud, hot springs, mining surfaces, soil	*Thiobacillus* *Thiomicrospira* *Achromatium* *Beggiatoa* *Thermotrix*
Anaerobic phototrophs	$H_2S \rightarrow S^0 \rightarrow SO_4^{2-}$	Anaerobic, H_2S, light	Shallow water, anaerobic sediments meta or hypolimnion, anaerobic water	*Chlorobium* *Chromatium* *Ectothiorhodospira* *Thiopedia* *Rhodopseudomonas*

Sulfur oxidizing bacteria can oxidize H_2S or elemental sulfur (S^0) for energy, producing sulfuric acid. Acidity of the microbial niche with pH lower than 1 had been produced by these sulfur oxidizing bacteria (Black, 2005). The oxidation of the most reduced sulfur compound, i.e. H_2S, occurs in stages, and the first oxidation step results in the formation of elemental sulfur, S^0. Here H_2S is used as electron donors by the microorganisms. When the supply of H_2S has been depleted, additional energy can be obtained from the oxidation of sulfur to sulfate. The final product of oxidation in most cases is sulfate (SO_4^{2-}). The total number of electrons involved between H_2S (oxidation state, -2) and SO_4^{2-} (oxidation state, +6) is 8. Less

energy is available when the intermediate products are produced like S^0 and thiosulfate ($S_2O_3^{2-}$) because of limited oxygen. Under oxygen limiting conditions, i.e. when oxygen concentration is below 0.1 $mg \cdot L^{-1}$, sulfur is the major end-product of the sulfide oxidation. On the other hand, sulfate is formed under circumstance of sulfide limitation. Some of the microbial sulfide degradation reactions are stated below (Brock and Madigan, 1991):

Aerobic zone

$$H_2S + 2O_2 \rightarrow SO_4^{2-} + H_2O \qquad \textit{Thiobacillus}$$

$$S + 2O_2 \rightarrow SO_4^{2-} \qquad \textit{Thiobacillus}$$

Microaerophilic zone

$$H_2S + 0.5O_2 \rightarrow S + H_2O \qquad \text{Sulfur bacteria}$$

Anaerobic zone

$$H_2S + CO_2 + light \rightarrow S + CH_2O \qquad \text{Anoxygenic prototroph}$$

$$SO_4^{2-} + 4[2H] \rightarrow H_2S + 2H_2O + 2OH^- \qquad \text{Sulfate-reducers}$$

Thiobacillus sp. is the most frequently used bacterial species in H_2S biotreatment (Sublette and Sylvester, 1987; Jensen and Webb, 1995; Hautakangas and Mihelcic, 1999). It is naturally present in the sanitary sewer system and treatment plant, and quickly converts H_2S to sulfate in a low growth, energy intensive manner. *Thiobacillus sp.* uses only carbon dioxide as its major carbon source when biodegrading H_2S, and no typical carbon sources were mentioned to have an inhibiting effect on its growth (Holt and Bergey, 1989). The genus Thiobacillus includes both acidophobic bacteria that prefer a pH near 7 and acidophilic bacteria that grow at low pH values, allowing efficient H_2S oxidation over a wide pH range. There are 18 known species of *Thiobacilli* in the natural environment. Table 2.6 shows the different pH range for them. Among these species, most attention has been paid to *Acidithiobacillus thiooxidans,* which is autotrophic and can oxidize

H_2S for its sole energy source and utilize CO_2 as the carbon source (Lizama and Sankey, 1993; Shinabe et al., 1995). It has the ability to grow and metabolize in highly acidic conditions (e.g. it grows well at pH 2 as shown in Table 2.6). Jaworska and Urbanek (1998) reported that the optimum temperature for *Acidithiobacillus thiooxidans* was 33°C. The shape of *Acidithiobacillus thiooxidans* is short rod, 0.5 by 1~2 μm, occurring singly, in pairs or in short chains. Colonies on thiosulfate agar are minute (<1.0 mm), transparent or whitish or yellow (Bergey and Holt, 1994), and usually appear after 2~3 days since inoculation. Other members of *Thiobacillus* have also been reported to oxidize H_2S, such as *T. thioparus* (Chung et al., 2000), *T. novellas* (Chung et al., 1998), and *T. denitrificans* (Sublette and Sylvester, 1987). A mixture of *Thiobacillus* has been reported to be used in bioreactors removing H_2S (Buisman et al., 1991; Jassen et al., 1995).

Table 2.6 Different pH range of the *Thiobacillus sp.* (www.dsmz.de)

Thiobacillus sp.	*Growth pH range*	*Optimum pH range*
Thiobacillus acidophilus	NA	3.5 - 4.5
Acidithiobacillus albertensis	NA	4.4 - 4.7
Thiobacillus aquaesulis	NA	6.0 - 7.6
Acidithiobacillus caldus	1.0 - 5.0	1.5 - 2.5
Thiobacillus cuprinus	3.0 - 7.0	3.5 - 4.0
Thiobacillus denitrificans	NA	6.8 – 7.0
Acidithiobacillus ferrooxidans	1.4-6.0	2.5 - 5.8
Thiobacillus halophilus	NA	7.3 – 7.5
Thiobacillus hydrothermalis	NA	6.0 – 7.5
Thiobacillus neapolitanus	3.0 - 8.5	6.2 - 7.0
Thiobacillus novellus	5.0 - 9.2	7.8 - 9.0
Thiobacillus plumbophilus	NA	6.0 - 7.0
Thiobacillus prosperus	2.0 - 7.0	2.5 - 3.0
Thiobacillus tepidarius	NA	6.0 – 6.9
Acidithiobacillus thiooxidans	**0.5 - 6.0**	**2.0 - 3.5**
Thiobacillus thioparus	4.5 - 10	6.6 - 7.2
Thiobacillus thyasiris	NA	7.0 – 7.6
Thiobacillus versutus	NA	7.0 - 8.5

The development of specialized consortia in filters inoculated with activated sludge is a long process which can take several months. To shorten the lag phase, pure or mixed cultures can be added (Cho et al., 1991b). These cultures can be obtained from culture collections or can be isolated from laboratory enrichments. However, applying pure culture on a full-scale biofilter is not practical. Acclimating activated sludge using specific "food" (the target pollutants) is recommended, and this has been well applied in the start-up and operation of recent biofilters.

2.3.2 Packing Medium

Selecting a proper biofilter medium is an important step towards the development of a successful biofiltration operation. Packing media not only supply a surface for the biomass to grow, but also play an important role in gas and liquid distribution, as well as in mass transfer. Desirable medium properties include a high specific surface area, structural integrity, high air and water permeability, low bulk density, high porosity, and providing a good source of microbial growth. Media used so far included natural materials such as soil, compost (Yang and Allen, 1994a), peat (Yoon and Park, 2002), wood bark (Smet et al., 1996), wood chips (Sheridan et al. 2002), lava rock (Cho et al., 2000), and synthetic materials such as ceramic saddles (Hirai et al., 2001), polyethylene Pall rings (Koe and Yang, 2000a), synthetic foams (Gabriel and Deshusses, 2003a), activated carbon (Guey et al., 1995), extruded diatomaceous earth pellets (Kinney et al., 1996) and glass beads (Munoz et al., 2006).

Natural organic packing materials have generally an advantage over synthetic media in providing nutrients for microbial growth. However, they have a main drawback

of the bed compaction resulting from the mineralization of the organics. The surface-to-volume ratios of natural materials are also typically low which results in low volumetric reaction rate. Moreover, their properties can be highly variable leading to undesirable problems. It has been found that during a long-term operation of a compost biofilter treating hexane, the nutrient availability may limit biofilter performance (Morgenroth et al., 1996). Nutrient limitation may also occur in biofilters with other natural media for odor removal during long-term operation. On the other hand, use of solely inert synthetic packing media requires proper seeding with nutrient, moisture and organisms. Therefore, a biotrickling filter, which has a continuous moisture and nutrient supply, is usually applied when using inert synthetic packing media. In order to combine the advantages of both natural and synthetic media, it is prevalent to use a mixed packing bed containing the two types of material. For example, Ergas et al. (1995) used a filter media consisting of air-dried compost, perlite, and crushed oyster shell. The compost consisted of 50% digested sewage sludge and 50% forest products. Perlite increased the porosity of the bed and the oyster shell provided calcium carbonate as a pH buffer. Shareefdeen and Baltzis (1993) used peat mixed with polyurethane foam, vermiculite and perlite for biofiltration of methanol vapor because of the large surface area provided for microbial adhesion and minimal pressure drop.

Besides the type of media, specific surface area is another important criterion that should be considered when selecting packing media. Effective specific surface area, which in most cases is approximated by the outer packing surface area per unit volume, is important because nearly all of the surface area of highly porous material such as activated carbon is inaccessible to the microorganisms (Schroeder, 2002). Tang et al. (1996) estimated the surface area of their sieved compost and chaff medium to be 180 $m^2 \cdot m^{-3}$. Peat has high surface area which results in high

adsorptive capacity. A high surface area provides access for biological growth and adsorption which are the two major mechanisms by which depletion of odor from the gas phase may occur. Adsorptive capacity in the organic medium allows the biofilter to withstand fluctuations in loading rates without compromising removal rate. Odorous compounds loadings higher than average can be accommodated on the solid surface. Conversely, microorganisms can gain their carbon and energy through loadings from compounds that are then desorbed from the surface.

2.3.3 Biofiltration System Configurations

There are many available configuration for biofiltration design and these vary in accordance to the site conditions where the proposed biofilter/biotrickling filter is to be located. Biofilters can either be open to the atmosphere or enclosed, while most biotrickling filters are enclosed. **Open-bed systems** are ideal for applications where space is not a constraint and are often used as low cost/performance biofilters. They are easily affected by weather conditions. Heavy rains can saturate the packing medium causing air flow problems; low temperature may slow down the microbial activities causing low removal efficiency. The advantages of an **enclosed system** include better control of the operational parameters for optimal performance of the biofiltration.

Whilst there are a few open-bed biofiltration systems, most that are reported in the literature and used frequently for industrial applications, are of the enclosed type. Within the enclosed systems, biofilters can be designed in many shapes (e.g. cylindrical, rectangular), and the foul gas is either blown through or draw in, as indicated in Figure 2.3. Water or nutrient solution may be applied periodically from the top of biofilters to supply necessary moisture and mineral nutrients maintaining

high activities of microorganisms immobilized on the packing surface. Biofilters can be operated in two or more individual beds, in parallel, or in series. Biofilters operated in parallel offer the flexibility to isolate individual beds for maintenance without completely shutting the total system down. Beds in series allow for the treatment of individual contaminants through different beds. For instance, the use of two-stage biofilters to treat waste air stream containing H_2S and VOCs (e.g. toluene, NH_3, MeSH, Me_2S, etc.) had been reported (Chung et al., 2001; Ruokojarki et al., 2001; Kim et al., 2002; Cox and Deshusses, 2002a).

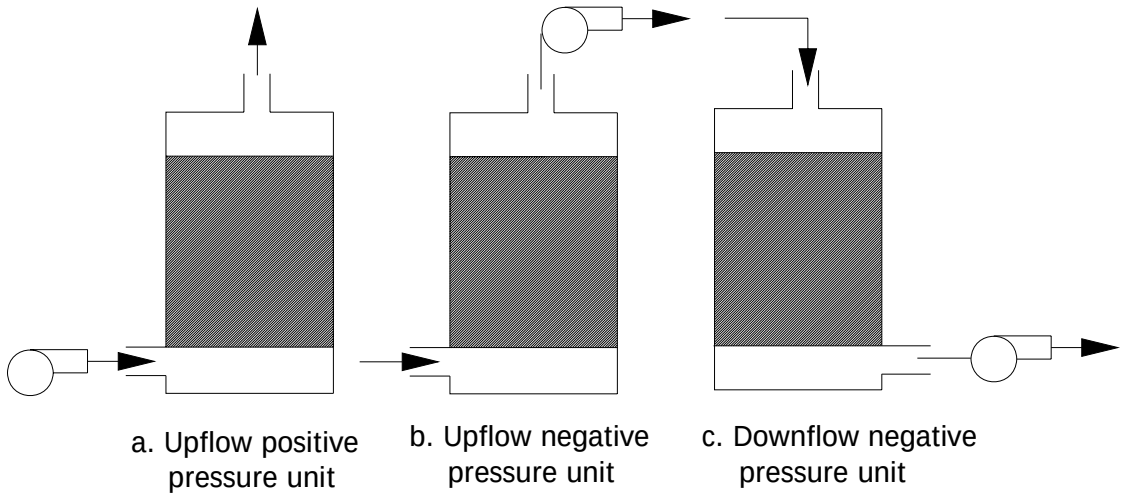

Figure 2.3 Typical configurations of biofilter

A biotrickling filter system looks almost like an enclosed bed biofilter with a liquid flow introduced into the bed together with the gas flow. Usually, a biofiltrickling filter stands vertically with counter-current (Figure 2.4a) or co-current (Figure 2.4b) gas-liquid flow direction. There are rare reports of applications on the use of cross-flow horizontal biotrickling filter (Zhou, 2000) as shown in Figure 2.4c. Also, a biotrickling filter can be designed as separate beds just like biofilters and placed in parallel, to offer the flexibility for industrial maintenance, or in series, to treat multi-pollutants.

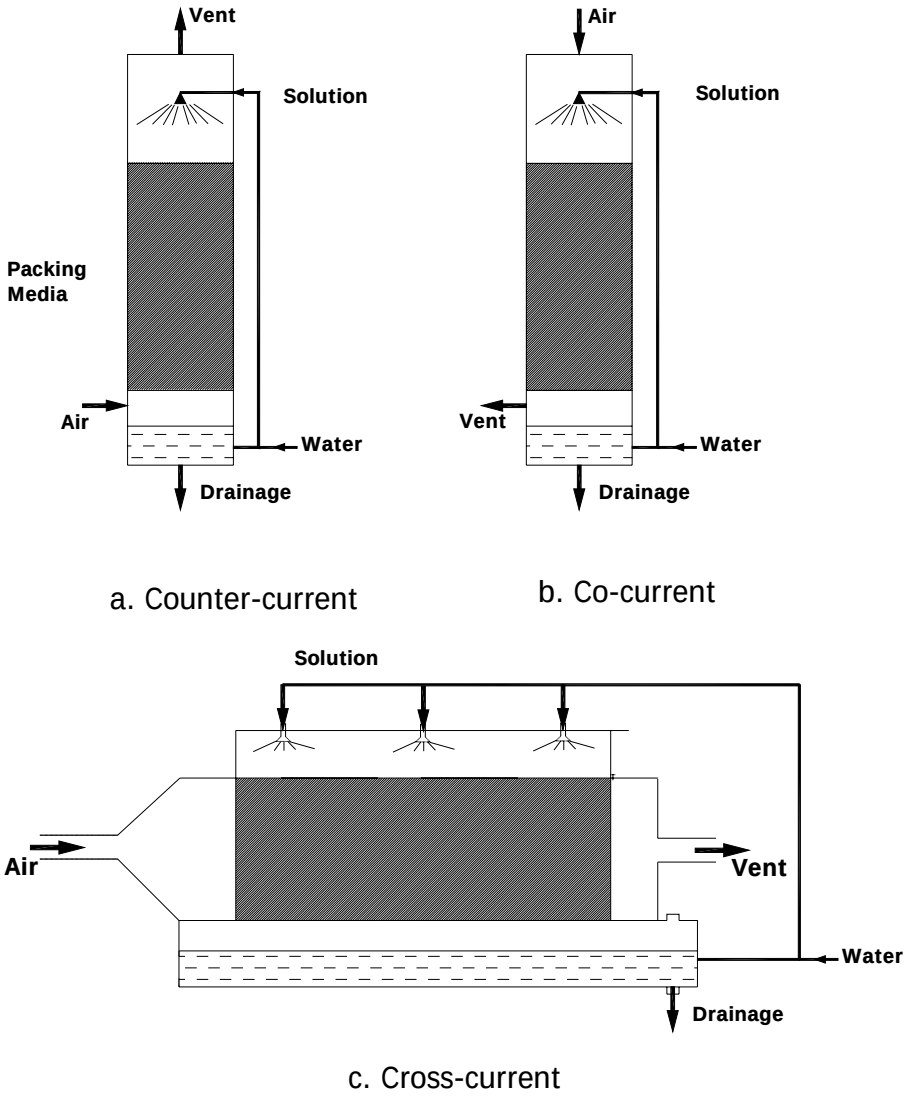

Figure 2.4 Existing configurations of biotrickling filter

2.3.4 Key Parameters Affecting Biofiltration Operations

There are numerous factors that may affect biofiltration operations including system pH, moisture content, nutrient supply, pressure drop, etc. To ensure stable performance over long periods of operation, some key operating parameters need to be carefully controlled. Typical operating conditions of biofiltration for waste air treatment are shown in Table 2.7. More detail descriptions of some key parameters will be given in the following sections.

Table 2.7 Typical operating conditions of biofiltration for waste air treatment

Parameter	Typical Value	
	Biofilter (Devinny et al., 1999)	**Biotrickling filter** (Cox and Deshusses, 2002b)
Bed height	1~1.5m (Single layer)	1~5 m
Cross section area	1~3000 m^2	1~3000 m^2
Waste air flow	50~3×10^5 $m^3 \cdot h^{-1}$	102~106 $m^3 \cdot h^{-1}$
Surface loading	5~500 $m^3 \cdot m^{-2} \cdot h^{-1}$	—
Bed void volume[a]	50%	• 90~95% (plastic rings, foam, random or structured packing); • ~50% (lava rock)
Empty bed gas retention time[b]	15~60s	2~60s
Pressure drop per m bed depth	0.2~1.0 cm water gauge (max. 10 cm)	<1 cm water gauge
Operating temperature	15~30°C	15~50°C
Inlet pollutant and/or odor conc	• 0.01~5 g·m-^{3} • 500~50,000 OU·m^{-3}	• 0.01~10 g·m^{-3} • 500~50,000 OU·m^{-3}
Inlet air relative humidity	>98%	—
Water content of the support material	60% by mass	—
pH	pH 6~8 (support material)	• ~7 (pH of recycle liquid remove VOCs that difficult to degrade) • 1~2 (pH of recycle liquid remove H_2S
Typical removal efficiencies	60~100%	60~100%
Trickling rate[c]	—	0.01~10 $m \cdot h^{-1}$
Liquid dilution rate[d]	—	0.1~2 day^{-1}

a. Value at startup; overtime, biomass growth will decrease bed porosity, typically by 10~30%.

b. The empty bed gas retention time is defined as the bed volume/air flow

c. Trickling flow rate/ bed cross section area.

d. Liquid feed rate/recycle liquid volume

2.3.4.1 pH

Each species of microorganisms is most active over a certain range of pH and will be inhibited or killed if conditions deviate from this optimal range. Most biological growths occur near a neutral pH and a wide deviation from it will impair the efficiency of the biofilter. A notable exception is the sulfur oxidizing bacteria which thrive at low pH though its growth will be inhibited when system pH is lower than a certain threshold. In a biofilter treating sulfur containing gases, sulfate and hydrogen ion will be produced and thus change the system pH during long term operation. Under some conditions, backwashing or adding buffering materials may have to be considered to control the pH of the packing media. For instance, crushed oyster shells were used extensively as a source of alkalinity for buffering and as a carbon source for the autotrophic bacteria responsible for nitrification and sulfide oxidation (Ergas et al., 1995; Kapahi and Gross, 1995). Maërl, a mineral support of marine origin containing 82% of calcium carbonate, was found by Bonnin et al. (1994b) to increase H_2S removal in biofilters at sewage treatment plants from 10 $g \cdot m^{-3} \cdot h^{-1}$ (peat without Maërl) to 50 $g \cdot m^{-3} \cdot h^{-1}$.

Yang and Allen (1994a) reported that the H_2S removal efficiency was highly dependent on pH below 3.2 but was almost independent of pH at higher values in a compost biofilter, and the maximum H_2S removal efficiency occurred at a compost pH value of 3.2. They suggested that the dominant active species present were acidophiles, which preferred an optimum pH near 3. Shinabe et al. (1995) indicated that the maximum specific H_2S removal rate was measured at pH 2.5 in a closed stirred tank reactor, and high specific H_2S removal rates were measured even at pH 1.0. Gabriel and Deshusses (2003a) revealed that the make-up water flow in their system was enough to maintain system pH between 1.5 and 2.2 so that no specific pH control was necessary. From these studies, it is difficult to determine an optimal

pH range for H_2S degradation, because most of the sulfur oxidizing bacteria are acidophilic and can tolerate low pH.

2.3.4.2 Moisture Content

Water is an important issue for microbial activity. Biological activity ceases if the moisture content of an organic material is too low. Control of moisture is not an issue in biotrickling filters, whereas it is important for biofilters. In practice, construction of biofilters without a means of adding water is unwise. Williams and Miller (1992) identified bed moisture content as the single most important parameter for biofilter viability. Optimal moisture contents varied from 20 to 60 wt.% in their review of operational biofilters. Heat generated by biological activity in a biofilter may increase the temperature of the bed medium above that of the inlet gas. Even if the gas enters the biofilter saturated with water, it will become unsaturated as its temperature rises after contact with the bed medium. Drying of the bed medium will occur. In addition, cracks, which may lead to bed channeling, can be formed in a dry bed, thus limiting the filter performance. Hence it is important to supply 100% humid air to a biofilter and/or irrigate the bed periodically to compensate for moisture loss so as to maintain the viability of the organic bed. Conversely, too much moisture leads to a slow mass transfer of odorous compounds into the biofilm, and anaerobic zones, where oxygen required for biooxidation is depleted, are formed within the bed. For this reason, the capacity of soil beds to remove odor drops significantly when they become too wet. Excessive moisture will also result in increased pressure drop through the packed bed.

Yang and Allen (1994a) found in their study of bench scale biofilter packed with compost that a moisture content of above 30 wt.% did not have much effect on H_2S

removal capacity. Below 30 wt.% of moisture, however, the removal efficiency decreased proportionately. The composts were able to recover from being dry to regain their former H_2S eliminating capacity in 1~3 days' time. And in their case, 40~60 wt.% water content resulted in the best biofilter performance. Pinnette et al. (1994) reported a loss of biological degradation of odorous compounds from sludge composting facilities when moisture content dropped below approximately 40 wt.%. The biofilter recovered its previous performance within 3 months after irrigation of the filter bed. Ottengraf and Van Den Oever (1983) kept moisture content in their VOC-eliminating biofilter at 50~70 wt.% for optimal biofilter operation. Removal of aromatic VOC and H_2S in the odor-removing biofilter of Ergas et al. (1995) increased dramatically and almost immediately when moisture content was increased from below 50 to 55 wt.%.

Peat and compost have good water holding capacities. Microbial activity in peat falls off if water content drops below 70 wt.% and rises when the water content goes above 85 wt.%. If moisture content goes below 30 wt.%, biological activity may ceases (Valentin, 1986). Soil is much less permeable than compost due to its smaller pore sizes. It is hydrophilic (dry compost is hydrophobic) and is thus difficult to rewet after drying out due to its highly porous structure (McNevin and Barford, 2000).

2.3.4.3 Nutrient Supply

Microorganisms growing in a vapor-phase bioreactor require nutrients such as nitrogen (N), phosphorus (P), potassium (K), sulfur (S), calcium (Ca), magnesium (Mg), sodium (Na), and iron (Fe), as well as an abundant carbon supply to form new cell material. In a biotrickling filter, nutrients are usually supplied with the

trickling recirculation liquid. In a biofilter, nutrients can be supplied with the humidification system or the packing can be periodically soaked in a nutrient solution. Kinney et al. (1996) developed an aerosol moisture delivery system for a laboratory biofilter system in which the packing was composed of diatomaceous earth pellets (Celite™ R-65). The aerosol particles were created from a nutrient solution using a nebulizer, resulting in a very small excess water stream, low head losses and stable performance in the treatment of toluene and methylene chloride.

Organic packing media in a biofilter such as compost have enough mineral nutrients and do not need extra nutrient supply. However, the rate of media degradation can be too slow to support effective biodegradation of target air pollutants (Gribbins and Loehr, 1998). Also, they may be depleted of nutrients during long term operation. Nutrient limitation has been reported in a compost packed biofilter treating hexane during a three month operation (Morgenroth et al., 1996). Inorganic and synthetic media, such as lava rock, plastic rings, or ceramic carriers don't have an appropriate supply of nutrients, if this type of media is used, additional nutrients must be added to the biofiltration bed. Usually N, P and K are added in the form of commercial fertilizer (Devinny et al., 1999) or secondary effluent from WWTPs (Wu et al., 2001; Martin et al., 2002). The nutrient issue in general is important for VOC control. For H_2S control, nutrient is less critical as H_2S degraders require little nutrients. Hence in many biofilters that are designed for H_2S control, secondary effluent can be used.

2.3.4.4 Pressure Drop

Gas phase pressure drop through a biofilter bed increases with increasing gas flow rate and diminishing particle size. Yang and Allen (1994a) reported increase in pressure drop of 0~35 $kPa \cdot m^{-1}$ which are reasonably linear with increasing gas

velocity (0~0.3 $m \cdot s^{-1}$) over a range of bed medium particle sizes (1~12 mm). Ergas et al. (1995) report pressure drops of 0.1~0.6 $kPa \cdot m^{-1}$ at corresponding superficial air velocities of 0.005~0.03 $m \cdot s^{-1}$ through the compost biofilter. These pressure drops were achieved by addition of 50% (by volume) perlite into the filter media. Pressure drop in biotrickling filter typically ranges from less than 0.098 $kPa \cdot m^{-1}$ at start-up to values over 1.47 $kPa \cdot m^{-1}$. Over time, the pressure drop increases as fine particles and microbial cells fill up the pores. Pressure drop should not be too high in order that energy costs can be kept low during the running of a biofilter. Schroeder (2002) reported that the packing medium should be replaced when pressure drop exceeds 1.47 $kPa \cdot m^{-1}$. Pressure drop appears to increase exponentially with decreasing particle size, especially with particles less than 1 mm (Brennan et al., 1996). Over watering and compaction of the filter bed over extended periods of usage will also give rise to prohibitive pressure drops (Pinnette et al., 1994).

Williams and Miller (1992) noted the unpredictability of pressure drop across differing bed media and recommend pilot testing of individual media. High pressure drop may cause excess energy cost of the biofilter as odorous air must be supplied at a greater pressure to achieve the same flow rate. The methods that alleviate pressure drop includes increasing packing particle size, decreasing bed porosity, or reconfiguring the biofiltration system (e.g. convert gas-liquid flow directions from counter-current to co-current or cross-current, divide bed height into several individual biofiltration systems in series). The abnormal low pressure drop in some long term operated biofiltration systems may indicate air flow distribution problems such as channeling. Monitoring of the pressure drop across the bed periodically is important for detection of cracks in the media and to prevent resultant short-circuiting of the bed by the air stream.

2.3.4.5 Porosity

Porosity is the percentage of the total volume of the packing bed that consists of pore space. Porosity and bulk density are important primarily for the effect they have on the gas phase pressure drop across the bed and the contact surface area where the foul gas contact with the biofilm on the packing medium. Too low porosity may cause extremely high pressure drop in the packed bed, and too high porosity will lead to low removal efficiency of the pollutants treated.

Appropriate porosity is diverse from different configurations of the biofiltration systems and different characterization of packing media used, considering both pressure drop related to energy costs and enough contact surface area related to necessary removal efficiency. Thus, from some researchers' experience, porosities for organic media range from 40 to 50% for soils and 50–80% for compost (Bohn, 1992); peat has typically 90% porosity with one-fifth of the pores being less than 30 μm in diameter (Valentin, 1986). It is often necessary to determine an optimal porosity of a specific proposed biofiltration system using a pilot scale system before full-scale application.

2.3.5 Mechanism of H_2S Oxidation

Many studies have investigated the mechanism of hydrogen sulfide oxidation by oxygen over different adsorbents and at different temperatures (Steijns et al., 1976; Ghosh and Tollefson, 1986; Mikhalovsky and Zaitsev, 1997; Yan et al., 2002). In general, H_2S can be oxidized to form sulfur and water. Steijns et al. (1976) indicated that elemental sulfur (one of H_2S intermediate oxidation products) could

be further oxidized to SO_2 at temperatures above 200 ^oC. This process involves a reaction on the surface layer between the chemisorbed oxygen and the dissociatively adsorbed hydrogen sulfide. Katoh et al. (1995) studied the oxidation mechanism of a mixture of H_2S, methanethiol and dimethylsulfide gases when they adsorbed on wet activated carbon fiber (ACF). They found that H_2S was oxidized to form elemental sulfur in micropores, and then the element sulfur reacted with H_2S to form polysulfide (H_2S_x). Moreover, the polysulfide and oxygen can produce a polysulfide radical on the surface of the ACF and react with H_2S to form polysulfide and SO_2. Mikhalovsky and Zaitsev (1997) used the x-ray photoelectron spectroscopy (XPS) to analyze the H_2S adsorption on activated carbon in an inert atmosphere which resulted in the formation of surface oxygen-containing complexes and elemental sulfur. Furthermore, the surface functional groups contributed significantly to the formation of SO_2 in H_2S oxidation. Bandosz and her co-workers (Bandosz, 1999; Bagreev and Bandosz, 2001; Bagreev et al., 2001a; Bandosz, 2002) investigated the effect of surface chemistry and pH on the H_2S adsorption on virgin and spent activated carbon, pointing out that the rate-limiting step is the reaction of the adsorbed hydrogen sulfide ion with oxygen.

Regarding the mechanisms of H_2S biological oxidation, H_2S can support the growth of a group of chemoautotrophic bacteria under aerobic conditions and a group of photoautrophic bacteria under strictly anaerobic conditions (See previous Table 2.6). Different conditions will result in different degradation mechanisms and bio-oxidation products, and this had been discussed in Section 2.3.1.

2.4 Biological Activated Carbon

Activated carbon has been most extensively used in adsorption towers for odor control well before the widespread use of the biofiltration technology. Biological systems that employ BAC has been used for the treatment of organic pollutants in water, wastewater (Voice et al., 1992; Scholz and Martin, 1997; Zhao et al., 1999; Mason et al., 2000; Xie and Zhou, 2002; Zhou and Xie, 2002), or air (Lee and Shoda, 1989; Liu and Barkley, 1994; Weber and Hartmans, 1995; Webster et al., 1996; Abumaizar et al., 1998; Aizpuru et al., 2003) and have been known to exhibit superior performance. The major function of activated carbon is to support the microorganisms and to act as a buffer for fluctuating loadings. Abumaizar et al. (1998) mixed 2 wt.% and 7.5 wt.% of activated carbon in compost filter media to remove BETX, and the biofilters packed with these mixed media achieved significantly higher performance and more stable operation than those biofilters that contained only compost. Weber and Hartmans (1995) found that the buffer capacity of the activated carbon depended on the desired concentration range of the inlet toluene vapor and on the time available for desorption. Fluctuations of inlet toluene concentration between 0 and 1000 $mg \cdot m^{-3}$ resulted in significant concentrations of toluene leaving the biofilter. However, when a selected type of activated carbon is used, these fluctuations could be decreased to about 300 $mg \cdot m^{-3}$, a level which subsequently can be completely degraded in a biofilter.

However, the application of BAC as packing media for bacteria immobilization, particularly in biological deodorization processes have rarely been investigated (Lee and Shoda, 1989; Medina et al., 1995; Webster et al, 1996). BAC should provide a more efficient odor treatment system compared to other conventional media, but supporting data for this assumption is not available yet. Compared to conventional biological systems, the enhanced biofilter performance achieved through the use of

BAC may be manifest in the terms of higher removal efficiency, shorter acclimation periods, and lower pollutant concentration in the effluent during step increases in influent pollutant concentration (Voice et al., 1992). Simultaneous bioregeneration of the carbon is an additional economic advantage to these systems, and this bioregeneration effect of activated carbon will be validated in this proposed study.

Although the micropores in activated carbon that contribute to adsorption are smaller than microbial cells so that they are inaccessible to the microorganisms, a biofilm containing bacteria can however form in the macropores on the external surface layer, and their "exoenzymes" can go into the micropores to degrade target component (Scholz and Martin, 1997). It is well known that the process of adsorption is faster than biodegradation. When a system encounter high pollutant loadings which the biofilm cannot digest timely, the contaminant molecules can pass through the macropores and the interstices of the biofilm into the much smaller micropores and activated sites on the carbon surface where it is adsorbed. And, when the system is subjected to relative low loadings, the absorbed molecules can desorb slowly for the bacteria to digest. Besides, activated carbon has excellent structural properties with uniform particle size and good resistance to crushing. It also has substantial water-holding capacities and provides good surface for microbial attachment (Devinny et al., 1999). BAC alone should provide a more efficient media, but adequate supporting data for this hypothesis does not exist. In this dissertation, the possibility of developing a compact system based on BAC alone will be comprehensively studied. The combined effects of the adsorption ability of activated carbon and the biodegradation ability of the biosystem shall be investigated thoroughly.

2.5 Mathematical Modeling

Efforts on biofilter modeling started in the early 1980s and was based on earlier work on submerged biofilm models (Devinny et al., 1999). The objectives were to organize experimental data and to understand simple relationships between pollutant removal and parameters such as media surface area, biological activity, biofilm thickness, etc. In addition, the interest exists in biofilter modeling for design and optimization purpose. It is able to predict the biofilter performance and finally optimize the biofiltration process under given conditions.

The early biofilter models assumed simple steady-state operation, basic mass balance principles, simple reaction kinetics, and a plug flow air stream (Ottengraf and Van Den Oever, 1983). Recently, with rapid increase in computer technology, more complex and accurate models have been developed. However, Ottengraf model (1983) is still the basis for future biofilter modeling and is the most commonly referenced (Devinny et al., 1999). The existing biofiltration models differ mainly in the following aspects: (1) phases considered in the model and details of inter-phase transport; (2) biofilm configuration, fully covered or partially covered; (3) biological reaction kinetics; (4) Adsorption on supporting surface if applicable; (5) diffusion in biofilm and/or packing surface; (6) capability of dynamic simulation. The contaminants must be transferred to the liquid/biofilm phase to be available for microbial metabolism. Thus vapor phase biological treatment involves three steps; gas-liquid transfer, liquid phase transport to the microorganisms, and microbial transformation of the contaminants. Two general process configurations exist, suspended growth/diffused aeration and packed beds. Suspended growth applications have been almost entirely associated with using contaminated air for aeration of activated sludge processes. Some of the earlier modeling works are summarized in Table 2.8.

Although many investigators have built mathematical models on biofilter and biotrickling filter in their efforts to understand and improve reactor performance (Table 2.8), the general applicability of biofilter models for design is still questionable. The values of model parameters remain uncertain, and some complex equations are difficult to solve. Design is still based on laboratory-scale test, derivation from published literature, or some field demonstration.

Table 2.8 Summary of existing biofiltration models

Model	Phases	Biofilm Configuration	Adsorption applicability on support	Biokinetics	Dynamic	Application
Hodge and Devinny, 1995	II phases: gas and solid/water	Not applicable	No	First-order	Yes	Ethanol
Deshusses et al., 1995a	III phases: gas, biofilm and sorption volume (water)	Uniform biofilm thickness and biomass density	No	Michaelis-Menten	Yes	MEK[a] & MIBK[b]
Tang et al., 1996	II phases: gas and biofilm	Uniform biofilm thickness and biomass density	No	Monod	No	TEA[c]
Abumaizar et al., 1997	III phases: gas, biofilm and carbon surface	Uniform biofilm thickness and biomass density but partially covered packing particles	Yes	Monod	Steady state	BTEX[d]
Alonso et al., 1998	III phases: gas, liquid and biofilm	The biofilm thickness varies with time, uniform biomass density	No	Monod	Quasi steady state	Toluene
McNevin et al., 1999	II phases: liquid and biofilm	The biofilm thickness is not applicable, the biomass density is a function of time and axial position	No	Monod	Yes	H_2S
Amanullah et al., 2000	III phases: gas, biofilm and solid support	Uniform biofilm thickness and biomass density	Yes	Michaelis-Menten	Yes	MEK
Li et al., 2002a	III phases: gas, liquid and biofilm	Uniform biofilm thickness, active biomass conc. as a function of time and position (both axial and radial)	No	Monod	Yes	H_2S
Den and Pirbazari, 2002	III phases: gas, biofilm/liquid and adsorbent	Uniform biofilm thickness and biomass density	Yes	Monod	Yes	TCE[e]
Kim and Deshusses, 2003	III phases: gas, liquid and biofilm (wetted and non-wetted)	Uniform biofilm thickness, biofilm is not fully wetted by liquid	No	Michaelis-Menten	Yes	H_2S
Spigno et al., 2004	II phases: gas and biofilm	Uniform biofilm thickness and biomass density	No	Monod	Yes	Phenol

a. Methyl ethyl ketone; b. Methyl isobutyl ketone; c. Triethylamine; d. Benzene, toluene, ethylbenzene, o-xylene; e. Trichloroethylene

CHAPTER 3
MATERIAL & ANALYTICAL METHODS

The material used (e.g. bacteria and carbon) and general analytical methods involved in this study are summarized and discussed in this chapter. Further information about laboratory experimental setup and system operation are addressed in Chapters 4, 5, 6, and 7.

3.1 Sulfide Degradation Bacteria

3.1.1 Culture Medium

In this study, Thiosulfate (TS) medium was used to acclimate the activated sludge to obtain the bacteria species to be immobilized onto the activated carbon pellets. The composition of the TS medium is shown in Table 3.1.

The preparation of the liquid medium proceeded as follows: 1) Stock KH_2PO_4-K_2HPO_4 solution was prepared in 10 multiples (30 $g \cdot L^{-1}$ each); 2) Solutions of NH_4Cl, $MgCl_2$, and trace elements mixture was prepared by using NaOH to adjust pH to 6.8±0.2 and 4.5±0.2 for different species of bacteria; 3) The above two solutions were autoclaved for 20 min at 15 psi and 121 ^oC, and were mixed together after cooling down; 4) Sodium thiosulfate solution of 4 multiples (40 $g \cdot L^{-1}$) and Cycloheximide solution of 40 multiples (2 $g \cdot L^{-1}$) were filtered into

the mixed liquor through a sterile filter (pore size = 0.22 μm) in a laminar flow chamber.

Table 3.1 Medium for the enriched culture

Medium for enriched culture		**Stored trace element solution**	
Chemical	Amount, /L	Chemical	Amount, /L
NH_4Cl	1.2 g	Na_2-EDTA	25 g
KH_2PO_4	3 g	$FeCl_2{\cdot}4H_2O$	3.58 g
K_2HPO_4	3 g	$CuCl_2{\cdot}2H_2O$	0.137 g
$MgCl_2{\cdot}6H_2O$	0.46 g	$ZnSO_4{\cdot}7H_2O$	11 g
Trace element	10 mL	$MnCl_2{\cdot}4H_2O$	2.5 g
Cycloheximide (Anti fungus)	50 mg	$CoCl_2{\cdot}7H_2O$	0.59 g
$Na_2S_2O_3{\cdot}5H_2O$	10 g	$(NH_4)_6Mo_7O_{24}{\cdot}4H_2O$	0.5 g
Agar (For plate culture)	15 g	$CaCl_2{\cdot}2H_2O$	10 g

Remark: the pH of medium was adjusted to 6.8±0.2 or 4.5±0.2 prior to autoclaving.

For the preparation of the solid medium, 10 g of Bacto^{TM} agar was added into the liquid medium before autoclaving. The autoclaved agar mineral medium was then cooled in a water bath at 60 ^{o}C prior to adding filtered sodium thiosulfate and Cycloheximide solution. The constant temperature of 60 ^{o}C will prevent the instability of $Na_2S_2O_3$ at high temperature and the solidification of agar at low temperature. The mouth of the bottle was flamed before and after adding filtered solution and the cap was flamed before covering the bottle. The warm gel liquid medium was poured into Petri dishes to make the agar plate, and left for solidification in a laminar flow chamber. Once cooled and solidified, the agar plates were stored in the refrigerator at 4 ˚C.

3.1.2 Activated Sludge Acclimation

From the engineering point of view, use of pure culture may pose some problems such as the difficulty to maintain the purity of the culture, and the initial pure

culture could be contaminated by other microbes. It is also difficult to determine how competent this pure culture is in an actual environment, it may die out when the environment changes. On the other hand, because of the lack of symbiotic function, the sulfide degradation efficiency of a pure culture may not be as high as that of mixed culture, in which a community of microbes can function together. Therefore, a mixed culture was preferred in this proposed study.

Sulfide oxidizing bacteria resources were obtained from a return activated sludge stream at the secondary sedimentation tank in a local wastewater treatment plant (Ulu Pandan WWTP). The fresh activated sludge was acclimated using liquid TS medium for a quick system set up. The acclimation of activated sludge proceeded as follows: One volume of activated sludge was added into 9 volume of liquid TS medium, and the mixed liquor was shaken on an autoshaker for 4 days, the initial mixed microbial liquor was designated as Generation One (G1), after that, 1/10 of the above mixed liquor was transferred into another 9 volume of fresh liquid TS medium, shaken for another 4 days and designated as G2, and so on. After three transfers (about 12 days), the bacteria seeds were ready for immobilization onto the activated carbon.

3.1.3 Growth Curve of the Mixed Culture

The pH, thiosulfate and sulfate concentration of the mixed culture, G2, were monitored while culturing in order to understand the fundamental microbial activity of sulfide degradation bacteria such as the growth curve. Iodometric method (refer to Section 3.3.2) was used to obtain the TS concentration, and the Flow Injection Analyzer with Ion Chromatograph (FIA/IC, Lachat, QuickChem 8000) was used to determine the sulfate concentration of G2. Figure 3.1 gives the time-variable of the media contents when acclimating with activated sludge, and

indirectly provides information on the lifetime curves of the mixed culture (G2).

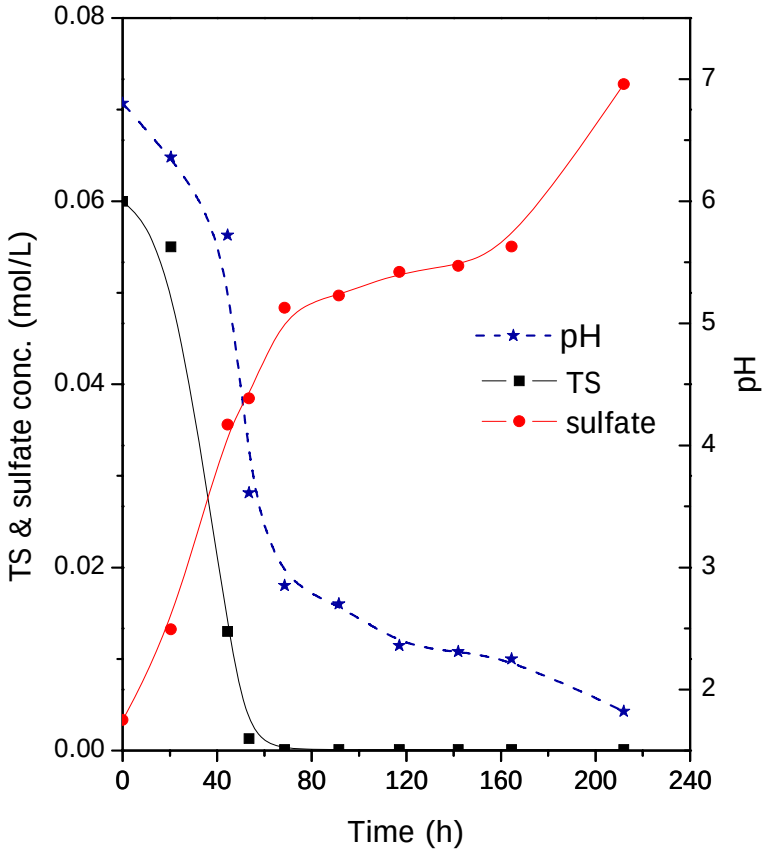

Figure 3.1 Time-variable of media contents of generation 2 of mixed culture

It can be seen from Figure 3.1 that the pH and TS concentration decrease in tandem. There is a sharp drop of TS as well as pH from the 20th hour to 50th hour, accompanied by the increase of sulfate concentration of the medium at the same time. After 60 hours' acclimation, the TS concentration decreased from 0.06 mol·L^{-1} to nearly zero, but sulfate concentration increased slowly with a stationary phase presented from around the 80th to 160th hour. This phenomenon showed that the exponential growth of the mixed culture, which degrades thiosulfate, occurred within 60 h from inoculation. The continuous increase of sulfate concentration after depletion of thiosulfate (i.e. after 60 h) suggested that the biodegradation of thiosulfate occurred step by step. Element sulfur might form first during the

depletion of TS, followed by a further oxidation to the end product, sulfate. This assumption was also verified by the witness of increasing turbidity within the shaking flask that contains the mixed culture, G2.

3.1.4 Bacteria Counting

Standard plate count method (Black, 2005) was used for counting viable cells in the biomass (Figure 3.2). This technique relies on the fact that only viable cell can divide and form a visible colony on an agar plate under proper condition. Because it is difficult to count more than 300 colonies on one agar plate, the original bacterial cultures were usually diluted before being transferred onto the agar plate (30~300 colonies per plate gave the most valid counts statistics). After the serial dilutions, a volume of 0.1 mL diluted culture broth was spread over the agar plate surface evenly by a sterile spreader. The inoculated plate was sealed by Parafilm^{TM} and placed in a 30 ^{o}C incubator for 2~7 days until the colonies appeared. The number of colonies counted on the plate was then multiplied by number of times of dilution to yield the concentration of bacteria in units of colony-forming units (cfu) per milliliter.

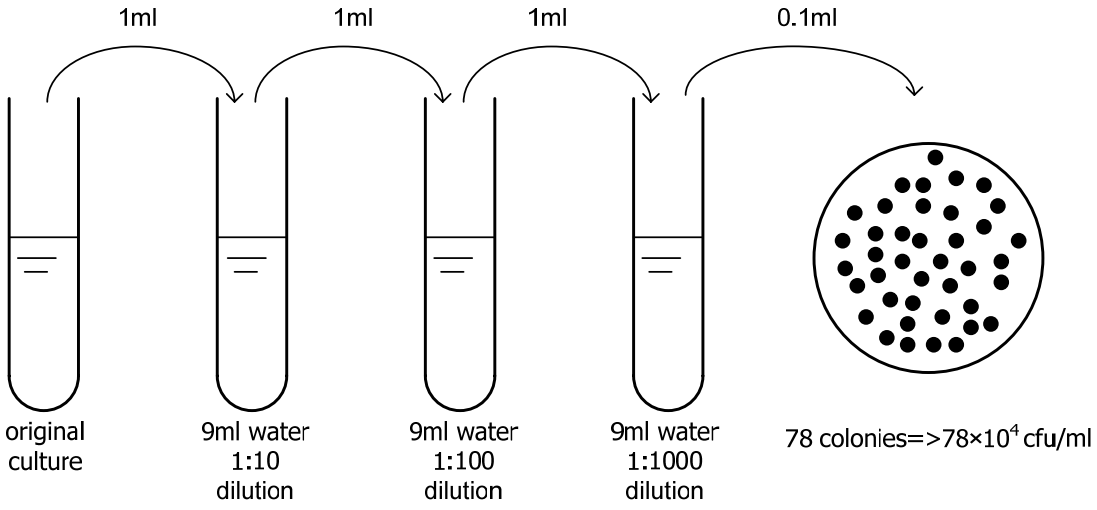

Figure 3.2 Serial dilution and standard plate count

3.1.5 Microbial Identification

The microbial isolation and identification of the acclimated activated sludge for immobilization onto activated carbon were carried out as follows:

3.1.5.1 Bacteria isolation

The schematic diagram of the isolation processes used in this study is shown in Figure 3.3.

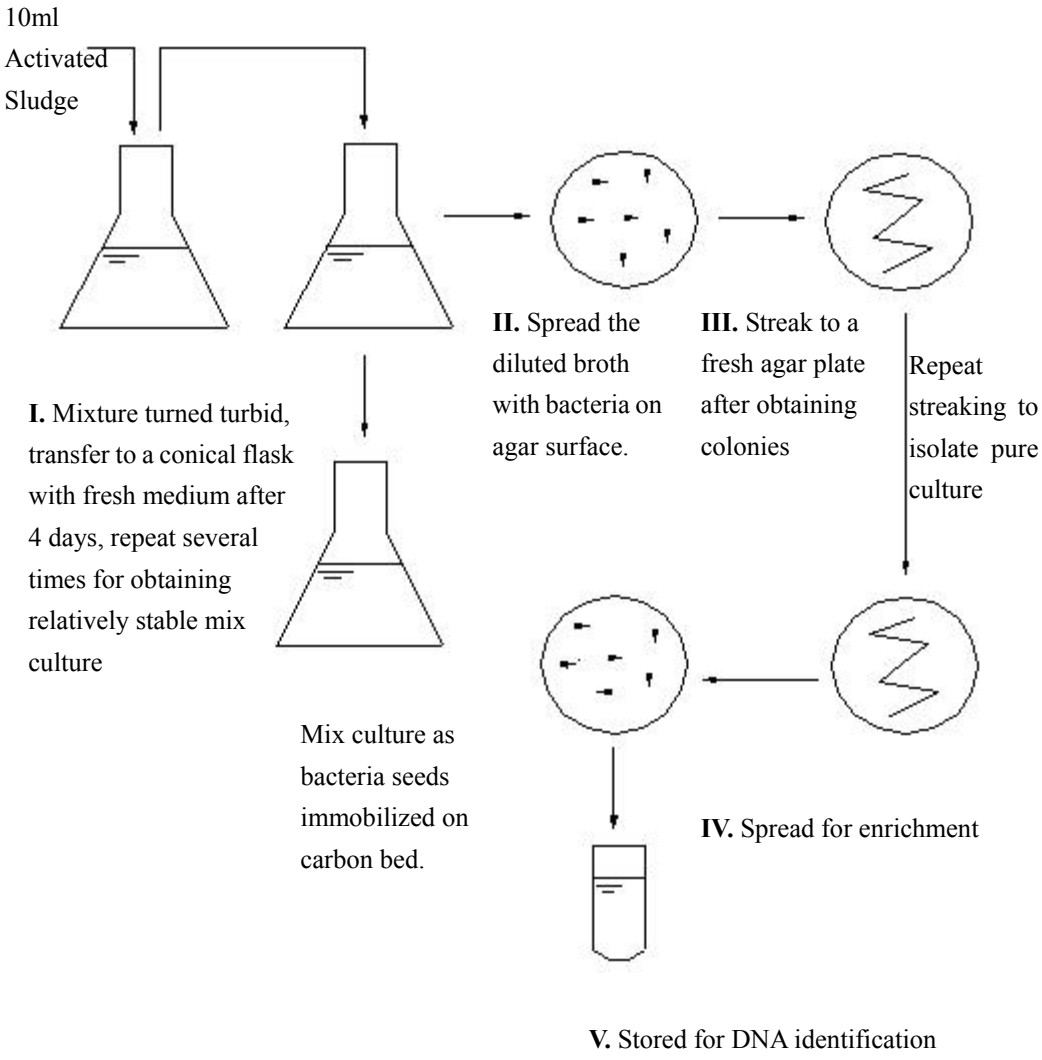

Figure 3.3 Process of isolating sulfide oxidizing bacteria from activated sludge

The isolation processes comprises 4 steps:

Step I. A volume of 10 mL activated sludge from the secondary sedimentation tank at a local WWTP in Singapore was added to 90 mL of liquid thiosulfate medium in a sterile conical flask. This process was done in a sterile environment. The cotton-sealed conical flasks were placed on an auto-shaker at 120 rpm for 4 days, and incubated at 30 ^{o}C. The continuous shaking ensured that the bacteria were kept in suspension so that there were sufficient nutrients available for them. After 2 days, the medium turned turbid, which indicated the growth of sulfide oxidizing bacteria from the activated sludge as well as the formation of sulfur solid deposits. The growth of bacteria was also observed by measuring the concentration variance of sodium thiosulfate and sulfate, which is the product of oxidization. An average of 4 days was needed to obtain a complete growth curve for the mixed culture. A volume of 10 mL of the above bacteria liquid, was then transferred to a sterile conical flask containing another 90 mL fresh medium to repeat the above procedures. These procedures were repeated 3 times to obtain a relatively stable mix culture. This mixed culture can be used for the development of biological activated carbon (BAC).

Step II. A volume of 1 mL of the third generation bacteria was serially diluted 10^6 times (using 0.85% of NaCl solution). 100 μL of the diluted bacteria liquid medium was then spread onto the thiosulfate medium plate in a Petri dish using a sterile spreader over the pH 7 and pH 4.5 agar surfaces, respectively. The Petri dishes were incubated at 30 ˚C in an incubator.

Step III. Bacteria colonies began to appear on the agar plates after about 2-7 days, the colonies on pH 4.5 agar plate surfaces, which appeared in 2 days, were growing much faster than those on pH 7 agar plates. A loop of the colonies was striped on a

new agar plate to obtain a purer culture. This procedure was repeated several times until several pure cultures were obtained. The pure cultures were stored in microbial tubes for later identification.

Step IV. Each kind of bacteria which can oxidize thiosulfate was ready to be identified by sequencing analysis. For storage of the pure culture, some colonies of each growing species were added to a mixture of 0.85 mL of liquid medium and 0.15 mL glycerol in the microbial tubes, and stored at -20 ^{o}C.

3.1.5.2 Morphological characterization

Microscopy (with gram staining): After obtaining the pure cultures, a drop of ultra pure water (UPW) was placed on a clean microscope slide. A loop of the bacteria colony was grabbed from the agar plate and mixed into the water droplet on the slide. Sample loop was flamed and cooled before and after grabbing the cultures. After air drying, the microbes were fixed on the slide by flaming. The crystal violet was applied onto the visible sample stain and kept for 1 min, washed by distilled water, and then flooded with iodine solution for 2 min. The slide was then washed under distilled water and decolorized to remove excess crystal violet and iodine. Once dried, the smear was counter-stained using red staining for 30 s. To remove the excess stain, the smear was washed again with water and dried before examination under a phase-contrast microscope at a magnification of 500X. As Figure 3.4 shows, the cells were observed to be rod shape, gram negative bacteria. The specific species will be determined by 16S rDNA identification, which will be discussed in Section 3.1.5.3.

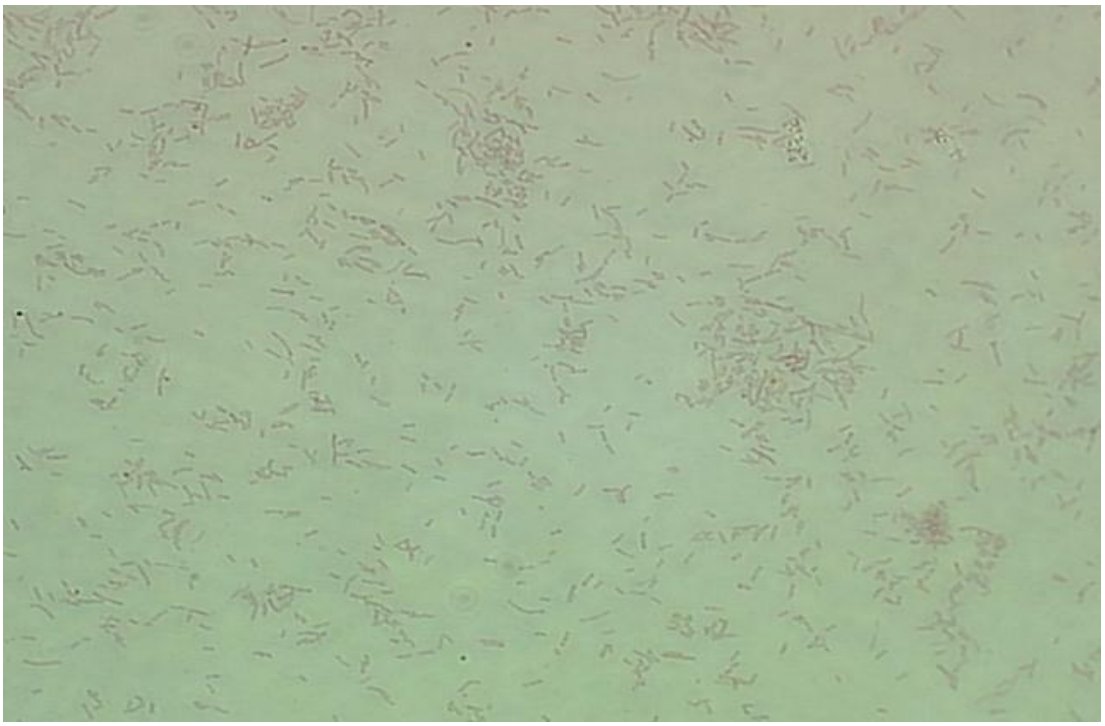

Figure 3.4 Morphology of sulfide degradation bacteria after gram staining

Scanning electronic microscopy (SEM): Enriched culture was filtered by 0.2 μm filter paper, then the filter paper was soaked in a breaker with 2% (v/v) glutaraldehyde for about 2 h in order to fix the microorganisms. The sample was then washed for 20 min three times with 0.1 M sodium cacodylate buffer. The washed sample was then dehydrated in 50%, 70%, 85%, and 95% ethanol each for 15 min before being stored in 100% ethanol. Following dehydration, the sample was dried using critical point drying equipment (E3000 Series). The dried sample was sputter-coated with gold at 20 mA in a high vacuum and low temperature cryo-chamber for 60 s, and then viewed with a scanning electron microscope (Stereoscan 420, Leica, Cambridge Instruments) at 15 KV. The sulfide oxidation bacteria in the mix culture was around 1 μm in size as seen from the SEM photograph of bacteria immobilized activated carbon (Figure 4.3). The methods of immobilizing bacteria onto carbon surface will be discussed in Chapter 4.

3.1.5.3 DNA identification

The microbial population in the sulfide degradation communities in the biofilters and acclimated activated sludge were examined and analyzed by denaturing gradient gel electrophoresis (DGGE) profiles of 16S ribosomal DNA fragments. The procedures are shown in Figure 3.5. DNA in the communities was extracted, and then the 16S rDNA fragments were amplified by polymerase chain reaction PCR, separated by DGGE, and finally identified by 16s ribosomal DNA. Premiers 27F and 1492R were used for PCR amplification (the procedural details are described in the following 6 steps).

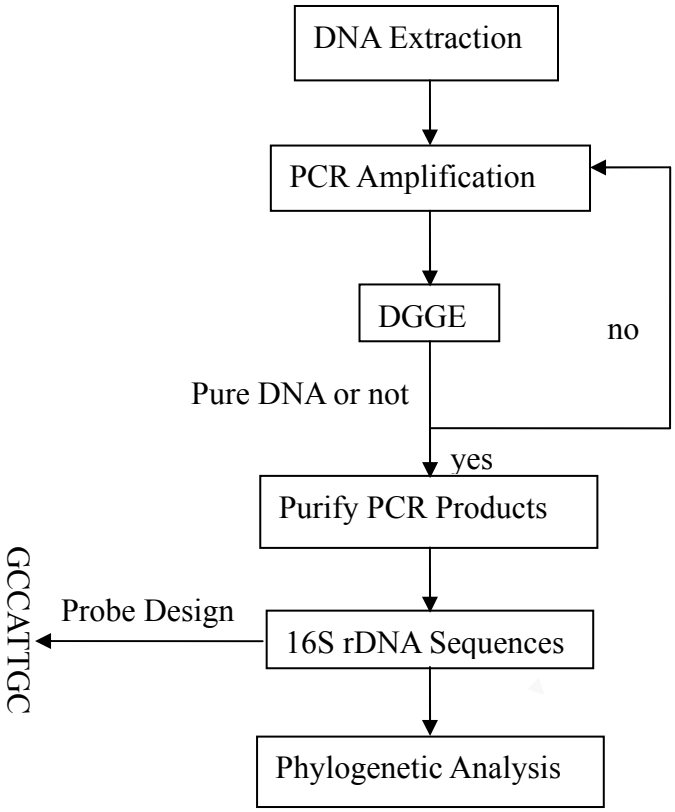

Figure 3.5 Flow chart of microbial community's diversity study

Step I. DNA extraction

Extraction from acclimated sludge: Cell pellets (100~200 mg wet weight) were suspended in 800 μL ultra pure water (UPW) first. An amount of 800 mg baked glass beads were placed into a Bead Beater tube of 2 mL, and then the suspended cells with 50 μg 20% sodium dodecyl sulfate (SDS) were also added into the Bead Beater tube. After topping off the Bead Beater tube with saturated phenol (pH 8.0, around 500 μL), the Bead Beater was run at 5000 oscillations/s for 3 min. Then the mixture was kept in 60°C water bath for 5 min. Subsequently, DNA extraction was carried out according to the protocols described previously (Watanabe et al., 1998a&b).

The above mixture was spun in SpeedVac for 10 min at 5000 rpm without vacuum. The aqueous layer was then removed and was extracted with the same volume (about 500 μL) of saturated phenol (pH 8.0, centrifuged at 10000 rpm for 5 min), followed by twice extractions using the mixed liquor containing saturated phenol and chloroform at a ratio of 4:1, and another twice extractions by chloroform (Spin in centrifuge at 10000 rpm for 5 min) in the same volume, respectively. All cell pellets were collected, and a 1/10 volume of 20% sodium acetate and 2 volumes of 95% ethanol was added and precipitated overnight at -20°C. The next day, precipitates were spun for 10 min in a microcentrifuge at 12000 rpm. The supernatant was removed and the cell pellet was washed twice with 80% ethanol (500 μL), dried, and suspended in 105 μL of UPW for 20 min. A volume of 5 μL of the suspension was taken for UV-vis wavescan from 250 to 400 nm. This 5 μL of the above mixed liquor was diluted 200 times and its optical density was read on a spectrophotometer. A 260/280 nm ratio of 1.9 to 2.0 was considered great, but anything above 1.65 was acceptable. Finally, the cell pellets were suspended to 2.5 $\mu g \cdot \mu L^{-1}$ of UPW and incubated at -20 °C until ready to use.

Extraction from BACs: BAC (10 g) was placed into 20 mL of 0.85% NaCl solution and re-suspended in a vortex for 10 min. The supernatant was collected and another 20 mL of 0.85% NaCl was added. The mixture was then sonicated for 9 min at 42 kHz and the supernatant was spun in a microcentrifuge at 4000 rpm for 20 min. After that, DNA of the received cell pellet was extracted following the method of DNA extraction from acclimated activated sludge as previously described above.

Step II. Polymerase Chain Reaction (PCR)

1) The tubes containing PCR Master Mix (Table 3.2) was placed into a programmable temperature cycle (Applied Biosystem, USA, Figure 3.6) with the following program:
   - 30 cycles of:
     - 94 °C for 1.5 min
     - 55 °C for 1.5 min
     - 72 °C for 2.0 min
   - 72 °C for 2.0 min (Final step)
   - 4 °C for store (Cooling)

Table 3.2 PCR master mix

Items	Per 100 µL Master Mix
10X Buffer B (for Taq)	10 µL
$MgCl_2$	6 µL
NP40 (0.05% NP40 in UPW, surfactant)	5 µL
dNTP (25:25:25:25)	0.8 µL
BSA	1 µL
Taq DNA Polymerase	1 µL
Primer 27F	2 µL
Primer 1492R	2 µL
Template(Extract DNA)	1 µL (~ 100 ng·µL^{-1})
Milli-Q H_2O	71.2 µL
Total Volume	100 µL

Figure 3.6 Programmable temperature cycle

2) DNA PCR products were checked by agarose gel electrophoresis, procedures as follows: An amount of 0.5 g agarose (Promega, USA) was dissolved into 50 mL 1X TAE (Tris-Acetate-EDTA) buffer, microwaved until agarose dissolved and the mixture turned into a clear solution. After the solution was naturally cooled to about 50 °C, 25 µL Ethidium Bromide (BioRad, England) was added, and the mixed liquor was homogenized by hand shaking. A comb was placed vertically in the gel tray about 1 inch from one end with the teeth 1~2 mm above the surface. The prepared gel solution was poured into the tray to a depth of about 5 mm. After 30 min's solidification at room temperature, the comb was removed, and the gel was placed in a mini-gel apparatus with combs (Minisubcell GT, BioRad, England) containing 250 mL 1X TAE buffer. With 2 µL of gel loading dye for every 5 µL of PCR products, the PCR products were loaded in the wells made by the comb, and electrophoresed at 90 mV for 40 min until dye markers had migrated an appropriate

distance, marked by a ladder. Finally, the gel was viewed under UV and photographed by a Kodak Digital Image Station 440CF (NEN Life Science Products). The fluorescent bands were the results of DNA product electrophoresis, which indicated that DNA extraction was successful. The remaining 95 µL PCR products were stored at -20 ºC for DGGE.

Step III. Denaturing Gradient Gel Electrophoresis (DGGE)

The DGGE was performed following the method described by Muyzer et al. (1993). Electrophoresis was conducted in a 1X TAE buffer solution at 85 V and 60 ºC for 15 h.

Step IV. Purify PCR products

QIAquick PCR Purification Kit Protocol (QIAGEN, Cat.No.28104, 28106) was applied to purify the PCR products. Pure products were stored at -20 °C.

Step V. Cycle sequencing for pure DNA products

The tubes containing the sequence reaction mix (Table 3.3) was placed in a programmable temperature cycle (Applied Biosystem, USA, Figure 3.6) with the following program:

- 25 cycles of:
  - 96 °C for 10 s
  - 50 °C for 5 s
  - 60 °C for 4 min
- 4 °C for store (Cooling)

After adding 2.0 µL of 3M sodium acetate and 50.0 µL 95% ethanol into the cycle sequencing products, the mixture was centrifuged for 20 min at 14000 rpm, followed by washing with 60 µL of 75% ethanol. After that, the mixture was again

centrifuged for 5 min, and then dried by vacuum centrifuging for 15 min, and finally stored at -20 °C.

Table 3.3 Sequencing reaction mix contents

Items	Volume
BigDye Terminator	5.0μL
Primer (3.2 mol·mL^{-1})	1.0μL
Purified 16s rDNA from Step IV	1.0μL
Sterilized MQ water	13.0μL

Step VI. Gene analysis by Gene Amp PCR system 9700 (Applied Biosystem. USA).

After the isolation and identification processes, three predominant species of sulfide oxidizing bacteria in the acclimated activated sludge (which later on will be applied onto the biofilters) were isolated in an acidic environment (pH 4.5 agar). These 3 species are different because the shapes of their colonies on the agar are different. Their partial sequencing of DNA were identified using the BLAST searching engine, and matched to be *Acidithiobacillus thiooxidans,* or the species similar to it. The similarities are shown as below:

1. *Acidithiobacillus thiooxidans*, similarity 100%
2. *Acidithiobacillus thiooxidans*, similarity 96%. It may be a species other than *Acidithiobacillus thiooxidans* but its partial DNA sequence is more like *Acidithiobacillus thiooxidans* than other known species, full DNA sequencing is recommended to be carried out so as to determine what it is exactly.
3. *Gamma Proteobacterium*, which is the mother group of *Acidithiobacillus thiooxidans*, similarity 94%

The similarity should be over 97% to be considered as belonging to the same species. Therefore, there are at least two new strong H_2S degradation species (except for *Acidithiobacillus thiooxidans)* in the acclimated activated sludge that would be applied later to produce BAC.

3.1.6 Optimal pH Investigation for the Mixed Culture Growth

A well mixed culture broth of 1 mL was inoculated into 39 mL of sterile media with different pH values (1.0, 2.5, 4.0, 5.5, 7.0 and 8.5) in a sterile environment. The viable microbe concentration of each inoculant was 3.3×10^4 cfu·mL^{-1} counted by plate count. Their respiration activities were observed by monitoring oxygen assimilation in the ecological niche by Micro-Oxymax system (Columbus, U.S.A, Figure 3.7). The most active niche among different pH can be considered as the optimal pH for the mixed culture growth.

Figure 3.7 Micro-Oxymax system

The activity of a microorganism consortium can be evaluated by a respirometer through measurement of its O_2 consumption rate. Figure 3.8 presents the O_2 accumulations in each bacterial consortium in diverse pH environment (pH 1.0, 2.5, 4.0, 5.5, 7.0 and 8.5) against time. Negative O_2 accumulation indicates that the microorganisms in the sealed niche are consuming O_2. Reactions in this niche are producing O_2 if O_2 accumulation becomes positive. Since aerobic bacteria are the type of bacteria that consume O_2, the more active the niche, the more negative the O_2 accumulation will be. It could be considered that the microbial activities ceased when O_2 accumulation increase and became positive. As Figure 3.8 shows, sulfide oxidizing bacteria cannot survive in a basic environment (pH > 7), and died out soon after being inoculated in a pH 8.5 medium. The microbial consortium appears to be the most active in pH around 5.5, and the bacteria can be active at pH as low as 1. This phenomenon is supported by data presented in Figure 3.9, which provides the information of the amount of sulfate produced in each of the bacterial consortium. There are 2 peak points of sulfate concentration in the bacterial broth after the microbial respiration experiments in the pH range of 1~9, one is at pH 5.5 (1.03 $g \cdot L^{-1}$) and the other is at pH 1 (0.66 $g \cdot L^{-1}$). Meanwhile, viable cells concentration both increased to 5.7×10^7 $cfu \cdot mL^{-1}$ in pH 5.5 and 2.9×10^6 $cfu \cdot mL^{-1}$ in pH 1 from an initial 3.3×10^4 $cfu \cdot mL^{-1}$ (plate counting), respectively. This phenomenon might be interpreted as follows: At pH 5.5, some relatively neutrophile bacteria species dominated the consortium. At lower pH, neutrophilic bacteria species decreased and acidophilic bacteria grew in the consortium, until at a pH of 1, acidophilic bacteria dominate the consortium. Considering that the bacteria consortium is also active at pH 1, biofilters based on it may work economically without pH control.

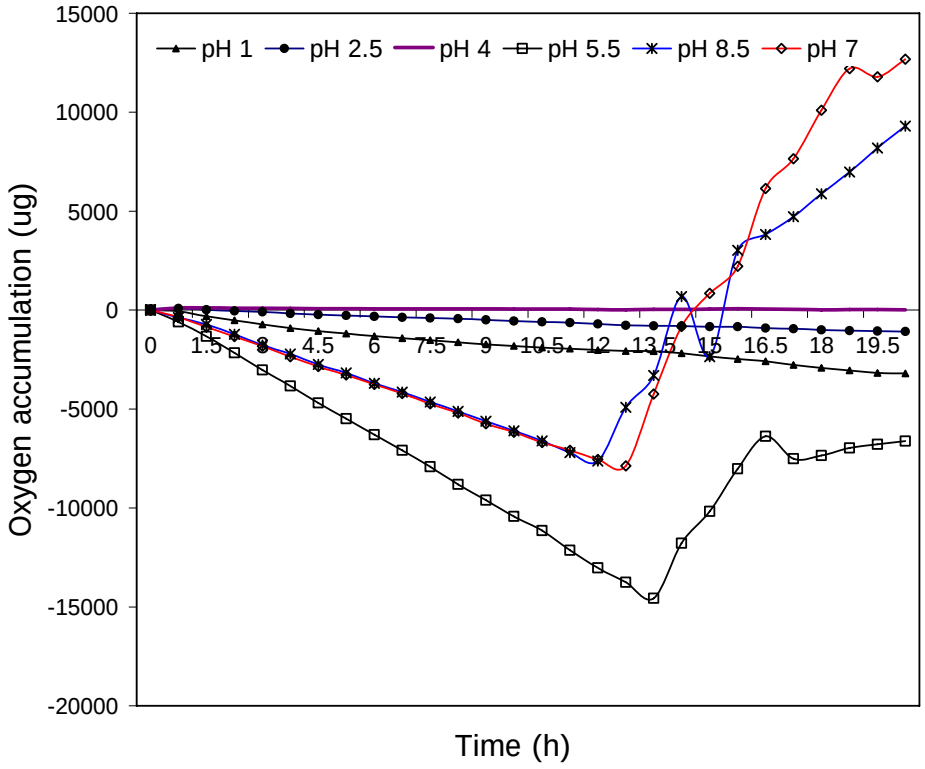

Figure 3.8 O_2 accumulations in respiration

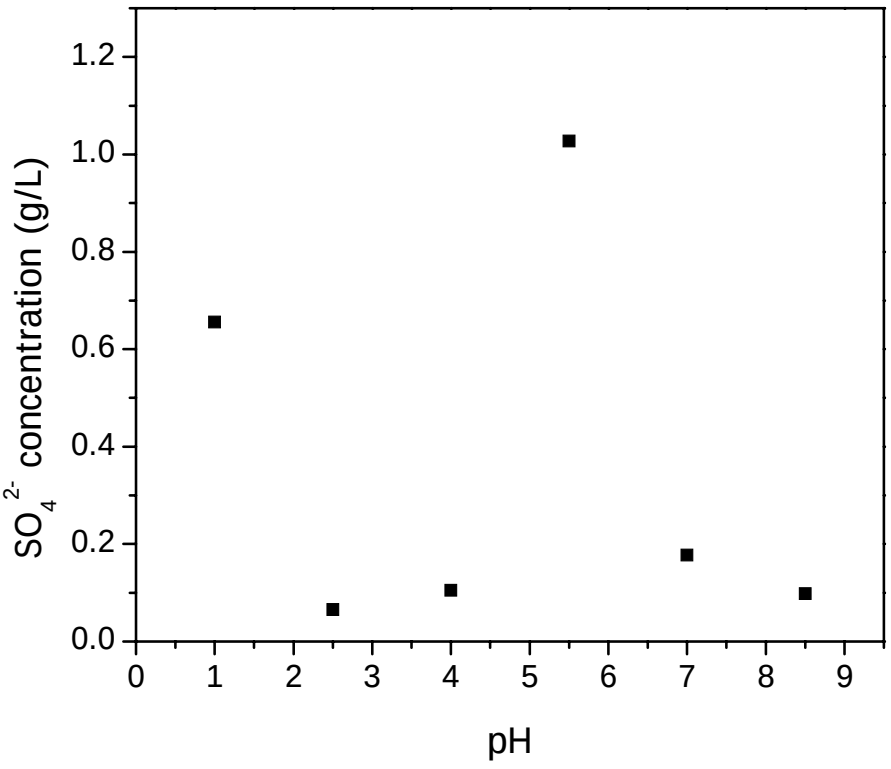

Figure 3.9 Sulfate (final oxidation products) concentrations vs. pH

3.1.7 Sulfate Concentration Impact on Mixed Culture Activities

An amount of 15 mL of well mixed culture broth as above was inoculated into 85 mL of sterile media with different initial sulfate concentration (0, 5, 10, 25, 50, 100 $g \cdot L^{-1}$, by dissolving appropriate amounts of Na_2SO_4) in 250 mL conical flask under a sterile environment. The flask without sulfate addition worked as control. All six flasks were shaken on an auto-shaker at 30 ^oC. Bacterial activities can be observed by monitoring the drop in pH with time. Any delay in the decrease of pH in the flask can be taken to represent the inhibition effect of sulfate acting on sulfide biodegradation.

Since the biooxidation of thiosulfate is a process that produces hydrogen ion and sulfate, the decrease in pH with time should represent the microbial activities indirectly, and the end product, sulfate concentration in the microbial niche should indicate the effect on the microbial growth. The pH drop curve of each microbial niche for different amounts of initial sulfate dosage is shown in Figure 3.10. The results show that for dosage of sulfate at concentrations from 5 $g \cdot L^{-1}$ to 25 $g \cdot L^{-1}$, there is little effect on the biodegradation of thiosulfate. However, if sulfate is allowed to accumulate up to 50 $g \cdot L^{-1}$, the degradation of thiosulfate is impeded. At 100 $g \cdot L^{-1}$ of sulfate concentration, biodegradation appears totally impeded. From these results, it appears that sulfate concentration in aqueous phase should be limited to less than 50 $g \cdot L^{-1}$ for *Acidithiobacillus Thiooxidans* to be effective on the biodegradation of H_2S.

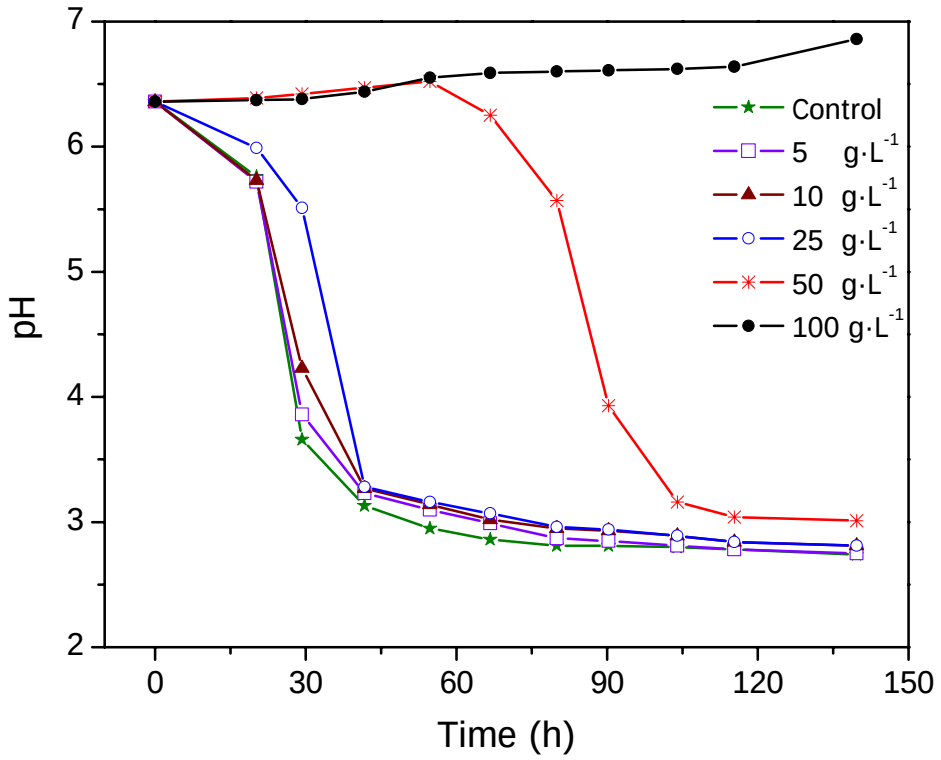

Figure 3.10 Initial sulfate impacts on bacterial growth

3.2 Physicochemical Characterization of Activated Carbon

Surface and pore features provide key information of a porous material. Activated carbon is a type of porous material with a large surface area. An evaluation of the possibility of using activated carbon as a support media in biofiltration was carried out in this research study. The activated carbon used for developing BAC was obtained from Calgon Carbon Corporation (Calgon AP460), which is a type of non-impregnated coal-based carbon. Coal as raw material ensures a high density product with good mechanical strength and low ash content. The characterization methods mentioned in this section can be applied on BAC as well.

3.2.1 Surface Properties

Carbon surface pH: The pH of the carbon suspension, which provides useful information about the average acidity/basicity of carbon surfaces, was measured in the following way: 0.4 g of each carbon sample was soaked in 20 mL UPW and swirled on an auto-shaker for 24 h to reach equilibrium. Then the sample was filtered and the pH of the solution was measured using a Horiba pH meter F-21 (Horiba Ltd. Japan). The results were referred to as "the pH of solution" for simplification, while it is actually the pH of the water extract of the activated carbon. Two replicate determinations for each sample were carried out for repeatability.

Carbon surface sulfur: Total sulfur contents in carbon samples were analyzed by x-ray fluorescence (XRF) technique using PANalytical PW 2400 x-ray spectrometer (Holland, Figure 3.11). Prior to analysis, carbon samples were ground into fine powder and freeze-dried for 24 h. Considering the morphology of carbon powder, the manufacture of a pure carbon pellet can hardly be done without the addition of a binder. As boric acid (H_3BO_3) is undetectable for XRF, 0.375 g of carbon powder was mixed with 1.125 g boric acid, and the mixture was homogenized in an agate mortar. The mixed powder was pressed at 350 bar pressure for 3 min to obtain the cylindrical pellet of 30.2 mm diameter, which was then used for XRF analysis.

Figure 3.11 PANalytical PW 2400 x-ray spectrometer (Holland)

Sulfates which are soluble would most likely be transferred into the aqueous phase. However, some sulfates that might remain at the carbon surface after the bioprocess are measured in the following way: 0.4 g of each carbon sample were soaked in 20 mL UPW and shaken on an auto-shaker for 24 h to reach equilibrium. Samples were filtered through a 0.2 μm membrane to remove particles. Sulfate concentration in the solution was determined by ion chromatography (IC-A3, Shimadzu, Japan, Figure 3.12). Calibration curve in the range of 0 to 1000 $mg \cdot L^{-1}$ was obtained using commercial standard solutions. The results were referred to as "sulfate concentration of solution" for simplification, while it is actually a water extract of the activated carbon. Two replicate determinations for each sample were carried out for repeatability.

Figure 3.12 Ion chromatography for anion (IC-A3, Shimazu, Japan).

FTIR Analysis: FTIR analysis was performed after grinding the carbon samples and mixing with potassium bromine (KBr) powder to prepare sample-KBr pellets. The BioRad Excalibur series FTS 3000 with DTGS detector was used as the analytical instrument (refer to Figure 3.13). Pellet thickness was kept constant by fixing the sample-in-KBr weight, using the same diameter, pelletizing pressure and time. Various amounts of the carbon were mixed with KBr powder in order to obtain the optimum concentration condition to achieve the highest absorbance of the sample peak. 1% sample concentration was founded to be an optimum. The instrumental settings were: resolution 4 cm^{-1} and sensitivity 1. Before each measurement, the instrument was run to establish the background, which was then automatically subtracted from the sample spectrum. KBr pellet prepared from the ground KBr powder was used as the background for virgin carbon, BACs and exhausted carbons, whilst for most cases, virgin carbon was used as the background for the BACs and exhausted carbons.

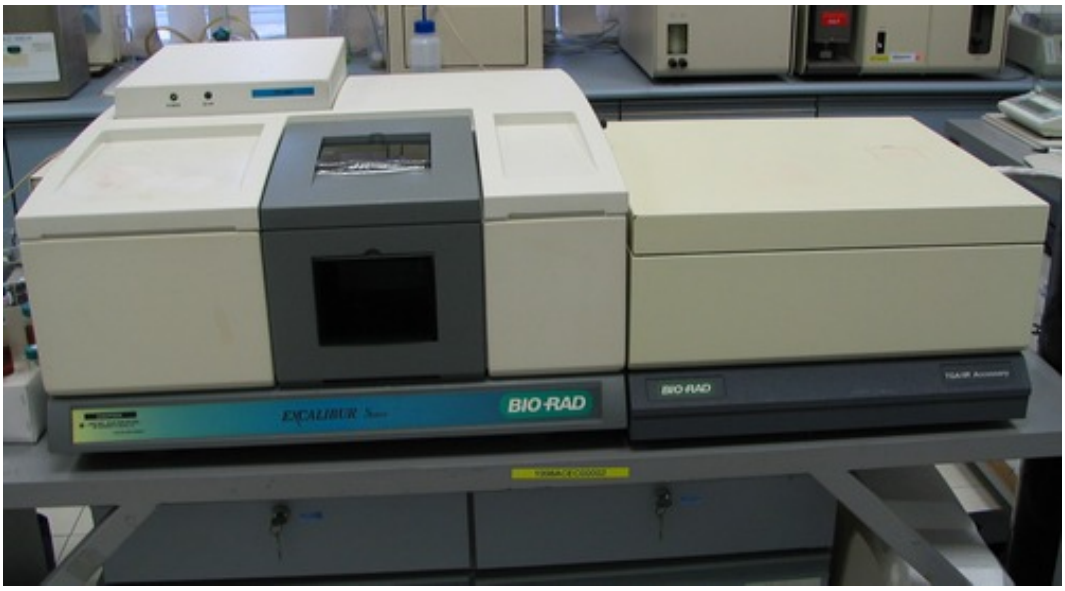

Figure 3.13 BioRad excalibur series FTS 3000 with DTGS detector

Thermal Analysis: Thermal analysis was conducted to evaluate the thermal desorption of different S-species adsorbed in carbon. The thermal gravimetric analyzer (TGA) used is Netzsch STA 409 from Germany (refer to Figure 3.14). The activated carbon pellet was placed onto the pan, and heating was carried out from room temperature to 1000 °C at 10 °C·min^{-1}. Nitrogen was channeled into the system at 50 mL·min^{-1}.

Figure 3.14 Thermal gravimetric analyzer (Netzsch STA 409, Germany)

CHNS analysis: CHNS analysis provides information on the combustible contents of C, N, H, and S in the samples. Among them, combustible sulfur species include H_2S and all those intermediates of H_2S oxidation, organic sulfur, excluding sulfates (S(VI), oxidation state of +6). The combustible elementary compositions (C, H, N, S) of carbon were measured using a thermo-analytical analyzer (PE2400 series II CHNS/O analyzer, PerkinElmer Instruments, USA, Figure 3.15). Three analyses for each sample were carried out for consistency.

Figure 3.15 PE2400 series II CHNS/O analyzer (PerkinElmer Instruments, USA)

3.2.2 Structure Analysis

SEM: Activated carbon surface structure and biofilm development on BACs were identified using SEM. Carbon samples (including BACs) were dried using a freeze dryer (EDWARDS) for about 16 h, coating with gold, prior to viewing with SEM. Details of SEM analytical procedure have been described previously in Section 3.1.5.2.

BET Test: Brunauer-Emmett-Teller (BET) measures indirectly the surface areas and pore volumes of porous material. In this study, the surface areas and pore volumes of virgin activated carbon, BACs and exhausted activated carbon pellets were measured by nitrogen adsorption using Micrometrics BET analyzer model ASAP 2010 (Figure 3.16). Carbon samples were first freeze vacuum dried for 24 h

before carrying out any identification. All the carbon samples (including dried BAC) were degassed to 1.33 Pa pressure at 70 °C prior to the BET analysis.

Figure 3.16 Micrometrics BET analyzer model ASAP 2010

Mercury Penetration: It is well known that the pores in activated carbon are classified into macropores (>50 nm), mesopores (2.0~50 nm) and micropores (0.4~2 nm). Microspores and mesopores are generally too small for access by microorganisms (~1 μm), and are inaccessible for bacteria. The property of macropores, some of which are larger than cells, can be obtained by the mercury porosimeter, AutoPore III series (Figure 3.17). Mercury penetrates under high pressure (up to 60000 psi) into the pores of porous materials (such as activated carbon) so as to determine the sizes and quantities of the pores (range in

0.003~360 μm) as well as density. The pressure required to fill the pores completely is inversely proportional to the size of the pores. The relationship is:

$$D = -\frac{1}{P} \cdot 4g \cdot \cos Q \qquad \text{Eq.3-1}$$

where D is the pore diameter, P is the applied pressure, g is the surface tension and q is the contact angle. The volume of mercury V penetrating the pores is measured directly as a function of applied pressure. This D-V information serves as a unique technique in the characterization of pore structure.

Figure 3.17 AutoPore III series of mercury porosimeters

3.2.3 H_2S Breakthrough Capacity Test

This dynamic test was carried out to evaluate the capacity of activated carbon for H_2S removal. ASTM D28 was used as the standard test method. The experimental set up is showed in Figure 3.18. Activated carbon was packed in a plastic tube (2.4 cm i.d.) at a fixed height of 25.6 cm. Glass beads were packed at the bottom and top of the carbon bed to enable a well-mixed gas flow. One part of 5% (v/v) H_2S was mixed together with 9 parts of moisture clean air (RH 100%) to form 0.5% moisture (RH 90%) H_2S test gas, which was delivered from the bottom of the carbon bed at a flow rate of 1300 $mL \cdot min^{-1}$. The linear gas flow velocity and gas retention time was kept at 4.79 $cm \cdot s^{-1}$ and 4.8 s. The experiment was conducted at room temperature, and the outlet H_2S concentration was measured by a Finch-com II portable H_2S monitor (Infitron Inc, Korea) until a breakthrough of 50 ppm_v was obtained. The time taken for breakthrough was recorded, and carbon breakthrough capacity in terms of both weight (grams of H_2S per gram of carbon) and volume (grams of H_2S per milliliter of carbon) was calculated.

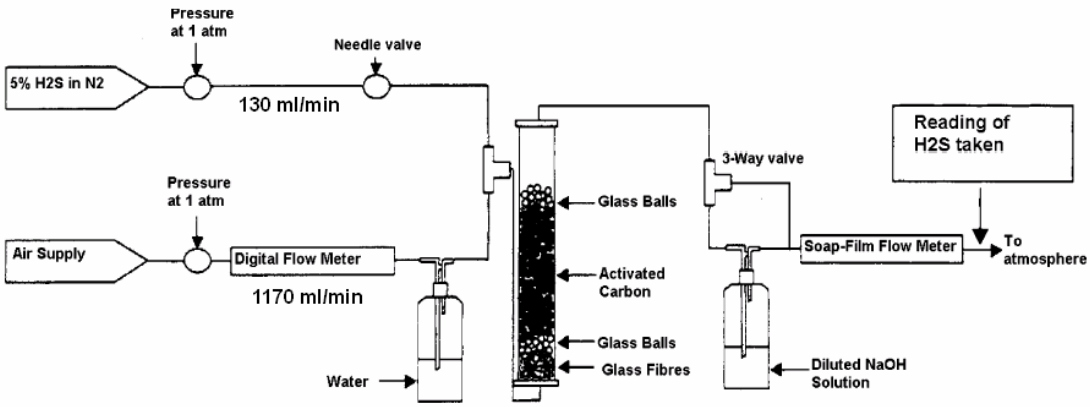

Figure 3.18 Schematics of activated carbon breakthrough capacity test

3.2.4 Activated Carbon Properties

The physical description of Calgon AP460, including density, pellet size, porosity, surface area, pore area distribution, pore volumes, average pore diameter, moisture content, and so on, is presented in Table 3.4. Figure 3.19 provided the direct image of how this sort of activated carbon looks like.

The H_2S adsorption capacity of Calgon AP460 is 5.5 wt.% by dry weight basis. Effective specific surface area, in most cases is approximated by the external packing surface area per unit gram. External surface area becomes a very important character of activated carbon when acting as a packing material in biofiltration because nearly all of the internal surface area is inaccessible to the microorganisms. Even the macropore average diameter, 0.02 μm, as shown in Table 3.4, in activated carbon is much smaller than the size of microorganisms which is around 1 μm. Figure 3.20 shows the cumulative pore areas at different pore radius. It can be seen from Figure 3.20 that most of the pore area is contributed by the pores with radius less than 0.01 μm, a size that cannot be utilized by microorganisms. Calgon AP460 is a type of non-impregnated carbon, with a pH environment (carbon initial pH = 7.96, refer to Table 3.4) that is more suitable for the growth of microorganisms on the carbon surface compared to alkaline impregnated carbons. Corsi and Seed (1995) recommended that 60 wt.% of a biofilter media should be composed of particles greater than 4 mm in diameter in order to prevent excessive head loss. The selected Calgon AP460 has a pellet diameter of 4 mm.

Table 3.4 Physical description of Calgon AP460

Parameters	Value	Method
Initial pH	7.96	pH meter
H_2S adsorption capacity, (dry weight basis), %	5.5	H_2S breakthrough test
Apparent (skeletal) density, $g \cdot mL^{-1}$	0.49	Mercury porosimeters (AutoPore III series)
Porosity, %	34	
Macropore area, $m^2 \cdot g^{-1}$	81.88	
Macropore volume, $mL \cdot g^{-1}$	0.43	
Average macropore diameter, µm	0.02	
Micropore volume, $mL \cdot g^{-1}$	0.28	BET test (Micrometrics ASAP 2010
Average pore diameter, nm	1.98	
Micropore surface area, $m^2 \cdot g^{-1}$	525.6	
External surface area, $m^2 \cdot g^{-1}$	505.9	
Pellet diameter, mm	4	Technical description from product menu
Hardness number, min	90	
Ash content, max% w/w	5	
Mesh size > US Mesh 6 (3.35mm), min %	95	
Ash content, max% w/w	12	
Moisture content, max% w/w	5	

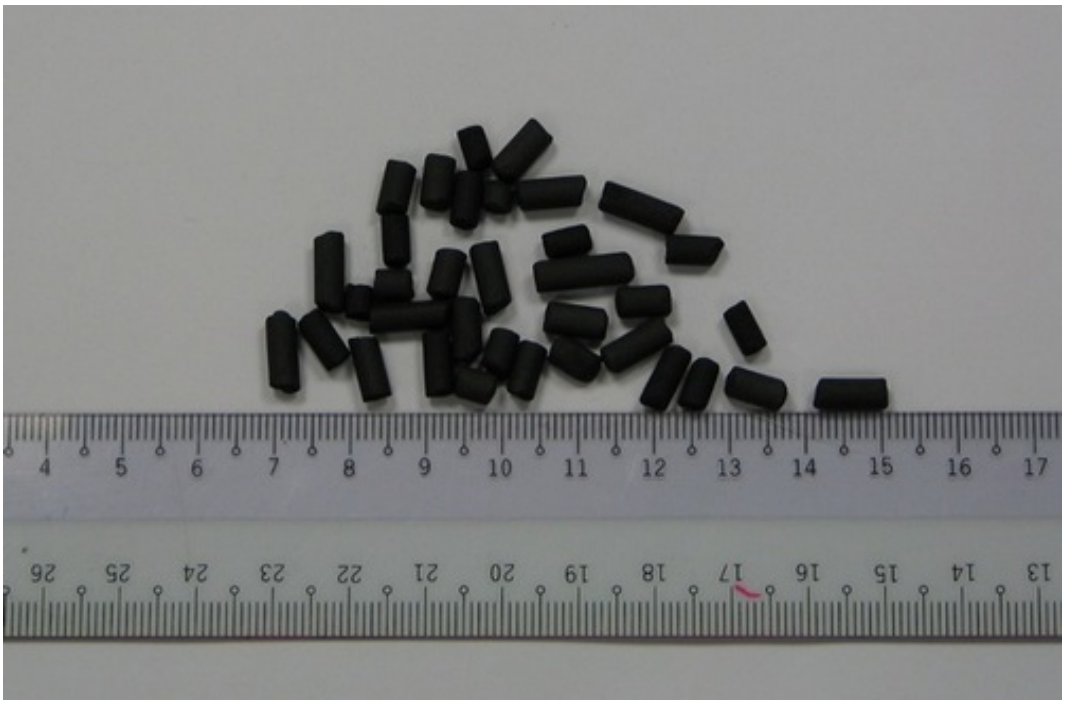

Figure 3.19 Calgon AP460

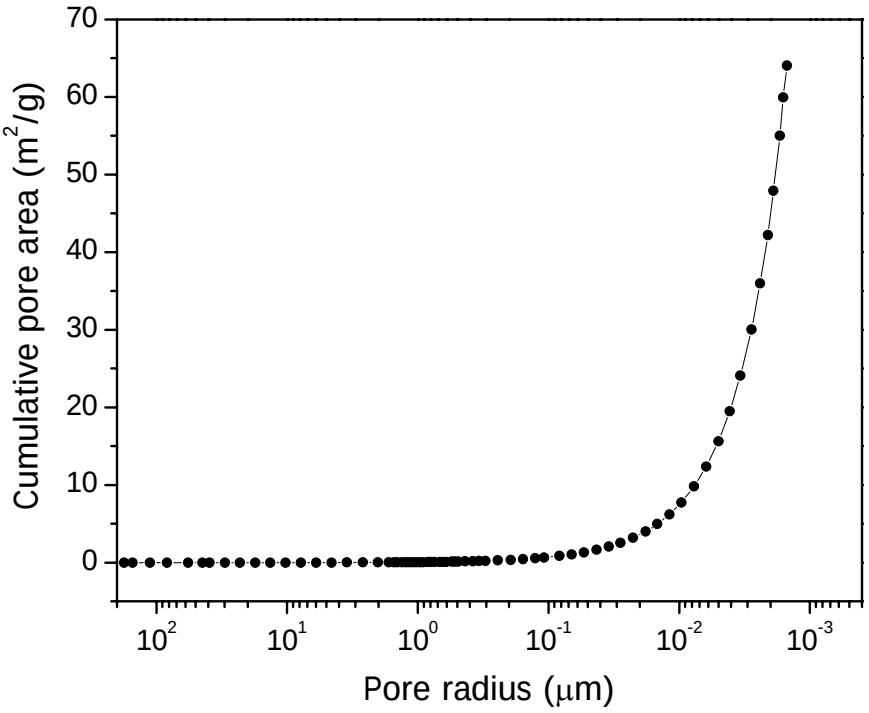

Figure 3.20 Cumulative pore areas vs. pore radius

3.3 Analytical Methods for Biofiltration Operation

3.3.1 Gas Sampling and Measurement

During the operation of an experimental biofilter in this study, periodical measurements of gas concentration and pressure drop were carried out from various sampling ports. Tedlar bags (SKC Inc., USA) were used to collect the gas samples. The outlet H_2S concentrations (generally around 1 ppm_v) were measured using a Jerome 631-X hydrogen sulfide analyzer (Arizona Instruments, USA, Figure 3.21a) and the inlet H_2S concentration (40~100 ppm_v) was determined using the Finch-com II portable H_2S monitor (Infitron Inc, Korea, Figure 3.21b). The Jerome analyzer is capable of measuring low level (ppb level, up to 50 ppm_v) of H_2S while the Finch-com monitor is more suitable for higher concentrations (ppm_v level, up to 100 ppm_v). The analysis of each gas sample was carried out

immediately after sampling to avoid the deterioration of H_2S sample. To eliminate any effect of residual H_2S in the Tedlar bags, all sample bags were flushed by clean air after each measurement. Three readings were taken for consistency.

a. Jerome 631-X H_2S analyzer (Arizona Instruments, USA)

b. Finch-com II portable H_2S monitor (Infitron Inc, Korea)

Figure 3.21 Devices that measuring H_2S concentration

3.3.2 Liquid Analysis

pH: The pH of the recirculation solution was measured using a Horiba pH meter F-21 (Horiba Ltd. Japan).

Determination of dissolved total sulfur (DTS): Direct DTS determination by ICP-OES (Inductively coupled plasma-optical emission spectrometry) was recommended as the most efficient method for routine determination of DTS in aqueous samples containing more than 1 ppm_v (Prietzel et al., 1996). The basic principle of the ICP-OES method is the activation of S atoms in Argon plasma and the quantification of the resulting emission spectrum at a characteristic wavelength. The intensity of the S emission spectrum is a direct function of S concentration in solution, irrespective of the type of S-containing compound and the oxidation status of the analyzed S atom. The ICP-OES method has been used successfully for S analysis in plant tissue after sample digestion and oxidation with various mixtures of acids and oxidants. It should be suitable for the determination of organic S compounds as well, if matrix and interference effects are excluded (Zhao et al., 1994; Prietzel et al., 1996). In this study, all aqueous samples were analyzed without pretreatment by Perkin Elmer Optima 2000DV apparatus at the S emission line of 180.669 nm in two replicate determinations. Nebulizations, background correction was carried out at a distance of 0.028 nm on each side of the peak of emission line. The entire optical system of the instrument was highly purged with N_2 to avoid the effect of O_2 absorption bands in the 170-200 nm region. The calibration graph was linear in the range between 1 and 50 ppm_v with R^2=0.999923. Thus, samples containing between 1 and 50 $mgS \cdot L^{-1}$ can be measured directly by ICP-OES; the determination range can be extended by pre-concentration or dilution of the aqueous samples.

Determination of sulfate: Sulfate concentration in the solutions were determined

by Ion Chromatography (IC-A3, Shimadzu, Japan), and the method has previously been described in Section 3.2.1.

Determination of thiosulfate: The thiosulfate concentration in liquid was determined in accordance to the iodometric method by titrating an amount of the liquid sample with standard iodine solution, using starch solution as the indicator. The titration volume at the end point was recorded and the TS concentration was calculated. Standard iodine solution of 0.0025 N and 0.00025 N were prepared as follows: 20 to 25 g KI was dissolved in a little amount of water together with 3.2 g iodine. After the iodine has been dissolved, the solution was diluted to 1000 mL and standardized against 0.0025 N and 0.00025 N $Na_2S_2O_3$, using starch solution as the indicator (APHA, 1999).

Bacteria concentrations: Bacteria concentrations in the recirculation water of biotrickling filter during the operations were counted by standard plate count method as previously described in Section 3.1.4.

CHAPTER 4
PRODUCTION OF BIOLOGICAL ACTIVATED CARBON

For this study, biological activated carbon (BAC) was produced by the immobilization of bacterial culture onto pelletized activated carbon (Calgon AP460). Figure 4.1 shows a simple flow chart where initially an acclimated bacterial solution was cultured from an activated sludge sample. The acclimated culture was then immobilized onto a batch of activated carbon to form BAC. The BAC was then used as the noval medium for H_2S biofiltration. Microbial diversity study and investigations to understand the removal mechanism using the BAC-based biofilters or biotrickling filters were then conducted.

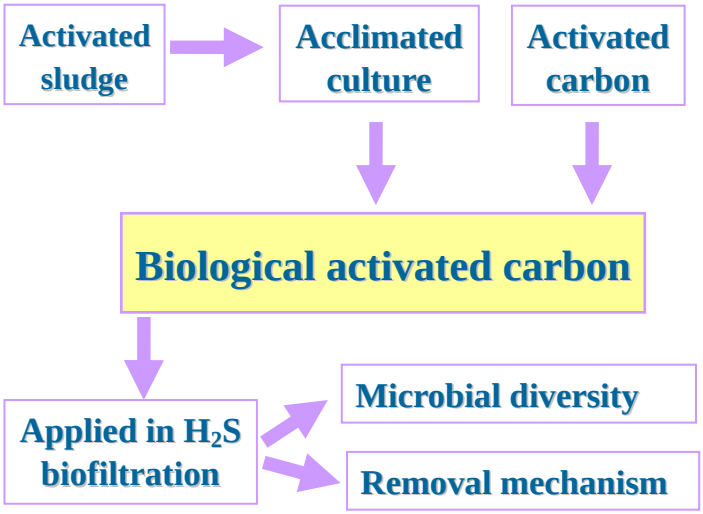

Figure 4.1 Flow chart of study on BAC application in biofiltration

4.1 Feasibility of Developing Biological Activated Carbon

As a well-known adsorbent and a supporting material for bacteria immobilization, activated carbon has been used alone or in combination with other material in a variety of biofiltration applications over the past decades. Nevertheless, the development of BAC for the purpose of treating odorous compounds (such as H_2S) in a biofilter has rarely been reported. By developing this BAC medium with some strains of bacteria immobilized onto the carbon surface, odorous compounds could possibly be firstly adsorbed by the activated carbon and then progressively released for microbial degradation. Therefore, the gas retention time (GRT) required for effective pollutant removal would be much shorter than those adopted by conventional biofilters. The BAC bed could then possibly be designed as small as an activated carbon adsorption tower. As the adsorbed compounds are embedded in the carbon pellet, the bacteria may have a longer time to degrade the "food" effectively. It is also expected that a well-developed BAC can treat odor more quickly and with a higher efficiency than a conventional biofilter.

Calgon AP460 is a grade of non-impregnated pelletized activated carbon with a neutral pH value (7.96). Although it has a lower H_2S adsorption capacity (5.5 wt.%) than alkaline activated carbon [22 wt.% (Yan et al., 2002), KOH impregnated], Calgon AP460 is more suitable for BAC development because of its lower pH as the *Thiobacillus* bacteria cannot grow in an alkaline environment. In addition, the favorable physical properties of Calgon AP460 (e.g. large external surface area, good water holding capacity, resistance to crushing, see Table 3.4) and the additional adsorption effect of carbon pore surfaces for odor removal, make it a good supporting media for bacteria immobilization. It is well known that the blockage of pores and interstices within/between carbon pellets by biomass/ metabolite is a concern in BAC development. A selection of carbon with a large

external surface area (like Calgon AP460) and certain bacteria would assist in minimizing the concern. *Acidithiobacillus sp.* is a chemolithoautotrophic bacterium that is known to produce less biomass or extracellular polymeric substances (EPS). Hence the potential to block the carbon pores is expected to be minimized. Therefore, *Acidithiobacillus sp.* was chosen as our interested bacteria species.

4.2 Biological Activated Carbon Production

According to Rafson's work (1998), the packing material should be normally inoculated prior to the system start-up in order to shorten the start-up and the acclimatization period. Three techniques for BAC production are investigated in this study. These include offline immersed immobilization, online immobilization in a biofilter and online immobilization in a biotrickling filter, depending on the types of biofiltration systems applied. The details of these three techniques are presented in this section.

4.2.1 Offline Immersed Immobilization

The offline immersed immobilization procedure is as follows: in a container, 1 volume of virgin activated carbon was immersed in 4 volume of acclimated activated sludge containing 10 $g \cdot L^{-1}$ thiosulfate at a pH of 7. After that, the container was put onto an auto-shaker and was continuously shaken at 120 rpm at room temperature. Since the biodegradation of reduced sulfur species produces hydrogen ion (H^+), the pH drop of the medium containing activated carbon and sludge would represent the growth of bacteria indirectly. The pH of the mixture was monitored daily and was adjusted using sodium hydroxide (NaOH) to 7 when it dropped to below 3. Sodium thiosulfate was added at a concentration of 10 $g \cdot L^{-1}$

each week to supply enough reduced sulfur. After 4 weeks of immobilization, a few pellets of carbon were taken out and viewed by using SEM. Figure 4.2 shows the carbon surface of an activated carbon pellet that does not have any bacteria grown on it, and Figure 4.3 shows the BAC surface formed by the immersed immobilization procedure. As shown, sulfide oxidizing bacteria (the rod shape cells sized about 1 μm) have been successfully immobilized on the carbon surface. The produced BAC pellets can be packed in a biofilter or biotrickling filter as and when they are needed.

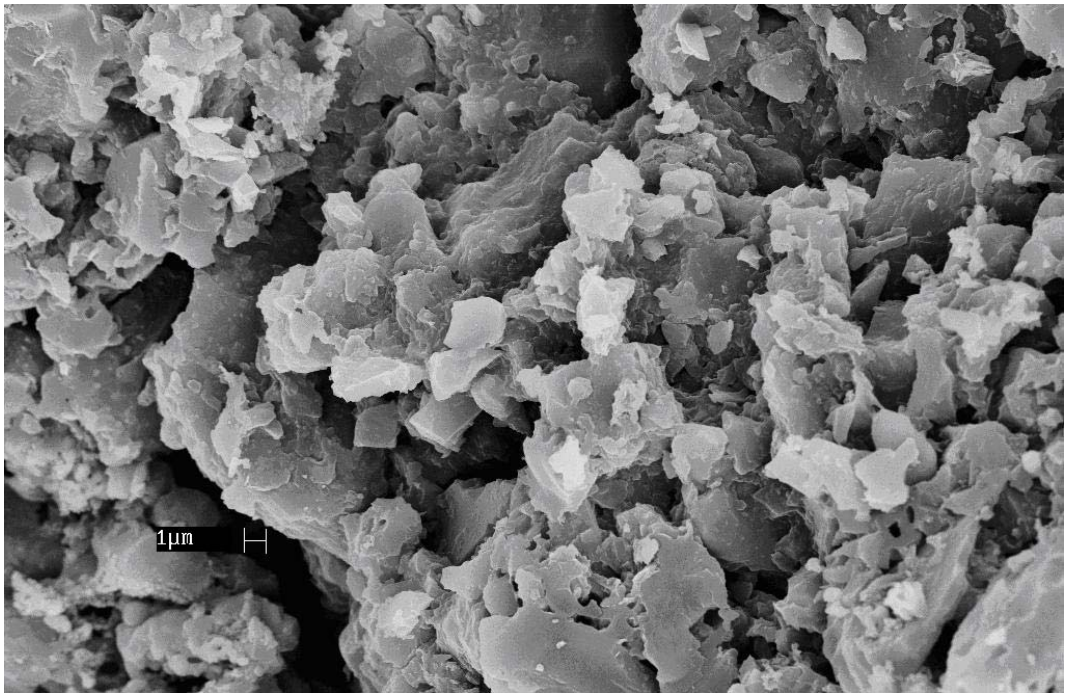

Figure 4.2 Activated carbon surface

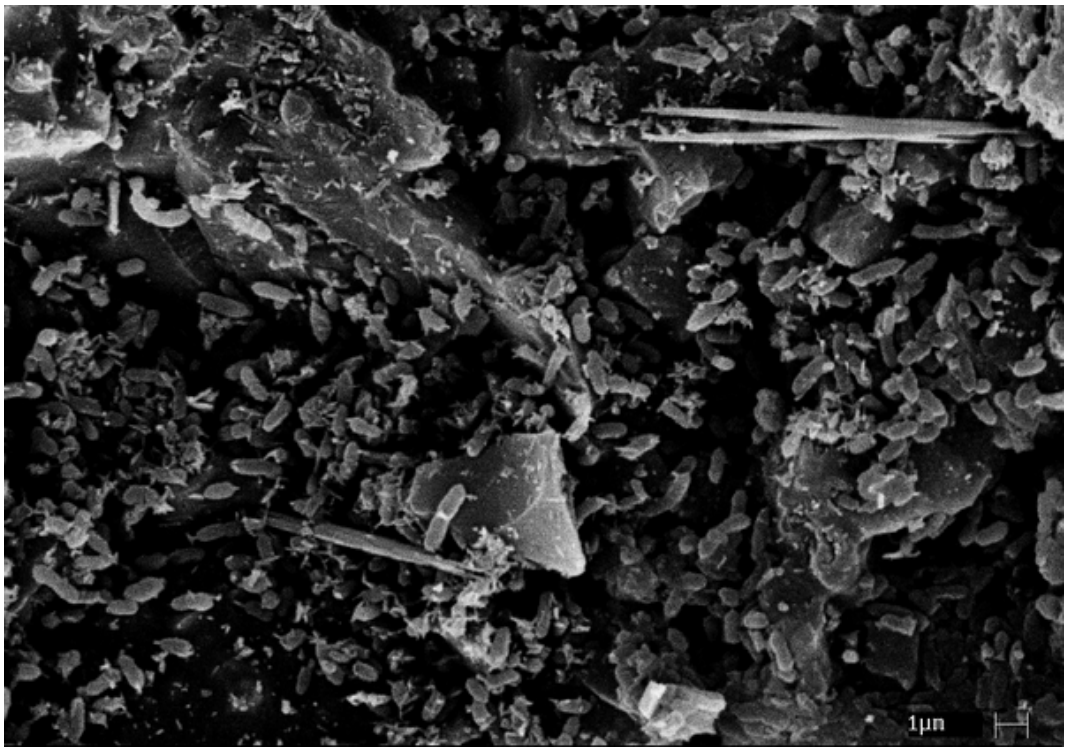

Figure 4.3 BAC surface formed by immersed immobilization

4.2.2 Online Immobilization in a Biofilter

In a full-scale application of BAC, it will be costly and impractical to provide huge culture containers for the immersion of the activated carbon for the production of BAC via off-line immersion as described in Section 4.2.1. Therefore, an alternative way of bacteria online immobilization was also investigated to provide the BAC needed for the biofilters in this study (details of configuration were descried in Chapter 5).

The online immobilization procedures used are as follows: the virgin activated carbon pellets were autoclaved and randomly stuffed into the biofilter bed to a designated height. A volume of acclimated activated sludge was added into 9 volumes of mineral medium (liquid medium without $Na_2S_2O_2 \cdot 5H_2O$, Table 3.1).

Then, 10 volumes of diluted sludge with a selective bacterial concentration was poured from the top of the biofilter bed to submerge the carbon bed completely. At the same time, a synthetic foul gas with a relatively low H_2S loading (< 15 $gH_2S \cdot m^{-3} \cdot h^{-1}$) was blown into the biofilter at a gas retention time of 21 s. The biofilter was then started and operated until stable removal efficiency for H_2S was obtained. The bacteria immobilization period lasted about 6 days. Samples of carbon pellets were taken from the middle of the biofilter bed after a run period of 16 days. The SEM photo of a sample is shown in Figure 4.4. As can be seen, a well-formed biofilm was evidenced over the carbon surface, and the production of BAC can be considered successful by this online immobilization method.

Figure 4.4 BAC surface after online immobilizing for 16 days in a biofilter

4.2.3 Online Immobilization in a Biotrickling Filter

Compared to a biofilter, a biotrickling filter has a continuous flow of liquid through the filter bed. Such a configuration provides a method for a continuous supply of the bacteria in the mobile phase (recirculation liquid) onto the packing bed.

In the horizontal biotrickling filter (HBTF) used in this study (to be introduced in Chapter 6), virgin activated carbon pellets were first packed randomly into all the segments of the HBTF. Sulfide oxidizing bacteria resources were obtained from acclimated activated sludge (See Section 3.1.2). An amount of 10 L of mineral resource with 2.03×10^{6} cfu·mL^{-1} of sulfide oxidizing bacteria concentration (counted by standard plate counting) was placed in the recirculation water tank. The sump was maintained at a volume of 10 L and the recirculation medium was refreshed by replacing 9/10 of total volume with fresh liquid medium (Table 3.1 but excluding TS) once every 4 days in order to maintain the bacteria concentration in the recirculation solution at a level of 10^{5}~10^{7} cfu·mL^{-1}. The flow rate of water stream was controlled at 2.4 L·min^{-1} and pH of the initial solution is ~4.5. At the same time, the synthetic foul gas with H_2S concentration of about 40~60 ppm_v was blown into the bed at a GRT of 16 s (H_2S loading 10~20 gH_2S·m^{-3}·h^{-1}), and the GRT was decreased stepwise to 6 s while keeping the inlet concentration within the range stated above. The H_2S removal efficiency stayed at almost 100% in the first 25 days of operation due to the carbon adsorption. Figure 4.5 shows the BAC surface after a run time of 60 days in this HBTF, and indicates that a satisfactory layer of biofilm has been formed over the carbon surface.

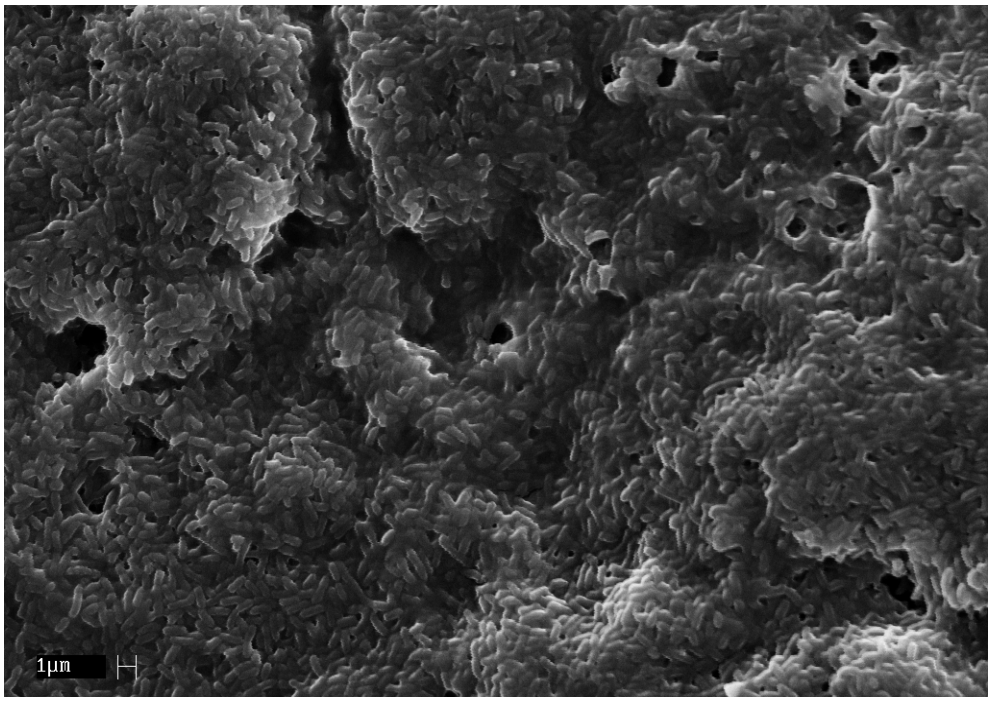

Figure 4.5 BAC surface after working for 60 days in a HBTF

The three different immobilization techniques investigated here show that any one of them will allow satisfactory immobilization of bacterial culture onto the surface of activated carbon pellets. BAC can hence be successfully produced by any one of the three methods. In general, there are a number of factors possibly influencing the performance of BAC in the course of biofilm formation on carbon surface such as thickness of biofilm and pore blockage of carbon. This point has not been explored in detail here as the focus of this study is the BAC application in a biofilter/ biotrickling filter, and understanding the mechanisms related to using BAC in the removal of H_2S. The optimized generation of BAC could be further studied in the future.

CHAPTER 5
USE OF BIOLOGICAL ACTIVATED CARBON IN A BIOFILTER TREATING H_2S

In this chapter, a laboratory-scale cylindrical biofilter system was set up to investigate the performance of BAC comprehensively (e.g. elimination capacity, removal efficiency). Various operating parameters were studied including H_2S inlet concentration, GRT, gas flow rate, and frequency of system irrigation, etc. Spent activated carbon (saturated with H_2S) was also investigated, targeting at the potential re-use or bio-regeneration. This study also looked into the biofilm and microbial diversity profiles in a biofilter for H_2S removal. At the end of the biofilter experimental run, packing material (BAC) at the top, middle and bottom sections of the biofilter were taken out for microbial analysis. SEM was used to observe the biofilm development on the activated carbon. The microbial communities in these three sections of the biofilter were examined by 16S ribosomal DNA based PCR denaturing gradient gel electrophoresis (DGGE).

5.1 Experimental Section

5.1.1 Biofilter System

A laboratory-scale biofilter system was designed and constructed. It consisted of parallel dual vertical columns, which could be operated simultaneously and

controlled separately (Figure 5.1). The packing material (Calgon AP460) was placed in a transparent and rigid Perspex tube, which has an inner diameter of 3.6 cm and a height of 30 cm. The carbon bed was packed inside the tube to a height of 20 cm and yielded a 0.2 L of packing volume. The packed material was supported by a plastic sieve plate to ensure a homogeneous distribution of the inlet gas across the bed. In this work, columns A and B are distinguished by whether the carbon bed is immobilized with bacteria or not. The composition and physical properties of the columns are summarized in Table 5.1.

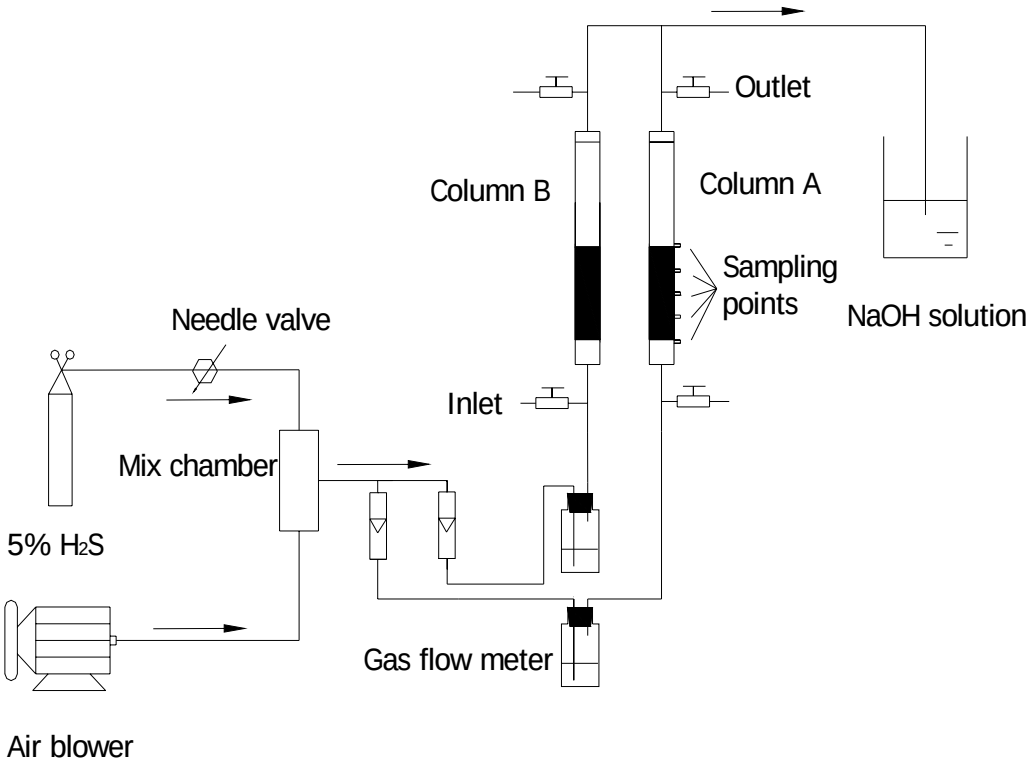

Figure 5.1 Schematic diagram of bench-scale biofilter system

Table 5.1 Physical properties of the biofilter columns

Physical Property	Column	
	A	B
Bacteria immobilization	With	Without
Wet carbon weight, W_1 (g)	183.4	181.6
Dry carbon weight, W_2 (g)	105.6	106.9
Moisture content, $m = (W_1-W_2)/W_1$ (%)	42.4	41.1
H_2S adsorption capacity, (wet weight basis, w/w%)	20.08[a]	0.44[b]
Diameter of column (cm)	3.6	3.6
Carbon surface area, $m^2 \cdot g^{-1}$	807	807
Diameter of carbon pellet (mm)	4	4
Height of media in each column, L (cm)	20	20
Volume of packing, V (L)	0.2	0.2
Bulk density, $d = W_1/V$ ($kg \cdot m^{-3}$)	917	908
Apparent density of activated carbon, ρ ($kg \cdot m^{-3}$)	490	490

a. H_2S consumption capacity for 100 days' biofilter running time;

b. H_2S exhausted capacity.

Sampling ports are located along the column for gas sampling and pressure measurements. The individual sampling ports are identified based on their locations along the biofilter column as inlet, 5 cm, 10 cm, 15 cm and outlet ports. The humidified air stream was prepared by blowing air through a gas wash bottle that contains water (the humidification chamber). Moreover, the bed was irrigated twice a day by submerging the bed in culture medium for 10 min and then releasing the solution. The desired H_2S inlet concentration was adjusted by the needle valve at the outlet of the 5% H_2S gas cylinder (balanced in N_2, Linde Gas Singapore Pte Ltd). Foul gas (containing various concentrations of H_2S) flow rates were controlled and measured using AALBORG (Orangeburg NY, USA) flow meters with units of $L \cdot min^{-1}$ located at the inlet of the wash bottle, blowing upward from the bottom inlet into the biofilter. Two additional pressure ports were installed at the top and bottom of the column in order to measure the pressure drop by a water manometer with a minimum reading of 1-mm water column. The column was sealed with fitted rubber

stoppers. The rubber stopper on the top of the column is removable so that water and mineral sources can be introduced into the filter material to maintain sufficient moisture and mineral nutrient contents in the bed. All the gas lines were 1/4-inch diameter Teflon tubing. The system was operated at room temperature of about 25 °C throughout all the experimental runs.

5.1.2 Bacteria Immobilization

An online immobilization (refer to Section 4.2.2) was adopted to start the biofilter in this study, and the procedures as follows: Virgin activated carbon pellets were autoclaved and stuffed into both columns randomly. A 5 mL of concentrated microbial broth was added into the 45 mL fresh mineral medium (liquid medium without $Na_2S_2O_3 \cdot 5H_2O$, Table 3.1). Then, 50 mL bacteria solution with a bacteria concentration of 1.96×10^8 cfu·mL^{-1} was poured from the top of the column A to submerge the carbon bed with 5mm water level above it. For column B, the control column, 50 mL distilled water was used instead of bacteria solution. At the same time, the synthetic foul gas with a low concentration of H_2S (about 20~50 ppm_v) was blown into both packing columns. The feed of H_2S provided energy source for the bacteria to grow. Upon completing the immobilization and acclimatization stage, the system was deployed for performance evaluation of BAC. The operating conditions during this period are tabulated in Table 5.2.

Table 5.2 Operating conditions for both columns

Operating Parameter	Range
Gas retention time (seconds)	3~ 21
Inlet H_2S concentration, C (ppm_v)	5 ~ 100
Gas flow rate, Q_g (L·min^{-1})	0.57~ 4
Superficial foul gas velocity, v (cm·s^{-1})	0.95~6.67
pH of the column	1.0 ~ 2.0

5.2 System Performance Evaluation

5.2.1 Performance during Startup Period

Figure 5.2a and Figure 5.2b shows the performance of the two biofilters during the initial 21 days of operation. Analysis of the H_2S removal performance during the startup period phase (GRT was adjusted to 21 s, Figure 5.2a) revealed that the removal efficiencies (RE) started to increase after 1 day of operation to reach a value of 90% for column A which contained the BAC, and 70% for column B which contained virgin carbon, about 6 days into the experimental run. The pH of the BAC declined to a value of 2 after 4 days of operation. The increase in RE correlated with the decline of pH, due to the production of H^+ and sulfate from the oxidation of H_2S. Acclimation lasted around 6 days, after which the H_2S RE remained high for the remaining duration of the study. H_2S inlet concentrations ranged from 10 to 125 ppm_v during the experimental run. Based on the data obtained, it can be considered that the biofilter with the BAC was ready for use after 6 days of startup period (Figure 5.2).

In Figure 5.2b, although a highly fluctuating inlet concentration was repeatedly observed during the 21 days of running time, the biofilter system was robust enough to consistently absorb and treat incoming H_2S with variable concentrations of 10~125 ppm_v. In order to confirm the formation of a suitable layer of biofilm on the carbon surface, a sample pellet of BAC was taken out from the middle of the media bed for analysis on the 16^{th} day of operation. The surface characteristics of the sample were determined by SEM. From the SEM photograph shown earlier in Figure 4.4, it can be seen that a biofilm containing rod shape bacteria is formed on the carbon surface. Dominant sulfur oxidizing bacteria species in this system was identified as *Acidithiobacillus Thiooxidans* (Section 3.1.5)

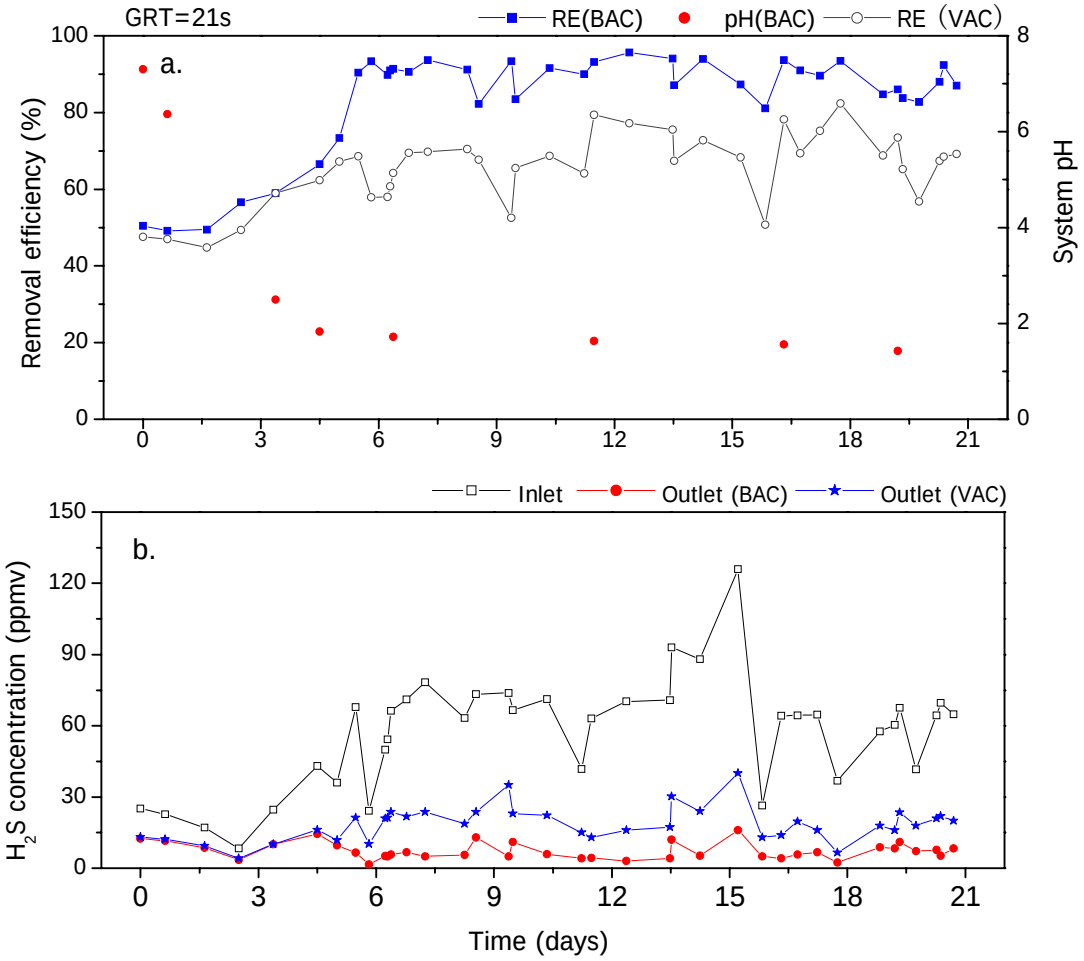

Figure 5.2 Performance of biofilter bed during the start-up period

a. Removal efficiency and pH vs. time; b. Inlet and outlet concentrations vs. time

During the startup period, the activated carbon pellets used in both column A and B had been soaked in a liquid medium (either bacterial solution for column A or water for column B). The water content of the wet carbon pellets averaged about 56 wt.%. As the existence of a water layer around the medium used in a biofilter would inhibit mass transfer of contaminants from the gas phase to the biofilm (Li et al., 2002a), it is hence not surprising that the average removal efficiency of the BAC biofilter in column A is less than 94%.

5.2.2 Long-term Performance

After 21 days startup period, the excess culture liquid medium was drained off, and another 79 days was taken to evaluate its long-term performance. During this period, the biofilters were irrigated twice per day to maintain the system moisture (refer to Section 5.1.1). Long-term performance of the biofilter trial is reported in Figure 5.3, expressed in the form of elimination capacity vs. loading rate. Pollutant loading rate is an important variable in a biofilter design. In this study, the loading rate changes were the result of the fluctuations in H_2S inlet concentration and the velocity of the influent gas when flow rates were varied. The biofilter containing the BAC consistently degraded more than 97% of the incoming H_2S loading when loading rate was less than 120 g $H_2S \cdot m^{-3} \cdot h^{-1}$ (Figure 5.3). At a loading rate above 120 g$H_2S \cdot m^{-3} \cdot h^{-1}$, the breakthrough of the BAC occurred, whereas a quasi-zero-order degradation regime was observed at loadings over 150 g$H_2S \cdot m^{-3} \cdot h^{-1}$, with RE gradually decreasing. The elimination capacity of BAC can reach 120 g$H_2S \cdot m^{-3} \cdot h^{-1}$ at a GRT of 2 s, higher than the maximum value (110g $H_2S \cdot m^{-3} \cdot h^{-1}$) previously reported at GRT around 2 s (Gabriel and Deshusses, 2003b). At a volumetric loading of 1600 $m^3 \cdot m^{-3} \cdot h^{-1}$ (87 ppm_v H_2S inlet concentration), a maximum elimination capacity of the BAC (181 g$H_2S \cdot m^{-3} \cdot h^{-1}$) at a RE of 94% was achieved.

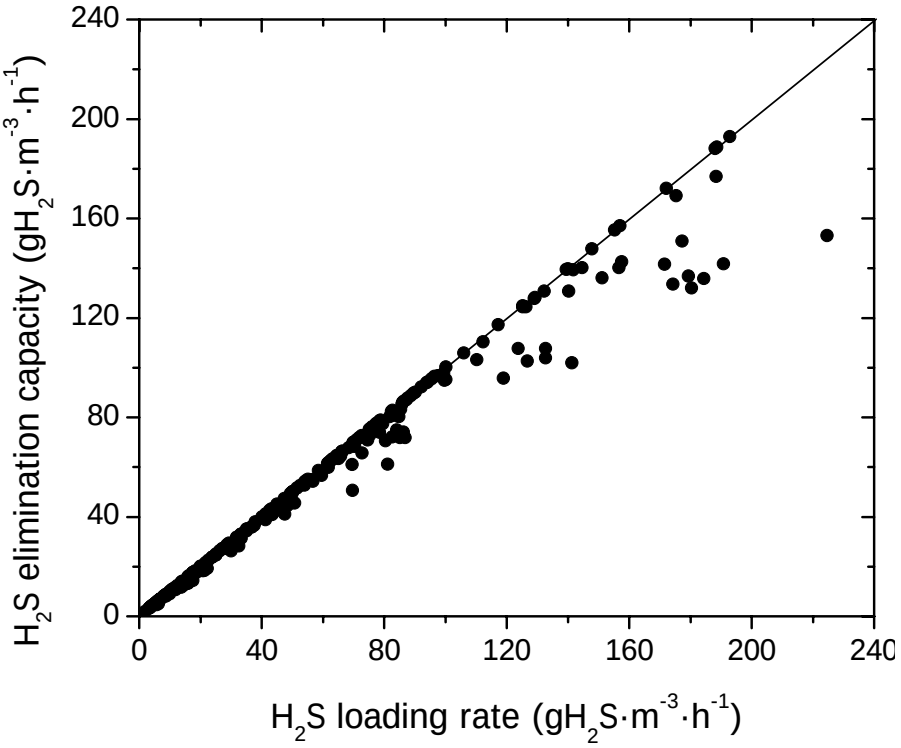

Figure 5.3 H_2S elimination capacity with loading rate at various gas retention times (from 2 to 21s)

The relationship between the inlet H_2S concentration, GRT, and H_2S removal efficiency is shown in Figure 5.4. The H_2S concentrations varied from 20 ppm_v to 100 ppm_v and at each H_2S setting, the GRT for the biofilter was changed from 6 to 1 s. BAC can work efficiently at a GRT of 4s or above in spite of the changes in the influent concentrations of H_2S. Reducing GRT further (< 4 s) as expected resulted in lower H_2S removal. Even so, removal efficiencies of 98% were commonly reached for inlet H_2S concentrations as high as 30 ppm_v when the system was operated at GRT as short as 2 s. Such performance is exceptionally high compared to other biofilters removing a low concentration of H_2S even at longer gas retention times (Sublette and Sylvester, 1987; Burgess et al., 2001; Koe et al., 2001; Wu et al., 2001). For most local wastewater treatment plants, H_2S concentration in the sewage air stream is typically less than 30 ppm_v. Hence, biofilters packed with BAC should be able to perform efficiently and can even remove H_2S effectively at short GRTs of as low as 2 s.

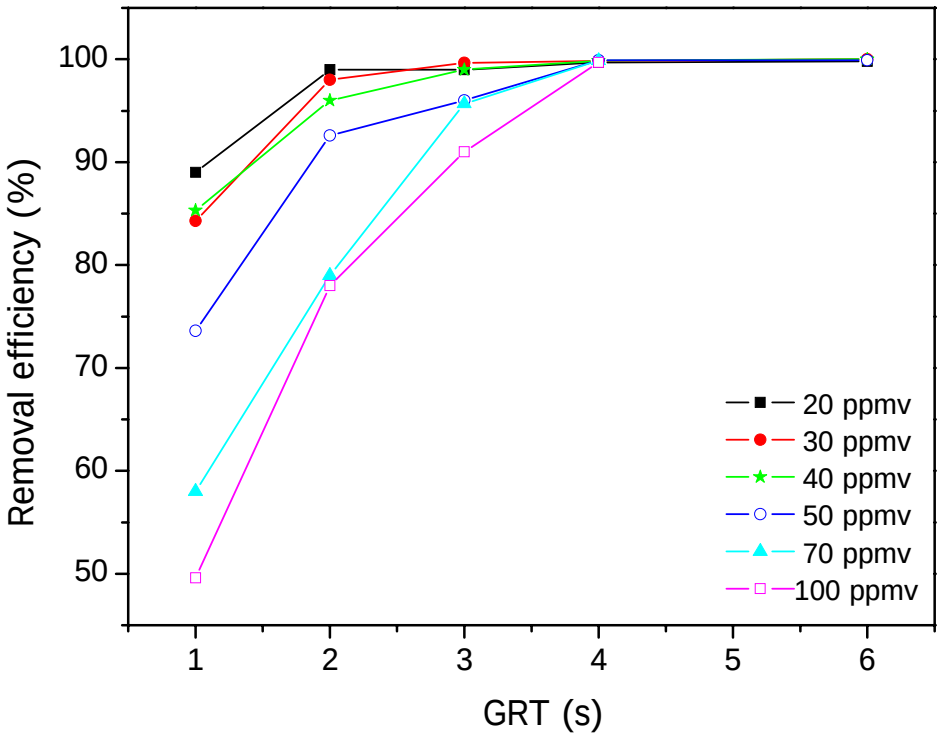

Figure 5.4 Biofilter performances under various H_2S inlet concentrations and gas retention times

Both the mass transfer rate and the bacteria utilization rate of H_2S should affect the H_2S biodegradation. As it was previously reported that H_2S could be metabolized by *Thiobacilli* within 1~2 s (Islander et al., 1991), the reduction of H_2S removal efficiencies under shorter GRT was most likely not due to the insufficient reaction time between the H_2S molecules and biomass, but due to the slower H_2S diffusion from the gas into the biofilm.

5.2.3 Biological Activated Carbon vs. Virgin Activated Carbon

Figure 5.5 shows the comparison of BAC and virgin activated carbon (VAC) on H_2S removal. H_2S RE of the VAC (the control column B) dropped sharply after working for 34 days, while the RE of the BAC could be maintained at a high level of over 99% for most of the time. H_2S removal capacity of VAC was then calculated based on 34

days of control column operation, and it was found that VAC had removed about 0.49 wt.% (wet weight basis) of H_2S in this control column. This value is close to the H_2S breakthrough capacity (0.44 wt.%, wet weight basis) of the VAC. For comparison with the capacity of the BAC to remove H_2S, the results indicated that the BAC had removed H_2S of 20.08% (wet weight basis) after operating for about 100 days and the biofilter was still capable of removing additional H_2S. The results primarily proved that BAC has an excellent performance on H_2S removal, and also, BAC could extend the life span of activated carbon.

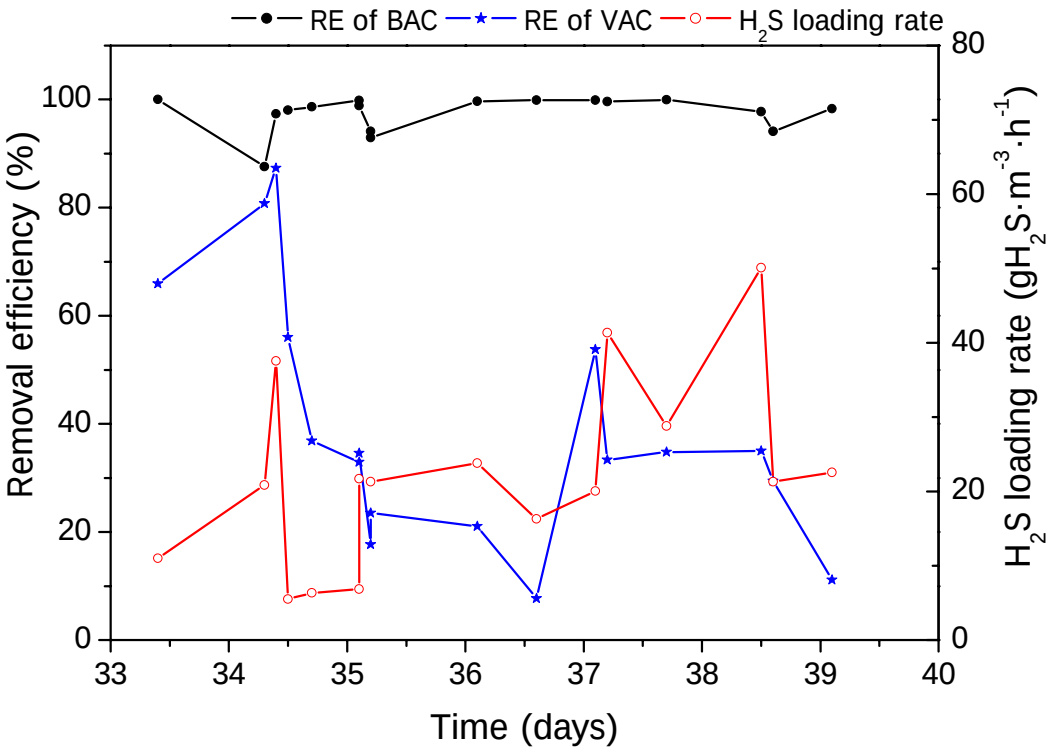

Figure 5.5 BAC vs. VAC on removal efficiency

5.2.4 Some Factors Influencing Performance

There are some limitations observed in this system. First, the accumulation of sulfate and excess biomass in the packing bed are problems frequently encountered. During the operation of the biofilter, white deposits were observed on the carbon surface, and the color of the bed progressively changed from black to whitish yellow from the bottom of the bed to the upper carbon layers. The rate of deposition seemed proportional to the rate of H_2S loading. A sudden increase in H_2S loading over a wide concentration range and prolonged operation at high H_2S loading rates caused the white-colored material to accumulate rapidly. This discoloration of the bed was companied by a rapid drop of the bed pH.

Extremely high system acidity was found to be harmful to the microorganism niche. In this study, active cell number in the microorganism niche dropped quickly when the system pH was below 1. The optimal pH of the sulfide oxidation mixed culture is 5.5 (Section 3.1.6). However, the average pH of the biofilter is about 1~2, the range within which high RE can still be achieved. Although low pH doesn't assist H_2S adsorption, it provides favorable conditions for the sulfide oxidization (Gabriel and Deshusses, 2003b). Further studies are needed to understand better the effect of low pH in BAC biofilters. The accumulation of sulfide biooxidation products, including sulfur, sulfate, thiosulfate, etc., may inhibit the system performance, and so does biomass. Dead cells and sulfide oxidation products accumulated on the packing could block the carbon surface pores and the pathway of gas stream thus causing the biofilter to be less efficient in pollutant removal.

Secondly, the bed was found to dry out easily unless it was irrigated periodically (e.g. twice per day as in this study) as the correct moisture content of biofilter media is another key parameter necessary for its good performance. Too high a moisture level will inhibit the mass transfer from the gas phase to the biofilm or adsorption surface

of the carbon. On the contrary, drying out of the media will definitely harm the healthy growth of microorganisms that are immobilized on the supporting media surface (Morales et al., 2003). Control of moisture requires an understanding of the drying of the packing media due to the changes in inlet air temperature and relative humidity, and also from metabolic heat production by pollutant oxidation.

The accumulation of excess biomass and oxidizing products, e.g. sulfur, could be reduced by periodic washing the media bed by water irrigation. This irrigation could also help maintain the moisture content of the packing bed for the development of a healthy biofilm. Washing the system with 50 mL deionized (DI) water for 10 min could remove about 40% of sulfate accumulated in the carbon bed, but it can only increase the pH by 0.1~0.2 units. Mohseni et al. (1998) reported that the activated carbon could become fouled with biomass after the startup of the biofilter system for a mixture of wood chips and spent mushroom compost amended with activated carbon. Similar phenomenon was also found in our peer study that applied *Pseudomonas sp.* on BAC to treat toluene (Koe and Liang, 2005). Nevertheless, such phenomenon was not found in this study. It is probably is due to the fact that H_2S degraders are mostly autotrophs and results in far less biomass production than heterotrophic VOC degraders.

5.2.5 Using Spent Activated Carbon as Packing Material

Spent carbon might be re-used and bio-regenerated by immobilized bacteria through the consumption of the H_2S molecules previously adsorbed in the activated carbon. One H_2S-exhausted carbon column was used to verify this hypothesis. Similar bacteria immobilization procedure was used for the exhausted carbon, followed by the biofilter performance evaluation. The results are shown in Figure 5.6. The initial pH of the spent activated carbon (SAC) is 2.5 compared to a pH of 7.96 for the VAC.

After an initial immobilizing period of 6 days (which is the same immobilization period as used for VAC) at a GRT of 24 s, the GRT was reduced to 12 s and then 6 s by increasing the gas flow through the biofilter. It was found that the BAC derived from the SAC work almost as well as that from the VAC. H_2S loading can reach as high as 125 $gH_2S \cdot m^{-3} \cdot h^{-1}$ at the 98% removal efficiency level. However, it needs at least a 6 s GRT to achieve a RE over 98%. The BAC generated from SAC is far from exhausted after 55 days of operation. Periodically the RE of the biofilter drops when the media bed dries out or clogging occurs. The results indicate that it is possible to develop BAC based on spent activated carbon. This could be a potential solution for the re-use of activated carbon in industrial application.

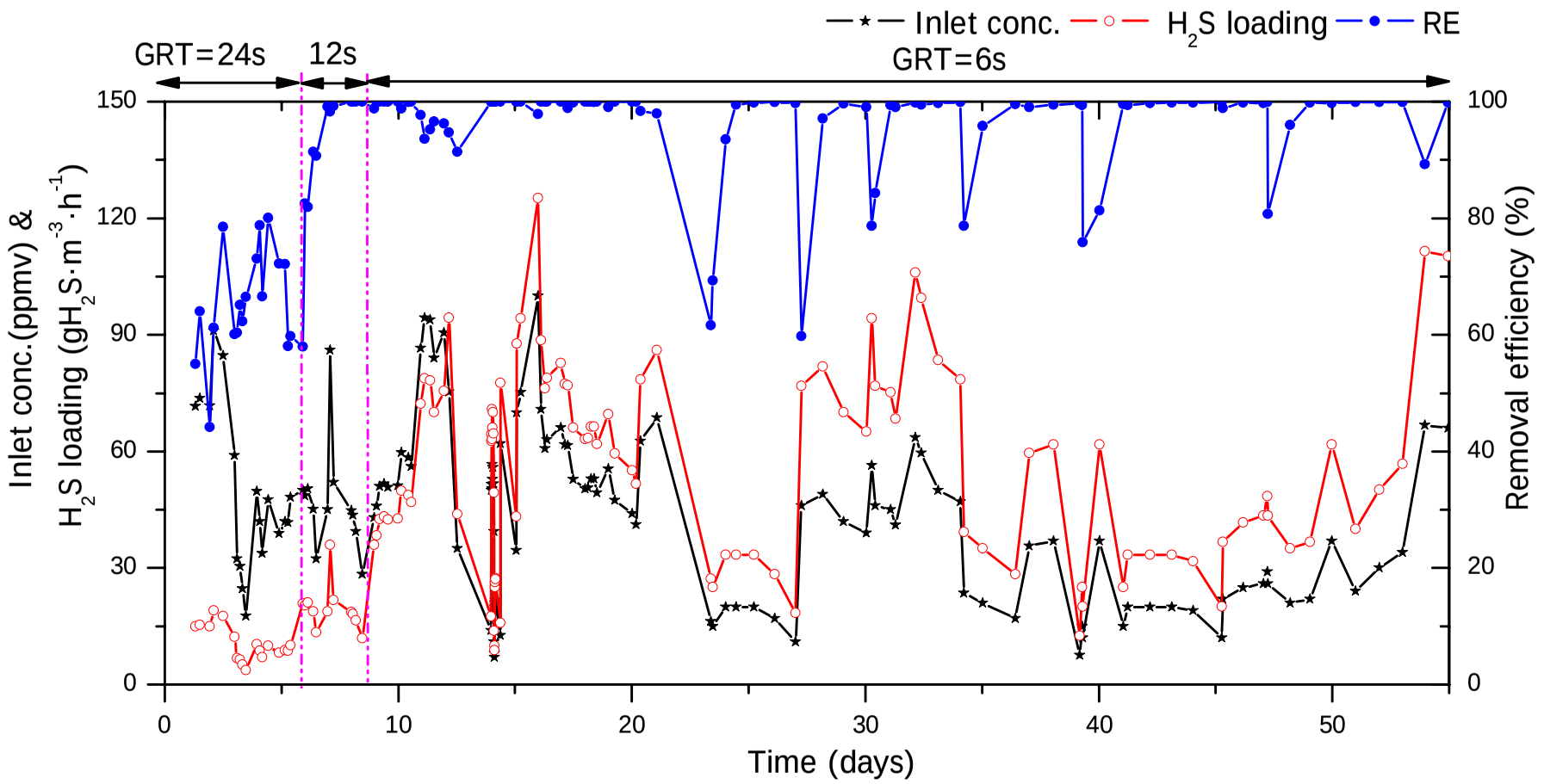

Figure 5.6 Performance of BAC developed from spent activated carbon

(H_2S saturated carbon)

5.3 Biofilm Identification

At the end of the biofilter (column A with BAC) operation, a sample of the BAC from the top, middle and bottom sections of the biofilter were taken out for microbial analysis. The results are presented here.

5.3.1 Biofilm Morphology

Scanning electron microscopy was performed to observe the microbial growth on the carbon surface. As shown in Figure 5.7, the bottom and the middle sections of the packing materials retained a thick layer of biofilm while the top section only had the bacteria growth in discrete form. White solid substances appeared with the biofilm from the sample taken from the bottom portion of the biofilter (Figure 5.7c). The pathway of sulfide biological oxidation by chemoautotrophs is suggested as: $H_2S \rightarrow S^0 \rightarrow S_2O_3^{2-} \rightarrow S_4O_6^{2-} \rightarrow S_3O_6^{2-} \rightarrow SO_3^{2-} \rightarrow SO_4^{2-}$ (Maier et al., 2000). High concentration of H_2S at the inlet caused the bacteria communities to be overfed so that H_2S may not be biological oxidized thoroughly. The yellowish white deposits on the carbon bed are likely to be the incomplete oxidation products of sulfide. In the middle of the bed, a well-formed biofilm with little white deposit was developed over the carbon surface (Figure 5.7b). A possible explanation is that the H_2S loading rate in the middle of the bed is comparable to the biodegradation rate which results mainly in sulfate, the complete oxidation product. Sulfate is soluble to water and can be washed off the bed by the irrigating medium. The discrete biofilm formed at the top of the bed is probably due to the low H_2S available at outlet portion of the biofilter (Figure 5.7a).

a. SEM photograph of the BAC on the top of the bed

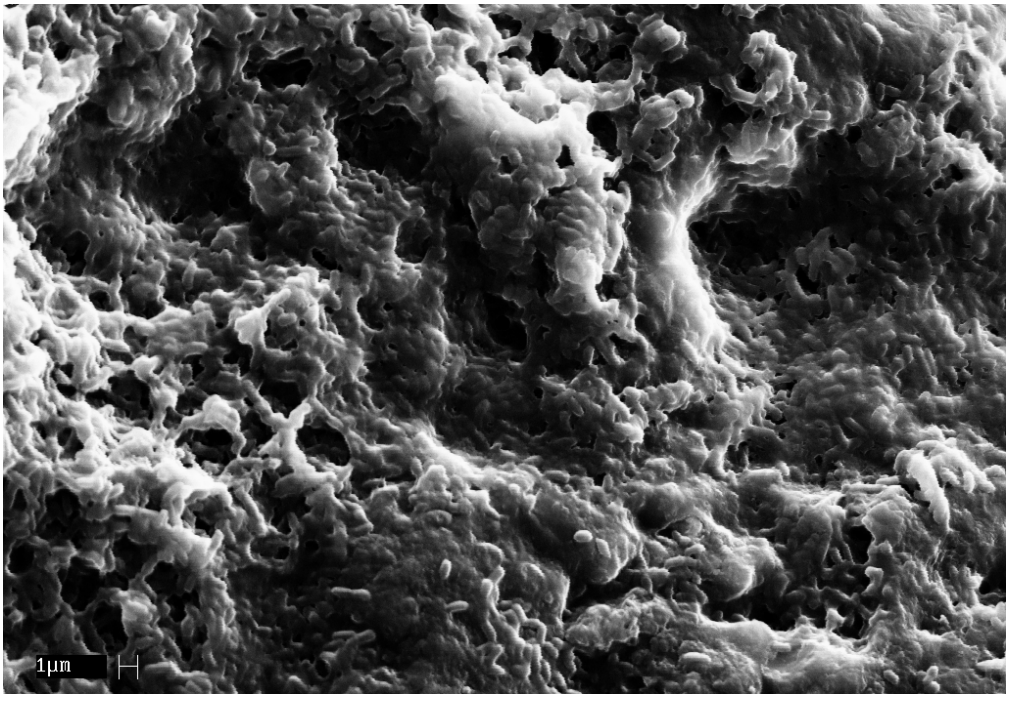

b. SEM photograph of the BAC in the middle of the bed

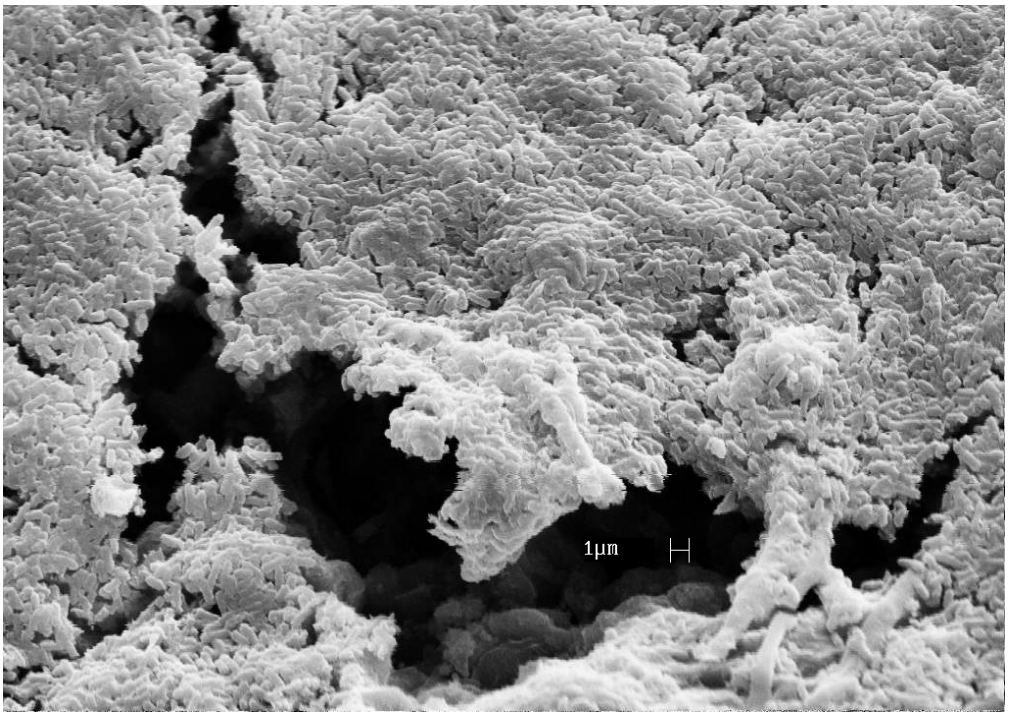

c. SEM photograph of the BAC at the bottom of the bed

Figure 5.7 Biofilm profiles on the carbon bed

5.3.2 Microbial Diversity Profiles

The fast growing bacteria in the microbial communities in the three sections of the biofilter were isolated and examined by 16S ribosomal DNA based PCR denaturing gradient gel electrophoresis (DGGE) as shown in Figure 5.8. One band stands for a strain of bacteria and the degree of darkness of the band indicates the relative cell concentration indirectly. As seen from Figure 5.8, there are at least 5 strains of bacteria with distinguished concentrations at the bottom of the bed, while for the sample taken at the middle and at the top of the biofilter bed, there are only 2 strains. The results show that the most active part of the system is at the bottom of the bed which is the inlet zone of the biofilter because more strains of bacteria are active in this zone. From the DNA identification, it was confirmed that the dominating bacteria are *Acidithiobacillus Thiooxidans* (Section 3.1.5).

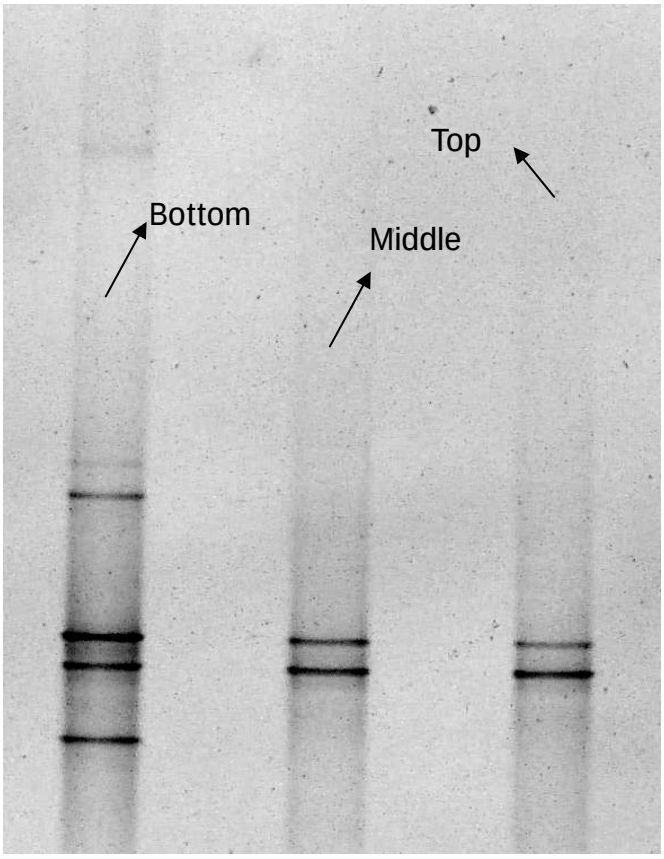

Figure 5.8 DGGE profiles of the PCR amplified 16S rDNA extracted from the carbon bed

Cultivable chemolithoautotrophic bacteria numbers and heterotrophic bacteria numbers were determined by plate-count method using TS agar plates and R_2A agar plates (used for culturing or counting heterotrophic bacteria), respectively. As Table 5.3 shows, the heterotrophic bacteria concentration increased from the top to the bottom whereas the chemolithoautotrophic bacteria were concentrated mainly in the top and middle sections. This may be due to the difference of oxygen supply. At the bottom of the bed, oxygen may not be sufficient for a large population of bacteria so that restrict chemolithoautrophic population growth and boost up heterotrophic bacterial growth. It can be concluded that the microbial community was dominated by heterotrophic species in the bottom half of the bed while chemolithoautrophic bacteria dominated on the top half. The biofilter bed is more acidic at the bottom half than top, which is due to more H_2S adsorbed and biodegraded at bottom of the bed to

produce more H^+. It can be seen that the ratios of mold to bacteria are increased from top to bottom because the acidic environment favored the growth of mold. The mold population increased from the top to bottom due to the decrease of pH from the top to the bottom.

Table 5.3 Cultivable heterotrophic vs. chemolithoautotrophic bacteria

Bed Sections	Heterotrophic		Chemolithoautotrophic	
	Bact. Conc. (cfu/cm^3 of packing)	Mold: Bacteria	Bact. Conc. (cfu/cm^3 of packing)	Mold: Bacteria
Top	400	1:1	2.7×10^6	N/A
Middle	5600	3.5:1	5.5×10^6	N/A
Bottom	34000	17:1.5	1.7×10^5	N/A

5.4 Conclusions

The performance of the bench scale biofilter trial showed that the BAC demonstrated a better performance than non-bacteria activated carbon as an odor adsorbent. Activated carbon was an excellent microorganism carrier in biofiltration suitable for the treatment of H_2S. Microorganisms immobilized on activated carbon were capable of extending the activated carbon's capacity and life span. Most of earlier studies on non-BAC biofilters require 10~30 s of GRT to achieve efficient removal of 20~100 ppm_v of H_2S, resulting in the elimination capacity of 110 $gH_2S\cdot m^{-3}\cdot h^{-1}$ or less. In this biofilter study, BAC could achieve a better performance with a short online immobilization period of 6 days, and a low GRT of up to 2 s particularly for low inlet concentration. Elimination capacity as high as 181 $gH_2S\cdot m^{-3}\cdot h^{-1}$ is achievable and the high performance could be maintained for at least 100 days of biofilter run. In addition, the use of spent activated carbon is also a possible medium that can be used

as a bioreactor packing material. This could possibly be a potential solution for the reuse of spent carbon in the industry.

Regarding the microbial community, the H_2S degrading bacteria can grow and form a satisfactory biofilm on the carbon surface for efficient removal of H_2S. Due to the different environment from the top to the bottom of a biofilter (e.g. oxygen supply, pH, etc.), the microbial niches at different position of the bed are diverse. The dominant bacterial population is *Acidithiobacillus Thiooxidans* identified by DNA sequencing. Classified by metabolism type, the microbial community is dominated by heterotrophic species in the bottom half (inlet portion) of the bed while chemolithoautrophic bacteria dominates that on the top half (effluent portion) of the bed. Mold concentrations increase with the decrease in pH in this biofilter.

From the above results, it can be seen that although both of the H_2S adsorption capacity and adsorption rate of the activated carbon were affected by the biofilm formation, the BAC could still provide an attractive, nutrient-rich environment for bacteria growth because of its good water holding capacity, large external surface area and H_2S adsorption capacity. The combined effects of carbon adsorption and biofilm degradation of H_2S enabled the BAC biofilter to achieve a better performance than those packed with non-bacteria activated carbon alone.

CHAPTER 6
USE OF BIOLOGICAL ACTIVATED CARBON IN A HORIZONTAL BIOTRICKLING FILTER

Whilst biofilters have been used successfully for odor abatement for many decades, the use of biotrickling filters for odorous air treatment is relatively new (Devinny et al., 1999). This Chapter discusses the use of the newly developed BAC in the biotrickling mode. In biotrickling filters, polluted air is passed, together with a recycled liquid, through a packed bed on which a pollutant-degrading biofilm develops. The reaction products are washed out of the medium and acidification of the media bed can thus be avoided. Therefore, biotrickling filters can offer superior performance over biofilters (Mpanias and Baltzis, 1998; Fortin and Deshusses, 1999). In addition, the presence of a free trickling liquid phase in the biotrickling system allows a better control of operation conditions.

The application of BAC in biological deodorization processes has rarely been investigated though our previous study (Koe et al., 2004; also summarized in Chapter 5) reported its excellent performance in a biofilter for H_2S removal. The excellent performance in treating H_2S as observed in our previous study shows the suitability of using BAC as a packing material. However, some critical obstacles of using BAC-packed biofilters in H_2S treatment remained. These include sulfur and biomass accumulation, and packing bed acidification. With continuous washing out of reaction products, a biotrickling filter may overcome these obstacles, facilitating

broader application of the BAC medium.

6.1 Why Horizontal Design

So far, many researchers have reported their work on traditional vertical biotrickling filters with co-current or counter-current flow (Chou and Huang, 1997; Kennes and Veiga, 2001; Wu et al., 2001; Cox and Deshusses, 2002b). Studies on cross-flow horizontal biotrickling filters (HBTFs) are rarely reported. As some WWTPs still use horizontal chemical scrubbers, information on HBTF performance will be useful when these horizontal chemical scrubbers are to be converted into biotrickling filters. A horizontal design is also expected to work well with a relatively low pressure drop compared to a vertical design (Zhou, 2000), particularly if a dense packing material (e.g. BAC) is used. In this chapter, a bench-scale cross-flow HBTF packed with BAC was set up to evaluate the suitability of using the novel BAC medium for H_2S treatment. The influence of a series of variable operation parameters [pH, sulfate accumulation, upset and recovery, pressure drop, gas-liquid (G-L) ratio, and shock loading] on the performance of the biotrickling filter were evaluated to achieve acceptable H_2S removal efficiencies, and are discussed to provide a better understanding of the process.

6.2 Experimental Section

A bench-scale HBTF system was used (Figure 6.1). The packing material (Calgon AP460) was placed in the three segments (shaded in Figure 6.1), each with dimensions of 15×15 cm with 10 cm in length. The three carbon compartments were sealed by gas tight silicon gel to the filter shell on the top and bottom to prevent the foul gas from bypassing the beds via the top or bottom air plenums. The general

properties of the bed are summarized in Table 6.1. The air stream was directed from left to right through the packing bed while the recirculation solution stream trickled down from the top of each segment. The desired H_2S inlet concentration was adjusted by mixing standard 10% H_2S gas (supplied by Soxal Gas, Singapore) with air supplied by an air blower. Four sampling ports are located along the bed from left (inlet) to right (outlet) of the biofilter for gas sampling and pressure measurements. The leftmost port is regarded as the inlet sampling port and the other three as outlet sampling ports (labeled 2 in Figure 6.1). The bed pressures at different sampling ports were measured using a water manometer capable of providing a minimum reading of 1-mm water column. Water samples were taken periodically for pH measurement, chemical analysis and viable bacterial counts. These analyses were carried out in accordance to the procedures described in Chapter 3. The system was operated at room temperature (~25 °C) throughout all the experimental runs.

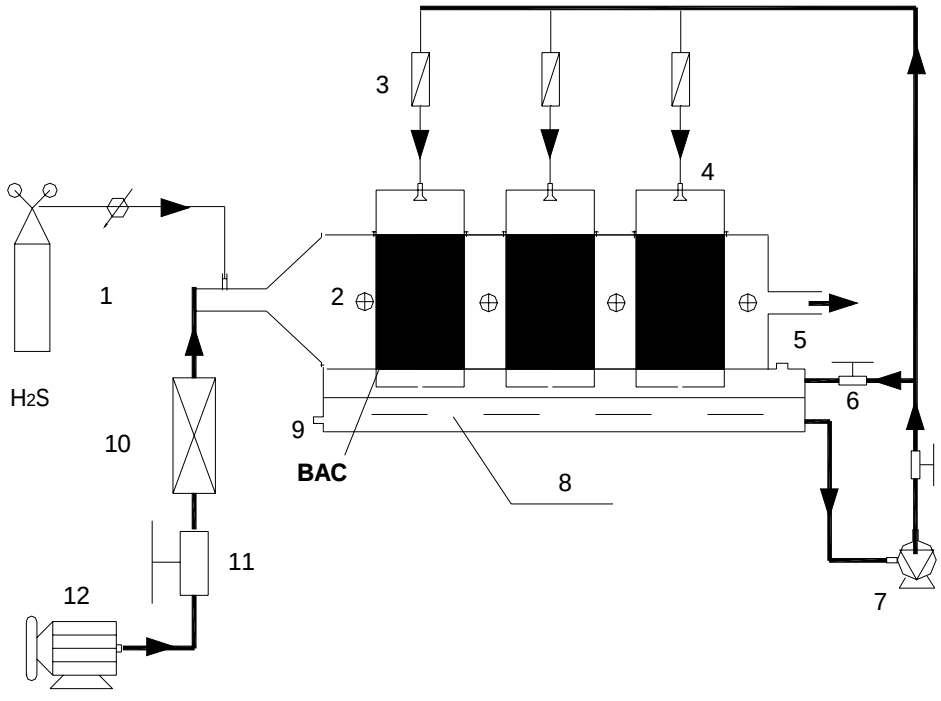

Figure 6.1 Schematic diagram of bench-scale horizontal biotrickling filter (HBTF) system.

(1. H_2S cylinder; 2. sampling ports; 3.liquid flow meter; 4. nozzle; 5. nutrient feeding port; 6. water valve; 7. water pump; 8. water tank; 9. water sampling port; 10. gas flow meter; 11. air valve; 12. air blower.)

Table 6.1 Physical properties of the HBTF

Physical Property	Parameters
Carbon commercial name	Calgon AP460
Immobilization bacteria	Mixed culture dominated by *Acidithiobacillus Thiooxidans*[a]
Wet carbon weight, W_1 (g)	4,914
Dry carbon weight, W_2 (g)	3,145
Moisture content, $m = (W_1-W_2)/W_1$ (%)	36
H_2S adsorption capacity, (dry weight basis, %)	5.5
H_2S elimination capacity for 120 days' HBTF operation (dry weight basis, %)	22.1
Bed dimensions, (cm)	15×15×10×3 [b]
Segment length, L (cm)	3×10
Packing volume, V (L)	6.4
Initial pH of the bed (pH of VAC)	7.96
Bulk density, $d= W_1/V$ ($kg \cdot m^{-3}$)	768
Surface area, $m^2 \cdot g^{-1}$	928
External surface area, $m^2 \cdot g^{-1}$	494
Diameter of carbon pellet (mm)	4
Bed porosity (%)	37
Apparent density of activated carbon, ρ ($kg \cdot m^{-3}$)	490

[a] See section 3.1.5

[b] Three segments in total

An in-situ immobilization of microorganisms was conducted as the start-up process following the procedures described in Section 4.2.3. The dominant species of sulfur oxidizing bacteria was identified as *Acidithiobacillus Thiooxidans* by partial 16S rRNA sequencing. The log phase of the mixed culture occurred at 25~50 h after inoculation in the thiosulfate medium. Upon completing the acclimatization and immobilization stage, the system was operated to provide performance data. The operating conditions during this experimental run are tabulated in Table 6.2.

Table 6.2 HBTF operating conditions

Operating Parameter	Range
Gas retention time (s)	3 ~ 16
Inlet H_2S concentration, C (ppm_v)	20 ~ 100
Gas flow rate, Q_g ($L \cdot min^{-1}$)	24 ~ 192
H_2S loading rate, ($gH_2S \cdot m^{-3} \cdot h^{-1}$)	6.26 ~ 167
Liquid recirculation rate, Q_l ($L \cdot min^{-1}$)	0.6 ~ 2.7
Gas-liquid ratio	32 ~ 160
Water trickling velocity ($cm \cdot s^{-1}$)	0.02 ~ 0.09
Superficial gas velocity, v ($m \cdot s^{-1}$)	0.018 ~ 0.071
Refreshing rate of recirculation solution	Once per 4 days
pH of recirculation solution	1.0 ~ 2.0

6.3 System Performance Evaluation

6.3.1 Performance during Start-up Period

The performance of the HBTF during the startup period (initial 25 days) is illustrated in Figure 6.2. The inlet H_2S concentration was varied in a range of 20~85 ppm_v with GRT reduced gradually from 16 to 8 s, and to 6 s, yielding a H_2S loading rate of 11~70 $gH_2S \cdot m^{-3} \cdot h^{-1}$. The removal efficiency during this period was calculated and recorded. Analysis during the startup phase revealed that the H_2S RE remained constant at 100% despite shortening the GRT from 16 to 6 s while inlet H_2S concentration varied within 20~85 ppm_v. This indicated that no acclimation period appear to be required for the biotrickling filter to perform efficiently. It is suspected that this excellent removal of H_2S is probably due to the adsorption characteristics of the activated carbon in use. During this initial stage, when the biofilm had yet to be formed completely on the carbon surface, the physical adsorption of activated carbon to H_2S could be the factor determining the bed performance. The pH of the recirculation nutrient solution (refer to Figure 6.2) initially increased up to 7.8 on the 3rd day of operation. This increase of pH initially may be caused by basic functional groups present on the carbon surface (Yan et al.,

2004a). When the recirculation solution was first passed through the carbon bed, chemical reactions might occur and these basic groups could partially release into the solution, thus accounting for the pH increase. Thereafter, the pH declined slowly to below 2 after 18 days of operation, indicating a continuous production of H^+ resulted from the oxidation and adsorption of H_2S. The use of BAC in a biotrickling filter appears to have a positive aspect during start-up in that the adsorption properties of the BAC dominates to allow excellent H_2S removal while the biofilm is being formed. For many non-BAC systems, an acclimation period (lasting 5~10 days) is normally required (Koe and Yang, 2000a; Koe and Yang, 2000b; Gabriel and Deshusses, 2003b).

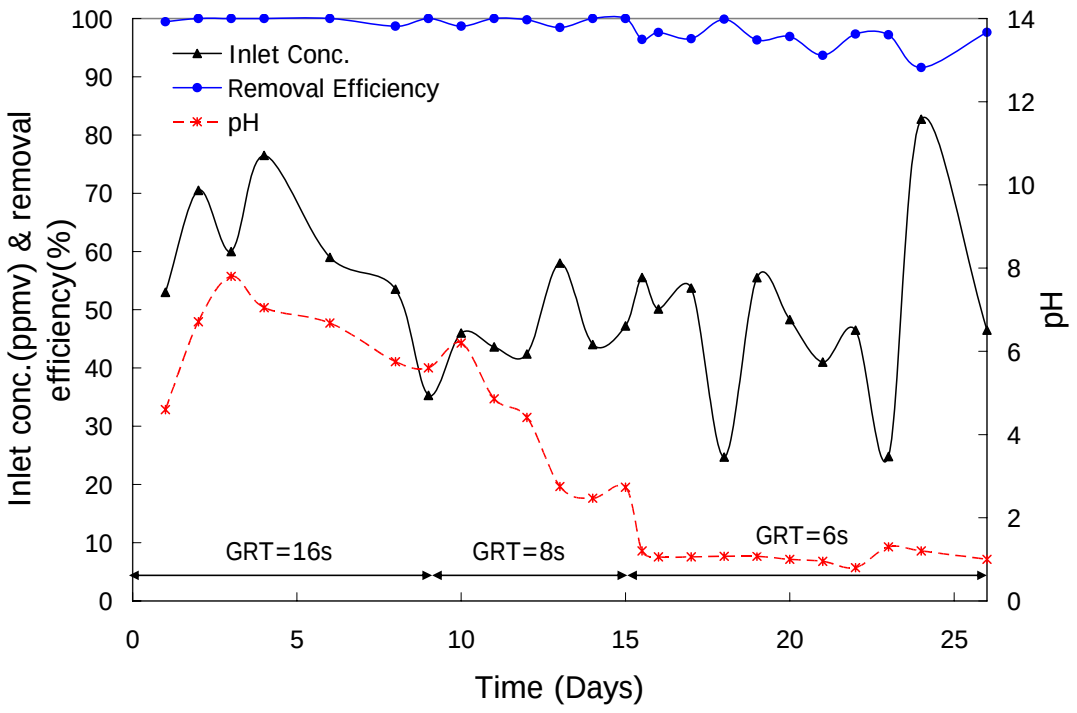

Figure 6.2 Performance of HBTF bed during the start-up period

6.3.2 Long-term Performance

Base on the pre-set parameters (Table 6.2), the long-term performance of HBTF for a period of 120 days was evaluated and reported in Figure 6.3. The system GRT was reduced gradually from 16 to 8 s, and to 6 s in the first 30 days, and was kept at 4 s for the rest of the experimental run. No significant difference in RE was observed during the first 40 days of operation when the H_2S concentration in the influent gas varied from 20 to 100 ppm_v, except that occasionally, a slight decrease in RE was observed due to the shock loading caused jointly by the decrease in GRT (labeled I in Figure 6.3) and increase in H_2S concentration (labeled II in Figure 6.3). For the remaining days of operation, nutrient deficiency and bacteria loss (labeled III in Figure 6.3) could be the major factors causing the drop in RE. The change of pH from 8 to 1 in the first 50 days of operation had only a negligible effect on system performance. During the 120 days of experimental run, a 10-day termination period was conducted to evaluate system behavior under this situation. Towards the end of the experimental period the packing bed was found to become clogged and the clogging and low pH environment appeared to influence the system performance (labeled IV and V in Figure 6.3).

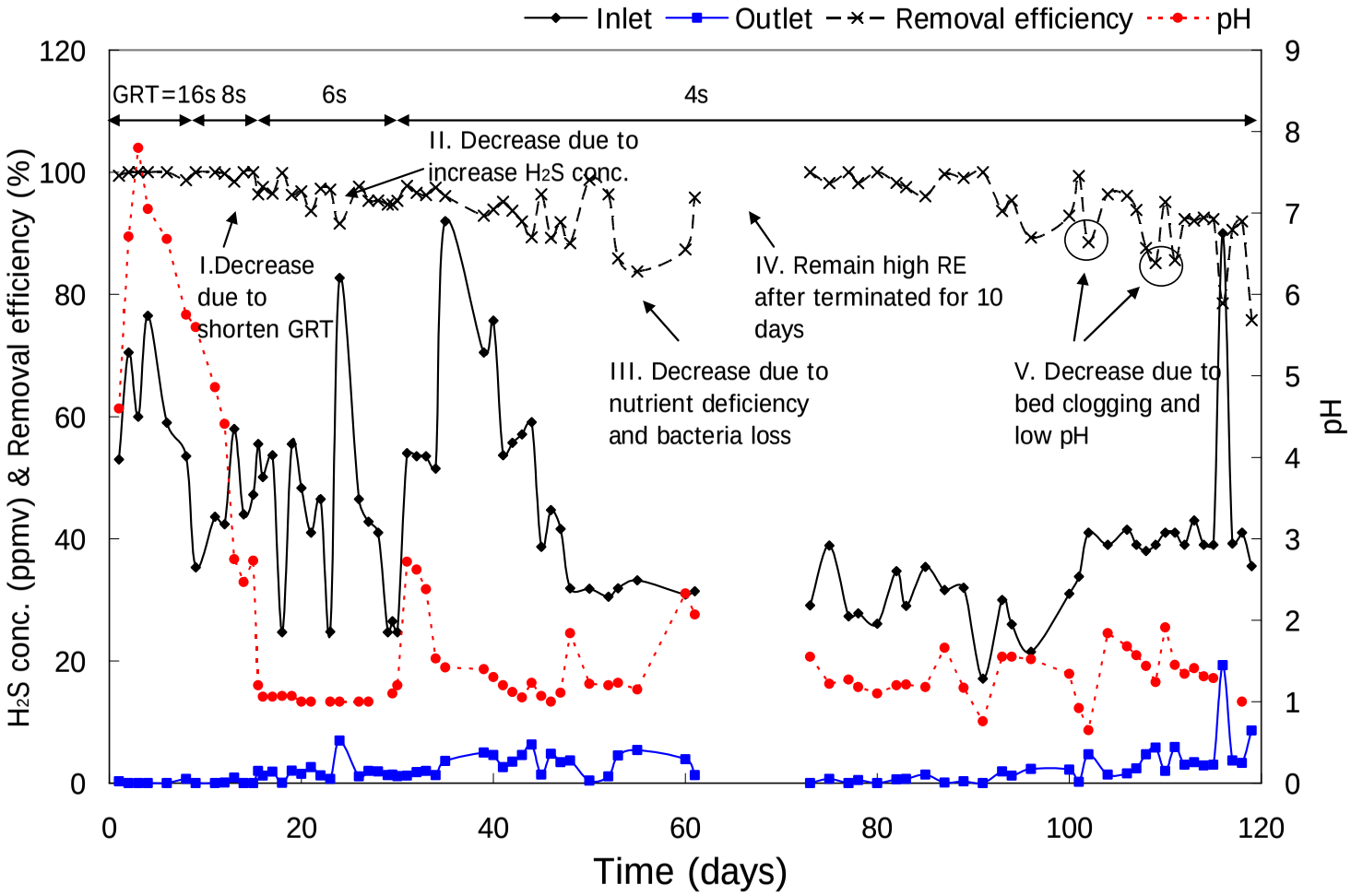

Figure 6.3 Representative profiles: long-term performance of the HBTF

The loading rate of H_2S is an important consideration in the system design, and is determined by the inlet pollutant concentration and GRT of the system. Similar with the study of the biofilter (discussed in Chapter 5), the loading changes in the biotrickling filter were due to the fluctuations in H_2S inlet concentration and the stepwise increase in gas flow rate. Elimination capacity of the BAC in the HBTF vs. loading rate is shown in Figure 6.4. At the loading rates of less than 100 $gH_2S \cdot m^{-3} \cdot h^{-1}$, the system consistently degraded over 90% of the inlet H_2S. When the loading rate was above 100 $gH_2S \cdot m^{-3} \cdot h^{-1}$, the breakthrough of the media bed occurred, whereas a quasi-zero-order degradation regime was observed at loadings over 130 $gH_2S \cdot m^{-3} \cdot h^{-1}$, with RE gradually decreasing. These specific breakthrough points are somewhat lower than those observed with the biofilter in the preceding chapter (Figure 5.3).

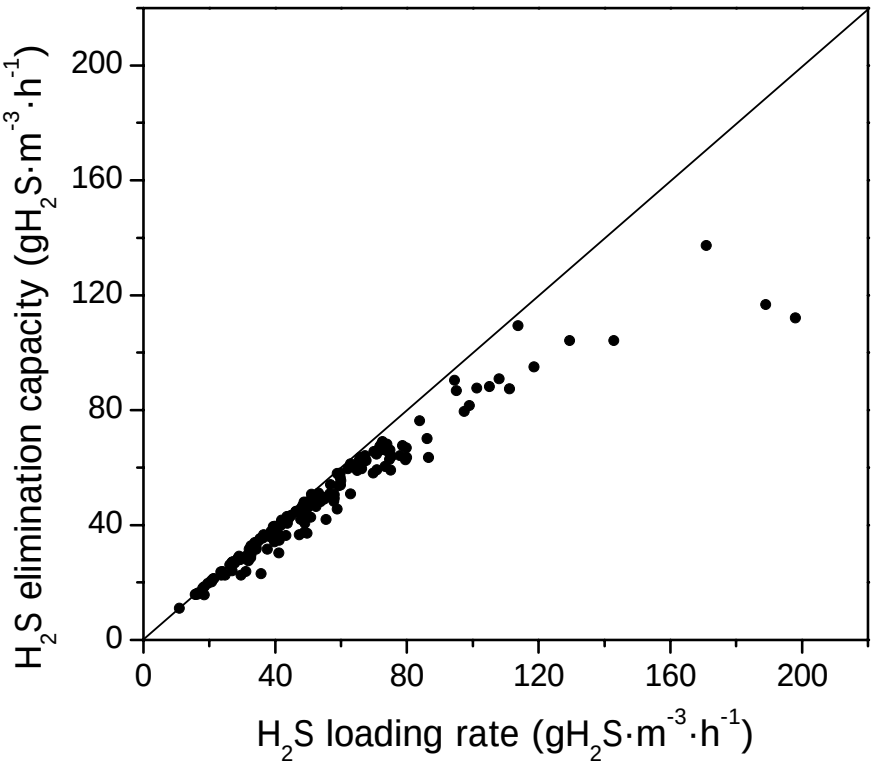

Figure 6.4 H_2S elimination capacity with loading rate
(Data include the 120 days of operation)

The HBTF efficiency at various GRT was also investigated. The inlet H_2S concentrations were increased from 20 to 90 ppm_v while GRT varied from 16 to 3 s. The relationship between the inlet H_2S concentration, GRT, and H_2S RE is shown in Figure 6.5. This BAC-based HBTF can work efficiently (over 96%) at a GRT of 6 s or above despite changes in the influent concentration, while any further reduction in GRT may cause a corresponding decrease in RE. REs of 98% were maintained when inlet H_2S concentration was kept at 20 ppm_v with a low gas retention time of 4 s. Such HBTF performance at short GRT (eg. 4 s) is not as good as that achieved in the previous biofilter trial (see Chapter 5), where high H_2S removal (over 98%) was achieved at a GRT as low as 2 s in treating H_2S gas stream of $\leq$30 ppm_v (Figure 5.4). There are two possible reasons for this: firstly, the existence of a continuous water layer surrounding the biofilm in a biotrickling unit would inhibit mass transfer of H_2S to the biofilm, thus lowering the RE substantially; secondly, the flow in the biotrickling filter is cross-current (horizontal configuration) rather than counter-current flow (vertical configuration) applied previously in the biofilter. Such horizontal configuration may reduce the contact area between gas and liquid/biofilm phase leading to a less efficient mass transfer of pollutants to the biofilm. This phenomenon indicates that mass transfer might become more significant in influencing reactor performance in a horizontal biotrickling filter, compared a vertical used biofilter (refer to Chapter 5). The slight reduction of H_2S RE for a biotrickling unit under short GRT was due not only to the insufficient reaction time between H_2S molecules and biomass, but also possibly due to the slower mass transfer of H_2S from the gas phase into the liquid/biofilm phase where bacteria degradation could occur.

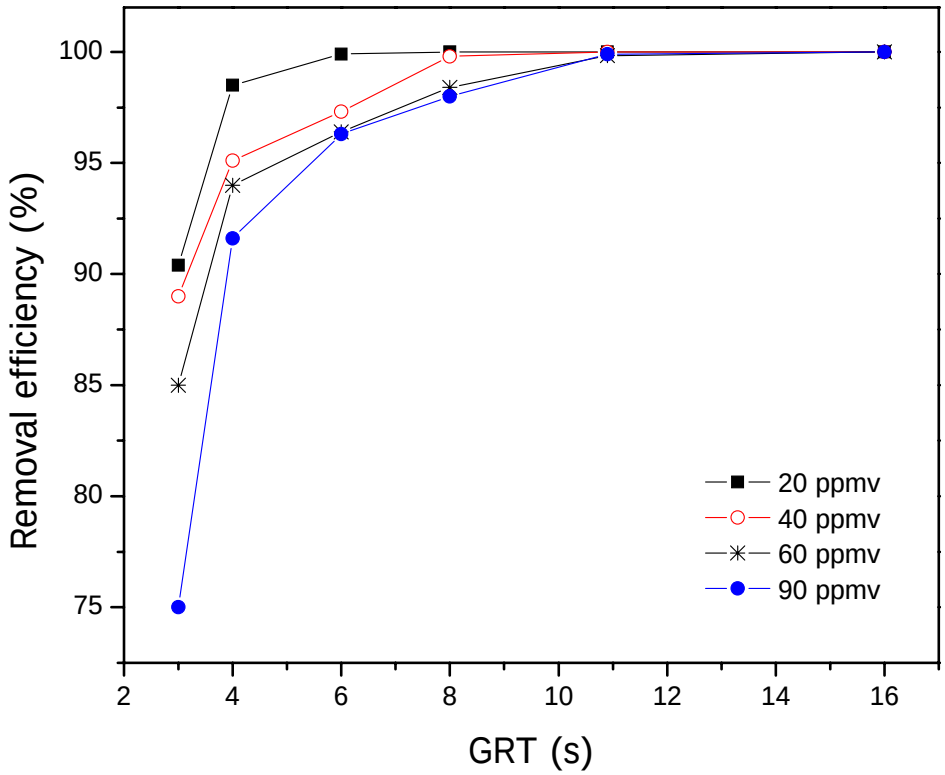

Figure 6.5 HBTF Performance under various H_2S loadings and gas retention time

6.3.3 Main Factors Influencing the Performance

Compared to the biofilter system, the accumulation of sulfur and/or excess biomass and drying of the packing bed was prevented from occurring in this HBTF system by the continuous trickling of liquid solution through the BAC bed. However, the performance of this HBTF is not as good when compared to a biofilter system in terms of RE at short GRT. This may suggest that the existence of a water layer surrounding the biofilm in the biofiltration unit somehow inhibits mass transfer as well as adsorption of H_2S into the biofilm, thus lowering RE substantially. Other main factors influencing the HBTF performance are discussed in the following text.

6.3.3.1 pH impact

The pH variation and H^+ accumulation in the recirculation liquid here have very little effect on HBTF performance during the whole run. However, it is harmful to the microorganism niche if the pH value is allowed to decrease to below 1 (labeled V in Figure 6.3, RE dropped from 99.4% to 88.5%). Dosing with alkali to adjust the pH of the system was conducted during the experiment. However, results obtained showed that bacteria levels are severely impacted. Figure 6.6 shows the variation of pH with bacterial concentration in the system. On day 34, when the pH of the recirculation solution was adjusted by NaOH addition from ~1.0 to 3.6, a dramatic decrease of bacterial concentration from 3.5×10^9 to 3.5×10^6 cfu·mL^{-1} was obtained. Alkali dosing appeared to cause a shock in the microbial niche resulting in significant destruction of bacteria. Satisfactory operation of the HBTF was obtained when the pH was maintained between 1.0 and 2.0. This can be achieved by periodically topping up the recirculation liquid with nutrients (such as N and P) for bacterial growth. Another way is to recirculate the system using a continuous flow of secondary effluent from a WWTP, thus removing excess H^+ and VOC accumulated in the recirculation liquid.

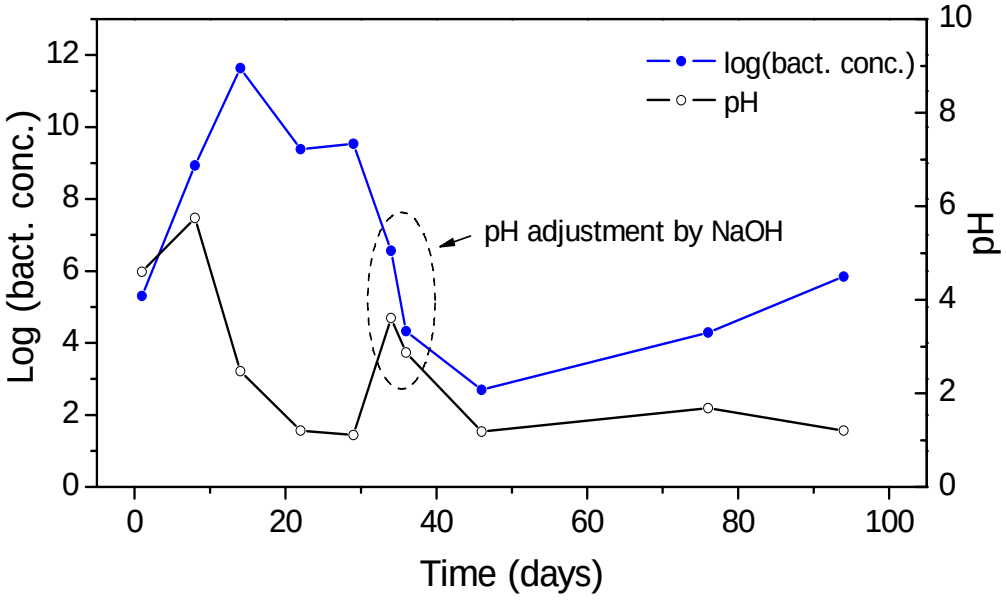

Figure 6.6 pH shock impact on bacteria growth

6.3.3.2 Sulfate accumulation

Sulfate accumulation in the recirculation liquid could also have a negative effect on HBTF performance. In this study, variable sulfate concentrations were prepared by spiking sodium sulfate into the recirculation solution. For the case where the pH of the recirculation solution was maintained at 1~2 and a GRT of 4 s was in operation for the biotrickling filter, the effect of sulfate accumulation on performance of the HBTF was evaluated. Figure 6.7 shows the variation of filter RE with changes in sulfate concentration. As shown, the RE is inversely proportional to sulfate concentration. For the three inlet H_2S condition (32, 40, and 55 ppm_v) tested, the decrease in RE follows the same trend. It could be concluded that better HBTF performance will result if sulfate levels in the recirculation solution are kept low. This can be achieved by increasing the rate at which the recirculation solution is being refreshed. This is consistent with the results presented in Section 3.1.7 (Figure 3.10) where high sulfate levels tend to inhibit bacterial degradation of H_2S.

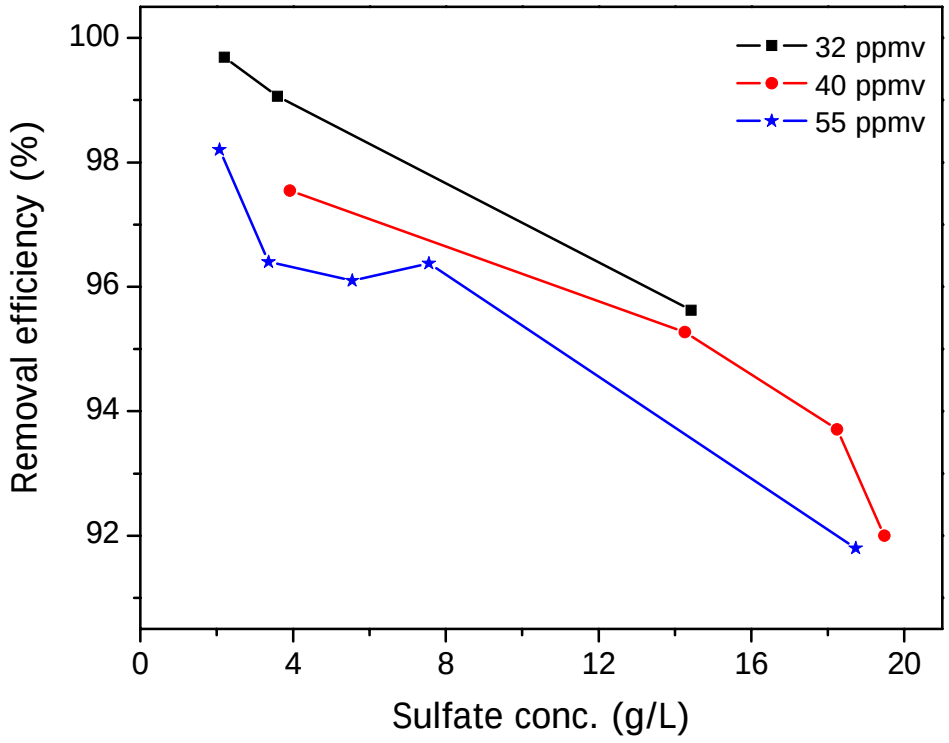

Figure 6.7 Effect of sulfate accumulation in the recirculation liquid on H_2S RE (Set GRT = 4 s, pH = 1~2)

6.3.3.3 Upset and recovery

Interruption in system operation may occasionally occur due to either mechanical or electrical failures. These failures may result in the termination of recirculation solution, gas feeding, or both. During the 120-day operation of this HBTF, the system was terminated for a period of 10 days (labeled IV in Figure 6.3, days 60~70). During the 10 days, the recirculation solution was kept running for about 2 h per day to maintain the necessary moisture of the bed, thus preventing the microorganisms from drying out. Thereafter, the HBTF system resumed operation as usual. The performance of the HBTF after the 10 days interruption is also shown in Figure 6.3. It showed that even after an interruption of as long as 10 days, the RE could still be maintained at a high level of 99.6% (labeled IV in Figure 6.3). This was surprisingly quite different from that previously reported by Koe and Yang (2000b), which had

found that the activity of microorganism was seriously inhibited after a termination of recirculation solution of 24 h. The most possible reason is that the microorganisms immobilized on the carbon surface might utilize the pre-adsorbed H_2S in the pores of activated carbon during the 10-day interruption. However, the underlying mechanisms are not clear and further study is needed to understand this phenomenon.

6.3.3.4 Pressure drop

Pressure drop is a measurement of the resistance to the flow in a packed system. It is dependent on the bed porosity and velocity of the flow going through the packed bed. The higher the bed porosity, the lower the pressure drop in the system. On the contrary, the higher the flow velocity, the higher the system pressure drop (Ergun, 1952). In this HBTF system, the pressure drop was found to be proportional to the gas velocity. The bulk density of the BAC (768 $kg \cdot m^{-3}$, refer to Table 6.1) is much higher than the Pall rings (124.1 $kg \cdot m^{-3}$) applied in a vertical biotrickling filter system conducted by Wu (2000), and the porosity of carbon bed at 37% (Table 6.1) is much lower than that of the Pall ring bed (86%, Wu, 2000). However, the pressure drop encountered in this HBTF is comparable with the filter system studied by Wu (2000). The comparisons showed that the horizontal design probably contributed a relatively low pressure drop in the system. The detailed pressure drop study on this HBTF and comparison with vertical biotrickling filters is given in **Appendix A**.

Nevertheless, problems related to pressure drop were still observed in this system despite the horizontal design. If operated under conditions of 0.075 $m \cdot s^{-1}$ gas velocity and a gas-liquid ratio of 40 for 60 days without backwash, the pressure drop in the HBTF increased dramatically from 131 $Pa \cdot m^{-1}$ to 653 $Pa \cdot m^{-1}$, an increase of almost 500%. This is most likely due to the biofilm growth and H_2S oxidation products deposited on the carbon medium. Such growth and deposits increase resistance to

the gas flow through the carbon bed. Backwashing can reduce 40% of the total pressure drop. It was also observed that the pressure drop in the HBTF decreased as much as 70% after the 10 days' termination of the HBTF system. This reduction of pressure drop was probably caused by the bacterial digestion of the accumulated sulfur on the carbon surface, thus increasing the porosity of the media bed. The digestion process however, might produce excess biomass in the biofilm, which may cause the packing bed to tend to clog up. However, the alleviation of pressure drop after 10 days' termination of the HBTF indicates that possibly the main contributor to the pressure drop in the studied HBTF is the deposition of H_2S oxidation products rather than the formation of biomass.

6.3.3.5 Gas-liquid ratio

In determining the optimal operation condition of the HBTF system, the gas-liquid volumetric ratio was also varied for the HBTF. The G-L ratio was increased from 32 to 160 with an inlet H_2S concentration of 30 ppm_v and a GRT of 4 s. It was observed that at very too low G-L ratio (i.e. 32), significant flushing of the HBTF system occurred, resulting in loss of bacteria and biofilm. On the other hand, too high G-L ratio (i.e. 160) caused the BAC bed to dry out quickly. Both of these extreme situations resulted in poor performance of the HBTF system. In order to achieve a long term efficient operation of the BAC-based HBTF, the G-L ratio had to be maintained within 60~80.

6.3.3.6 Shock Loading

The current horizontal bioreactor was subjected to shock loading test to ascertain its capacity to buffer and recover from a shock H_2S loading. As shown in Figure 6.8, the bioreactor was subject to a sudden increase in inlet H_2S concentrations from 20 to 60

ppm_v levels over a 1 h interval at a GRT of 4 s. The bioreactor was operated with and without the trickling of recirculation solution, respectively. In the latter case, the recirculation solution was shut off while other operation parameters remained the same as that adopted for the HBTF. It was found that the horizontal bioreactor could achieve high RE of 99.8% in both cases for the treatment of the foul gas containing 20 ppm_v of H_2S. After the abnormal high loading, the bioreactor could recover quickly in around half an hour. However, the RE dropped from 99.8% to about 92% at the highest loading of H_2S (60 ppm_v) to the HBF (horizontal biofilter without recirculation solution), while the RE dropped to 81% at the highest loading of H_2S in the HBTF (horizontal biotrickling filter with recirculation solution). The different performances of the two phases under shock loading show that the non-trickling biofilter has a more robust buffer effect than biotrickling filter. This phenomenon again validated that the excess liquid film over the carbon surface in the biotrickling filter does appear to have a negative effect on the mass transfer of pollutant.

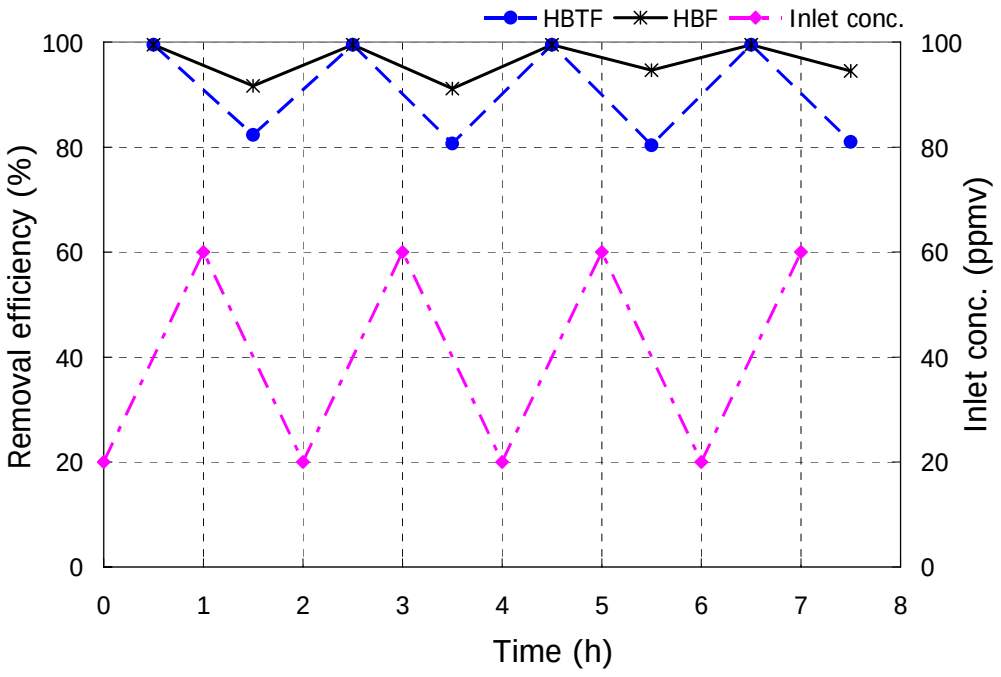

Figure 6.8 Shock loading tests at conditions of HBTF and HBF

6.4 Conclusions

The experimental runs with the HBTF provided new information on the capacity of the BAC to be used as a novel medium for the treatment of H_2S-contaminated waste gas. A BAC-based HBTF was found to achieve a performance comparable to that of a biofilter. The HBTF can be operated at a low GRT (as low as 4 s) and still provide high removal of H_2S. The elimination capacity of the BAC can be as high as 100 $gH_2S \cdot m^{-3} \cdot h^{-1}$. HBTF using the BAC can perform efficiently without the need for lengthy start-up or acclimation periods. Moreover, use of the HBTF reduced or avoided the problems caused by the limitations from biofilter design, such as the sulfur and biomass accumulation, and bed acidification. However, although a BAC-based HBTF can achieve a high performance, it is not as good as a biofilter in terms of performance under short GRT or resistance to shock loadings. This phenomenon to some extent was accounted for by the liquid layer formed over the carbon surface resulting in an inhibition of the mass transfer of H_2S into the biofilm. The liquid layer could also lead to a high bed density to cause an increase in the pressure drop of the biotrickling system. Fortunately, and as an important advantage, the horizontal design alleviated the pressure drop problem significantly.

CHAPTER 7
REMOVAL MECHANISMS OF BIOLOGICAL ACTIVATED CARBON AND MATHEMATICAL MODELING

The preceding chapters (Chapters 5 & 6) focused on the feasibility of applying BAC to treat H_2S in a biofilter and a biotrickling filter and provided information on the performance of the BAC in these bioreactors. The experimental data indicated that activated carbon immobilized with bacteria is a potential packing material of the biofilters. The much higher removal capacity of BAC, compared to using activated carbon alone, could be attributed to the role played by the biofilm in metabolizing adsorbed sulfur and sulfur compounds, hence releasing the adsorption sites for further H_2S uptake by carbon (Ng et al., 2004; Yan et al., 2004b). However, there are still a lot of unknowns concerning microbial immobilization on carbon and the different roles of biodegradation and adsorption of packing material in the H_2S biofiltration. The mechanism of using BAC in treating H_2S has rarely been reported, and therefore, further investigations are needed.

This chapter attempts to evaluate the mechanisms of H_2S abatement using BAC with the focus on providing a better understanding to different contributions of adsorption and biodegradation on the overall H_2S removal capacity compared to carbon adsorption only. Firstly, the mechanism studies focused on the surface properties and chemistry of BAC bed and their relationship with the performance of BAC

treating H_2S in a HBTF as described in Chapter 6. Further, a set of parallel columns were set up to evaluate in-depth the combined effect of adsorption and biodegradation in the BAC-based biotrickling filter, with particular attention paid to the sulfur bearing species distribution. A mathematical model, which considered H_2S diffusion in the biofilm and adsorption on carbon surface simultaneously, is presented to describe the kinetics behavior of the transformation of H_2S in the BAC.

7.1 Mechanism Study on the H_2S Removal by BAC in the HBTF

In this section, a series of BAC samples were taken periodically from different locations during the operation of the bench-scale horizontal, cross-flow biotrickling filter as described in Chapter 6. The samples are expected to differ in the surface properties [evaluated by Braunner-Emmett-Teller (BET) test]. The surface chemistry of the BAC samples, together with virgin carbon and exhausted carbon (after H_2S breakthrough test, non-microbial immobilization), was fully evaluated using surface pH, carbon-hydrogen-nitrogen-sulfur (CHNS) elemental analyses, Fourier transform infrared (FTIR) and thermal analyses. The results obtained here provided new information on the advantage of using BAC where the combined contribution of physical adsorption and biodegradation of the new medium for treating H_2S was investigated.

7.1.1 Experimental Section

This study was based on the bench-scale horizontal, cross-flow biotrickling filter (HBTF) system (details refer to Chapter 6). A center and a side series of carbon samples were taken from the bed at 0, 5, 10, 15, 20, 25 and 30 cm distance from the inlet to outlet and labeled as C1 to C7 and S1 to S7, respectively. The sampling locations are shown in Figure 7.1. The two sets of samples stated above were taken

on the 60th day and 200th day into the experimental run. These two sets of carbon samples were used to represent the extent of various reactions including adsorption and biodegradation that had occurred in the BAC bed.

BET tests with the BAC samples provided information to explain the effects of microbial growth and to some extent, the relationship between the presence of immobilized culture on the carbon porosity. The samples conducted with BET analysis in this study not only included the two sets of BAC taken along the carbon bed (center and side) on the 60th and 200th day of the HBTF run, but also virgin carbon (as received, non-bacterial) as well as H_2S exhausted carbon (activated carbon saturated with H_2S after breakthrough test, see Section 3.2.3). Changes of carbon surface pH were monitored by a pH meter. Biofilm development was observed by SEM directly while the diversity of sulfide oxidation (bio/non-bio) products was investigated by FTIR, thermal and CHNS elemental analyses. Detailed analysis conditions and procedures have been presented previously in Chapter 3.

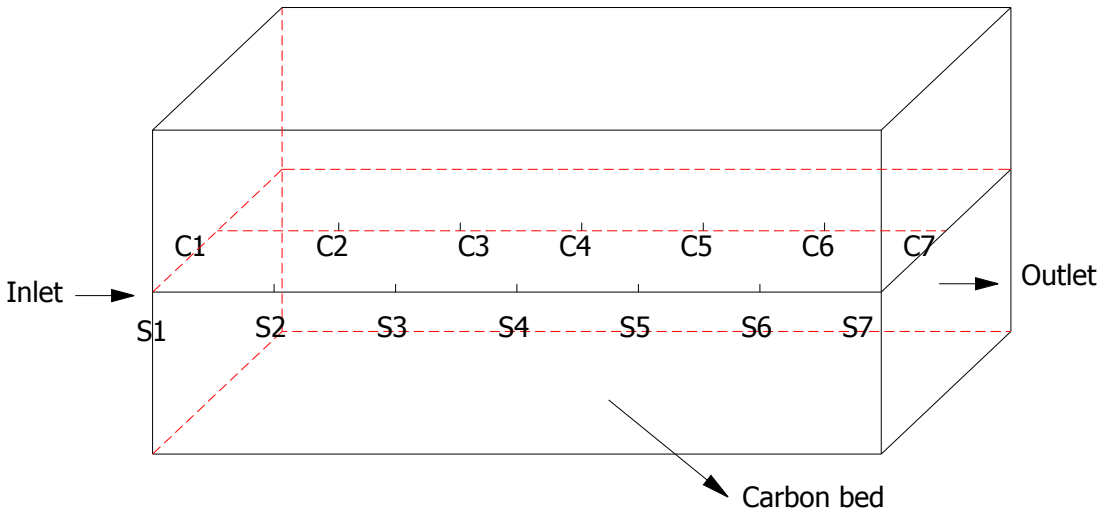

Figure 7.1 Schematic diagram of sampling locations

7.1.2 Results and Discussion

7.1.2.1 Effects of biofilm development on BAC performance

The pore and surface characteristics of BAC together with virgin and exhausted carbon were identified using BET test and the results are presented in Table 7.1 and Figure 7.2. The data tabulated are the mean values of sample duplicates. For discussion, virgin carbon results shall be used here as reference. Compared to virgin carbon, the changes of pore volume and surface area of the exhausted carbon are caused by the physical chemisorption of H_2S, while those of BAC would reflect the co-effects of adsorption and biodegradation.

Table 7.1 Braunner-Emmett-Teller (BET) test results of BAC bed

		Distance from the inlet (cm)	pH	Average Pore Diameter, nm	Micropore volume ($mL \cdot g^{-1}$)	Surface Area ($m^2 \cdot g^{-1}$ of packing)		
						External	Micropore	BET surface area
Carbon Sample on day 60	**Center**	5	2.53	2.019	0.168	504.7	372.2	876.9
		15	2.53	1.953	0.178	539.4	400	939.4
		25	2.45	1.942	0.219	349.2	476.7	825.9
		Average	***2.50***	***1.971***	***0.188***	***464.4***	***416.3***	***880.7***
	Side	5	2.42	2.01	0.163	504.3	363.2	867.5
		15	2.38	1.969	0.202	340.6	439.9	780.5
		25	2.40	1.942	0.213	236.2	460.6	696.8
		Average	***2.40***	***1.974***	***0.193***	***360.4***	***421.2***	***781.6***
Carbon Sample on day 200	**Center**	0	1.86	1.951	0.159	533.1	359.2	892.3
		5	1.89	2.035	0.181	464.1	403.8	867.9
		10	1.86	1.951	0.225	327.0	488.0	815.0
		15	1.89	1.955	0.229	383.1	506.0	889.1
		20	1.87	1.945	0.225	321.3	489.1	810.4
		25	1.89	1.968	0.208	397.3	453.8	851.1
		30	1.94	1.944	0.239	332.4	518.4	850.8
		Average	***1.89***	***1.964***	***0.209***	***394.0***	***459.8***	***853.8***
Virgin Carbon (AP460)			7.96	1.980	0.276	505.9	525.6	1031.5
Exhausted Carbon (AP460)			2.61	2.024	0.078	182.1	397.1	579.2

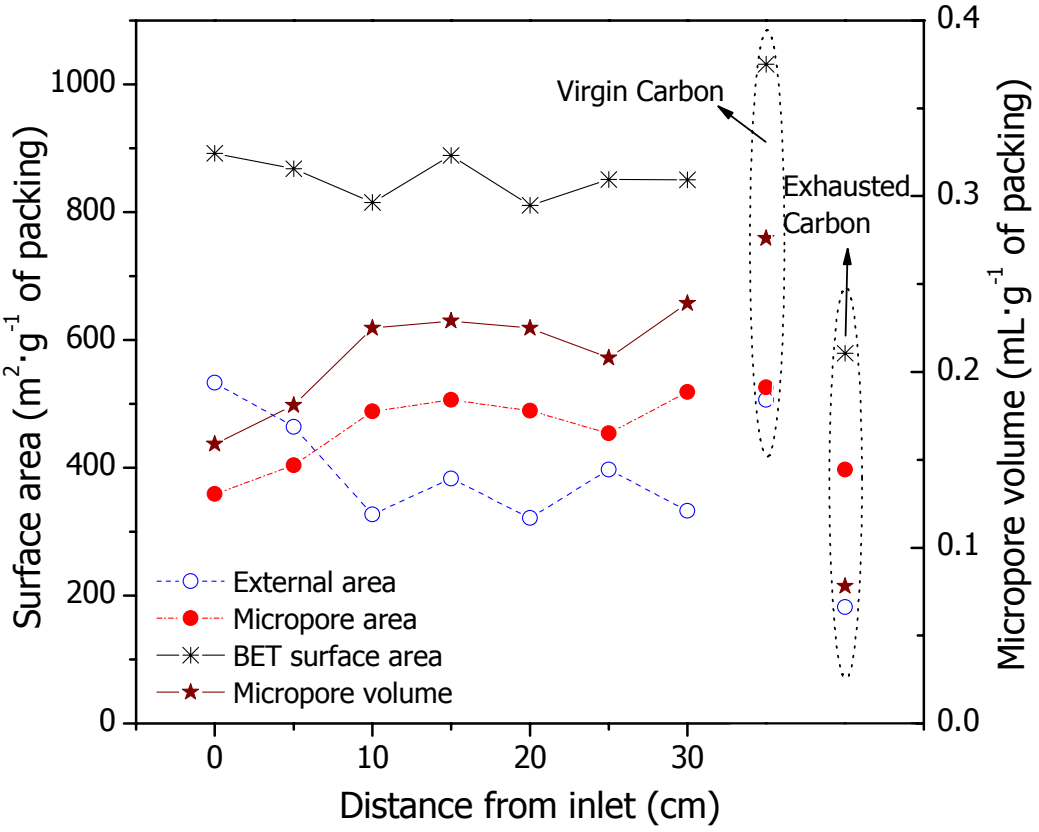

Figure 7.2 BET profiles of BAC along the HBTF bed after 200 days' operation

As Table 7.1 shows, Calgon AP460 (virgin carbon) has a micropore volume of 0.276 $mL \cdot g^{-1}$ and a BET surface area of 1031.5 $m^2 \cdot g^{-1}$[the sum of external surface area (505.9 $m^2 \cdot g^{-1}$) and micropore surface area (525.6 $m^2 \cdot g^{-1}$)]. Exhausted carbon (that is saturated with H_2S) has a significantly smaller micropore volume of only 0.078 $mL \cdot g^{-1}$ and a BET surface area of 579.2 $m^2 \cdot g^{-1}$ (external surface area of 182.1 $m^2 \cdot g^{-1}$ and micropore surface area of 397.1 $m^2 \cdot g^{-1}$). These data show that the physical/chemical adsorption of H_2S accounts for the severe reduction of the micropore volume and the external surface area of the virgin carbon sample. The slight increase of average pore diameter from virgin carbon (1.980 nm) to exhausted carbon (2.024 nm) could indicate that most H_2S adsorption take place in pores of small diameters. This finding is similar to the previous observation reported by Adib et al. (1999a), which established a good correlation between the H_2S breakthrough capacity with the volume in pores between 0.5 and 1.0 nm width. Therefore, it can be

concluded that the physical/chemical adsorption of H_2S most likely occupy the micropores (0.4~2 nm diameter) than the mesopores (2.0~50 nm diameter) or macropores (> 50 nm diameter).

The BAC samples taken from the HBTF carbon bed after 60 days of operation represents carbon samples on which the biofilm had been newly formed. The BAC samples taken from the center line of the HBTF bed has an average micropore volume of 0.188 $mL \cdot g^{-1}$ and an average BET surface area of 880.7 $m^2 \cdot g^{-1}$ (external surface area of 464.4 $m^2 \cdot g^{-1}$ and micropore surface area of 416.3 $m^2 \cdot g^{-1}$) (Table 7.1). Compared to the virgin carbon, the adsorption plus biodegradation of H_2S on the BAC does reduce the micropore volume and the surface area of BAC, though those reductions are far less than those observed in the H_2S exhausted carbon. These data implied that most of micropores in the BAC remained available for further reaction, and is quite different with the observation of the H_2S exhausted carbon where the adsorbed H_2S occupied mainly the micropores. The average pore diameter of the BAC taken from the center line is 1.971 nm, which is not too different than that of the virgin carbon (1.98 nm). It does appear that the formation of the biofilm after 60 days of operation did not impact upon the micropore volume of the carbon sample. The formation of the biofilm probably blocked some of the external pores on the carbon surface but have insignificant effects on the micropores. Bacteria cells were too large (~1 μm) to enter the mesopores and micropores of the carbon sample. They stayed on the carbon external surface and formed the biofilm. Some H_2S oxidation products of small molecules and enzymes of biomass could enter the carbon macropores to utilize the adsorbed H_2S and free the micropores that were previously occupied by H_2S initially (Scholz and Martin, 1997). Similar phenomena, compared to virgin and exhausted carbon, were found in the BAC samples taken from the side line of the HBTF bed on day 60 and those taken from the center line on day 200.

When the BAC-based HBTF operated for 200 days, the BAC samples taken from the center line has an average micropore volume of 0.209 $mL \cdot g^{-1}$ and average BET surface area of 853.8 $m^2 \cdot g^{-1}$ (external surface area of 394.0 $m^2 \cdot g^{-1}$ and micropore surface area of 459.8 $m^2 \cdot g^{-1}$) (Table 7.1). Compared to the surface properties of the BAC samples taken from the center line on day 60, the BET surface area reduced a little, while the micropore volume had increased with the length of operation (from 0.188 $mL \cdot g^{-1}$ to 0.209 $mL \cdot g^{-1}$). These data confirmed that the biofilm on carbon surface prefer to occupy larger pores rather than the micropores that are preferred by the adsorption process. The average pore diameter of the BAC decreased slightly for the HBTF operating till day 200 (1.964 nm) from that on day 60 (1.971 nm) and virgin carbon (1.980 nm). It provided positive evidence that the biofilm occupied the macropores and utilized the adsorbed H_2S that is preferentially adsorbed in the micropores.

Concerning BET surface properties of the BAC along the HBTF bed on day 60, as Table 7.1 shows, the external surface areas and average pore diameters of BAC samples along the HBTF bed decreased while micropore surface areas and volumes increased from inlet to outlet at both center line and side samples. This indicates that although the biofilm is already formed on the 60^{th} day of operation (to be confirmed with SEM images in the following text), the physical adsorption of H_2S still occupy an important role with H_2S mostly adsorbed in micropores (Yan et al., 2004a). The higher H_2S concentration near the inlet served as a higher driving force allowing the penetration of H_2S across the biofilm followed by adsorption in the micropores. Hence H_2S and its oxidation products of small molecules occupied more micropore area/volume at the inlet than at other locations. However, for the 200^{th} day BAC sample taken along the center line of the HBFT, the BET surface tests for center samples did not show any definite variation of surface properties with sampling locations along the BAC bed. This implied that biodegradation probably play a more

important role than adsorption in the removal of H_2S in the HBTF.

From the results of the BET tests, the mechanisms of BAC treating H_2S differ with that of purely activated carbon adsorption. For the exhausted carbon, H_2S is adsorbed mainly in micropores. Certain tendencies of carbon surface properties could be seen along the bed from the inlet to the outlet (Yan et al., 2004a). For the BAC, where a biofilm is coated over the carbon surface, H_2S might penetrate into the carbon pores through the biofilm, and physical/chemisorption plays a role in the overall H_2S elimination at the initial stage of biofilm development (i.e., 60 days' of the HBTF run). However, with further development of the biofilm (i.e., 200 days' of the HBTF run), biodegradation became predominant, thus leading to a more uniform distribution of carbon surface properties along the BAC bed.

7.1.2.2 Change of carbon surface pH

The pH values of virgin carbon and H_2S exhausted carbon are 7.96 and 2.61, respectively (Table 7.1). The change of pH from basic to acidic values accounted for the dissolution of H_2S in the water film and the formation of sulfuric acids during the H_2S adsorption on the carbon surface. Unlike H_2S adsorption by a carbon tower, the pH values of BAC from each location along the HBTF bed were almost constant. After the HBTF ran for 60 days, the carbon pH value is around 2.50 and didn't differ much at different positions of the bed. There is, however, a further decrease of the pH to about 1.89 after 200 days of HBTF run. A lower carbon surface pH may indicate different sulfide oxidation products on BAC compared to carbon adsorption (Yan et al., 2004a). Since the local pH in the pore system has a significant effect on the efficiency of H_2S dissociation and its oxidation to various sulfur species (Adib et al., 2000; Bandosz, 2002), the biofilm over the BAC surface should affect the H_2S oxidation products. The continuous decrease in the pH of the BAC surface with HBTF operation may be due to the acid accumulation in the system.

7.1.2.3 Biofilm identification using SEM

The SEM image of virgin carbon (Figure 4.2) suggests a very open, ordered macropore structure of Calgon AP460. With the eventual operation of the HBTF, the carbon pellets were gradually coated with biofilm. Figure 7.3 (a, b and c) show the SEM image of a BAC pellet taken at a location 5 cm from the inlet of the HBTF. Figure 7.3a shows a well-formed biofilm over the carbon surface after the HBTF has operated for 60 days. On observing the cross section of the BAC pellet as Figure 7.3b shows, microorganisms may grow in the macropores located on carbon surface as long as the pore sizes are bigger than the bacteria cells. On the 200th day of HBTF operation, the biofilm over the carbon surface becomes sticky and thick as Figure 7.3c shows. Dead cells, extracellular polymeric substances (EPS) and sulfur-bearing species together with fungi are found to accumulate on the carbon surface. Also, there existed some large interstices/gaps on the biofilm allowing H_2S to pass through to achieve H_2S adsorption on the micropores of the BAC.

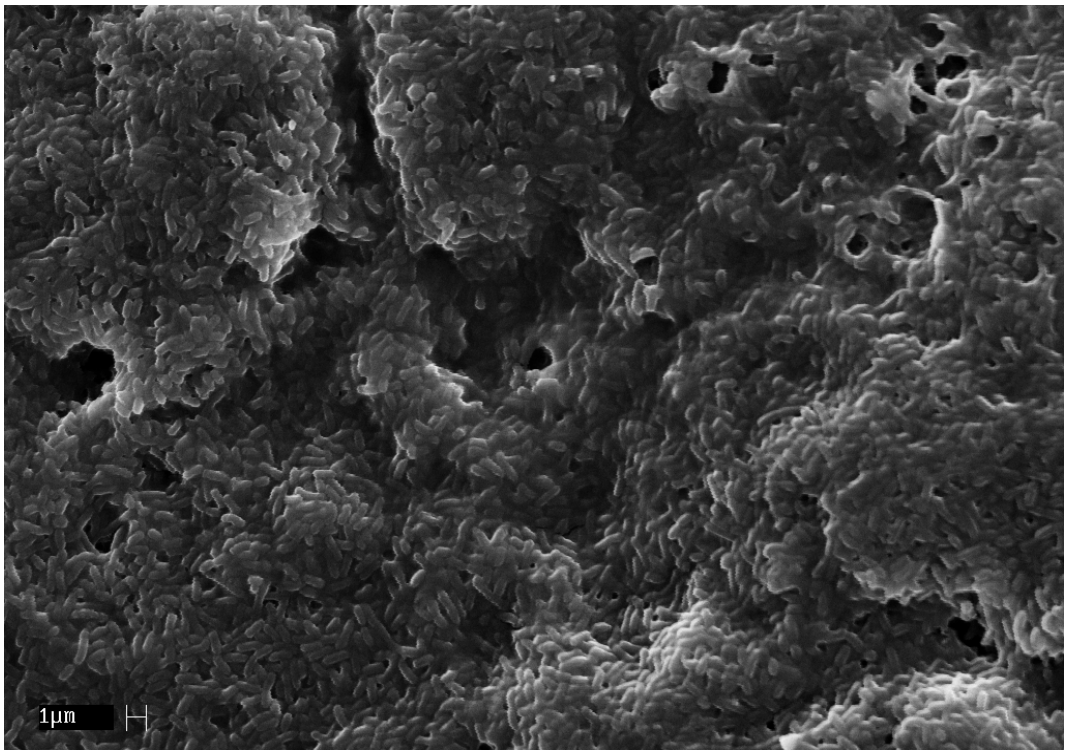

a. BAC on day 60

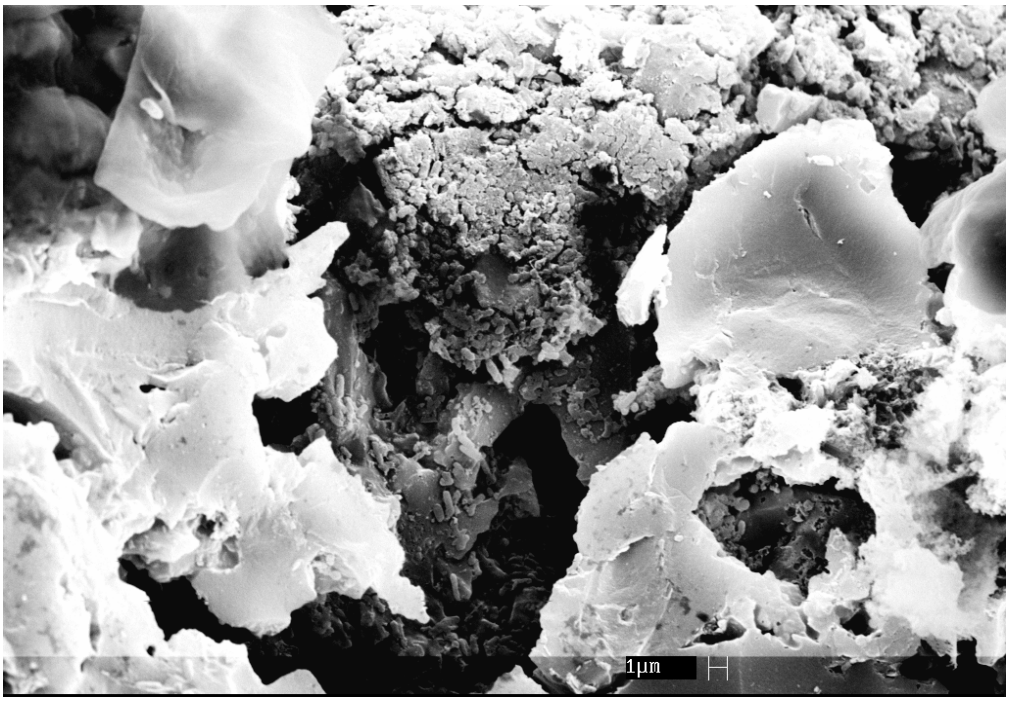

b. Cross section of BAC on day 60

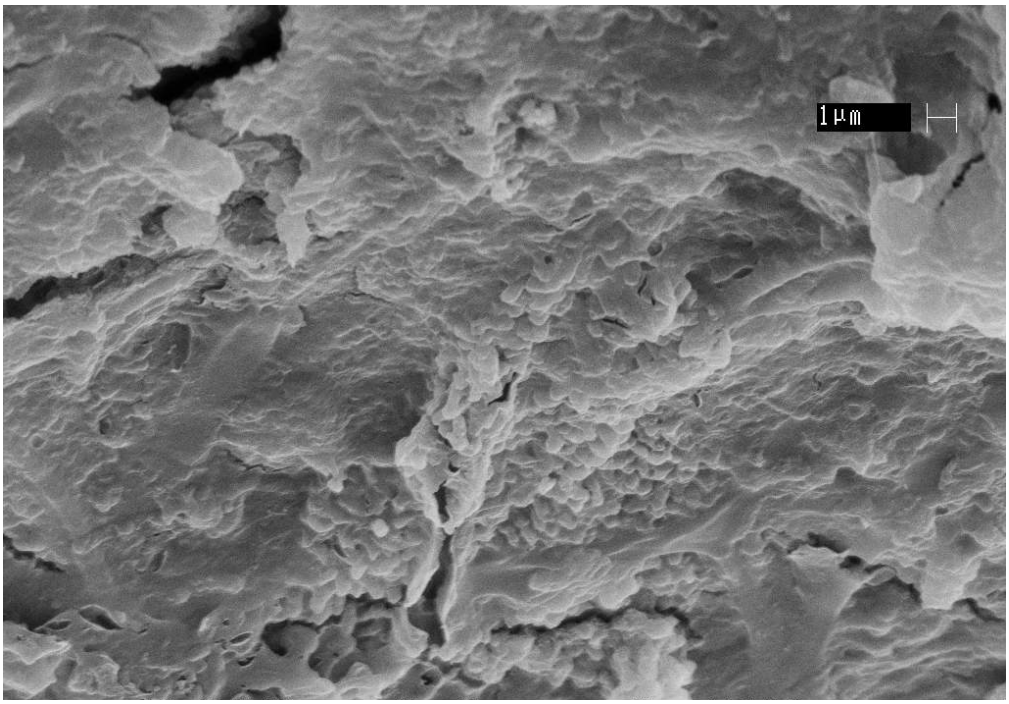

c. BAC on day 200

Figure 7.3 Scanning electron micrographs of representative pellets of carbon
(BAC samples are taken from 5 cm from inlet of the HBTF bed)

7.1.2.4 Sulfide oxidation products on BAC

Calgon AP460 can adsorb 5.5 wt.% (dry weight basis) of H_2S (refer to Table 6.1). After 200 days HBTF run, the BAC has eliminated 35.3 wt.% (dry weight base) of H_2S and remain far from exhausted because the available surface area (853.8 $m^2 \cdot g^{-1}$) is higher than the that of the H_2S exhausted carbon (579.2 $m^2 \cdot g^{-1}$) [refer to virgin carbon (1031.5 $m^2 \cdot g^{-1}$), Table 7.1]. This indicated that most of the H_2S removed by the BAC is via the process of biodegradation rather than carbon adsorption, or could be due to the synergetic effects of biodegradation and adsorption. In the processes of H_2S biodegradation, H_2S is used as electron donors by the sulfide oxidizing bacteria. The oxidation of H_2S occurs in stages: the first oxidation step results in the formation of elemental sulfur, S^0. When the supply of H_2S has been depleted, additional energy can be obtained from the oxidation of sulfur to sulfate. The final product of oxidation in most cases is sulfate (SO_4^{2-}). The intermediate products could be elemental sulfur (S^0), thiosulfate ($S_2O_3^{2-}$), tetrathionate ($S_4O_6^{2-}$), trithionate ($S_3O_6^{2-}$), sulfite (SO_3^{2-}) etc. Some of the related reactions are stated below:

$$2H_2S + O_2 \rightarrow 2H_2O + 2S^0 \qquad \Delta G_0 = -343.32 \text{ kJ/mol} \qquad \text{Eq.7-1}$$

$$2HS^- + O_2 \rightarrow 2S_0 + 2OH^- \qquad \Delta G_0 = -169.35 \text{ kJ/mol} \qquad \text{Eq.7-2}$$

$$2HS^- + 4O_2 \rightarrow 2SO_4^{2-} + 2H^+ \qquad \Delta G_0 = -732.58 \text{ kJ/mol} \qquad \text{Eq.7-3}$$

$$S_0 + H_2O + 1.5O_2 \rightarrow SO_4^{2-} + 2H^+ \qquad \Delta G_0 = -589.1 \text{ kJ/mol} \qquad \text{Eq.7-4}$$

$$S_2O_3^{2-} + H_2O + 2O_2 \rightarrow 2SO_4^{2-} + 2H^+ \qquad \Delta G_0 = -409.4 \text{ kJ/mol} \qquad \text{Eq.7-5}$$

$$CO_2 + H_2O + E. \rightarrow [CH_2O] + O_2 \qquad \text{Eq.7-6}$$

ΔG^0 is the change in Gibbs energy under standard pressure and temperature conditions. Eq.7-1 to Eq.7-4 show that sulfide oxidizing involved a two-step process comprising an initial oxidation to elemental sulfur followed by a slower additional oxidation to sulfate. The initial oxidization need much less energy than the additional oxidization. Under oxygen limiting conditions (i.e. oxygen

concentration is below 0.1 mg·L^{-1}), elemental sulfur is the major end product of the sulfide oxidation as show in Eq.7-1 and Eq.7-2. Otherwise, sulfate is formed under circumstance of sulfide limitation following Eq.7-3 to Eq.7-6.

FTIR analysis

The surface functional groups on BAC surface and oxidation products of H_2S on BAC were first identified using Fourier transform infrared spectroscopy (FTIR). Figure 7.4 shows the spectra of the exhausted carbon and BACs on day 60 and day 200 in the HBTF bed after responses of virgin carbon as background data are subtracted. These FTIR spectra of BAC are quite similar to those observed using activated carbon adsorption alone (Yan et al., 2004a). The peaks at around 1,120 cm^{-1} and 580 cm^{-1} represent the vibration from SO_4^{2-} indicating that the dominant oxidation product of H_2S in the HBTF is sulfuric acid. The peaks at around 1120 cm^{-1} were integrated and the areas are indicated in Figure 7.4 to represent the content of the formed sulfuric acid. Comparing the carbon samples taken from different positions and operation time, the amount of sulfuric acid accumulated on the carbon surface are diverse on day 60 (from C_2 to C_4, and C_6, the area unit changes from 12.6 to 4.8 and 9.4, Figure 7.4a), but on day 200 it does not change much with the location of the bed (8.2~9.5 area unit, Figure 7.4b). The yield of oxidation product reflected partially the activities of biofilm during the initial period of HBTF operation (i.e. on day 60). Over the 200 days of HBTF operation, the trickling liquid solution possibly removed the accumulated oxidation products off the bed resulting in a more homogeneous FTIR response in the anaphase.

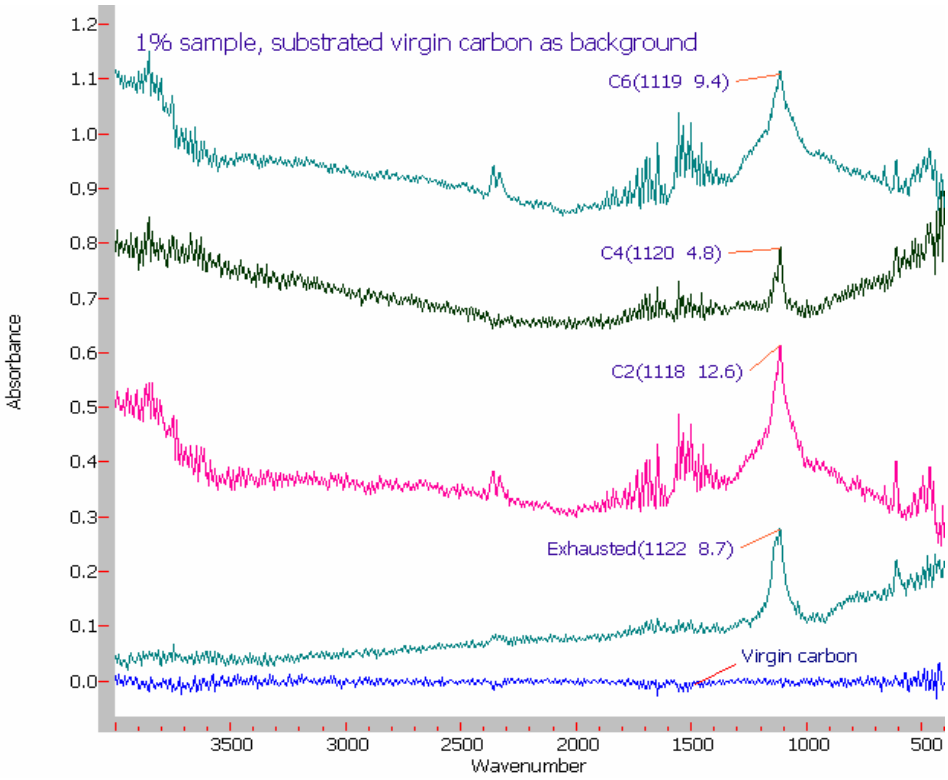

a. BAC from HBTF at 60 days of operation.

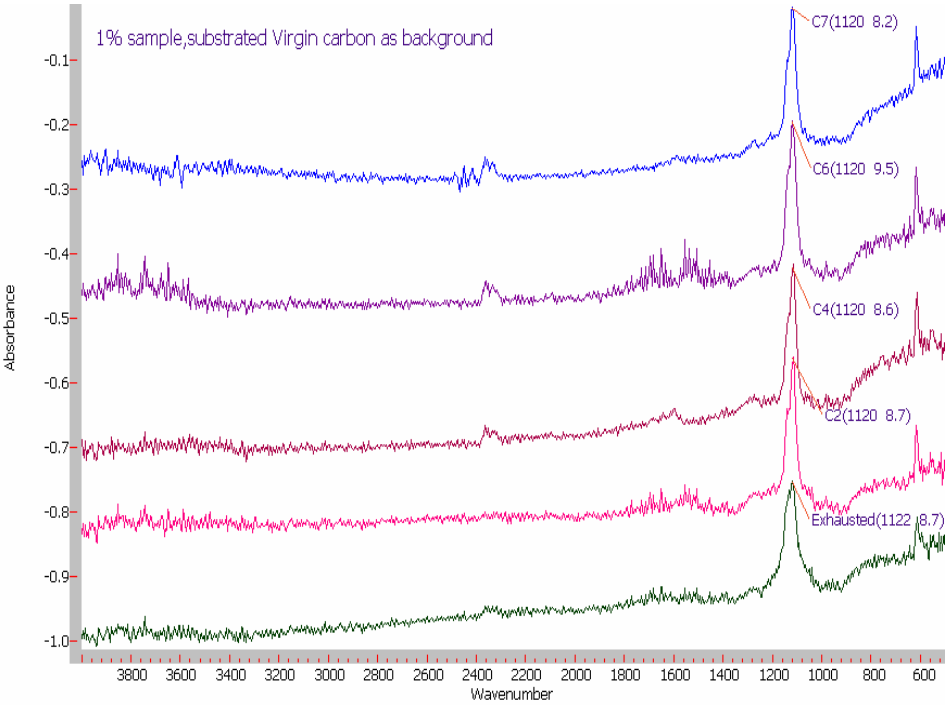

b. BAC from HBTF at 200 days of operation.

Figure 7.4 FTIR spectra of BAC from HBTF after operation and of exhausted carbon

(subtract virgin carbon as reference, C2 = carbons at 5 cm; C4 = carbons at 15 cm; C6 = carbons at 25 cm; C7 = carbons at 30 cm from the inlet of the bed)

Thermal analysis

Thermal analysis was conducted to further analyze the products of surface oxidation on BAC. The differential thermogravimetric (DTG) curves of the virgin carbon, exhausted carbon and BAC at selected locations from centerline of the bed are presented in Figure 7.5. Each peak corresponds to weight loss due to desorption of species from the activated carbon at the specific temperature. The higher the peak or the larger the peak area indicates more weight loss. The figures shown here begin at 200 °C, so the peak for water loss that occurs at around 140 °C is not seen. The DTG curves of the exhausted carbon showed a prominent peak (P1) at around 280 °C and a weak peak (P2) at around 490°C. Since these peaks are not present in the virgin carbon response, it can be concluded that they are formed by H_2S adsorption and oxidation. Previous work revealed that the first peak is due to desorption of oxidized sulfur species (SO_2, SO_4^{2-}, etc), while the second peak comes from elemental sulfur species (Adib et al., 1999a; Bandosz, 2002). The exact locations of the two peaks vary in temperature due to the different physical and chemical characteristics of activated carbon (Bagreev and Bandosz, 2002), but it is in agreement that the peak relative to oxidized sulfur comes before the element sulfur peak.

In Figure 7.5, the P2 peak (representing elemental S) is small for the exhausted carbon and is hardly detectable for all the tested BAC samples taken from the HBTF bed. Compared to the exhausted carbon, the negligible P2 response observed with BAC samples indicated that the biofilm presence on carbon may enhance the adsorbed H_2S oxidation to sulfate. The P1 area (representing contents of oxidized sulfur) slightly decreased from the inlet to the outlet of the bed (C_2 to C_4, and to C_6) with their area units changing from 3.91 to 3.55 and 3.53 on day 60 (Figure 7.5a) and from 5.83 to 5.37 and 5.26 on day 200 (Figure 7.5b). The increased content of oxidized S species on BAC collected on day 200 (when compared to day 60), indicates clearly the further adsorption/biodegradation of H_2S on BAC for a longer period of HBTF operation. The

weight loss of P1 for BAC on day 60 are less than that of exhausted carbon (4.59 wt.%), whilst those for BAC on day 200 are all higher than that of exhausted carbon.

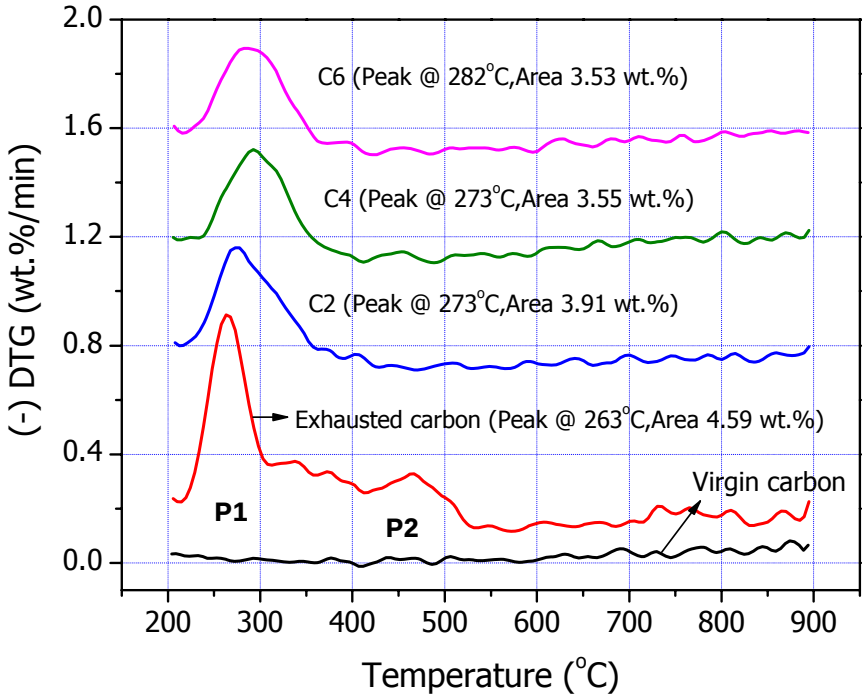

a. At 60 days' operation.

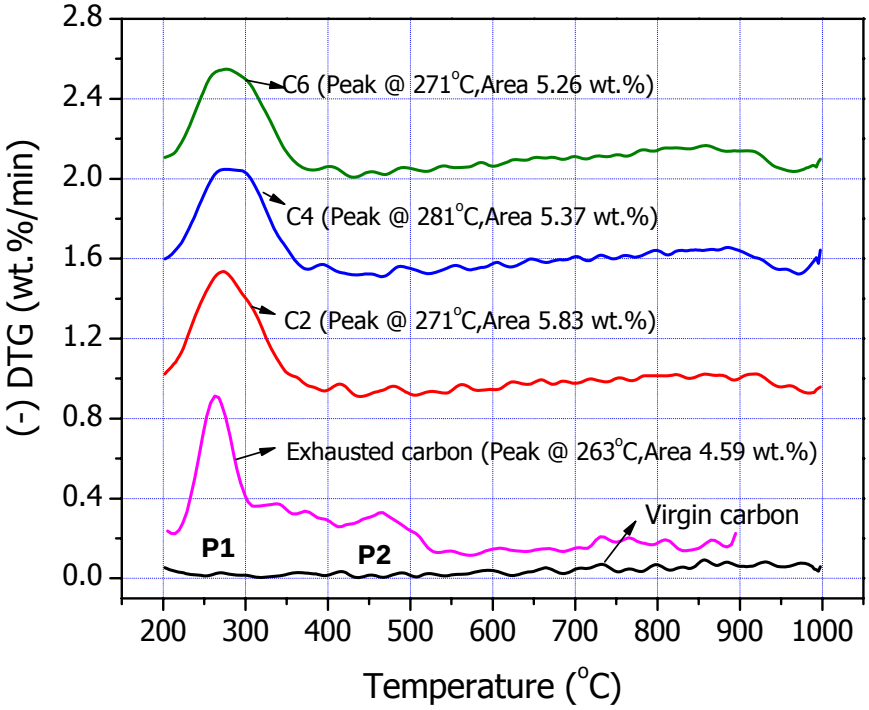

b. At 200 days' operation.

Figure 7.5 DTG curves of the exhausted carbon and BAC from the HBTF bed.

(C2 = carbons at 5 cm; C4 = carbons at 15 cm; C6 = carbons at 25 cm; C7 = carbons at 30 cm from the inlet of the bed)

The filtrates obtained from carbon surface pH measurement were analyzed by ion chromatography (IC), and no distinguish peaks other than sulfate was found in the IC spectra. This positively indicates that the biofilm enhanced sulfide oxidation on the BAC surface, and that the oxidation intermediates remained in low concentration and were non-detectable by IC.

Elemental analysis

FTIR spectra, DTG curves and IC spectra all showed that the dominant sulfide oxidation products on BAC are sulfate, which has the highest oxidation valence of sulfur [S(VI)] and is non-combustible. In order to obtain the content of combustible sulfur-bearing species, if any, present on BAC, CHNS elemental analysis (including C, H, S, and N) was conducted. Figure 7.6 shows an example of combustible C, H, N, S contents (wt.%) for the center and side BAC samples of the HBTF bed on day 200. Results of the elemental analysis of virgin and exhausted carbons are also shown. Results of side and center BAC samples on day 60 demonstrated similar tendencies as shown in Figure 7.6 and are therefore not given here. Compared to virgin carbon, the carbon content in BAC (Figure 7.6) was slightly decreased due to accumulation of combustible sulfur-bearing species and biomass on the bed. The contents of hydrogen and sulfur in BAC were therefore higher than those in virgin carbon, but the increase in sulfur content in BAC was not as much significant as that found with the exhausted carbon sample.

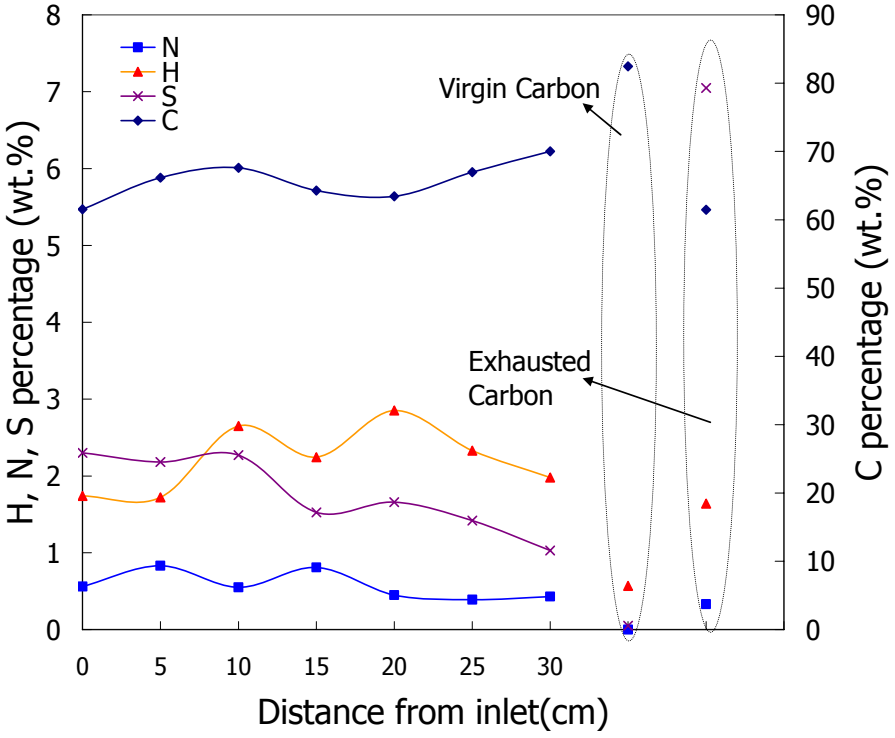

a. BAC samples from centerline

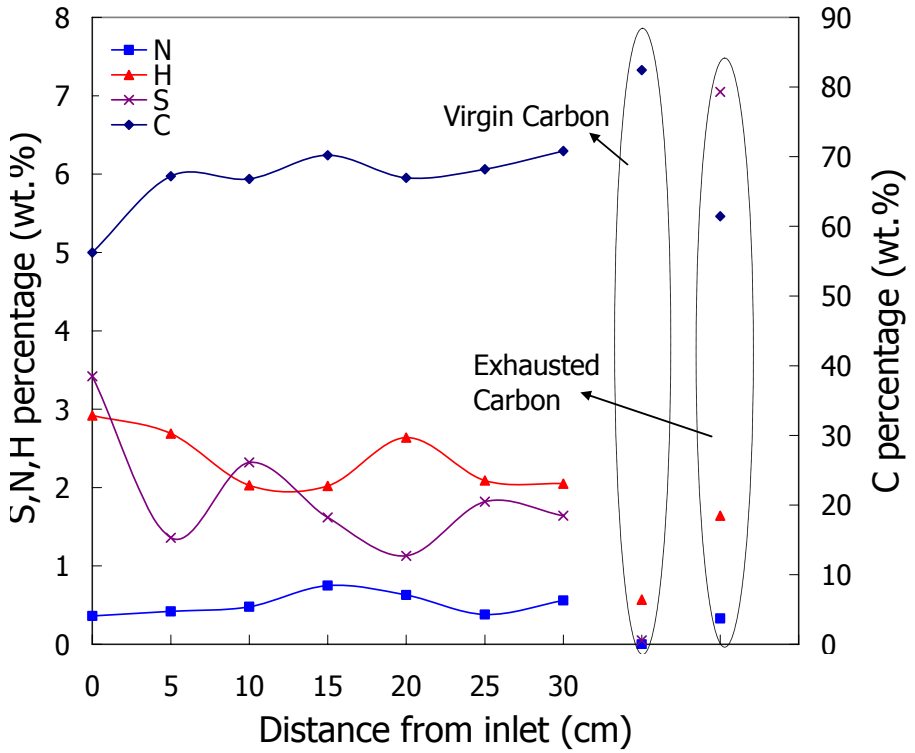

b. BAC samples from sideline

Figure 7.6 C, H, N, S contents of virgin carbon, exhausted carbon and BAC along the HBTF bed on day 200.

Sulfur content

Figure 7.7 is plotted to show the change of combustible sulfur-bearing species along the bed at both center and side locations of the HBTF. The combustible sulfur-bearing species could be any intermediate oxidation products of H_2S [excluding S(VI)] formed through either physical/chemisorption or biological oxidation. On day 60 (Figure 7.7a), a decreasing trend of the content of combustible sulfur on BAC is observed from the inlet to the outlet of the HBTF bed. In comparison to the side samples, a much sharper decrease in sulfur content from inlet to outlet locations was observed for the samples taken along the centerline of the HBTF. This probably may be due to the difficulties of H_2S diffusion to the side of the carbon bed. A different observation was however noted on day 200 (Figure 7.7b). The combustible sulfur is much higher in quantity than those found on day 60. Contents of the side samples are more variable than center samples due to possibly poor water distribution at the side of the bed.

The contents of combustible sulfur-bearing species in a sample each of exhausted and virgin carbon are also plotted in Figure 7.7. The 7.05 wt.% value for exhausted carbon is much higher than that of the BAC samples (the highest sulfur content: 1.79 wt.% for 60 days' and 3.42 wt.% for 200 days' HBTF run). In other words, the intermediate oxidation products of sulfur [combustible, excluding S(VI)] on BAC are much less than those of the exhausted carbon, regardless of the larger content of sulfates [S(VI), indicated by P1 in thermal analysis, Figure 7.5] in the BAC previously observed. Again, this is another positive evidence that the biofilm on the BAC enhanced the oxidation of H_2S on the carbon surface, resulting in the formation of sulfate, which is noncombustible.

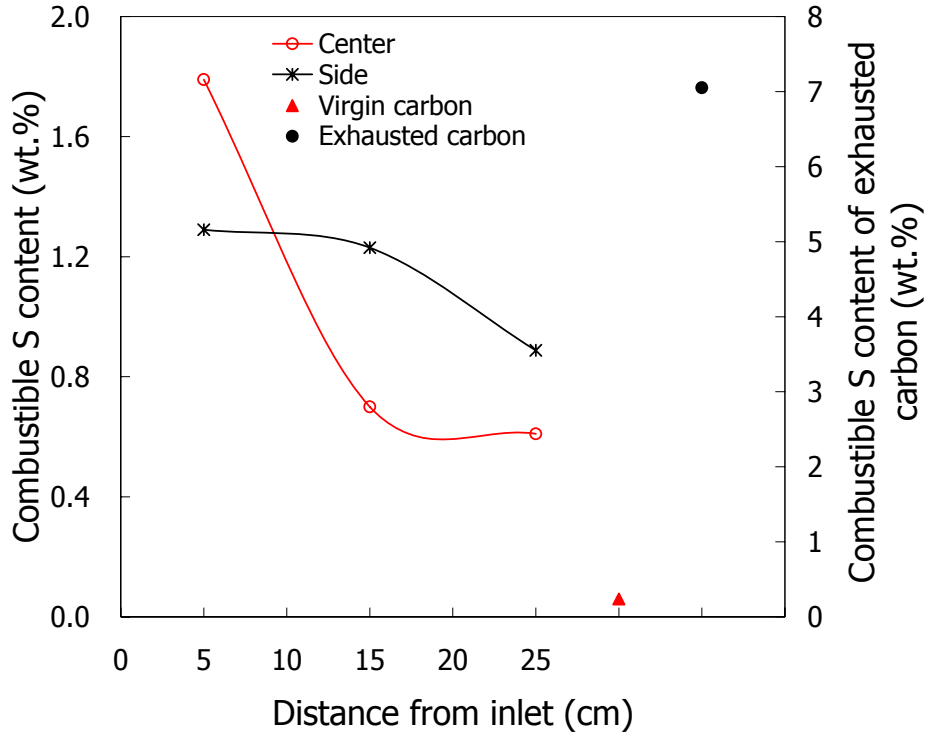

a. At 60 days' operation.

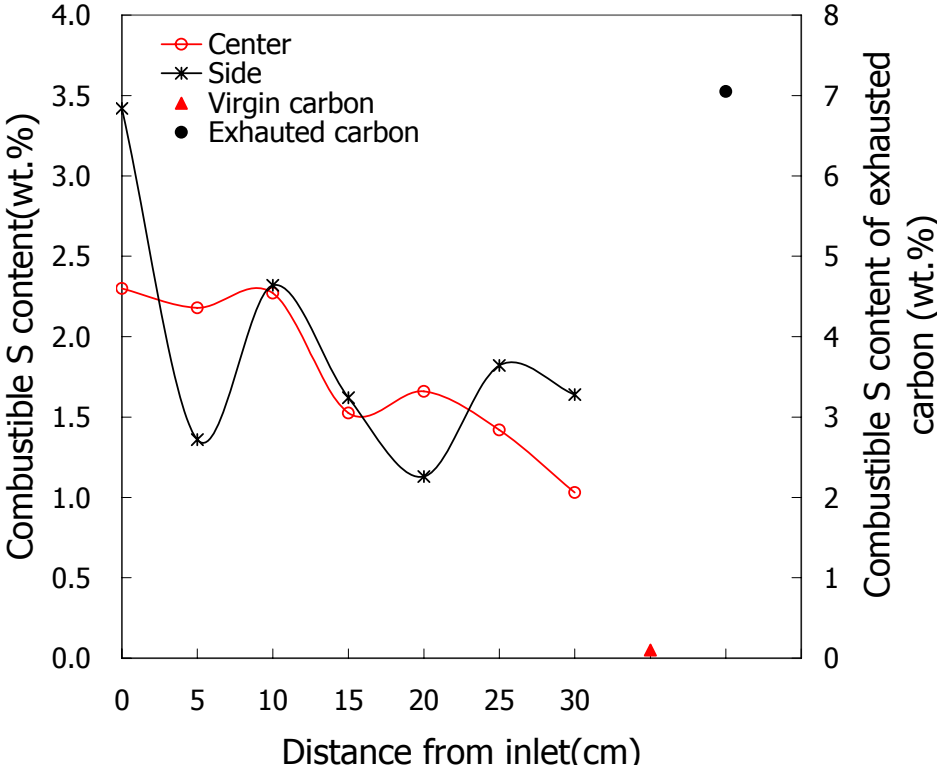

b. At 200 days' operation

Figure 7.7 Combustible sulfur content profiles along the HBTF bed

7.2 Combined Effect of Adsorption and Biodegradation of BAC on H_2S Biotrickling Filtration

In this section, four parallel laboratory-scale biofiltration columns packed with different media were set up and evaluated for the treatment of H_2S. Surface chemistry of the used carbons [BAC or virgin activated carbon (VAC)] in all these columns was studied to provide further insights on to the combined effects of biodegradation and adsorption when the novel BAC is used.

7.2.1 Experimental Section

Figure 7.8 shows the schematic diagram of a four-column biofilter system that was designed and constructed for this study phase. The four glass columns, which are identified as A, B, C, and D, could be run simultaneously and controlled separately. The biofilter bed material is enclosed in each glass tube which has an inner diameter of 4 cm and packing height of 5 cm. Column A (biotrickling filter with 20% BAC + 80% glass beads), B (trickling filter with 20% VAC + 80% glass beads), C (20% BAC + 80% glass beads but without trickling solution adsorption column), and D (100% glass beads acting as a trickling filter) are distinguished according to the amount and kind of activated carbon used in the column and the mode of liquid medium in operation. Figure 7.8 and Table 7.2 provide the details of the set-up. In column A, the H_2S removal was expected to be attributed to the combined action of biodegradation by the biofilm on the BAC (1), adsorption on the solid (glass beads + carbon) (2) and adsorption in the trickling liquid (3). For column B which does not have the presence of bacteria, H_2S removal was expected to be attributed to only adsorption on combination of the solid (glass beads + carbon) (2) and in the trickling liquid (3). Column C was operated as a biofilter system without liquid trickling. Hence H_2S removal was therefore attributed to the adsorption on the solid (glass

beads + carbon, 2) only. Finally column D served as a reference column, as only inert materials (glass beads) were packed in it. H_2S removal in column D therefore only accounted for the adsorption in the liquid trickling through it (3). The role of glass beads in column A, B and C is to dilute the carbon packing in order to obtain a reasonable breakthrough time. Glass beads of 5 mm in diameter were selected for use because of its comparable apparent surface area (78.5 mm^2) with that of carbon pellet used - Calgon AP460 (108.1 mm^2). Activated carbon was mixed with the glass beads in a volume ratio of 1:4, which enabled a reasonable breakthrough time (~120 h) to be obtained for the series of experiment.

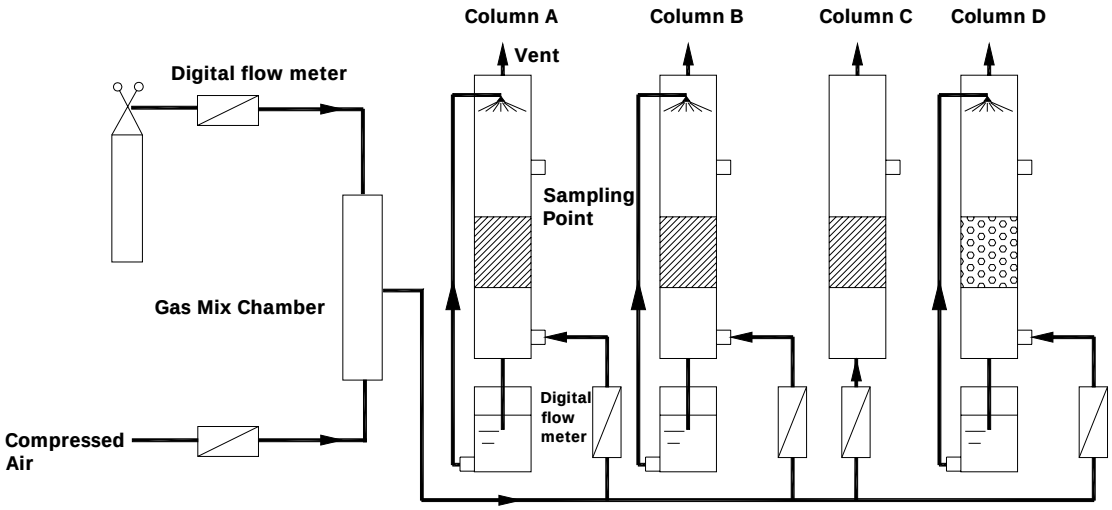

Figure 7.8 Schematic of four-column biofiltration system

(Column A: 20% BAC + 80% glass beads with liquid medium recirculation; Column B: 20% VAC + 80% glass beads with liquid medium recirculation; Column C: 20% VAC + 80% glass beads without liquid medium recirculation; Column D: 100% glass beads with liquid medium recirculation)

Table 7.2 Physical properties and part of the results in parallel columns

Physical Properties	Columns			
	A	B	C	D
Operating Pattern	Biotrickling filter	Trickling filter	Adsorption column	Trickling filter
Packing materials	BAC+ glass beads	VAC+ glass beads	VAC+ glass beads	Glass beads
Activated carbon weight, W_2 (dry base, g)	7.79	7.77	7.78	0
Glass beads weight (5mm diameter), W_g (g)	79.72	79.7	79.74	100.82
Volume percentage of activated carbon, (%,v/v)	20	20	20	0
Diameter of the columns (cm)	4	4	4	4
Bed Height, L (cm)	5	5	5	5
Volume of media, V (mL)	62.8	62.8	62.8	62.8
H_2S inlet concentration, C (ppm_v)	45	45	45	45
Gas retention time, t (s)	4	4	4	4
Gas flow rate, Q_g ($L \cdot min^{-1}$)	0.944	0.944	0.944	0.944
Liquid flow rate, Q_l ($mL \cdot min^{-1}$)	0.71	0.71	0	0.71
Recirculation medium volume, V_1 (L)	0.5	0.5	0	0.5
Running time, t (h)	120	120	120	120
Total H_2S feed, (g S)	0.4	0.4	0.4	0.4
H_2S removed in whole run, EC[a] (g S)	0.119	0.082	0.044	0
TSS[b] increasing during the run, ($g \cdot L^{-1}$)	1.13	0.33	-	-

[a]EC: Elemination capacity;

[b]TSS: Total suspended solid

H_2S inlet concentration was fixed at 45 ppm_v by mixing 1% (v/v) standard hydrogen sulfide (Linde Gas, Singapore) at 4.30 $mL \cdot min^{-1}$ with air at 940 $mL \cdot min^{-1}$. The total synthetic foul gas at a flow rate of 944.3 $mL \cdot min^{-1}$ was directed into the experimental columns as shown in Figure 7.8. The superficial gas velocity and retention time of the gas passing through the column were kept at 1.25 $cm \cdot s^{-1}$ and 4 s, respectively. Each column was operated for 120 h in total. An amount of 500 mL of recirculation liquid medium (refer to Table 3.1) was used and a hydraulic retention time (HRT) of 88.45 min, wherever applicable was maintained. The experiments were all conducted at room temperature of about 25 ^oC. The H_2S concentrations were measured at the outlet of the bed using Jerome 631-X H_2S analyzer (Arizona Instrument, USA).

An offline immobilization of microorganisms onto the carbon surface (in column A) was applied to produce the BAC in accordance to the procedures described previously in Section 4.2.1. Periodic sampling of trickling liquid medium was carried out during the column runs, and carbon samples were taken out and subjected to analysis on completion of the experiment. Dissolved total sulfur (DTS), sulfate concentrations, and pH in the aqueous phase were determined as per procedures described previously in Section 3.3.2. For the solid phase, total sulfur contents, pH, sulfate, and combustible sulfur species in the carbon samples, were measured as discussed in Section 3.2.1.

7.2.2 Results and Discussion

7.2.2.1 Performance comparison of the Biofiltration systems

Figure 7.9 illustrates the H_2S removal profiles of column A,B and C during the experimental duration of 120 h. Except for the inlet H_2S input curve (set constant as 45 ppm_v), the other three curves represent the outlet concentration-time profile from column A, B, and C, respectively. Results from column D was not plotted as the H_2S broke through the glass beads within 3 min after passage of the H_2S gas stream. This indicated that the adsorption of H_2S by the liquid film and the glass beads had insignificant contribution to the removal of H_2S. Experimental run of column D was terminated early on breakthrough and therefore, the adsorption of H_2S on glass bead surface was ignored. The outlet H_2S concentration of column B was always lower than that of column C during the column runs indicating that the trickling liquid over the VAC (in column B) provided a measure of H_2S removal. As shown in Figure 7.9, the outlet H_2S concentration profile of column A against time was fluctuating within 20~40 ppm_v, while columns B and C that involve only carbon adsorption had a gradual increase (less fluctuation) of outlet H_2S concentration profile against time. As shown in Table 7.2, total sulfur feeding (in form of H_2S) for each column was 0.4 g

during the 120 h of operation. For the duration of 120 h, column C got its breakthrough point had removed 11% of the incoming H_2S (0.044/0.4, Table 7.2), while column B had removed 20.5%of the fed H_2S (0.082/0.4, Table 7.2). This additional removal of H_2S by column B probably was due to the sulfur oxidation products transferred from the solid phase (glass beads + carbon) to the aqueous phase in the liquid trickling bed. The H_2S removal for column A (which had BAC) was 29.8% of the incoming H_2S during the 120 h run (0.119/0.4, Table 7.2). The increase of total suspended solid (TSS) in the recirculation solution during the whole run for column A was 1.13 $g \cdot L^{-1}$ (Table 7.2). This value was almost three times higher than that of column B (0.33 $g \cdot L^{-1}$). This might be due to the growth of biomass in the aqueous phase and some insoluble H_2S oxidation products that were flushed into the recirculation solution.

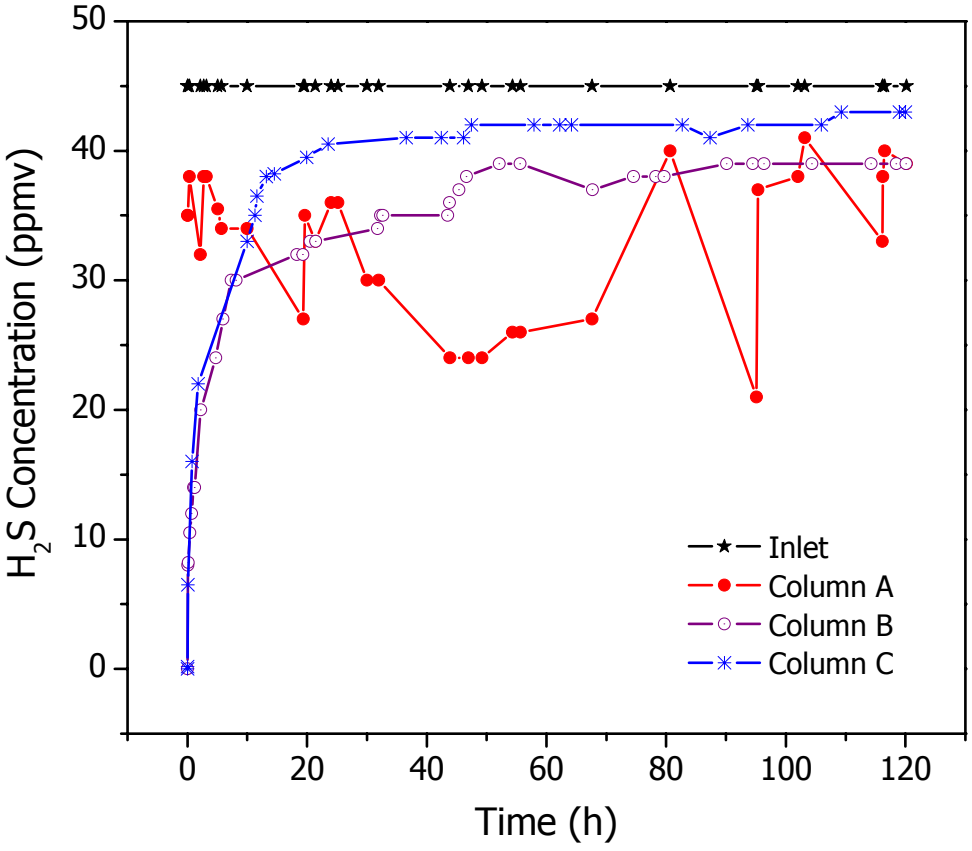

Figure 7.9 H_2S elimination profile in the biofiltration system

Figure 7.10 shows the pH profiles of the recirculation solution in the trickling systems (column A and B) that were monitored during the experimental runs. As Figure 7.10 shows, the initial pH value of the liquid medium was 6.6. The pH value of recirculation liquid in column A decreased continuously to 5.9 at the end of the 120 h run, while that of column B remained almost constant. It is well known that the biodegradation of sulfide will create hydrogen ions. Therefore, the pH of the recirculation medium will decrease if biodegradation takes place in the aqueous phase. In column B where only physical/chemical adsorption occurred, complex chemical reactions might take place on the carbon surface during the adsorption process to form S-bearing complex (Yan et al., 2002). The adsorbed H^+ in column B may not however be washed off easily, thus the pH of recirculation solution remained constant in the trickling system for column B which was packed with non-biologically activated carbon (VAC). It is desirable to avoid significant pH drop in a biofiltration system so as to prevent highly acidic environment which can cause damage the microbial growth in biofilters, especially if pH is below 1 (Section 6.3.3.1).

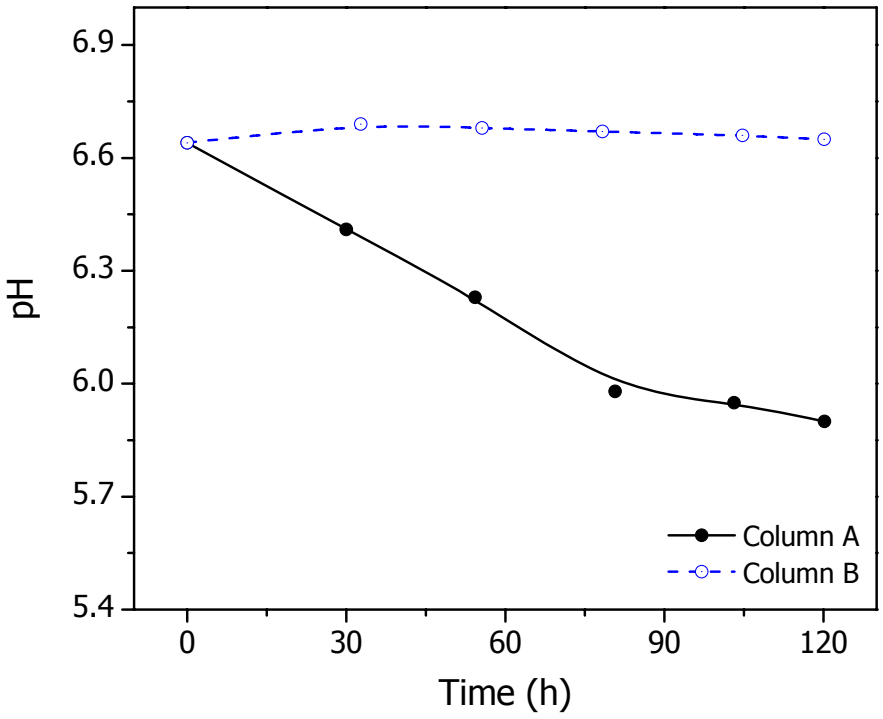

Figure 7.10 pH profiles of the aqueous phase in biotrickling system

7.2.2.2 Sulfide oxidation products analysis

In the process of H_2S biodegradation, H_2S is used as electron donor by the bacteria. The oxidation of H_2S occurs in stages such as $H_2S \rightarrow S^0 \rightarrow S_2O_3^{2-} \rightarrow S_4O_6^{2-} \rightarrow S_3O_6^{2-} \rightarrow SO_3^{2-} \rightarrow SO_4^{2-}$ (Maier et al., 2000). An investigation on the distribution of sulfur oxidation products during the biofiltration of H_2S will eventually contribute to a better understanding of this process.

Aqueous phase

The changes of total sulfur content (T-S, measured by ICP-OES) and sulfate sulfur content (S-S, measured by IC) in the aqueous phase are plotted in Figure 7.11. As Figure 7.11 shows, the initial T-S concentration in the liquid medium is 12.3 $mg \cdot L^{-1}$, and S-S concentration, 1.4 $mg \cdot L^{-1}$. In the BAC biotrickling filter (column A), T-S and S-S concentrations increased greatly during the biotrickling filter run, and finally reached 239 $mg \cdot L^{-1}$ (T-S) and 222 $mg \cdot L^{-1}$ (S-S) in the aqueous phase, respectively. For column B which involved adsorption only, both T-S and S-S contents in aqueous phase increased mildly and remain at relatively low level (37 $mg \cdot L^{-1}$ of T-S and 16 $mg \cdot L^{-1}$ of S-S at the end of operation, respectively) throughout the column run. It shows that the additional biodegradation on BAC enhanced the adsorptive oxidation of H_2S in total due to possibly the further bio-oxidation of adsorbed H_2S and other reduced sulfur-bearing species.

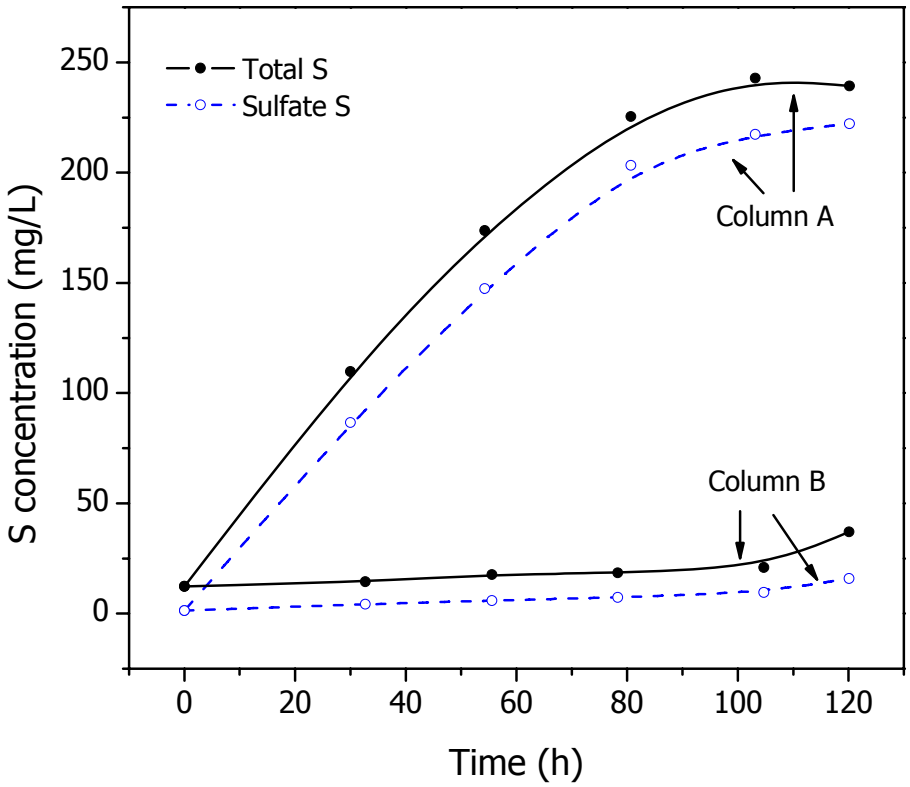

Figure 7.11 Time-variable total and sulfate sulfur concentration in aqueous phase.

Figure 7.12 illustrates the different patterns of the S-S percentage (%) changes in T-S throughout the runs for columns A and B. Both the BAC and the VAC have demonstrated a continuously increase of sulfate percentage versus run time. In column B (carbon adsorption only), S-S percentage increased mildly, and at the end of the run, it accounts for 43% of the total soluble sulfur in the aqueous phase. While in column A (packed with BAC), the S-S percentage increased greatly to around 80% of the T-S during the first 30 h with a slower rate of increase after that. With the growth of bacteria during the biotrickling filters run, more and more sulfate was produced and resulted in the increase of the S-S percentage of the T-S. Finally, the S-S content in the aqueous phase reached 93% of the T-S in the BAC system (column A) and 43% of the T-S in the VAC system (column B).

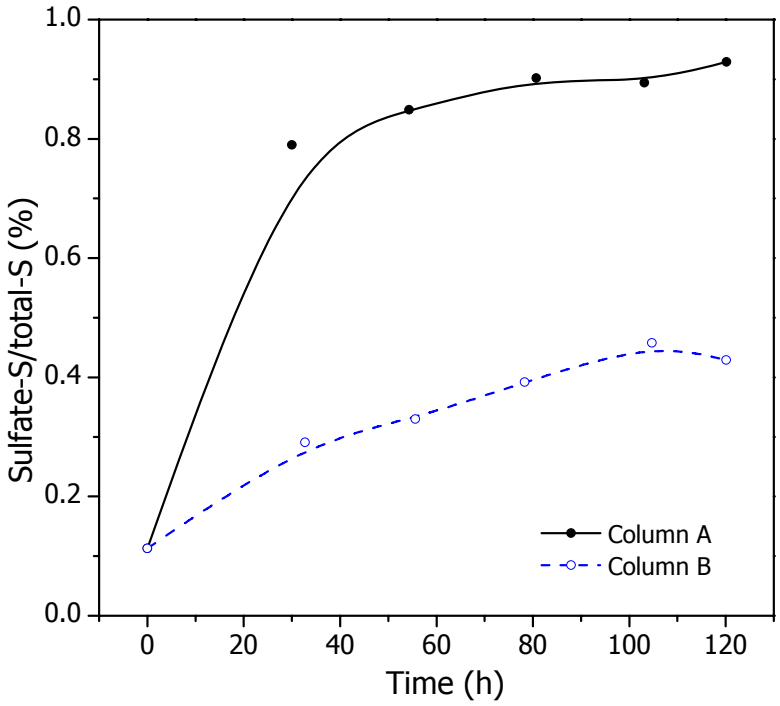

Figure 7.12 Percentages of sulfates in total sulfur in aqueous phase.

Solid phase

The combustible sulfur-bearing species (C-S) on carbon surface (measured by CHNS analyzer) include H_2S, organic sulfur and any intermediate oxidation products of H_2S, excluding sulfates [S(VI)], formed through either adsorption or biological oxidation of H_2S. Sulfate at the carbon surface is soluble so that it most likely will be transferred to the aqueous phase when carbon was subjected to washing by ultra pure water (UPW). Therefore, S-S on the carbon surface was determined by measuring the sulfate concentration in the water that was extracted from the carbon (details in Section 3.2.1). The T-S on the carbon was measured by XRF. Distinguishing these three types of sulfur content can assist to provide additional understanding of the different effects of adsorption and biodegradation on H_2S removal and oxidation products distribution on the BAC medium.

Variable sulfur content in the solid phase of the biofiltration systems, measured by different approaches, are shown in Table 7.3. As previously mentioned (Section 3.2.1), the pH value of the carbon surface was determined by UPW extraction of the

carbon pellets. The T-S content in the carbon is supposed to be equal to the sum of S-S and C-S. But unfortunately, a poor mass balance of sulfur distribution in the three forms was seen in Table 7.3, which was most likely due to the different analytical approaches and methods being applied. Only those data from the same approach (presented in the same column) are comparable.

As Table 7.3 shows, the surface pH of VAC is 7.96. After the immobilization with bacteria, the pH of the BAC surface decreased to 3.44 due to the accumulation of H^+ produced by bacterial metabolism. The pH value of the BAC increased to 5.34 after the 120 h run of column A. This is probably due to the produced H^+ on BAC surface being washed off by the recirculation solution. For column B and C, the relatively slight pH decreases might be due to the adsorption of H_2S onto the carbon bed. Comparing the T-S on the carbon surfaces in the three used columns, although column A had the recirculation solution trickling through, where the soluble sulfur might be washed off the carbon bed, the BAC accumulated the most sulfur (2.33 wt.%) on its surface among the three. In column B, 1.23 wt.% of sulfur accumulated on carbon surface, which is more than that adsorbed in column C (0.84 wt.%). These data confirmed that moisture may help the adsorption of H_2S as Yan et al. (2002) reported previously. For the S-S, the amount of sulfate accumulated on the BAC surface (0.28 wt.%) is much more than the trickling VAC column (B, 0.034 wt.%). It was most likely due to the better performance of column A in removing H_2S which lead to a higher S-S than that in column B. Without liquid trickling, more S-S deposited on activated carbon in column C (0.20 wt.%) than that in column B. It is because that in column B, the produced sulfate was washed off the carbon pellets by the recirculation solution, while there is no transfer of sulfate in column C. Still, more C-S (0.56 wt.%) was fixed on column A than the other two columns (0.14 and 0.34 wt.%, respectively). This indicated that the biofilm on carbon surface did improve the carbon adsorption capacity of H_2S.

Table 7.3 Sulfur profile in solid phase

Samples	pH	Total sulfur conc. (wt.%)	Sulfate sulfur conc. (wt.%)	Combustible sulfur conc. (wt.%)
VAC	7.96	-	-	0.06
Original BAC	3.44	1.50	0.040	0.35
Used BAC from column A	5.34	2.33	0.28	0.56
Used VAC from column B	6.84	1.23	0.034	0.14
Used VAC from column C	6.92	0.84	0.20	0.34

-: undetectable

7.3 Mathematical Modeling of the Biofiltration Kinetics in the BAC- based HBTF

A simplified 2-D linear force driving (LDF) kinetic model was developed in this section to understand and simulate the experimental HBTF process on the basis of dynamic mass balance, which incorporates several phenomena including convection, dispersion in the gas phase, partial coverage of biofilm on supporting medium surface, interface mass transfer between gas/biofilm, direct adsorption, and biological reactions in the biofilm. Biodegradation of H_2S in the biofilm was described using Michaelis-Menten relationship and homogeneous surface diffusion model (HSDM) was used to predict the dynamic adsorption of the system (Traegner and Suidan, 1989). Several constants, such as biodegradation rate, mass transfer rate, and adsorption equilibrium constant were determined by bench experiments. The model equations were solved analytically for some parameters and numerically by MATLAB.

7.3.1 Model Description

The model proposed in this study describes transport, physical adsorption and biological processes that occur during the biofiltration. As foul gas passes through the biofilter, dispersion, advection, adsorption, diffusion, bioreaction, and the characteristics of the biofilm over activated carbon surface will affect the efficiency of contaminant removal (Figure 7.13).

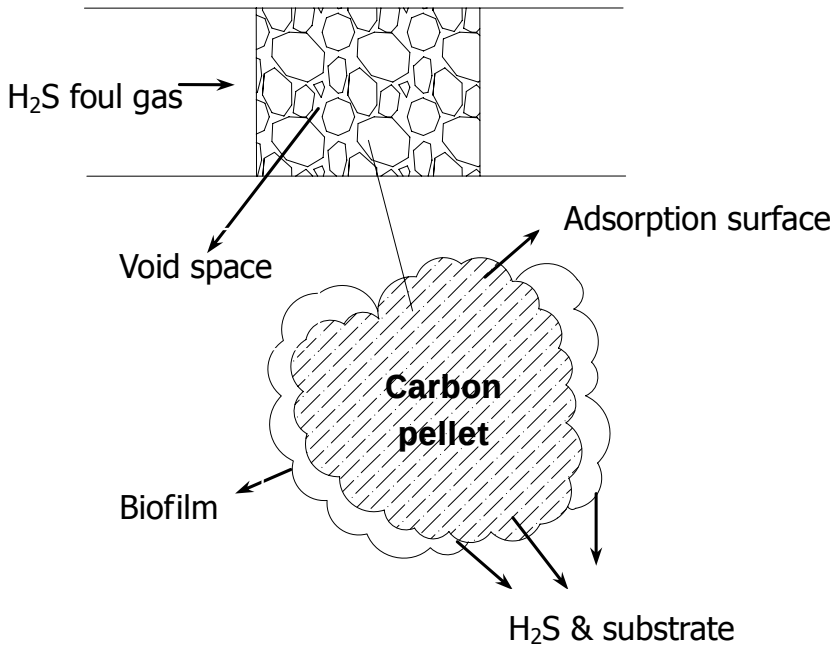

Figure 7.13 Biophysical model for the horizontal biotrickling filter

It is not possible to consider every phenomenon that occurs in the filter. Therefore, several simplifying assumptions are made in developing the theoretical model and are listed as follows:

1. An axially dispersed plug flow is assumed for the gas flow through the packed bed, and gas flow rates are sufficiently high to neglect axial dispersion; isotherm operation and the ideal gas law apply for the gas phase.
2. The frictional pressure drop is assumed to be negligible; oxygen limitation was not considered in this study.
3. The rate of biodegradation depends on the concentration of substrate.
4. The packing material is not entirely covered with the biofilm. The exposed patches of carbon solid surface contact with the air stream directly. Adsorption of the pollutant on the solid particles occurs primarily through the portion of the surface that is not covered with the biofilm. The biofilm adsorption (gas-biofilm interface) and the solid adsorption from the biofilm (biofilm-solid interface) are negligible.
5. The biofilm is modeled as a flat plate. It is a reasonable approximation because the thickness of the biofilm is much smaller compared to the diameter of the carbon pellet. The biofilm has a finite and constant thickness and density. And the concentration of substrate in the biofilm at the interface (gas-biofilm) is assumed to be in equilibrium with the concentration in the bulk gas. The substrate is assumed to contact the biofilm and transport within the biofilm through diffusion only and characterized by Fick's law (Montgomery, 1985). These concepts were illustrated for a carbon pellet in Figure 7.14.
6. At steady state, microorganisms are considered to be uniformly distributed throughout the biofilm and the whole biofilter.
7. There is no net biomass accumulation in the biofilter bed.
8. The kinetics of substrate reactions in the biofilm surrounding the activated carbon pellets follow the Michaelis-Menten relationship, with H_2S the only rate-limiting substrate, developed for enzyme mediated reactions:

$$-r_b = \frac{k_{max} C_f}{K_s + C_f}, \qquad \text{Eq.7-7}$$

where C_f = substrate concentration in the biofilm, $g \cdot m^{-3}$; k_{max} = maximum degradation rate, $g \cdot m^{-3} \cdot s^{-1}$; K_s = half-saturation constant (Michaelis constant), $g \cdot m^{-3}$; and r_b = substrate biodegradation rate, $g \cdot m^{-3} \cdot s^{-1}$. This biokinetics can be simplified as first-order at low substrate concentration and zero-order at high concentration. The H_2S is used as an energy source, and it is assumed that carbon source (CO_2 in this case) is not rate-limiting.

9. In order to simplify the model, the carbon pellets are assumed to be spherical although Calgon AP460 is cylindrical. The substrate concentration is assumed to decrease from the particle surface, where its concentration is in equilibrium with bulk gas phase, to a value of zero at some radial distance from the center of the pellet. The intraparticle substrate concentration inside carbon pellet is considered to be radially uniform.
10. The rate of mass transfer around the boundary of the carbon pellet is approximated by a linear driving force (LDF) model.

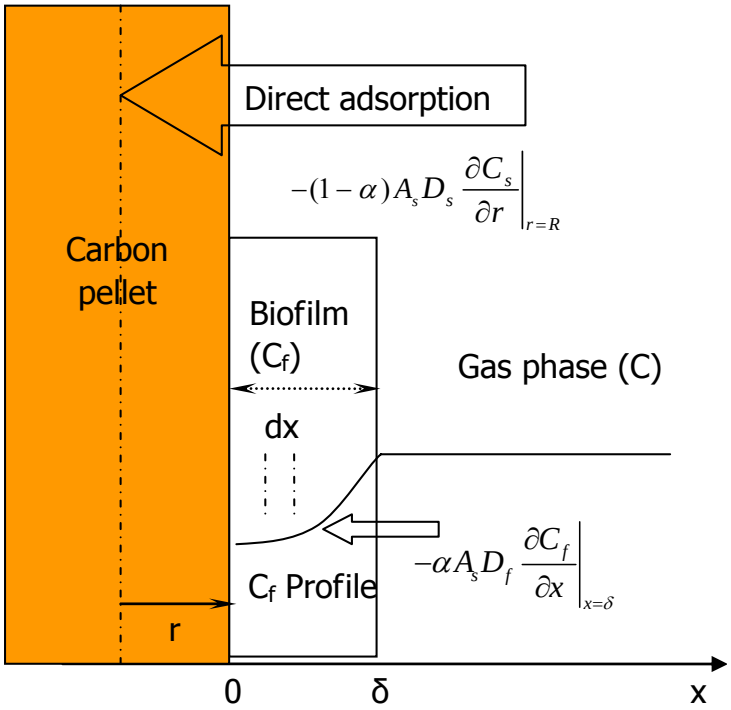

Figure 7.14 Schematic concept of the biofiltration model.

The fundamental phenomena governing the transport of substrates (H_2S) in gas-phase are dispersion, advection and diffusion, as well as in this work the biodegradation in the biofilm and adsorption on the solid phase. Based on the above assumptions, the transient biofilter operation is described using the following equations.

Mass balance in gas phase The mass balance of the substrate (H_2S) from air to the biofilm/solid phase, which considers the dispersion, advection and mass transfer to the biofilm/solid phase (to the biofilm by diffusional flux, to the solid support media by adsorption), can be modeled as:

$$\frac{\partial C}{\partial t} = D\frac{\partial^2 C}{\partial z^2} - v\frac{\partial C}{\partial z} - \left(\alpha A_s D_f \left.\frac{\partial C_f}{\partial x}\right|_{x=\delta} + (1-\alpha) A_s D_s \left.\frac{\partial C_s}{\partial r}\right|_{r=R} \right), \qquad \text{Eq.7-8}$$

where C = concentration of substrate in air phase, $g \cdot m^{-3}$; z = distance of travel in filter, m; α = percentage coverage of the particle by the biofilm; A_s = effective diffusion surface area per volume of packing (specific area), m^{-1}; D = dispersion coefficient of substrate in air phase, $m^2 \cdot s^{-1}$; v = axial interstitial gas velocity, $m \cdot s^{-1}$; D_f = diffusivity of substrate in the biofilm, $m^2 \cdot s^{-1}$; C_f = concentration of substrate in biofilm, $g \cdot m^{-3}$; x = distance in biofilm, 0~δ μm; D_s = internal pore diffusivity of substrate within activated carbon pellet, $m^2 \cdot s^{-1}$; C_s = concentration of substrate in carbon, $g \cdot m^{-3}$; r = radius distance in carbon pellets, m; R = equivalent radius of carbon pellet (spherical), m; and t = time, h.

Balance in biofilm phase

$$-\alpha A_s D_f \left.\frac{\partial C_f}{\partial x}\right|_{x} + \alpha A_s D_f \left.\frac{\partial C_f}{\partial x}\right|_{x+\Delta x} + \alpha A_s \Delta x \cdot r_b = 0 . \qquad \text{Eq.7-9}$$

Balance in solid phase The mathematical description of the substrate concentration as a function of radial distance in the carbon particle which was developed by Traegner and Suidan (1989) was used. It is derived from a material balance for a

spherical shell with thickness, dr, which for steady state is:

$$\frac{\partial C_s}{\partial t} = D_s\left(\frac{\partial^2 C_s}{\partial r^2} + \frac{2}{r}\frac{\partial C_s}{\partial r}\right). \qquad \text{Eq.7-10}$$

Boundary conditions:

$$\left.\frac{\partial C_s}{\partial r}\right|_{r=0} = 0, \qquad \text{Eq.7-11}$$

$$C_s\big|_{r=R} = C \qquad \text{Eq.7-12}$$

Applying first order adsorption kinetics in this case (Appendix B): $\frac{\partial C_s}{\partial t} = k_{ad}C$, Eq. 7-10 becomes:

$$\frac{\partial^2 C_s}{\partial r^2} + \frac{2}{r}\frac{\partial C_s}{\partial r} = \frac{k_{ad}C}{D_s}, \qquad \text{Eq.7-13}$$

where k_{ad} is the first order reaction rate constant that describes adsorption on activated carbon particles, s^{-1}. Solving Eq.7-13 under the boundary conditions of Eq. 7-11 & 7-12 yields the following:

$$\frac{C_s}{C} = 1 + \frac{k_{ad}}{6D_s}\left(r^2 - R^2\right). \qquad \text{Eq.7-14}$$

First-order biodegradation kinetics

When the substrate concentration in the gas phase is very low, $C_f << K_s$, Eq.7-7 reduces to a first-order rate equation: $r_b = -k_1 C_f$. At steady state, a mass balance on the substrate for a differential element in the biofilm of a carbon pellet (Figure 7.14) is derived from Eq. 7-9 by substituting r_b with $-k_1 C_f$:

$$-A_s D_f \left.\frac{\partial C_f}{\partial x}\right|_x + A_s D_f \left.\frac{\partial C_f}{\partial x}\right|_{x+\Delta x} - k_1 C_f A_s \Delta x = 0, \qquad \text{Eq.7-15}$$

where k_1 = first-order reaction rate constant, s^{-1}. Dividing both sides by A_s and Δx, and taking the limit as Δx approaches zero, yield:

$$D_f \frac{\partial^2 C_f}{\partial x^2} - k_1 C_f = 0 . \qquad \text{Eq.7-16}$$

The boundary conditions, assuming reaction limited kinetics, are

$$\left.\frac{\partial C_f}{\partial x}\right|_{x=0} = 0 , \qquad \text{Eq.7-17}$$

$$C_f\big|_{x=\delta} = \frac{C}{H} , \qquad \text{Eq.7-18}$$

where H is Henry's Law constant. The solution of Eq.7-16 to Eq. 7-18 is:

$$C_f = \frac{C}{H}\frac{\cosh\left(\Phi\frac{x}{\delta}\right)}{\cosh\Phi} , \qquad \text{Eq.7-19}$$

where Φ = "Thiele modulus" and is defined as $\Phi = \delta\sqrt{\frac{k_1}{D_f}}$.

Assuming that dispersion is negligible when the system is at steady state, Eq.7-8 reduces to:

$$-v\frac{\partial C}{\partial z} - \left(\alpha A_s D_f \left.\frac{\partial C_f}{\partial x}\right|_{x=\delta} + (1-\alpha)A_s D_s \left.\frac{\partial C_s}{\partial r}\right|_{r=R}\right) = 0 . \qquad \text{Eq.7-20}$$

Combine Eq.7-14, 7-19, 7-20:

$$-v\frac{\partial C}{\partial z} = \alpha A_s D_f \left(\frac{\Phi}{\delta H}\tanh\Phi\right)\cdot C + \frac{(1-\alpha)A_s k_{ad} R}{3}\cdot C . \qquad \text{Eq.7-21}$$

Therefore, for the initial condition of $C\big|_{z=0} = C_0$, the solution of Eq.7-21 yields $C_g(z)$, the steady state gas-phase concentration of pollutant at bed length, z:

$$\frac{C}{C_0} = e^{-(E+F)\cdot z} , \qquad \text{Eq.7-22}$$

where $E = \frac{\alpha D_f A_s}{v}\left(\frac{\Phi}{\delta H}\tanh\Phi\right)$; $F = \frac{(1-\alpha)A_s k_{ad} R}{3v}$ at steady state of biodegradation before the carbon pores are saturated with H_2S. Here E can be considered to roughly represent the effect of biodegradation, and F evaluates the effect of adsorption. From Eq. 7-22, we can expect that the outlet concentration of H_2S is determined by the combined effect of biofilm degradation and carbon adsorption.

Zero-order biodegradation kinetics

For sufficient high substrate concentration, $C>>K_s$, Eq.7-7 reduces to a zero-order rate expression. In this case, Eq. 7-16 becomes:

$$D_f \frac{\partial^2 C_f}{\partial x^2} - k_0 = 0 . \qquad \text{Eq.7-23}$$

With boundary conditions of Eq.7-17 & 7-18, we obtain:

$$C_f = \frac{k_0 x^2}{2D_f} - \frac{k_0 \delta^2}{2D_f} + \frac{C}{H} . \qquad \text{Eq.7-24}$$

Following the same procedure as the in previous section, at steady state of biodegradation before the carbon pores are saturated with H_2S, the gas concentration at bed length, z, is

$$C = \left(C_0 + \frac{3\alpha k_0 \delta}{(1-\alpha) k_{ad} R} \right) e^{\frac{-(1-\alpha) A_s k_{ad} R}{3\nu} \cdot z} - \frac{3\alpha k_0 \delta}{(1-\alpha) k_{ad} R} . \qquad \text{Eq.7-25}$$

In this study, the highest H_2S inlet concentration is 200 ppm_v, which is still within the concentration range of first-order kinetics (Yang and Allen, 1994b). Due to the small size of the experimental biofilters used in this study, higher H_2S concentration can cause great harm to the microbial niche in the BAC-based biofilter because of the extremely low pH it caused. For this study, however, the BAC-based biotrickling filter can work efficiently at a H_2S loading of less than 113 $gH_2S \cdot m^{-3} \cdot h^{-1}$ (see Chapter 6). Therefore, zero-order kinetics cannot be validated by the experiment data in this HBTF.

7.3.2 Experimental Setup

Data from the bench-scale horizontal, cross-flow biotrickling filter (HBTF) system (details refer to Chapter 6) were used to evaluate the suitability of the mathematical model developed here. After the 120 days of operational run for the HBTF, the

system was conditioned and maintained to work at steady state, keeping the gas-liquid volumetric ratio at 40. The gas samples from each sampling point were extracted and measured under this stable set of conditions. The HBTF was considered to work steadily when the readings from each sampling point did not change much (variation less than ±5% of the average reading) over a period of 1 h. Gas sampling procedures and analytical conditions were previously presented in Section 3.3.

7.3.3 Model Parameter Estimation

The model proposed in this study was validated by using the results for some parameters available from some key published models developed by others (Hodge and Devinny, 1995; Abumaizar et al., 1997; Amanullah et al., 1999; Devinny et al., 1999; Den and Pirbazari, 2002; Li et al., 2002; Martin et al., 2002; Li et al., 2003). Other parameters that were unique to this proposed model were determined by batch experiments conducted in this study. The set of model parameters are tabulated in Table 7.4. Details of the model parameter estimation are provided in **Appendix B.**

Table 7.4 Values of model parameters preset

Parameters	Symbol	Initial Input Value	Source
Percentage coverage of the particle by the biofilm	α	0.7	(Devinny et al., 1999)
Effective diffusion surface area per volume of bed	A_S (m^{-1})	820.9	Batch experiments
Biofilm thickness	δ (μm)	35.7	Batch experiments
Effective diffusion coefficient in biofilm	D_f ($m^2 \cdot s^{-1}$)	1.61×10^{-9}	Perry's Handbook
Bed porosity	ε	0.37	HBTF
Equivalent radius of carbon particle	R (m)	2.7×10^{-3}	Calculated
Half saturation coefficient	K_s ($g \cdot m^{-3}$)	0.0279	(Kim and Deshusses, 2003)
First order biodegradation rate constant, $=k_{max}/K_S$	k_1 (s^{-1})	14.9	Batch experiments
Zero order biodegradation rate constant, $=k_{max}$	k_0 ($g \cdot m^{-3} \cdot s^{-1}$)	0.415	Calculated by k_1
Thiele modulus $\Phi = \delta\sqrt{k_1 / D_f}$	Φ	9.62×10^{4}	Calculated
First-order adsorption rate constant	k_{ad} (s^{-1})	2.18 (Range:2.04~2.31)	Breakthrough test
Distribution coefficient between biofilm & air ($C_g/C_f \approx H$)	H	0.42	Perry's Handbook

7.3.4 Comparison of Experimental Data and Model Simulation

Yang and Allen (1994b) reported that H_2S biodegradation rate followed either first-order kinetics when the inlet concentration was below 200 ppm_v, or zero-order biodegradation kinetics when the inlet concentration was above 400 ppm_v, or fractional-order kinetics when the inlet concentration fell in between. In this study, only first-order biodegradation kinetics was investigated due to the low H_2S concentration applied (0~200 ppm_v throughout the HBTF run). In this HBTF, 200 ppm_v of H_2S running through the packing bed at a short GRT of 4 s provided a high loading of 250 $gH_2S \cdot m^{-3} \cdot h^{-1}$, which is actually more than twice the reported maximum elimination capacities not only of this HBTF but also other biofiltration systems (Wu et al., 2001; Burgess et al., 2001b; Elias et al., 2002; Oyarzun et al.,

2003; Gabriel and Deshusses, 2004; Martin et al., 2004). Hence, for practical reasons, higher H_2S inlet concentration greater than 200 ppm_v was not applicable for the HBTF conducted in this study.

Figure 7.15 gives the normalized gas phase concentration profiles for the HBTF at various GRTs and inlet concentrations under first order biodegradation kinetics as predicted using Eq.7-22. The measured values of H_2S concentration relative to the inlet concentration (C/C_0) at the different sampling points in the bed under steady state are provided for a comparison. In each case, the data points represent an average of three readings.

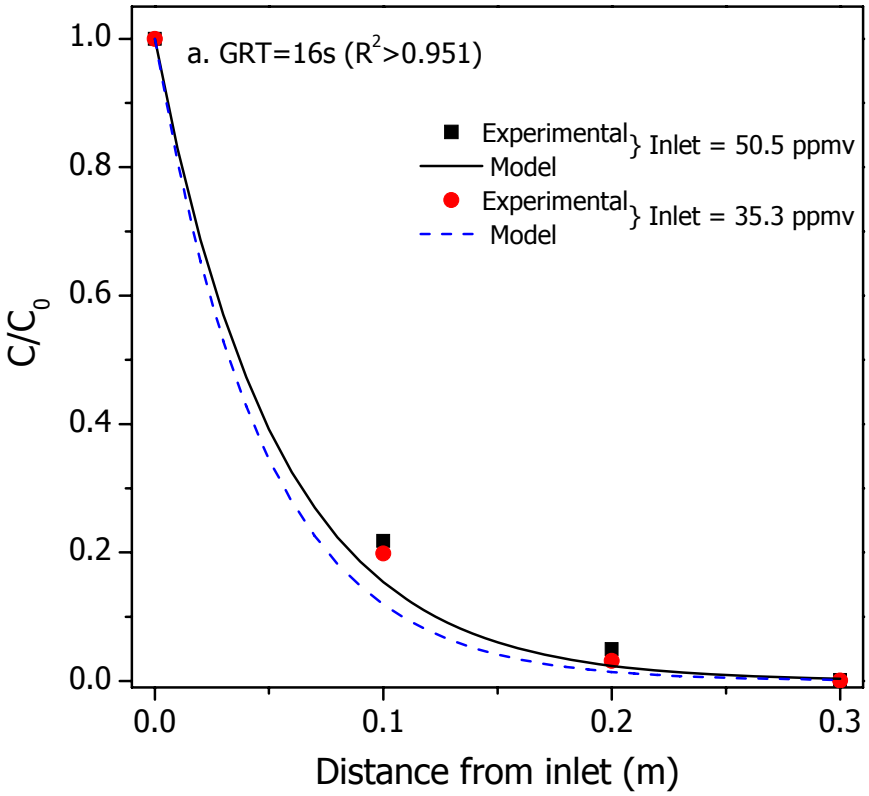

Figure 7.15 Experimental and model gas phase concentration profiles in HBTF
a. under GRT=16s
(First-order biodegradation kinetics of H_2S elimination) (cont'd)

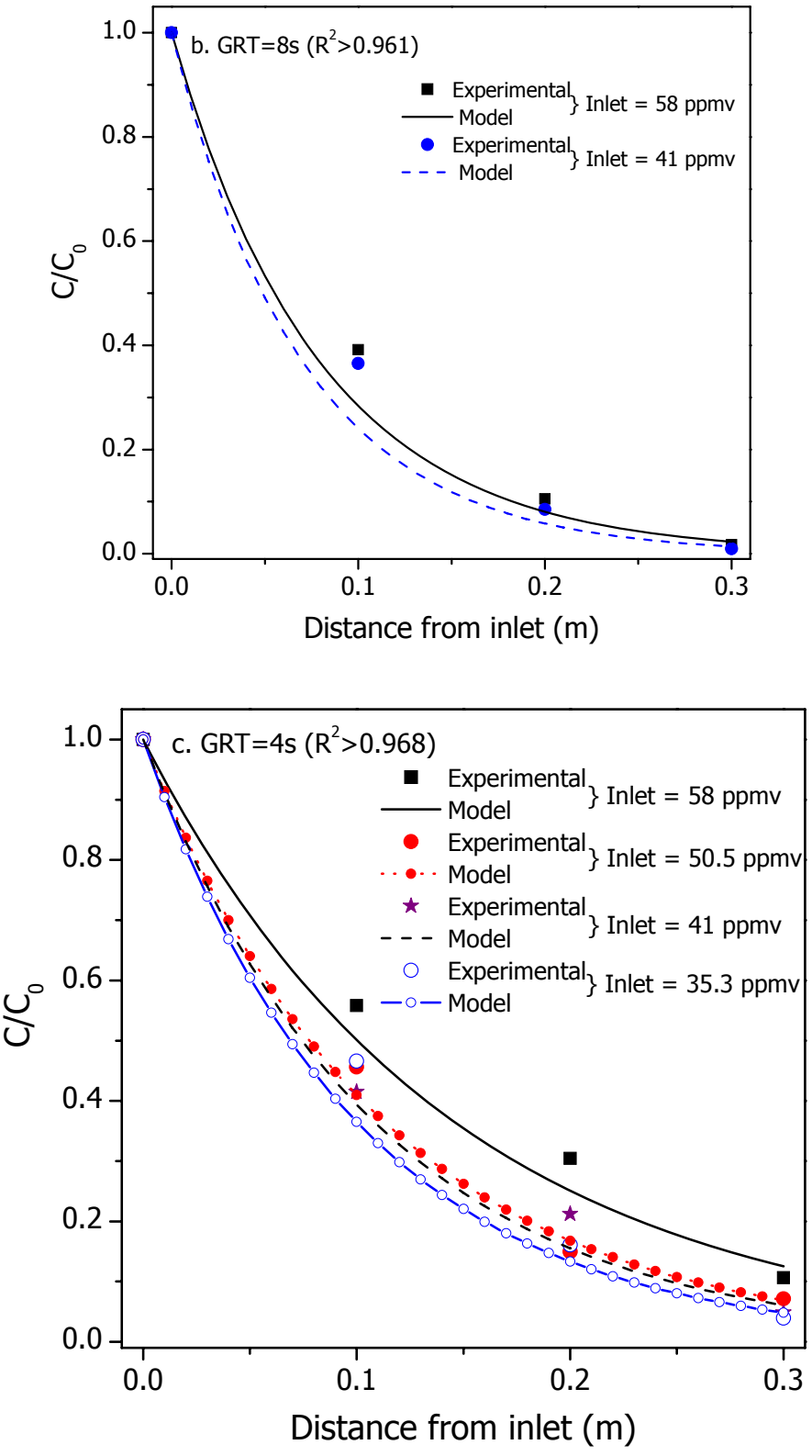

Figure 7.15 Experimental and model gas phase concentration profiles in HBTF

b. under GRT=8s

c. under GRT=4s

(First-order biodegradation kinetics of H_2S elimination) (cont'd)

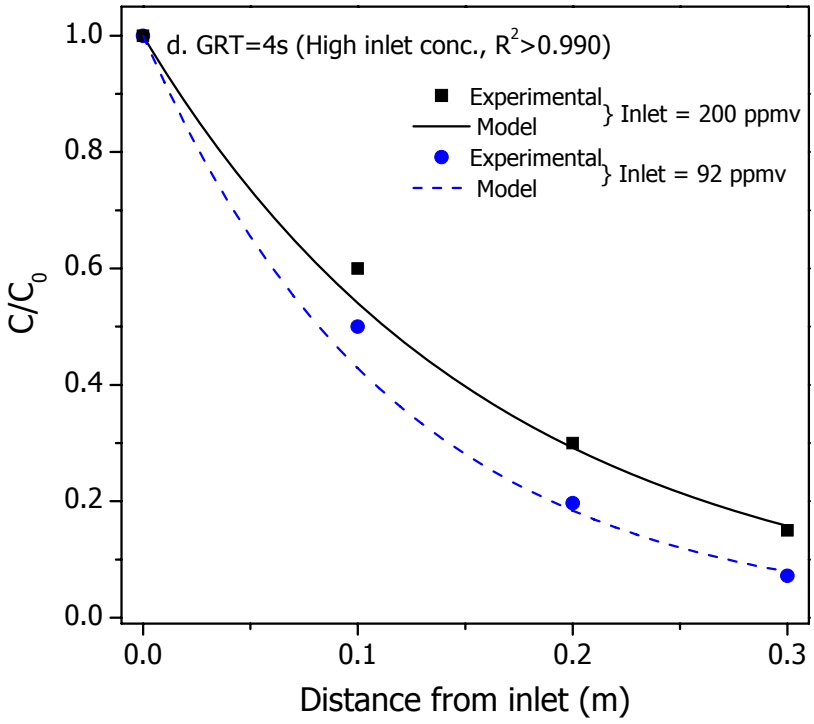

Figure 7.15 Experimental and model gas phase concentration profiles in HBTF d. under GRT=4s and high inlet H_2S concentration over 90 ppm_v (First-order biodegradation kinetics of H_2S elimination).

In Figure 7.15, it is found that the theoretical and experimental concentration values show a good agreement (average R^2>0.95). With varied H_2S inlet concentrations in a range of 35~200 ppm_v and operating at a GRT of 16~4 s (Figure 7.15a to 7.15d), the theoretical and experimental concentration values show reasonable agreement, except that the model predicted slightly lower concentrations than the actual measurements for the locations in the middle of the bed. As shown in Figure 7.15c, the inlet concentration has little effect on RE on both the theoretical and experimental data for low inlet concentration range (i.e. C_0 <60 ppm_v). With an increase in the initial concentration up to 200 ppm_v (Figure 7.15d), the H_2S removal in the HBTF still follows the first biodegradation kinetics with better fit of the data to the model.

Model predictions were also generated based on an assumption of F = 0 in Eq. 7-22, to indicate a full coverage of the carbon surface by biofilm resulting in no carbon

adsorption on the carbon surface. The results are presented in Figure 7.16 where the plot for the case of 'biodegradation + adsorption' is also given, to illustrate the respective contributions of carbon adsorption and biodegradation. As shown, the 'biodegradation only' plot does not fit the experimental data set, while the "biodegradation + adsorption" curve is a better fit. This illustrates that for the BAC system, biodegradation alone only contributed part of the overall RE and that adsorption of the carbon surface is significant. For the experimental conditions (C_0 = 50 ppm_v, GRT = 4 s) there exist a balance of adsorption on the carbon surface and degradation by the biofilm thus resulting in an efficient removal of H_2S by the biologically activated carbon bed.

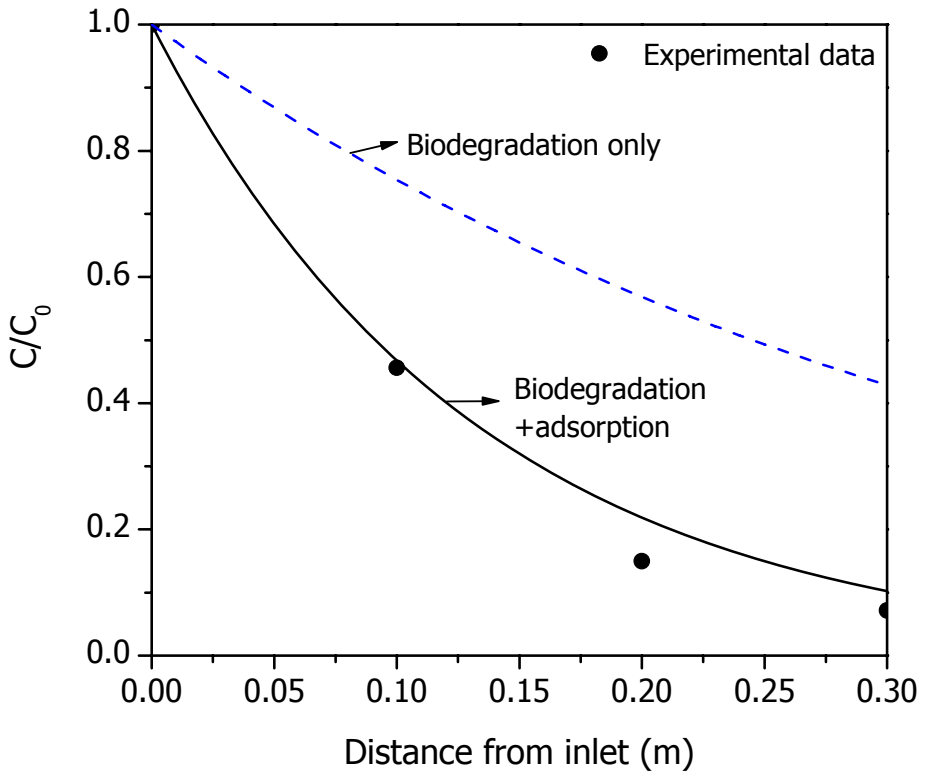

Figure 7.16 Comparison of model simulations of with/without adsorption of gas phase concentration profiles in the HBTF.

(C_0 = 50 ppm_v, GRT = 4 s and gas superficial velocity = 0.075m·s^{-1})

7.3.5 Sensitivity Analysis

Sensitivity analyses were conducted for two specific objectives: (1) to study the effects of various parameters on predicted biofilter performance and (2) to determine which conditions must be altered. The parameters considered for the sensitivity study include four mass transfer parameters (k_{ad}, D_f, A_s, α) and two biokinetic parameters (k_1 or k_0, δ). All these parameters were evaluated by varying 50% of both upper and lower bounds of the preset values shown in Table 7.4. Model simulations were then run at the H_2S concentration of 50 ppm_v (average H_2S inlet concentration for the HBTF) and gas superficial velocity of 0.075 $m \cdot s^{-1}$ (GRT = 4 s). The results of the sensitivity studies are shown in Figure 7.17.

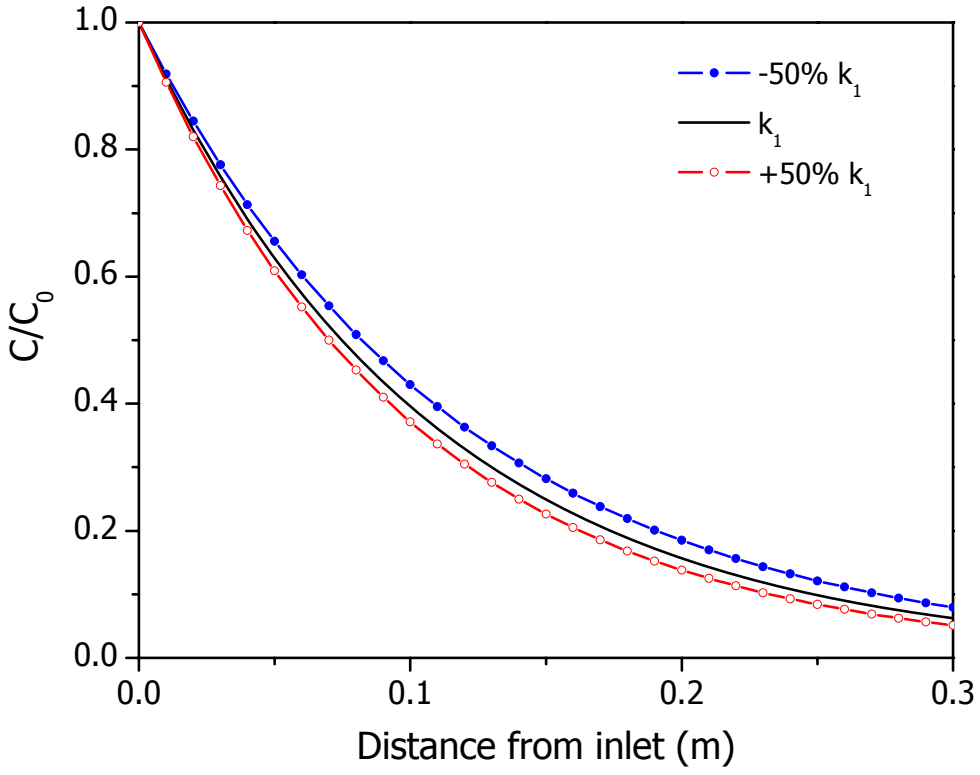

a. k_1 (First-order biodegradation rate constant)

Figure 7.17 Model sensitivity analyses on first-order biodegradation kinetics (cont'd)

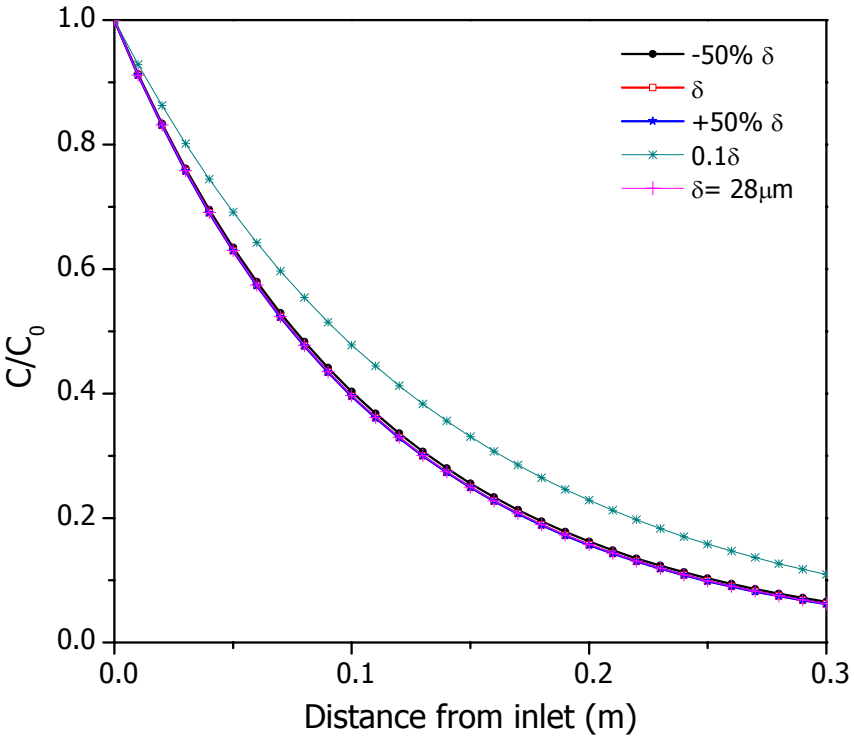

b. δ (Biofilm thickness)

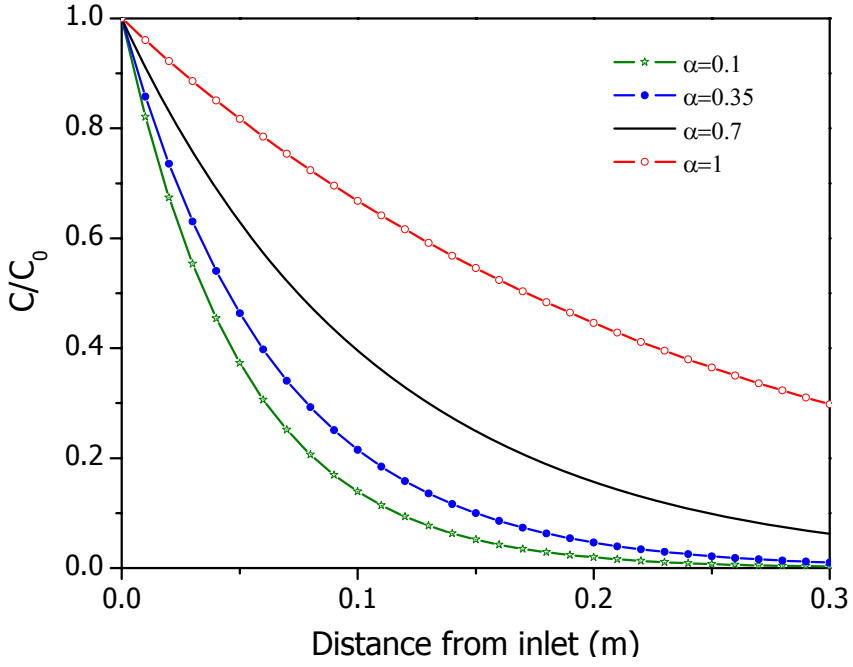

c. α (coverage percentage of the pellets by biofilm)

Figure 7.17 Model sensitivity analyses on first-order biodegradation kinetics (cont'd)

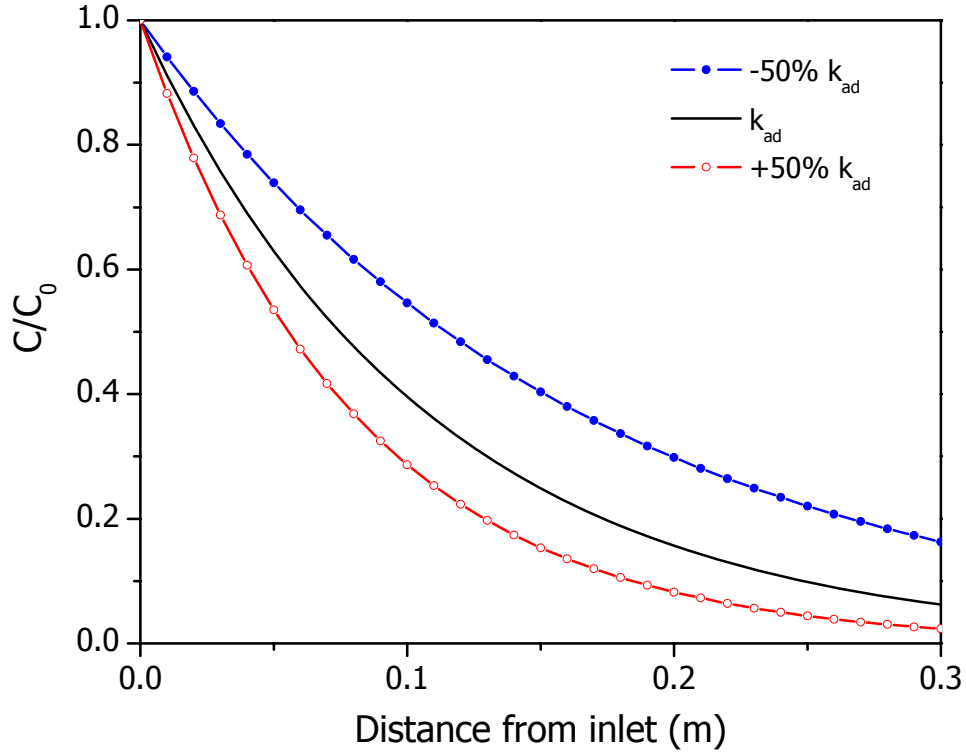

d. k_{ad} (First order adsorption rate constant)

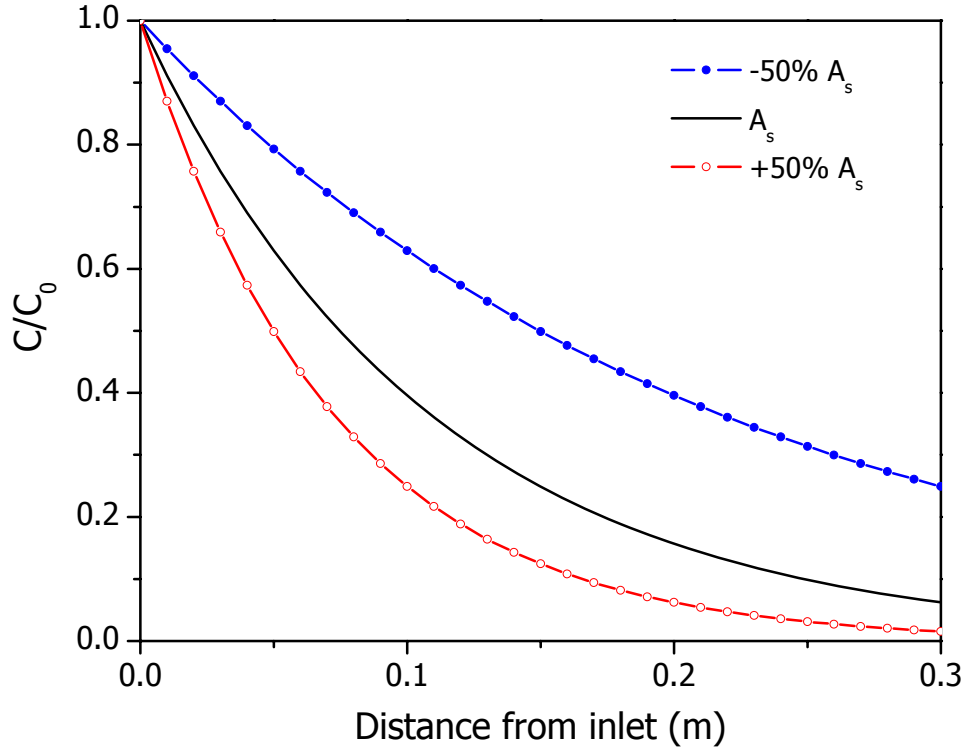

e. A_s (Effective diffusion surface area per volume of bed)

Figure 7.17 Model sensitivity analyses on first-order biodegradation kinetics

It can be seen from Figure 7.17 that mass transfer parameters including the percentage coverage of biofilm on pellets (α), first order adsorption rate constant (k_{ad}) and effective diffusion surface area (A_s), affect the steady state performance more significantly than biokinetic parameters. The results of sensitivity studies for the biokinetic parameters, k_1 and δ, are shown in Figure 7.17a and 7.17b, respectively. As evident from Figure 7.17a, under steady state, an increase of 50% in k_1 value yielded an improvement of H_2S removal efficiency by 1.1% while a decrease of 50% of k_1 value reduced the RE by 1.7%. The biofilm thickness (δ) had almost no effect on the RE in this study (Figure 7.17b), less or additional 50% biofilm thickness (experimentally measured at 35.7 μm, Appendix B) led to no change of system RE. However, if the value of δ is lowered to < 28 μm, the calculated results of removal biofilm thickness of 35.7 μm (Table 7.4) exceeded the critical value (28 μm, calculated), there is hence no obvious change of RE for varied biofilm thickness. Within the range of 0~28 μm, the thinner the biofilm, the lower the system RE (0.1δ curve, Figure 7.17b).

Note that the diffusivity of substrate (H_2S) in the biofilm (D_f) is always accompanied by the first order biodegradation rate constant (k_1) in the modeling equations (Eq.7-22). The sensitivity of D_f is regarded as the same as k_1 and is thus not shown here. The results of sensitivity study for other mass transfer parameters are reported in Figures 7.17c~7.17e. Figure 7.17c shows the effects of variations in the percentage of biofilm covering the carbon pellet (α), a parameter that generally has a profound influence on the steady state RE of the biofilter as it directly affects the contribution of carbon adsorption and the biodegradation of H_2S in biofilters that used BAC. Too much a biofilm coverage will decrease the RE of system because the process of biodegradation is generally slower than the adsorption process and pore blockage by biomass might become significant. A full coverage of biofilm over carbon pellet (100% coverage, $\alpha = 1$) leads to an increase of 29.5% of the effluent

concentration compared to the case where coverage is only 10% ($\alpha = 0.1$). Devinny et al. (1999) revealed that a value of $\alpha = 30\%$ was found to be best in describing most biofiltration experiments, but no experimental confirmation was obtained for his reported value. It is not possible to determine the percentage of carbon surface area covered by biofilm in the HBTF conducted in this study. As there are additional water and nutrient supplied to the HBTF when against a biofilter system, it is assumed here that 70% of the carbon surface was likely to be covered by biofilm. The biofilm thickness (δ) was calculated based on this assumption.

First order adsorption rate constant k_{ad} and effective diffusion surface area A_s also have profound impact on the system performance because they influence the H_2S adsorption onto activated carbon directly (Figure 7.17d and 7.17e). A 50% increase of A_s lead to 4.7% improvement of RE while a 50% increase in k_{ad} lead to 3.8% increase of RE. On the other hand, the system performance drop 18.7% at 50% decrease of A_s and 10.1% at 50% decrease of k_{ad}. The influences of k_{ad} and A_s to the system performance are fairly comparable.

The above model sensitivity studies demonstrate that the mass transfer parameters are important factors for consideration in order to achieve a good system performance. Compared to the biokinetic parameters, the mass transfer parameters have more significant impact on the system RE. Also, carbon adsorption accounted for a significant portion of the HBTF performance. This phenomenon suggests that the process, described by the model, was most likely limited by the mass transfer of H_2S in the biofilter, either on carbon surface or in the biofilm. Theoretically, the system performance can be improved through increasing contact surface areas and reducing biofilm coverage so as to enhance the mass transfer. However, more surface area may increase the head loss of the biofilter and less biofilm will directly weaken the microbial biodegradation of a biofilter.

7.4 Conclusions

Studies on surface properties and chemistry of BAC used in HBTF provided a comprehensive understanding to the mechanisms involved in the process. Porosity and surface area investigations of BAC revealed a correlation between the available surface areas and pore volume with the extent of microbial immobilization and H_2S uptake. SEM photographs show the direct carbon structure and biofilm coated on the carbon surface. Results of FTIR spectra, DTG curves and CHNS elemental analysis indicated a less diversity of H_2S oxidation products on BAC than those previously observed with exhausted carbon caused by H_2S adsorption only. The predominant oxidation product of H_2S on BAC is sulfuric acid, which may cause the system pH to decrease continuously with the operation of biotrickling filter.

The combined effects of carbon adsorption and biodegradation of BAC in treating H_2S are investigated in-depth through four well-designed parallel columns. The physical/chemical adsorption of H_2S on carbon surface tended to produce complex sulfur-bearing species (other than sulfate) as confirmed too by other researchers (Bandosz, 1999; Adib et al., 1999b; Yan et al., 2004a). Biological degradation of H_2S however, produces mostly sulfate. The BAC used in this study was found to produce mainly sulfate during the removal of H_2S. Therefore, it can be concluded that the oxidation of H_2S adsorbed on carbon surface was enhanced by the biofilm on the carbon surface.

From the mathematical modeling of the H_2S removal kinetics in the BAC-based HBTF, it was found that the theoretical first order biodegradation kinetics is generally a good predictor of the experimental profiles obtained for relatively low inlet concentrations (e.g. < 200 ppm_v). It is in accordance with other researchers'

work on vertical biofilters (Hodge and Devinny, 1995; Abumaizar et al., 1997; Amanullah et al., 1999; Li et al., 2002a). In this study, the derived model, using independently measured equilibrium and kinetics parameters, appears adequate in describing the experimental results generated from the HBTF. It showed theoretically that the direct adsorption of carbon bed strongly affected the performance of a BAC-based HBTF. Biodegradation by the biofilm is also a major contributor to the H_2S removal mechanisms. The rate-limiting step of H_2S elimination was the mass transfer in the bioreactor, either on carbon surface or in the biofilm.

CHAPTER 8
CONCLUSIONS AND RECOMMENDATIONS

8.1 Conclusions

After a systematic investigation, two major tasks were completed in this dissertation: (1) assessment of the feasibility of immobilizing bacteria on pelletized activated carbon to create biological activated carbon (BAC), and (2) the application of BAC as the packing medium for the biofiltration or biotrickling filtration of odorous hydrogen sulfide gas. Fundamental studies were also carried out to provide further insight into the mechanism and kinetics of H_2S elimination on activated carbon surface in the presence of the biofilm for the biofilter/biotrickling filter bed. In spite of the limited range of experiment runs that have been carried out, the results obtained enabled the following conclusions to be made:

- From the initial characterization, activated carbon was found to be an excellent microorganism carrier. Its excellent structural properties, with uniform particle size, high water-holding capacity and good resistance to crushing, provided a good surface for microbial attachment. Besides, it has a large surface area (around 1000 $m^2 \cdot g^{-1}$) compared to other synthetic biofilter supporting materials (i.e. Pall rings, lava rock, polyurethane foam), thus providing additional adsorption effect for odor removal. Therefore, BAC, which allows for the combined processes of biodegradation and adsorption to occur, is expected to

perform well as a packing medium for the removal of gaseous H_2S.

- A mixed culture of sulfide oxidation bacteria (dominated by *acidithiobacillus thiooxidans*) acclimated from activated sludge could be immobilized on the surface of pelletized activated carbon (Calgon AP460) resulting in a new and novel medium (biological activated carbon). There are three ways to immobilize bacteria onto the carbon surface: offline immersed immobilization, online immobilization in a biofilter and online immobilization in a biotrickling filter. All the three methods can be used successfully to produce the BAC.

- The performance of the bench scale biofilter trial shows that the BAC demonstrated a better performance than activated carbon as an odor adsorbent. Microorganisms immobilized on activated carbon was capable of extending the activated carbon's capacity (20.08 wt.% of BAC with 100 days of operation compared to 0.44 wt.% of carbon adsorption only) and its life span. In the biofilter trial carried out in this study, BAC achieved a good performance after a short online immobilization period of 6 days. At a low GRT of up to 2 s and particularly for low inlet H_2S concentration (e.g. <30 ppm_v), excellent H_2S removal efficiency was obtained. Elimination capacity as high as 181 $gH_2S \cdot m^{-3} \cdot h^{-1}$ is achievable and the high performance could be maintained for at least 100 days of the biofilter run. In addition, the use of spent activated carbon (SAC) as a possible medium for the development of BAC was demonstrated in this study. This could possibly be a potential solution for the reuse of spent carbon in the industry.

- Studies on the microbial community in the biofilter bed revealed that the microbial niches at different positions of the filter bed were diverse, which

could be due to the different environments (e.g. oxygen supply, pH, etc.) along the bed. Classified by metabolism type, the microbial community was dominated by heterotrophic species in the bottom half of the bed (inlet portion) while chemolithoautrophic bacteria dominated on the top of the bed (outlet portion). Mold concentration increase with the decrease in pH in the biofilter.

- The experimental runs with the horizontal biotrickling filter (HBTF) provided new information on the capacity of the BAC to be used as a novel medium for the treatment of H_2S-contaminated waste gas. A BAC-based HBTF was found to achieve a performance comparable to that of a biofilter. The HBTF can be operated at a low GRT (as low as 4 s) and still provided high removal of H_2S. The elimination capacity of the BAC can be as high as 100 $gH_2S \cdot m^{-3} \cdot h^{-1}$. HBTF using the BAC can perform efficiently without the need for lengthy start-up or acclimation periods. Moreover, use of the HBTF reduced or avoided the problems caused by the limitations associated with the biofilter design, such as the sulfur and biomass accumulation, and bed acidification. However, the HBTF did not perform as good as a BAC-based biofilter when subjected to conditions of short GRT and shock loading. This study has argued that to some extent the inferior performance of the HBTF was accounted for by the liquid layer that was formed over the carbon surface, thus possibly inhibiting the mass transfer of H_2S into the biofilm. The liquid layer could also lead to a high bed density so that an increase in the pressure head of the biotrickling system could occur. Fortunately, and as an important advantage, the horizontal design adopted here alleviated the pressure drop problem significantly.

- Porosity and surface area investigation of BAC treating H_2S revealed a correlation between the available surface area and pore volume with the extent

of microbial immobilization and H_2S uptake by the BAC. SEM photographs show the direct carbon structure and biofilm coated on the carbon surface. Results of FTIR spectra, DTG curves and CHNS elemental analysis indicate a less diversity of H_2S oxidation products (sulfate predominated) on the BAC than those previously observed with exhausted carbon caused solely by H_2S adsorption.

- The combined effects of carbon adsorption and biodegradation of BAC in removing H_2S are investigated in-depth through four well-designed parallel columns. The physical/chemical adsorption of H_2S on the carbon surface tends to produce complex sulfur bearing species (other than sulfate), while the biodegradation of H_2S produces mostly sulfate in this study. BAC was found to produce mostly sulfate during the removal of H_2S. Therefore, it can be concluded that the oxidation of absorbed H_2S was enhanced by the biofilm on the carbon surface. The predominant oxidation product of H_2S is sulfuric acid, which may cause the system pH to decrease continuously during the operation of the biotrickling filter.

- The theoretical first order biodegradation kinetics showed a good agreement with the experimental profiles under low inlet concentrations (e.g. <200 ppm_v) for the HBTF system. This is in accordance with results of other researchers who had worked on vertical biofilters. The mathematical modeling attempted here is probably the first known attempt to model the process occurring in a horizontal biotrickling filtration packed with BAC. The derived model, using independently measured equilibrium and kinetics parameters, appears adequate for describing the experimental results generated from the HBTF runs. It showed theoretically that the direct adsorption of carbon bed would strongly

affect the performance of the BAC-based HBTF (under a GRT of 4 s). At the same time the biofilm also contributed to some extent to the removal of H_2S. The rate-limiting step of H_2S elimination was the mass transfer in the bioreactor, either on the carbon surface or in the biofilm. In this HBTF, the biofilm thickness (including the thickness of liquid film over the biofilm) exceeded the calculated critical value above which, the system performance is affected.

Overall, it is believed that the biofilm could enhance the oxidation of H_2S adsorbed on BAC surface. Although the H_2S adsorption by carbon might be affected by the biofilm, the activated carbon could still provide an attractive, nutrient-rich environment for bacteria growth. Therefore, a good combination and balance of biodegradation and physical/chemical adsorption does occur in the BAC during the removal of H_2S. Such an efficient system could lead to a long-term satisfactory removal of odorous H_2S in a biofilter/biotricking filter.

8.2 Recommendations

Although BAC has been found to be a promising and excellent packing material for use in biofiltration, there is a need for further investigation into the use of BAC in the biofiltration technology. Some recommendations related to the aforesaid research are made for possible future studies:

- **Intermittent biotrickling filtration:** BAC application in a biofilter has the limitations of packing bed clogging that results in channeling, bed acidification, and carbon surface pore blockage during the operations. When it is applied in a biotrickling filter, the continuous liquid trickling may inhibit the mass transfer of H_2S into the biofilm. An intermittent trickling system, which has water

trickling at fixed time intervals, may alleviate the mass transfer problem in the biotrickling filter. Further studies to confirm the effectiveness of intermittent trickling could be useful for the development of new and better biofilters.

- **BAC application on other gas contaminants:** BAC application in biofiltration for the removal of H_2S has been studied in this work. H_2S is one of the many odorous compounds that exist at significant level in sewage air. It would be useful to conduct further studies on the presence of non-H_2S compounds on the BAC operation. Some volatile organic compounds (VOCs) and odorous sulfur compounds, such as toluene, triethylamine, methyl ethyl ketone, methyl isobutyl ketone, benzene, ethylbenzene, o-xylene and ammonia, can be applied separately or in a mixture in a BAC-based biofiltration system to find out the applicability of BAC for odor or VOC control.

- **Spent activated carbon:** The performance of BAC developed from spent activated carbon (SAC) which saturated with H_2S or VOCs in a biofilter has been preliminary assessed in Section 5.2.5, and was found to work well, at least not very different from the performance of BAC developed from virgin activated carbon. The use of SAC for BAC development has two major advantages: Firstly, it will reduce the cost of a biofiltration system as packing material represents a significant fraction of total cost. Secondly, SAC with adsorbed target pollutants could offer additional food source for bacteria assimilation at initial biofilm development stage. Thus the startup time of SAC-based biofilters can be substantially reduced. Additional studies on the viability of using SAC as a potential packing material for biofiltration could provide new knowledge in this field.

- **Field development and evaluation:** The conclusions drawn from this study were based on the laboratory scale experiments using synthetic foul gas containing different concentrations of H_2S. In a real sewage gas, besides the presence of H_2S, other odorous compounds and VOCs are present. Some concerns, such as high pressure drop, packing media channeling, and trickling liquid distribution problems, which were not significant in a lab-scale system, could be important in a full scale system. The findings from this study which is based on bench setup may have provided some useful information but numerous additional considerations should be addressed at full scale particularly for the development of the individual components of the system, such as bioreactor configuration, reactor vessel, air and liquid distribution system, pretreatment system, moisture control system, and etc. Further studies under field situation should provide new information on BAC performance for sewage air treatment.

REFERENCES

Abumaizar, R. J., Kocher, W. and Smith, E. H. (1998) "Biofiltration of BETX Contaminated Air Streams Using Compost-activated Carbon Filter Media." J. Hazardous Material, Vol.60, pp. 111-126.

Abumaizar, R. J., Smith, E. H. and Kocher, W. (1997) "Analytical model of dual-media biofilter for removal of organic air pollutants." J. Environ. Eng-ASCE, Vol.123, No.6, pp. 606-614.

Abumaizar, R. J., Smith, E. H. and Kocher, W. (1997) "Analytical Model of Dual-media Biofilter for Removal of Organic Air Pollutants." J. Environ. Eng.-ASCE, Vol.123, No.6, pp. 606-614.

Adib, F., Bagreev, A. and Bandosz, T. J. (1999a) "Effect of Surface Characteristics of Wood-Based Activated Carbons on Adsorption of Hydrogen Sulfide." J. Colloid Interface Sci., Vol.214, No.407-415.

Adib, F., Bagreev, A. and Bandosz, T. J. (1999b) "Effect of pH and Surface Chemistry on the Mechanism of H_2S Removal by Activated Carbons." Journal of Colloid and Interface Science, Vol.216, No.2, pp. 360-369.

Adib, F., Bagreev, A. and Bandosz, T. J. (2000) "Analysis of the Relationship between H_2S Removal Capacity and Surface Properties of Unimpregnated Activated Carbons." Environ. Sci. Technol., Vol.34, No.4, pp. 686-692.

Aizpuru, A., Malhautier, L., Roux, J.-C. and Fanlo, J. L. (2003) "Biofiltration of a

Mixture of Volatile Organic Compounds on Granular Activated Carbon." Biotech. Bioeng., Vol.83, No.4, pp. 479-488.

Alonso, C., Suidan, M. T., Kim, B. R. and Kim, B. J. (1998) "Dynamic Mathematical Model for the Biodegradation of VOCs in a Biofilter: Biomass Accumulation Study." Environ. Sci. Technol., Vol.32, No.20, pp. 3118-3123.

Amanullah, M., Farooq, S. and Viswanathan, S. (1999) "Modeling and simulation of a biofilter." Industrial & Engineering Chemistry Research, Vol.38, No.7, pp. 2765-2774.

Amanullah, M., Farooq, S. and Viswanathan, S. (1999) "Modeling and Simulation of a Biofilter." Indust. Eng. Chem. Res., Vol.38, No.7, pp. 2765-2774.

Amanullah, M., Viswanathan, S. and Farooq, S. (2000) "Equilibrium, Kinetics, and Column Dynamics of Methyl Ethyl Ketone Biodegradation." Indust. Eng. Chem. Res., Vol.39, No.9, pp. 3387-3396.

APHA (1999) Standard Methods for the Examination of Water and Wastewater. 20th ed., American Public Health Association, Washington DC, USA.

ASCE, (1989) Manuals and Reports on Engineering Practice No. 69, Sulfide in Wastewater Collection and Treatment Systems. New York, American Society of Civil Engineers, pp. 4-15.

Atlas, J. E. and Bartha, R. (1981) Microbial Ecology: Fundamentals and Applications. Addison-Wesly Pulb. Company, MA.

Bagreev, A. and Bandosz, T. J. (2001) "H_2S Adsorption/Oxidation on Unmodified Activated Carbons: Importance of Prehumidification." Carbon, Vol.39, No.15, pp. 2303-2311.

Bagreev, A. and Bandosz, T. J. (2002) "H_2S Adsorption/Oxidation on Materials

Obtained Using Sulfuric Acid Activation of Sewage Sludge-derived Fertilizer." J. Colloid Interface Sci., Vol.252, pp. 188-194.

Bagreev, A., Adib, F. and Bandosz, T. J. (2001) "pH of activated carbon surface as an indication of its suitability for H2S removal from moist air streams." Carbon, Vol.39, No.12, pp. 1897-1905.

Bagreev, A., Adib, F. and Bandosz, T. J. (2001a) "pH of Activated Carbon Surface as An Indication of its Suitability for H_2S Removal from Moist Air Streams." Carbon, Vol.39, No.12, pp. 1897-1905.

Bandosz, T. J. (1999) "Effect of Pore Structure and Surface Chemistry of Virgin Activated Carbons on Removal of Hydrogen Sulfide." Carbon, Vol.37, No.3, pp. 483-491.

Bandosz, T. J. (2002) "On the Adsorption/oxidation of Hydrogen Sulfide on Activated Carbons at Ambient Temperatures." J. Colloid Interface Sci., Vol.246, pp. 1-20.

Bergey, D. H. and Holt, J. D. (1994) Bergey's Mannual of Determinative Bacteriology. 9th ed. Williams and Wilkins, Baltimore.

Black, J. G. (2005) Microbiology: Principles and Explorations. 6th Edition. Chichester: Wiley, New York.

Bonnin, C., Coriton, G. and Martin, G. (1994a) "Biodeodorization Processes: From Organic Media Filters to Mineral Beds." VDI Berichte, Vol.1104, pp. 217-230.

Bonnin, C., Martin, G. and Gragnic, G. (1994b) "Biopurification of odorous gases in urban wastewater treatment plant". Vigneron, S., Hermia, J. and Chaouki, J.(Eds), Proceedings of The Second International Symposium on Characterization and Control of Odours and VOC in he Process Industries, Louvain-la-Neuve, Belgium.

Brandy, J., Fanlo, J. L. and Le Cloirec, P. (1995) "Deodorization of Gaseous Emissions By a Bioscrubber." Odours VOC's J., Vol.1, pp. 192-197.

Brennan, B. M., Donlon, M. and Bolton, E. (1996) "Peat Biofiltration as an Odour Control Technology for Sulphur-based Odours." J. Chart. Inst. Wat. Environ. Manag., Vol.10, No.3, pp. 190-198.

Brock, T. D. and Madigan, M. T. (1991) Biology of Microorganisms. 6th Ed., Prentice Hall, Imprint Englewood Cliffs, N.J.

Buisman, C. J. N., Ijspeert, P., Hof, A., Jassen, A. J. H., Ten Hagen, R. and Lettinga, G. (1991) "Kinetic Parameters of a Mixed Culture Oxidizing Sulfide and Sulfur with Oxygen." Biotech. Bioeng., Vol.38, pp. 913-820.

Burgess, J. E., Parsons, S. A. and Stuetz, R. M. (2001) "Developments in Odour Control and Waste Gas Treatment Biotechnology: A Review." Biotechnology Advances, Vol.19, No.1, pp. 35-63.

Burgess, J. E., Parsons, S. A. and Stuetz, R. M. (2001b) "Developments in Odour Control and Waste Gas Treatment Biotechnology: A Review." Biotechnology Advances, Vol.19, No.1, pp. 35-63.

Carlson, D. A. and Leisner, C. P. (1966) "Soil Beds for the Control of Sewage Odors." J. Wat. Pollut. Control Feder., Vol.38, No.5, pp. 829-834.

Chin, M. and Davis, D. D. (1993) "Global Sources and Sinks of OCS and CS_2 and Their Distrubutions." Global Biogeochemical Cycles, Vol.7, pp. 321-337.

Cho, K. S., Ryu, H. W. and Lee, N. Y. (2000) "Biological Deodorization of Hydrogen Sulfide Using Porous Lava as a Carrier of *Thiobacillus Thiooxidans*." J. Biosci & Bioeng., Vol.90, No.1, pp. 25-31.

Cho, K. S., Zhang, L., Hirai, M. and Shoda, M. (1991) "Removal Characteristics of

Hydrogen Sulfide and Methanethiol by *Thiobacillus sp.* Isolated from Peat in Biological Deodorization." J. Ferment. Bioeng., Vol.71, No.1, pp. 44-49.

Chou, M. S. and Huang, J. J. (1997) "Treatment of Methylethylketone in Air Stream by Biotrickling Filters." J. Environ. Eng.-ASCE, Vol.123, No.6, pp. 569-576.

Chung, Y. C., Huang, C. P., Pan, J. R. and Tseng, C. P. (1998) "Comparison of Autotrophic and Mixotrophic Biofilters for H_2S Removal." J. Environ. Eng.-ASCE, Vol.124, No.4, pp. 362-367.

Chung, Y.-C., Huang, C. and Tseng, C.-P. (2001) "Biological Elimination of H_2S and NH_3 from Waste Gases by Biofilter Packed with Immobilized Heterotrophic Bacteria." Chemosphere, Vol.43, No.8, pp. 1043-1050.

Chung, Y.-C., Huang, C., Tseng, C.-P. and Rushing Pan, J. (2000) "Biotreatment of H_2S- and NH_3-containing Waste Gases by Co-immobilized Cells Biofilter." Chemosphere, Vol.41, No.3, pp. 329-336.

Chung, Y.-C., Lin, Y.-Y. and Tseng, C.-P. (2005). "Removal of High Concentration of NH3 and Coexistent H2S by Biological Activated Carbon (BAC) Biotrickling Filter". Bioresource Technology. Vol.96, No.16, pp.1812-1820.

Cook, L. L., Gostomski, P. A. and Apel, W. A. (1999) "Biofiltration of Asphalt Emissions: Full-scale Operation Treating Off-gas from Polymer-modified Asphault Production." Environ. Prog., Vol.18, pp. 178-187.

Corsi, R. L. and Seed, L. (1995) "Biofiltration of BTEX: Media, Substrate, and Loadings Effects." Environ. Prog., Vol.14, No.3, pp. 151-158.

Cox, H. H. J. and Deshusses, M. A. (2002a) "Co-treatment of H_2S and Toluene in a Biotrickling Filter." Chem. Eng. J., Vol.87, No.1, pp. 101-110.

Cox, H. H. J. and Deshusses, M. A. (2002b) Biotrickling Filters for Air Pollution

Control. The Encyclopedia of Environmental Microbiology. Bitton, G. (Editor-in-Chief), J. Wiley & Sons. **2:** 782-795.

De Zwart, J. M. M. and Kuenen, J. G. (1992) "C_1-cycle of Sulfur Compounds." Biodegradation, Vol.3, pp. 37-59.

Den, W. and Pirbazari, M. (2002) "Modeling and design of vapor-phase biofiltration for chlorinated volatile organic compounds." Aiche Journal, Vol.48, No.9, pp. 2084-2103.

Deshusses, M. A., Hamer, G. and Dunn, I. J. (1995a) "Behavior of Biofilters for Waste Air Biotreatment .1. Dynamic-Model Development." Environ. Sci. Technol., Vol.29, No.4, pp. 1048-1058.

Devinny, J. S., Deshusses, M. A. and Webster, T. S. (1999) Biofiltration for air pollution control. Lewis Publishers, Boca Rotan, FL.

Diks, R. M. M. and Ottengraf, S. P. P. (1991a) "Verification Studies of a Simplified Model for the Removal of Dichloromethane from Waste Gases Using a Biological Trickling Filter: Part I." Biopr. Eng., Vol.6, No.93-99.

Elias, A., Barona, A., Arreguy, A., Rios, J., Aranguiz, I. and Penas, J. (2002) "Evaluation of a Packing Material for the Biodegradation of H_2S and Product Analysis." Process Biochem., Vol.37, pp. 813-820.

Ergas, S. J., Shroeder, E. D., Chang, D. P. Y. and Morton, R. L. (1995) "Control of Volatile Organic Compound Emissions Using a Compost Biofilter." Wat. Environ. Res., Vol.67, No.5, pp. 816-821.

Ergun, S. (1952) "Fluid Flow Through Packed Columns." Chem. Eng. Prog., Vol.48, No.2, pp. 89-94.

Fortin, N. Y. and Deshusses, M. A. (1999) "Treatment of Methyl Tert-butyl Ether

Vapors in Biotrickling Filters. 1. Reactor Startup, Steady State Performance, and Culture Characteristics." Environ. Sci. Technol., Vol.33, No.17, pp. 2980-2986.

Gabriel, D. and Deshusses, M. A. (2003a) "Performance of a Full-scale Biotrickling Filter Treating H_2S at a Gas Contact Time of 1.6 to 2.2 Seconds." Environ. Prog., Vol.22, No.2, pp. 111-118.

Gabriel, D. and Deshusses, M. A. (2003b) "Retrofitting Existing Chemical Scrubbers to Biotrickling Filters for H_2S Emission Control." PNAS, Vol.100, No.11, pp. 6308-6312.

Gabriel, D. and Deshusses, M. A. (2004) "Technical and Economical Analysis of the Conversion of a Full-scale Scrubber to Biotrickling Filter for Odor Control." Wat. Sci. Technol., Vol.50, No.4, pp. 309.

Ghosh, T. K. and Tollefson, E. L. (1986) "Kinetics and Reaction Mechanism of Hydrogen Sulfide Oxidation Over Activated Carbon in the Temperature Range of 125-200 ^{o}C." Can. J. of Chem. Eng., Vol.64, No.6, pp. 969-976.

Grant, W. D. and Long, P. E. (1981) Environmental Microbiology. Halsted Press, New York.

Gribbins, M. J. and Loehr, R. C. (1998) "Effect of Media Nitrogen Concentration on Biofilter Performance." J. Air & Wast. Manage. Assoc., Vol.48, pp. 216-226.

Guey, C., Degorce-Dumas, J. R. and Le Cloirec, P. (1995) "Hydrogen Sulfide Removal on Biological Activated Carbon." Odours VOC's J., Vol.1, pp. 144-145.

Hattermer-Fery, H. A., Travis, C. C. and Land, L. (1990) "Benzene: Environment Partitioning and Human Exposure." Environ. Res., Vol.53, pp. 221-232.

Hautakangas, H. and Mihelcic, J. R. (1999) "Optimization and Modeling of Biofiltration for Odour Control". Proceedings of WEF's 72nd Annual Conference

and exposition, New Oelean, LA.

Hirai, M., Kamamoto, M., Yani, M. and Shoda, M. (2001) "Comparison of the Biological H_2S Removal Characteristics among Four Inorganic Packing Materials." J. Biosci & Bioeng., Vol.91, No.4, pp. 396-402.

Hodge, D. S. and Devinny, J. S. (1995) "Modeling Removal of Air Contaminants by Biofiltration." J. Environ. Eng.-ASCE, Vol.121, No.1, pp. 21-32.

Holt, J. G. and Bergey, D. H. (1989) Bergey's Manual of Determinative Bacteriology. 8th Edition. Williams & Wilkins, Baltimore.

Islander, R. L., Devinny, J. S., Mandfeld, F., Postyn, A. and Shih, H. J. (1991) "Microbial Ecology of Crown Corrosion in Sewers." Environ. Eng., Vol.117, No.6, pp. 751-771.

Jassen, A. J. H., Sleyster, R., Van Der Kaa, C., Jochemsen, A., Bonstsema, J. and Lettinga, G. (1995) "Biological Sulfide Oxidation in a Fed-batch Reactor." Biotech. Bioeng., Vol.47, pp. 327-333.

Jaworska, M. and Urbanek, A. (1998) "The Influence of Oxygen Concentration in Liquid Medium on Elemental Sulfur Oxidation by *Thiobacillus thiooxidans*." Bioproc. Eng., Vol.18, pp. 201-205.

Jensen, A. B. and Webb, C. (1995) "Treatment of H_2S-containing Gases: A review of Microbiological Alternatives." Enzyme and Microbial Technology, Vol.17, No.1, pp. 2-10.

Jin, Y. M., Veiga, M. C. and Kennes, C. (2005). "Effects of pH, CO2, and flow pattern on the autotrophic degradation of hydrogen sulfide in a biotrickling filter". Biotechnology and Bioengineering. Vol.92, No.4, pp.462-471.

Kapahi, R. and Gross, M. (1995) "Biofiltration for VOC and Ammonia Emissions

Control." BioCycle, Vol.36, No.2, pp. 87-90.

Katoh, H., Kuniyoshi, I., Hirai, M. and Shoda, M. (1995) "Studies of the Oxidation Mechanism of Sulphur-containing Gases onWet Activated Carbon Fiber." Appl. Cataly. B: Environ., Vol.6, pp. 255-262.

Kelly, D. P. and Smith, N. A. (1990) "Organic Sulfur Compounds in the Environment." Adv. Microbiol. Ecol., Vol.11, pp. 345-385.

Kennes, C. and Thalasso, F. (1998) "Waste Gas Biotreatment Technology." J. Chem. Technol. Biotechnol., Vol.72, pp. 303-319.

Kennes, C. and Veiga, M. C. (2001) Bioreactors for Waste Gas Treatment. Kluwer Academic Publishers, Dordrecht.

Kim, H. S., Kim, Y. J., Chung, J. S. and Xie, Q. (2002) "Long-term Operation of a Biofilter for Simultaneous Removal of H_2S and NH_3." J. Air & Waste Manag. Assoc., Vol.52, No.12, pp. 1389-1398.

Kim, S. and Deshusses, M. A. (2003) "Development and Experimental Validation of a Conceptual Model for Biotrcikling Filtration of H_2S." Environ. Prog., Vol.22, No.2, pp. 119-128.

Kinney, K. A., Plessis, C. A. d., Schroeder, E. D., Chang, D. and Scow, K. M. (1996) "Optimizing Microbial Activity in a Directionally-switching Biofilter". Proceedings of Conference on Biofiltration, University of Southern California, U.S.A.

Koe, L. C. C. and Liang, J. (2005) "Comparison of Two-stage and Single-stage Biofiltration for H_2S and Toluene Co-treatment". Proceedings of Congress on Biotechniques for Air Pollution Control, La Coruna, Spain

Koe, L. C. C. and Yang, F. (2000a) "A Bioscrubber for Hydrogen Sulphide Removal." Wat. Sci. Technol., Vol.41, No.6, pp. 141-145.

Koe, L. C. C. and Yang, F. (2000b) "Evaluation of a Pilot-scale Bioscrubber for the Removal of Hydrogen Sulfide." J. Chart. Inst. Wat. Eng., Vol.14, pp. 432-435.

Koe, L. C. C., Duan, H. Q., Tong, D. J., Yan, R. and Chen, X. G. (2004) "Preliminary Study of Using Activated Carbon as Biofilter Packing Material for Treatment of H_2S". Proceedings of Enviro04 Convention & Exhibition, Sydney.

Koe, L. C. C., Wu, L., Loo, Y. Y. and Wu, Y. (2001) "Field Trial Testing of a Biotrickling Filter for Sewage Odor Control". Proceedings of A&WMA's 94th Annual Conference & Exhibition., Florida, U.S.A.

Kowal, S., L., F. J., Degorce-Dumas, J. R. and Le Cloirec, P. (1992) "Deodorization with a Biofilter Using a Consumable Support: Example of BSE Process for Hydrogen Sulfide Removal." Poll. Atm., pp. 34-42.

Lanting, J. and Shah, A. S. (1992) "Biological Removal of Hydrogen Sulfide from Biogas". Proceedings of 46th Purdue Industrial Waste Conference, Chelsea, Lewis Publishers, Inc.

Laustsen, T. A., Marran, K. S., Little, H. L. and Coladonato, S. (1999) "Design Parameters for a Biofilter that Successfully Treats Volatile Organic Compounds from a Combined Sewer". Proceedings of WEFTEC'99, New Orlean, LA.

Lee, S. K. and Shoda, M. (1989) "Biological Deodorization Using Activated Carbon Fabric as a Carrier of Microorganisms." J. Ferment. Bioeng., Vol.68, No.6, pp. 437-442.

Leson, G. and Winer, A. M. (1991) "Biofiltration: An Innovative Air Pollution Control Technology for VOC Emission." J. Air & Wast. Manage. Assoc., Vol.41, No.10, pp. 1045-1054.

Li, H. B., Crittenden, J. C., Mihelcic, J. R. and Hautakangas, H. (2002) "Optimization of biofiltration for odor control: Model development and parameter

sensitivity." Water Environment Research, Vol.74, No.1, pp. 5-16.

Li, H. B., Mihelcic, J. R., Crittenden, J. C. and Anderson, K. A. (2003) "Field Measurements and Modeling of Two-Stage Biofilter that Treats Odorous Sulfur Air Emissions." Journal of Environmental Engineering-Asce, Vol.129, No.8, pp. 684-692.

Li, H., Crittenden, J. C., Mihelcic, J. R. and Hautakangas, H. (2002a) "Optimization of Biofiltration for Odor Control: Model Development and Parameter Sensitivity." Wat. Environ. Res., Vol.74, No.1, pp. 5-16.

Li, X. Z., Wu, J. S. and Sun, D. L. (1998) "Hydrogen Sulphide and Volatile Fatty Acid Removal from Foul Air in a Fibrous Bed Bioreactor, Water Science Technology." Wat. Sci. Technol., Vol.38, No.3, pp. 323-329.

Liu, P. K. T. and Barkley, N. (1994) "Engineered Biofilter for Removing Organic Containminants in Air." J. Air & Waste Manage. Assoc., Vol.44, pp. 299-303.

Lizama, H. M. and Sankey, B. M. (1993) "Conversion of Hydrogen-Sulfide by Acidophilic Bacteria." Appl. Microbiol. Biotechnol., Vol.40, No.2-3, pp. 438-441.

Maier, R. M., Pepper, I. L. and Gerba, C. P. (2000) Environmental Microbiology., Academic Press, San Diego.

Malhautier, L., Gracian, C., Roux, J.C., Fanlo, J.L. and Le Cloirec, P. (2003). "Biological Treatment Process of Air Loaded with an Ammonia and Hydrogen Sulfide Mixture". Chemosphere. Vol.50, No.1, pp.145-153.

Martin, R. W., Li, H. B., Mihelcic, J. R., Crittenden, J. C., Lueking, D. R., Hatch, C. R. and Ball, P. (2002) "Optimization of Biofiltration for odor control: Model calibration, validation, and applications." Wat. Environ. Res., Vol.74, No.1, pp. 17-27.

Martin, R. W., Mihelcic, J. R. and Crittenden, J. C. (2004) "Design and Performance Characterization Strategy Using Modeling for Biofiltration Control of Odorous Hydrogen Sulfide." J. Air & Waste Manage. Assoc., Vol.54, No.7, pp. 834-844.

Mason, C. A., Ward, G., Abu-Salah, K., Keren, O. and Dosoretz, C. G. (2000) "Biodegradation of BTEX by Bacteria on Powdered Activated Carbon." Biopr. Eng., Vol.23, pp. 331-336.

McNevin, D. and Barford, J. (2000) "Biofiltration as an Odour Abatement Strategy." Biochemical Engineering Journal, Vol.5, No.3, pp. 231-242.

McNevin, D., Barford, J. and Hage, J. (1999) "Adsorption and Biological Degradation of Ammonium and Sulfide on Peat." Wat. Res., Vol.33, No.6, pp. 1449-1459.

Medina, V. F., Webster, T. S. and Devinny, J. S. (1995). "Treatment of Gasoline Residuals by Granular Activated Carbon Based Biological Filtration." J. Environ. Sci. Health, Part A. Vol.30, No.2, pp.407-412.

Mikhalovsky, S. V. and Zaitsev, Y. P. (1997) "Catalytic Properties of Activated Carbons I. Gas-phase Oxidation of Hydrogen Sulphide." Carbon, Vol.35, No.9, pp. 1367-1374.

Mohseni, M., Allen, D. G. and Nichole, K. M. (1998) "Biofiltration of Alpha-pinene and Its Application to the Treatment of Pulp and Paper Air Emission." TPPI J., Vol.81, No.8, pp. 205-211.

Montgomery, J. M. (1985) Water treatment principles and design. Wiley, New York.

Morales, M., Hernandez, S., Cornabe, T., Revah, S. and Auria, R. (2003) "Effect of Drying on Biofilter Performance: Modeling and Experimental Approach." Environ. Sci. Technol., Vol.37, No.5, pp. 985-992.

Morgenroth, E., Schroeder, E. D., Chang, D. P. Y. and Scow, K. M. (1996) "Nutrient Limitation in a Compost Biofilter Degrading Hexane." J. Air & Waste Manag. Assoc., Vol.46, No.4, pp. 300-308.

Morton, R. and Caballero, R. (1996) "The Biotrickling Story." Wat. Environ. Technol., Vol.8, No.6, pp. 39-45.

Mpanias, C. J. and Baltzis, B. C. (1998) "An Experimental and Modeling Study on the Removal of Mono-chlorobenzene Vapor in Biotrickling Filters." Biotechnol. Bioeng., Vol.59, No.3, pp. 328-343.

Munoz, R., Arriaga, S., Hernandez, S., Guieysse, B. and Revah, S. (2006). "Enhanced hexane biodegradation in a two phase partitioning bioreactor: Overcoming pollutant transport limitations". Process Biochemistry. Vol.41, No.7, pp.1614-1619.

Ng, Y. L., Yan, R., Chen, X. G., Geng, A. L., Gould, W. D., Liang, D. T. and Koe, L. C. C. (2004) "Use of Activated Carbon as a Support Medium for H_2S Biofiltration and Effect of Baceteria Immobilization on Available Pore Surface." Appl. Microbiol. Biotechnol., Vol.66, pp. 259-265.

O'Neill, D. H. and Phillips, V. R. (1992) "A Review of the Control of Odour Nuisance from Livestock Buildings: Part 3, Properties of the Odorous Substances which have been Identified in Livestock Wastes or in the Air around them." Journal of Agricultural Engineering Research, Vol.53, pp. 23-50.

Ottengraf, S. P. P. and Van Den Oever, A. H. C. (1983) "Kinetics of Organic Compound Removal from Waste Gases with a Biofilter Filter." Biotech. Bioeng., Vol.25, pp. 3089-3102.

Oyarzun, P., Arancibia, F., Canales, C. and Aroca, G. E. (2003) "Biofiltration of High Concentration of Hydrogen Sulphide Using Thiobacillus Thioparus." Process

Biochemistry, Vol.39, No.2, pp. 165-170.

Patnaik, P. (1999) A Comprehensive Guide to the Hazardous Properties of Chemical Substance. 2nd ed., John Wiley, New York.

Pinnette, J. R., Giggey, M. D., Marcy, G. J. and O'Brien, M. A. (1994) "Performance of Biofilters at Two Agitated Bin Composting Facilities". Proceedings of A&WMA's 87th Annual Conference & Exhibition., Ohio.

Planker, T. W. (1998) Masking and Odor Neutralization. Odor and VOC control Handbook (Rafson eds). McGraw-Hill. New York.

Pomeroy, R. D. (1982) "Biological Treatment of Odorous Air." J. Wat. Pollut. Control Fed., Vol.54, No.12, pp. 1541-1545.

Prietzel, J., Cronauer, H. and Strehl, C. (1996) "Determination of Dissolved Total Sulfur in Aqueous Extracts and Seepage Water of Forest Soils." Int.J. Environ. Anal. Chem., Vol.64, No.3, pp. 193-203.

Prokop, W. H. and Bohn, H. L. (1985) "Soil Bed System for Control of Rendering Plant Odors." JAPCA, Vol.35, pp. 1332-1338.

Rafson, H. J. (1998) Odor & VOC Control Handbook. McGraw-Hill, New York.

Ruokojarki, A., Ruuskanen, J., Martikaninen, P. J. and Olkkonen, M. (2001) "Oxidation of Gas Mixutes Containing Dimethyl Sulfide, Hydrogen Sulfide, and Methanethiol Using a Two-stage Biotrickling Filter." J. Air & Wast. Manage. Assoc., Vol.51, pp. 11-16.

Scholz, M. and Martin, R. J. (1997) "Ecological Equilibrium on Biological Activated Carbon." Wat. Res., Vol.31, No.12, pp. 2959-2968.

Schowengerdt, R. W., Hunter, B. and Hanson, R. E. (1999) "Incremental Hydrogen Sulfide Loading and Diurnal Fluctuation of Three Operation Biofilters".

Proceedings of WEFTEC'99, New Orleans, L.A.

Schroeder, E. D. (2002) "Trends in application of gas-phase bioreactor." Rev. Environ. Sci. & Biotechnol., Vol.1, pp. 65-74.

Shareefdeen, Z. and Baltzis, B. C. (1993) "Biofiltration of Mechanol Vapor." Biotech.Bioeng., Vol.41, pp. 512-524.

Sheridan, B. A., Curran, T. P. and Dodd, V. A. (2002). "Assessment of the influence of media particle size on the biofiltration of odorous exhaust ventilation air from a piggery facility". Bioresource Technology. Vol.84, No.2, pp.129-143.

Shinabe, K., Oketani, S., Ochi, T. and Matsumura, M. (1995) "Characteristics of Hydrogen Sulfide Removal by T*hiobacillus Thiooxidans KS1* Isolated from a Carrier-packed Biological Deodorization System." J. Ferment. Bioeng., Vol.80, No.6, pp. 592-598.

Smet, E., Chasaya, G., Van Langenhove, H. and Verstraete, W. (1996) "The Effect of Inoculation and the Type of Carrier Material Used on the Biofiltration of Methyl Sulfides." Appl. Microbiol. Biotechnol., Vol.45, pp. 293-298.

Smet, E., Lens, P. and Van Langenhove, H. (1998) "Treatment of Waste Gases Contaminated with Odorous Sulfur Compounds." Crit. Rev. Environ. Sci. Technol., Vol.28, No.1, pp. 89-117.

Sorial, G. A., Smith, F. L., Suidan, M. T. and Biswas, P. (1995) "Evaluation of a Trickling Bed Biofilter Media for Toluene Removal." J. Air & Wast. Manage. Assoc., Vol.45, pp. 801-810.

Spigno, G., Zilli, M. and Nicolella, C. (2004) "Mathematical Modelling and Simulation of Phenol Degradation in Biofilters." Biochemical Engineering Journal, Vol.19, No.3, pp. 267-275.

Steijns, M., Derks, F., Verloop, A. and Mars, P. (1976) "The Mechanism of the Catalytic Oxidation of Hydrogen Sulfide : II. Kinetics and Mechanism of Hydrogen Sulfide Oxidation Catalyzed by Sulfur." Journal of Catalysis, Vol.42, No.1, pp. 87-95.

Sublette, K. L. and Sylvester, N. D. (1987) "Oxidation of Hydrogen Sulfide by Thiobacillus Denitrificans: Desulfurization of Natural Gas." Biotechnol. Bioeng., Vol.29, pp. 249-257.

Swanson, W. J. and Loehr, R. C. (1997) "Biofiltration: Fundamentals, Design and Operations Principles, and Applications." J. Envion. Eng., Vol.123, No.6, pp. 538-546.

Tan, X., Wang, F., Bi, Y., He, J., Su, Y., Braeckman, L., de Bacquer, D. and Vanhoorne, M. (2001) "Carbon Disulfide Exposure Assessment in a Chinese Viscose Filament Plant." International Journal of Hygiene and Environmental Health, Vol.203, No.5-6, pp. 465-471.

Tang, H. M., Hwang, S. J. and Hwang, S. C. (1996) "Waste Gas Treatment in Biofilters." J. Air & Wast. Manage. Assoc., Vol.46, No.4, pp. 349-354.

Thalasso, F., Naveau, H. and Nyns, E. J. (1996) "Effect of Dry Period in a 'mist-foam' Bioreactor Designed for Gaseous Substrate." Environ. Technol., Vol.17, pp. 909-913.

Traegner, U. K. and Suidan, M. T. (1989) "Evaluation of Surface and Film Diffusion Coefficients for Carbon Adsorption." Wat. Res., Vol.23, No.3, pp. 267-273.

Turk, A., Mahmood, K. and Mozaffari, J. (1993) "Activated Carbon for Air Purification in New-York-City Sewage-Treatment Plants." Water Science and Technology, Vol.27, No.7-8, pp. 121-126.

Valentin, F. H. H. (1986) "Peat Beds for Odour Control: Recent Developments and Practical Details." Filtration & Separation, Vol.23, No.4, pp. 224-227.

Van Lith, C., Leson, G. and Michelsen, R. (1997) "Evaluating Design Option for Biofilters." J. Air & Wast. Manage. Assoc., Vol.47, pp. 37-48.

Verschueren, K. (1983) Handbook of Environmental Data on Organic Chemicals. Van Nostrand Reinhold Company Inc., New York.

Vincent, A. and Hobson, J. (1998) "Odour Control." CIWEM monographs on best practice no. 2. London, UK: Chart. Instit. Wat. Environ. Manag., pp. 31.

Voice, T. C., Pak, D., Zhao, X. and Hickey, R. F. (1992) "Biological Activated Carbon in Fluidized Bed Reactors for the Treatment of Groundwater Contaminated with Volatile Aromatic Hydrocarbons." Wat. Res., Vol.26, No.10, pp. 1389-1401.

Watanabe, K., Teramoto, M., Futamata, H. and Harayama, S. (1998b) "Molecular Detection, Isolation, and Physiological Characterization of Functionally Dominant Phenol-degrading Bacteria in Activated Sludge." Applied and Environmental Microbiology, Vol.64, No.11, pp. 4396-4402.

Watanabe, K., Yamamoto, S., Hino, S. and Harayama, S. (1998a) "Population Dynamics of Phenol-degrading Bacteria in Activated Sludge Determined by gyrB-targeted Quantitative PCR." Applied and Environmental Microbiology, Vol.64, No.4, pp. 1203-1209.

Weber, F. J. and Hartmans, S. (1995) "Use of Activated Carbon as a Buffer in Biofiltration of Waste Gases with Fluctuating Concentration of Toluene." Appl. Microbiol. Biotechnol., Vol.43, No.2, pp. 365-369.

Webster, T. S., Devinny, J. S. and Torres, E. M. (1996) "Microbial Ecosystem in Compost and Granular Activated Carbon Biofilters." Biotech. Bioeng., Vol.53, No.3, pp. 296-303.

WEF/ASCE, (1995) Odor Control in Wastewater Treatment Plants. Water Environment Federation (WEF) manual of practice no.22, American Society of Civil Engineers (ASCE) manuals and reports on engineering practice no. 82, USA: WEF/ASCE, pp. 203-216.

Williams, T. O. and Miller, F. C. (1992) "Biofilters and Facility Operations." BioCycle, Vol.33, No.11, pp. 75-79.

WPCF, (1979) Odor Control for Wastewater Facilities (Manual of Practice No.22). Washtington D.C., Water Pollution Control Federation, pp. 8.

Wu, L. (2000) "Using Biotrickling Filter to Treat Odorous Off-gas from municipal Wastewater Treatment Facilities." M.Eng. Thesis, National University of Singapore.

Wu, L., Loo, Y. Y. and Koe, L. C. C. (2001) "A Pilot Study of a Biotrickling Filter for the Treatment of Odorous Sewage Air." Wat. Sci. Technol., Vol.44, No.9, pp. 295-299.

Xie, Y. F. and Zhou, H. J. (2002) "Using BAC for HAA Removal Part 2: Column Study." J. AWWA, Vol.94, No.5, pp. 126-134.

Yan, R., Chin, T., Ng, Y. L., Duan, H. Q., Liang, D. T. and Tay, J. H. (2004a) "Influence of Surface Properties on the Mechanisms of H_2S Removal by Alkaline Activated Carbons." Environ. Sci. Technol., Vol.38, No.1, pp. 316-323.

Yan, R., Liang, D. T., Tsen, L. and Tay, J. H. (2002) "Kinetics and Mechanisms of H_2S Adsorption by Alkaline Activated Carbon." Environmental Science & Technology, Vol.36, No.20, pp. 4460-4466.

Yan, R., Ng, Y. L., Chen, X. G., Geng, A. L., Gould, W. D., Duan, H. Q., Liang, D. T. and Koe, L. C. C. (2004b) "Batch Experiment on H_2S Degradation by Bacteria Immobilized on Activated Carbons." Wat. Sci. Technol., Vol.50, No.4, pp. 299-308.

Yang, Y. H. and Allen, E. R. (1994a) "Biofiltration Control of Hydrogen Sulfide 1. Design and Operational Parameters." J. Air & Waste Manage. Assoc., Vol.44, pp. 863-868.

Yang, Y. H. and Allen, E. R. (1994b) "Biofiltration Control of Hydrogen Sulfide 2. Kinetics, Biofilter Performance and Maintenance." J. Air & Waste Manage. Assoc., Vol.44, No.1315-1321.

Yoon, I. K. and Park, C. H. (2002) "Effects of Gas Flow Rate, Inlet Concentration and Temperature on Biofiltration of Volatile Organic Compounds in a Peat-packed Biofilter." J. Biosci & Bioeng., Vol.93, No.2, pp. 165-169.

Zhao, F., McGrath, S. P. and Crosland, A. R. (1994) "Comparison of 3 Wet Digestion Methods for the Determination of Plant Sulfur by Inductively-Coupled Plasma-Atomic Emission-Spectroscopy (Icpaes)." Commun. Soil Sci. and Plant Anal., Vol.25, No.3-4, pp. 407-418.

Zhao, X., Hickey, R. F. and C. Voice, T. (1999) "Long-term Evaluation of Adsorption Capacity in a Biological Activated Carbon Fluidized Bed Reactor System." Water Research, Vol.33, No.13, pp. 2983-2991.

Zhou, D. Z. (2000) "Biological Treatment of Sewage Air Using a Horizontal Biotrickling Filter." M.Eng.Thesis, National University of Singapore.

Zhou, H. J. and Xie, Y. F. (2002) "Using BAC for HAA Removal Part 1: Batch Study." J. AWWA, Vol.94, No.4, pp. 194-200.

APPENDIX A
PRESSURE DROP STUDY

Pressure drop is the resistance to flow in the bioreactor system. It is a major factor that determines the amount of energy needed to force the contaminated gas through a bioreactor. Pressure drop is related to the superficial velocity and the particle size of the packing material (Yang and Allen, 1994a). In order to investigate the effect of biofilter configuration on pressure drop variation across the filter beds used this study, pressure drop measurements were conducted under three gas-liquid (G-L) flow conditions. These were counter-current, co-current and cross-current as shown in Figure A.1. For each G-L flow condition, pressure drops were measured for water saturated activated carbon with and without liquid trickling. The pressure drop in horizontal design (cross-current) will be compared to that of vertical designs (co-current and counter-current) purposely.

Figure A.1a and Figure A.1b show the vertical setups used for pressure drop tests under co- and counter-current G-L flow conditions, respectively. The packing heights of both setups were 45 cm and the internal diameter of the column was 10 cm. Figure A.1c presents the horizontal setup under cross-current flow condition. The total packing length was 30 cm and the cross-sectional area of the packing bed was 0.0225 m^2 (15×15 cm). The pressure head was measured using a manometer filled with water.

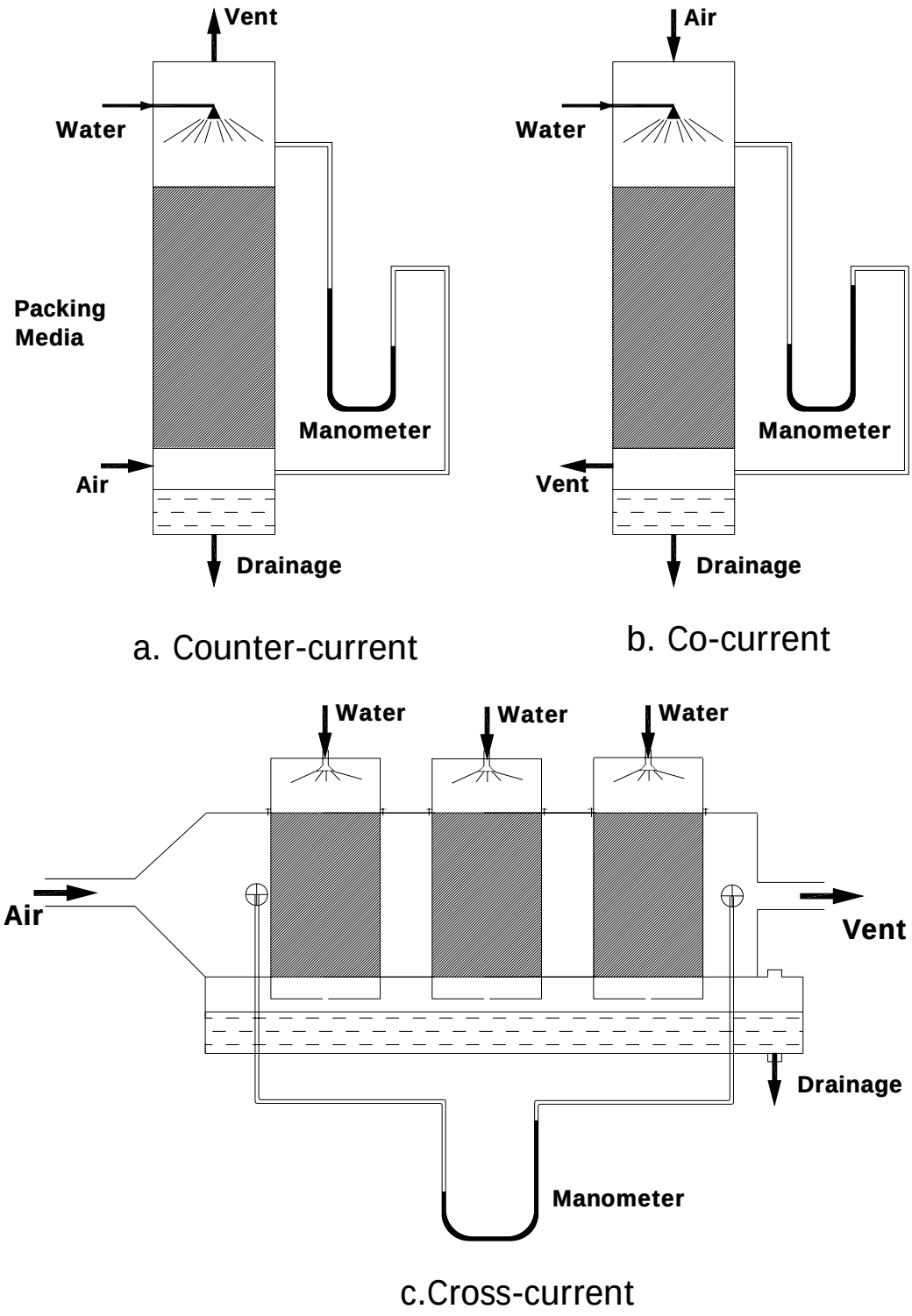

Figure A.1 Schematic diagram for pressure drop test

As Moregan-Sagastume et al. (2001) reported, pressure drop of a packing bed increased with the increasing of gas velocity. The degree to which the pressure drop increased depended on the type of packing material used, and also on the range of air velocities at which the linear behavior became nonlinear. In considering a monophasic fluid system (i.e. homogeneous mixture between gas and water), Ergun (1952) established the following relationship (Eq. A-1) of the pressure drop (ΔP) with respect to the porosity of the bed through an ideal porous fixed-bed plug-flow reactor:

$$\frac{\Delta P}{H} = \frac{150\mu v_0}{d_p^2}\frac{(1-\varepsilon)^2}{\varepsilon^3} + \frac{1.75\rho v_0^2}{d_p}\frac{1-\varepsilon}{\varepsilon^3} \qquad \text{Eq. A-1}$$

where ΔP is the pressure drop across the bed; μ is the air dynamic viscosity, ρ is the density of air; v_0 is the superficial air velocity; d_p is the effective diameter of the particles; ε is the bed fractional void volume or effective porosity and H is the bed height.

Curves of pressure drop against superficial air velocity, which have a linear behavior at low air velocities, have been widely reported for natural, porous packing materials (Madamba et al., 1994). These types of curves can be satisfactorily modeled by a modified Ergun (M-E) equation (Eq. A-2), which takes into account the dependence on porosity of the viscous and kinetic energy losses (Macdonald et al., 1979)

$$\frac{\Delta P}{H} g_c = \frac{A\mu v_0}{d_p^2}\frac{(1-\varepsilon)^2}{\varepsilon^{3.6}} + \frac{B\rho v_0^2}{d_p}\frac{1-\varepsilon}{\varepsilon^{3.6}} \qquad \text{Eq. A-2}$$

in which g_c is the gravitational constant; A and B are constants, respectively. In the modified M-E equation, Macdonald et al. (1979) replaced the constants 150 and 1.75, and ε^3 from the original quasi-empirical Ergun equation (Eq.A-1; Ergun, 1952) by A, B, and $\varepsilon^{3.6}$. These modifications to the original Ergun equation (Eq. A-1)

account for particle roughness and a better porosity function (Macdonald et al., 1979). The first term in the modified M-E equation takes into account viscous energy losses, proportional to $(1-\varepsilon)^2/\varepsilon^{3.6}$, and the second term accounts for kinetic energy losses, proportional to $(1-\varepsilon)/\varepsilon^{3.6}$. The parameter A is considered to be independent of particle roughness and equals to 180, but B is dependent on surface roughness, varying from 1.8 for the smooth particles to 4.0 for the roughest particles.

Nominate $K_1 = \frac{A\mu}{g_c d_p^2}\frac{(1-\varepsilon)^2}{\varepsilon^{3.6}}$, $K_2 = \frac{B\rho}{g_c d_p}\frac{(1-\varepsilon)}{\varepsilon^{3.6}}$, Eq.A-2 can be simplified as:

$$\frac{\Delta P}{H} = K_1 v_0 + K_2 v_0^2 \qquad \text{Eq. A-3}$$

Figure A.2 shows the variations of the pressure drop across the bed versus the superficial air velocity passing by these three biofilter systems. As shown in Figure A.2, the experimental data from the biofilters with dry or wet carbon without liquid trickling, or with liquid trickling under co-, cross- and counter-current G-L flow directions fit the modified M-E Equation (Eq. A-2) well. Pressure drop increases with increase gas velocity and follows a polynomial (Figure A.2a) and linear (Figure A.2b) relationships. Due to the different configurations of the biofilters investigated in this study (Figure A.1), the different G-L flow directions creates different water resistance to gas flow through the porous bed so that the void volume (ε) available for convection is varied. In this study, A, B, μ, g_c, d_p, ρ are constants, K_1 and K_2 are proportioned to $(1-\varepsilon)^2/\varepsilon^{3.6}$ and $(1-\varepsilon)/\varepsilon^{3.6}$, respectively. Therefore, the higher the ε, the lower the K_1 and K_2 value.

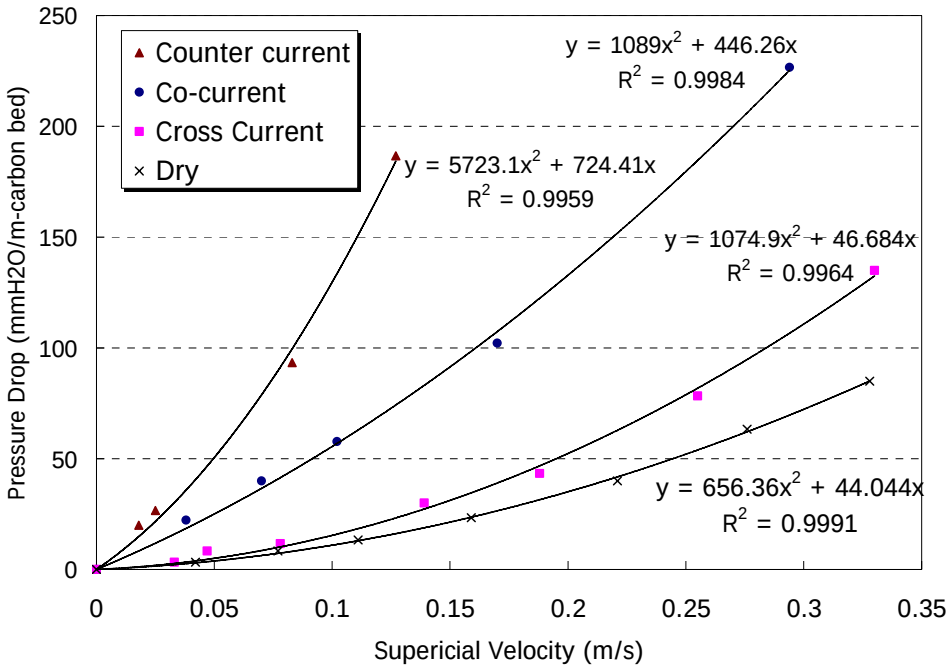

a. Nonlinear relationship at high air velocity

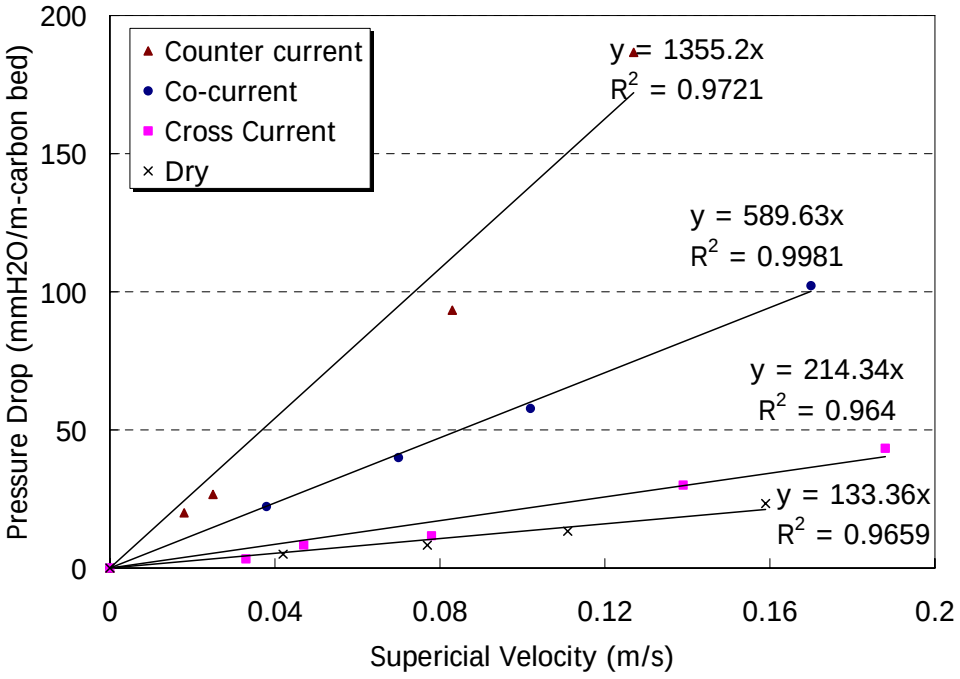

b. Linear relationship at low air velocity

Figure A.2 Pressure drop per unit length of carbon bed with various G-L flow directions as a function of gas velocity

When the system is running at high superficial air velocity, the pressure drop per unit bed length followed the polynomial relationship (Eq. A-3). As Figure A.2a shows, K_2 value under cross-current flow condition (1074.9) is much less than the other two flow directions [counter-current (5723.1) and co-current (1089)], and approaches to the dry carbon bed whose K_2 value is 656.34. The same tendency was found in K_1 values [counter-current (724.41) > co-current (446.26) > cross current (46.68) $\approx$ dry bed (44.04)]. Under counter-current flow, the water resistance to gas flow through the bed is more than that under co-current flow, and that under co-current flow would be more than that under cross-current flow (horizontal design). The comparison shows that horizontal design may have a great potential in relieving pressure drop which would reduce the energy consumption of a biofilter.

At a low superficial gas velocity, the kinetic energy loss (the second term of the modified M-E equation) in the packing bed could be ignored. The relationship between pressure drop per unit bed length and superficial air velocity becomes linear:

$$\frac{\Delta P}{H} = K_1 v_0 \qquad \text{Eq. A-4}$$

With linear relationship between pressure drop and the air velocity at a slope of K_1 (Figure A.2b), K_1 value under the cross-current flow condition (214.34) is much less than the other two flow directions [counter-current (1355.2) and co-current (589.63)], and approaches to the dry carbon bed (133.36).

Diameter of carbon pellet, one of the parameters that influence the bed porosity, affects the pressure drop indirectly. The comparison on pressure drop between different pellet diameters at a low superficial air velocity through the packing bed is tabulated in Table A.1. The pressure drop caused by Calgon AP460 (I.D. = 4 mm) is less than half of that caused by Calgon AP360 (I.D. = 3 mm) when the packing

bed is operated in the same conditions (Note: pressure drop is proportional to K_1 value, Table A.1). Larger pellet size may lead to a less pressure drop of the packing bed. Yang and Allen (1994a) reported that the pressure drop created by particles of 1 mm or less is about 200 times of that caused by an equivalent bed composed of particles of 12 mm or greater in size. For the application of all kinds of packing media in biotrickling filtration, at least 4 mm of particle size is needed (Bibeau et al., 2000; Elias et al., 2002). However, too large particle sizes, which may lead to extremely high bed porosity, would reduce the G-L contact surface area and thus decrease the system RE. Therefore, in an industrial design, the largest particle size packing with the least pressure drop is usually chosen to meet the limit of odor emission standard.

Table A.1 Comparison of K_1 value for the AP460 and AP360

G-L follow Direction	AP460		AP360	
	Liquid Trickling Velocity (cm/s)	K_1 value	Liquid Flow Rate (L/min)	K_1 value
Dry	0	133 (0.966)	0	515 (0.976)
Cross-Current	0.021	214 (0.964)	0.037	611 (0.978)
Co-Current	0.021	590 (0.998)	0.034	902 (0.990)
Counter-Current	0.021	1355 (0.972)	0.034	2752 (0.974)

Remarks: 1. Numbers in the brackets are the R^2 values;

2. Data from AP360 refer to (Tong, 2004);

3. The difference between AP360 & AP460 is the average pellet diameter: AP360 => 3 mm, AP460 => 4 mm.

APPENDIX B
MODEL PARAMETERS ESTIMATION

B.1 Henry's constant (H)

System temperature will impact the partial pressure of a component in the gas phase in equilibrium with a specified solution concentration. According to Montgomery (1985), from a thermodynamic analysis, the temperature dependence of the Henry's constant (H) can be modelled by a Van't Hoff-type relation, given in the integrated form by:

$$\log H = \frac{-\Delta H}{RT} + K \qquad \text{Eq.B-1}$$

where ΔH (kcal/kmol) is the heat absorbed in the evaporation of 1 mole of component from solution at constant temperature and pressure, R is the gas constant (1.987 kcal·kmol^{-1}), K is an empirical constant. The values of ΔH and K for H_2S are as follows: ΔH = 1845 kcal·kmol^{-1}; K = 5.88 (Montgomery, 1985).

It indicates that the temperature dependence of H is nearly linear within the range of 15~35 °C as shown in Table B.1. Therefore, it is necessary to consider the effect of temperature in the process when estimating the values of H. In this proposed study, the temperature was maintained at around 25 °C so that a value of 0.42 was taken for H_2S Henry's constant.

Table B.1 Henry's constant of H_2S at different temperatures
(Montgomery, 1985)

T (°C)	T (K)	H (atm)	H (dimensionless)
15	288.15	454	0.339
20	293.15	515	0.378
25	298.15	583	0.420
30	303.15	656	0.466
35	308.15	736	0.514

B.2 Bed porosity (ε)

The bed porosity (ε) of HBTF was defined and calculated as follows:

$$\varepsilon = \frac{bulk \cdot volume \cdot of \cdot bed - \frac{mass \cdot of \cdot carbon}{density \cdot of \cdot carbon}}{bulk \cdot volume \cdot of \cdot bed} \qquad \text{Eq. B-2}$$

The calculated bed porosity is 0.37.

B.3 Effective diffusion surface area (A_s)

The specific surface area for effective diffusion is determined as:

$$A_s = \frac{Volume \cdot fraction \cdot filled \cdot with \cdot particles \times area \cdot of \cdot one \cdot particle}{Volume \cdot of \cdot one \cdot particle}$$
$$= \frac{(1-\varepsilon) \times (2\pi r_c^2 + 2\pi r_c l)}{\pi r_c^2 l} = 2(1-\varepsilon)(\frac{1}{l} + \frac{1}{r_c}) \qquad \text{Eq. B-3}$$

where ε is the bed porosity, l is the average length of activated carbon, m; and r_c is the average carbon pellet radius, m. The average length and radius of Calgon AP460 are measured to be 6.6 mm and 2.0 mm, respectively. Therefore, the calculated A_s is 820.9 m^{-1}.

B.4 Equivalent radius of carbon pellet (*R*)

The equivalent radius of carbon pellet is the radius of a sphere (assumed in carbon adsorption kinetic model) whose volume is equal to a carbon cylindrical pellet (The shape of Calgon AP460). R is determined as:

$$\frac{4}{3}\pi R^3 = \pi r_c^2 l \Rightarrow R = \sqrt[3]{\frac{3r_c^2 l}{4}} \qquad \text{Eq. B-4}$$

Substitute r_c (2.0 mm) and l (6.6 mm) into Eq. B-4 and results in R = 2.7 mm.

B.5 Biofilm thickness (δ)

The biofilm thickness (δ) was estimated from biomass measurements conducted after a series of biokinetic experiment using appropriate empirical correlations (Pirbazari et al., 1993)

$$\delta = \frac{\Delta W_1}{0.99\rho_l N_p A_p} \qquad \text{Eq. B-5}$$

where ΔW_1 = weight of biomass, g; ρ_l = aqueous density, g·m^{-3}; N_p = number of the particles; A_p = apparent surface area of particles, m^2.

Five sets of BAC (each set contained about 50 pellets) were taken out of the HBTF randomly after the HBTF run to measure the biofilm thickness. The initial weight was noted as W_1, the samples were dried for 10 h under 105 ^{o}C followed by weighing as W_2 (the dried sample). Therefore, $\Delta W_1 = W_1 - \frac{W_2}{1\text{-}m}$, where m = average moisture content of Calgon carbon AP460, %. According to Table 6.1, the moisture content is 36%. The apparent surface area was calculated as the surface area of cylinder. Finally, the average value for biofilm thickness (δ = 35.7 μm) was calculated by Eq. B-5 and was used as the preset biokinetic parameter in the model calculation.

B.6 First order biodegradation rate constant (k_1)

Data from a set of batch experiments were used to estimate the biodegradation parameters (k_1) by a model calibration exercise. In a 250 mL conical flask, 10 mL of bacteria seeds (2.03×10^6 cfu·mL^{-1}) was added into the 90 mL liquid medium given in Table 3.1. Sodium thiosulfate (as bacteria energy source) was adopted to avoid the difficulty of measuring H_2S concentration changes in a conical flask. The flasks were shaken on an auto-shaker at 120 rpm under room temperature (~25 ^oC). Thiosulfate concentration was monitored during the culturing. The reaction rate constant k_1 was determined by performing linear regression between the natural logarithm (*ln*) of the relative concentration of C/C_0 and the time (t) at the microbial exponential growth phase following as Eq.B-6 shows:

$$\frac{C}{C_0} = e^{-k_1 t} \qquad \text{Eq.B-6}$$

Finally, the average value of k_1 (14.9 s^{-1}) was obtained from three batch flask cultures.

B.7 First order adsorption rate constant (k_{ad})

To estimate k_{ad} under the steady-state condition, four parallel identical H_2S breakthrough tests were set up. The internal diameter of the columns was 2 cm. They were filled with 2.62 g of activated carbon (Calgon AP460) to a height of 2 cm. Figure 3.18 shows the setups of the H_2S breakthrough test. Different concentrations of H_2S gas stream (6~35 ppm_v) were passed through the columns at a gas superficial velocity of 2 cm·s^{-1}. The problem is that the steady-state position for fixed-bed adsorption is at exhaustion, at which point there is no removal rate to measure. Measuring the removal rate prior to this time yields a theoretically

unsteady-state rate constant that is then applied to a steady-state condition. The compromise was accepted in this study. To some extent the measurement of k_{ad} in the active adsorption zone simulates the activity of activated carbon pellets in the HBTF, even at steady state, where diffusion and biodegradation keep the external BAC surface "active" throughout. The measurements of the outlet concentration profiles against time revealed an exponential increasing function. Therefore, the first-order adsorption rate constant (k_{ad}) for the varied inlet H_2S concentrations could be estimated by performing a linear regression analysis of the constant pattern profiles. Finally, the calculated k_{ad} value was between 2.04~2.31 s^{-1}, and the initial input average value of k_{ad} was obtained, at 2.18 s^{-1}.

REFERENCES FOR APPENDICES

Bibeau, L., Kiared, K., Brzezinski, R., Viel, G. and Heitz, M. (2000) "Treatment of Air Polluted with Xylenes Using a Biofilter Reactor." Water Air and Soil Pollution, Vol.118, No.3-4, pp. 377-393.

Elias, A., Barona, A., Arreguy, A., Rios, J., Aranguiz, I. and Penas, J. (2002) "Evaluation of a Packing Material for the Biodegradation of H_2S and Product Analysis." Process Biochem., Vol.37, pp. 813-820.

Ergun, S. (1952) "Fluid Flow Through Packed Columns." Chem. Eng. Prog., Vol.48, No.2, pp. 89-94.

Macdonald, I. F., El-Sayed, M. S., Mow, K. and Dullien, F. A. L. (1979) "Flow Through Porous Media-the Ergun Equation Revisited." Ind. Eng. Chem. Fundam., Vol.18, No.3, pp. 199-208.

Madamba, P. S., Driscoll, R. H. and Buckle, K. A. (1994) "Bulk Density, Porosity and Resistance to Airflow of Garlic Slices." Drying Technol., Vol.12, No.4, pp. 937-954.

Montgomery, J. M. (1985) Water treatment principles and design. Wiley, New York.

Morgan-Sagastume, F., Sleep, B. E. and Allen, D. G. (2001) "Effects of Biomass Growth on Gas Pressure Drop in Biofilters." J. Envion. Eng., pp. 388-396.

Pirbazari, M., Ravindran, V., Badriyha, B. N., Craig, S. and McGuire, M. J. (1993)

"GAC Adsorber Design Protocol for the Removal of Off-flavors." Wat. Res., Vol.27, No.7, pp. 1153-1166.

Tong, D. J. (2004) "Use of Activated Carbon as Biofiltration Packing Material." M.Eng.Thesis, Nanyang Technological University.

Yang, Y. H. and Allen, E. R. (1994a) "Biofiltration Control of Hydrogen Sulfide 1. Design and Operational Parameters." J. Air & Waste Manage. Assoc., Vol.44, pp. 863-868.

PUBLICATIONS

1. Yan, R., Chin, T., Ng, Y.L., Duan, H.Q., Liang, D.T., and Tay, J.H. (2004). "Influence of surface properties on the mechanisms of H_2S removal by alkaline activated carbons". Environ. Sci. Technol., Vol.38, No.1, pp.316-323.

2. Yan, R., Ng, Y.L., Chen, X.G., Geng, A.L., Gould, W.D., Duan, H.Q., Liang, D.T., and Koe, L.C.C. (2004). "Batch experiment on H_2S degradation by bacteria immobilized on activated carbons". Wat. Sci. Technol., Vol.50, No.4, pp.299-308.

3. Koe, L.C.C., Duan, H.Q., Tong, D, Yan, R. and Chen, X.G. (2004). "Preliminary Study of Using Activated Carbon as Biofilter Packing Material for Treatment of H_2S". Proceedings of Enviro04 Convention & Exhibition, Sydney, Australia.

4. Duan, H.Q., Koe, L.C.C. and Yan, R. (2005). "Treatment of H_2S using a Horizontal Biotrickling Filter Based on Biological Activated Carbon: Reactor Setup and Performance Evaluation". Appl. Microbiol. Biotechnol., Vol.67, pp.143-149.

5. Duan, H.Q., Yan, R. and Koe, L.C.C. (2005). "Investigation on the Mechanism of H_2S Removal by Biological Activated Carbon in a Horizontal Biotrickling Filter". Appl. Microbiol. Biotechnol., Vol.67, No.3, pp.350-357

6. Koe, L.C.C., Duan H.Q. and Yan, R. (2006) "Biological Activated carbon for H_2S Removal in Biotrickling filter". Proceeding WEF and AWMA Odors and Air Emissions, Maryland, USA

7. Duan, H.Q., Koe, L.C.C., Yan, R. and Chen X.G. (2006) “Biological treatment of H_2S using Pellet Activated Carbon as a carrier of microorganisms in a biofilter. Water Research, Vol.40, pp.2629-2636

8. Duan, H.Q., Yan, R., Koe, L.C.C. and Wang, X.L. (2006) “Combined Effect of Adsorption and Biodegradation of Biological Activated Carbon on H_2S Biotrickling Filtration”. Chemosphere, Vol. 66, No.9, pp.1684-1691